PHD

Vehicle and engine biodiesel investigations

Ali, Hasan

Award date:
2011

Awarding institution:
University of Bath

Vehicle and Engine Biodiesel Investigations

Hasan A. M. Ali

A thesis submitted for the degree of Doctor of Philosophy

University of Bath

Department of Mechanical Engineering

August 2011

Table of Contents

TABLE OF CONTENTS I
LIST OF FIGURES VII
LIST OF TABLES XIII
ACKNOWLEDGMENTS XIV
ABSTRACT XV
LIST OF NOTATIONS XVI
CHAPTER 1 INTRODUCTION 1
1.1 Background 1
1.2 Project Aims 3
1.3 Project Objectives 3
1.4 Summary of Chapters 4
1.5 Papers Published From This Work 6
CHAPTER 2 LITERATURE REVIEW 7
2.1 Introduction 7
2.2 FAME Production 10
2.2.1 Feedstock 10
2.2.2 Transesterification Process 11
2.3 FAME Properties 12
2.3.1 Cetane Number (CN) 14
2.3.2 Heat of Combustion 16
2.3.3 Density and Kinematic Viscosity 16
2.3.4 Cold Flow 17
2.3.5 Oxidation Stability 18
2.4 FAME Performance in Diesel Engines 19
2.4.1 Compatibility 19
2.4.2 Lubrication and Wear 20
2.4.3 Fuel Injection System 21
2.4.4 Exhaust After-Treatment System 22
2.4.5 Engine out Emissions 23
2.4.5.1 Particulate Matter (PM) and Smoke 23
2.4.5.2 Nitrogen Oxides (NO_X) 24
2.4.5.3 Hydrocarbons (HC) 26
2.4.5.4 Carbon Monoxide (CO) 26
2.5 Review of Vehicle Experiments with Biodiesel 27

2.5.1 Particulate Matter (PM) and Smoke Opacity 27
2.5.2 Nitrogen Oxides (NO_X) 29
2.5.3 Hydrocarbons (HC) 30
2.5.4 Carbon monoxide (CO) 31
2.5.5 Power and Fuel Consumption 32
2.6 Review of Engine Experiments with Biodiesel 32
2.6.1 Engine out Emissions 33
2.6.2 Combustion and Heat release 34
2.6.3 Power and Fuel Consumption 38
2.7 Unregulated Emissions with Biodiesel 39
2.8 Review of Engine Simulation with Biodiesel 40
2.8.1 Background 40
2.8.2 Simulation Reviews 41
2.9 Engine Calibration with Biodiesel 44
2.9.1 Background 44
2.9.2 Engine Optimization Reviews 44
2.10 Conclusions 47
CHAPTER 3 BIODIESEL VEHICLE TRIALS 50
3.1 Introduction 50
3.1.1 Aims and Objectives 50
3.1.2 Approach 51
3.2 Experimental Facility 51
3.2.1 Experimental Cell 51
3.2.2 Vehicle 52
3.2.3 Fuels 53
3.2.4 Facilities 54
3.2.4.1 Emissions Measurement 54
3.2.4.2 Fuel Consumption Measurement 56
3.3 Experimental Program 57
3.3.1 NEDC 57
3.3.2 Bath Full Load Cycle 58
3.4 Design of Experiments (DoE) 59
3.5 NEDC Results 61
3.5.1 NEDC CO Emissions 61
3.5.2 NEDC THC Emissions 64
3.5.3 NEDC NO_X Emissions 66

3.5.4 NEDC PM Emissions 68
3.5.5 Engine Strategy Investigations 70
3.5.6 Catalyst Performance Investigations 73
3.5.6.1 Catalyst Conversion Efficiency 73
3.5.6.2 Exhaust Temperature Investigations 77
3.5.6.3 HC Speciation Investigations 78
3.5.7 Fuel Consumption (FC) 80
3.5.8 NEDC Surface Response Model 82
3.6 Full Load Results 87
3.6.1 Dynamometer Tractive Force 87
3.6.2 Power Drop Investigation 90
3.7 Conclusions 93
CHAPTER 4 BIODIESEL ENGINE SIMULATION 96
4.1 Introduction 96
4.2 Ricardo WAVE Software 96
4.3 WAVE Model Sensitivity to Fuel Properties 97
4.3.1 Fuel properties 98
4.3.1.1 Selecting Fuel Properties 98
4.3.1.2 Fuel Property Values 99
4.3.2 Simulation Set Up 104
4.3.2.1 Engine Model 104
4.3.2.2 Creating Fuel Files 106
4.3.2.3 Experimentally Obtained Data 106
4.3.2.4 Running the WAVE model 107
4.4 Experimental Approach 108
4.4.1 MODDE 7 Software Package 108
4.4.2 Experimental Design Process 109
4.5 Results and Discussion 110
4.5.1 Effect of Fuel properties on the Fuel Evaporation 110
4.5.2 Effect of Fuel properties on the Combustion Process 113
4.6 Conclusions 118
CHAPTER 5 BIODIESEL ENGINE TRIALS 120
5.1 Introduction 120
5.2 Aims and Objectives 120
5.3 Experimental Facility 121
5.3.1 Measuring equipment 122

5.3.1.1 Engine dynamometer 123
5.3.1.2 CP CADET V12 123
5.3.1.3 ATI Vision 123
5.3.1.4 CAS System 124
5.3.1.5 MEXA Analysers 124
5.3.1.6 In-Cylinder Pressure Measurement 124
5.3.1.7 Crank Shaft Encoder 125
5.3.1.8 Temperature Measurement 125
5.3.2 Engine Specification 125
5.3.3 Fuel Injection System 126
5.3.4 Fuels 127
5.4 Approach 129
5.5 In Cylinder Investigation: Fixed Engine Load 129
5.5.1 Fuel Injection Process 130
5.5.2 Combustion Analysis 131
5.5.3 Emissions Analysis 135
5.6 In Cylinder Investigation: Fixed Pedal position 138
5.6.1 Combustion Analysis 138
5.6.2 Emissions Analysis 141
5.7 In Cylinder Investigation: Fixed Pedal position and deactivated Pilot injection 144
5.7.1 Combustion Analysis 144
5.7.2 Fuel Injection Process 147
5.7.3 Ignition Delay Investigation 149
5.7.4 Effect of Deactivation of Pilot Injection 151
5.8 Conclusions 154
CHAPTER 6 BIODIESEL ENGINE CALIBRATION SENSITIVITY 156
6.1 Introduction 156
6.2 Approach 156
6.3 Varying the EGR Rate 157
6.3.1 1500 RPM 10% pedal 157
6.3.2 1500 RPM 17% pedal 160
6.3.3 2250 RPM 15% pedal 163
6.3.4 2250 RPM 22% pedal 164
6.4 Varying Rail Pressure 166
6.4.1 1500 RPM 10% pedal 166
6.4.2 1500 RPM 17% pedal 169
6.4.3 2250 RPM 15% pedal 171

6.4.4 2250 RPM 22% pedal 173

6.5 Varying Main Injection Timing 175

6.5.1 1500 RPM 10% pedal 175

6.5.2 1500 RPM 17% pedal 178

6.5.3 2250 RPM 15% pedal 180

6.5.4 2250 RPM 22% pedal 182

6.6 Varying Pilot Injection Timing 183

6.6.1 1500 RPM 10% pedal 184

6.6.2 1500 RPM 17% pedal 187

6.6.3 2250 RPM 15% pedal 189

6.6.4 2250 RPM 22% pedal 191

6.7 Conclusions 192

CHAPTER 7 BIODIESEL OXIDATION CATALYST PERFORMANCE 194

7.1 Introduction 194

7.2 Background 195

7.3 Aims and Objectives 197

7.4 Experimental Facility 197

7.5 Approach 198

7.6 DOC Performance during NEDC 199

7.6.1 NEDC CO Emissions 200

7.6.2 NEDC HC Emissions 201

7.6.3 NEDC NO_X Emissions 202

7.7 Thermal Impact of Using RME Biodiesel 203

7.7.1 Catalyst Brick temperature 203

7.7.2 Continuous Conversion Efficiency 206

7.7.2.1 Continuous CO Conversion 206

7.7.2.2 Continuous HC Conversion 207

7.7.2.3 Continuous Passive NO_X Conversion 209

7.8 Chemical Impact of Using Biodiesel on DOC 211

7.8.1 CO Light-off Curve: NEDC Idle periods 211

7.8.2 HC Light-off Curve: NEDC Idle periods 212

7.8.3 Passive NO_X Light-off Curve: NEDC Idle periods 214

7.9 Further Investigations into Chemical Impact of biodiesel on DOC 216

7.9.1 Transient Engine Ramp 216

7.9.1.1 Light-off Curves during Transient Engine Ramp 217

7.9.1.2 Emissions Investigation during Transient Engine Ramp 220

7.9.2 Altering the engine calibration 222

7.10 Conclusions 228

CHAPTER 8 FINAL CONCLUSIONS 230

8.1 Overall Conclusions 230

8.2 Recommendations for Future Work 236

CHAPTER 9 REFERENCES 237

CHAPTER 10 APPENDICES 249

Appendix A: Baseline Diesel Fuel Specification 249

Appendix B: RME Biodiesel Fuel Specification 250

Appendix C: The Student T Test P values 251

List of Figures

Figure 2.1, Formation of Methyl Ester from Triglycerides, adopted from [10] 11

Figure 2.2, Cetane Number Trend Lines for Methyl Esters [21] 15

Figure 2.3, Effect of Iodine Number on NO_X Emissions [24] 25

Figure 2.4, Instantaneous rate of heat release for 50 percent of rated engine load at 1400 RPM. 34

Figure 2.5, Rate of heat release analysis [8] 35

Figure 2.6, Needle lift and fuel injection line profiles [64] 36

Figure 2.7, Heat Release Rates [88] 37

Figure 2.8, Simulation results of pressure and HRR [99] 42

Figure 2.9, Effects on emissions and FC due to changes in engine Parameters [102] 45

Figure 2.10, Heat Release Rate at 2000 RPM and 12 bar BMEP [103] 46

Figure 3.1, University of Bath chassis dynamometer testing facility 52

Figure 3.2, University of Bath chassis dynamometer and CVS system layout 54

Figure 3.3, Fuel system layout 56

Figure 3.4, New European drive cycle (NEDC) 57

Figure 3.5, Full Load Method 58

Figure 3.6, The impact of the biodiesel blend ratio and ambient temperature on the NEDC tailpipe bag CO emissions 62

Figure 3.7, The impact of the biodiesel blend ratio and ambient temperature on the NEDC pre-catalyst CO emissions 64

Figure 3.8, The impact of the biodiesel blend ratio and ambient temperature on the NEDC tailpipe THC emissions 65

Figure 3.9, The impact of the biodiesel blend ratio and ambient temperature on the NEDC pre-catalyst THC emissions 65

Figure 3.10, The impact of the biodiesel blend ratio and ambient temperature on the NEDC tailpipe bag NO_X emissions 66

Figure 3.11, The impact of the biodiesel blend ratio and ambient temperature on the NEDC pre-catalyst NO_X emissions 67

Figure 3.12, The impact of the biodiesel blend ratio and ambient temperature on the NEDC tailpipe PM emissions 69

Figure 3.13, The impact of the biodiesel blend ratio and ambient temperature on the NEDC tailpipe opacity 69

Figure 3.14, Impact of B50 biodiesel on Engine Map Transition (NEDC 25°C ambient Temperature) 70

Figure 3.15, Impact of B50 Effect RME on Cumulative Pedal Position (NEDC 25°C ambient Temperature) 71

Figure 3.16, Impact of Ambient Temperature on Engine ECU Map Transition 72

Figure 3.17, NEDC CO Catalyst Conversion Efficiency 73

Figure 3.18, NEDC THC Catalyst Conversion Efficiency 75

Figure 3.19, Catalyst CO conversion efficiency relative to cycle time 75

Figure 3.20, Catalyst THC conversion efficiency relative to cycle time 76

Figure 3.21, The impact of B50 biodiesel on NEDC engine-out exhaust gas temperature at 25°C ambient temperature 77

Figure 3.22, The impact of the biodiesel blend ratio on the average NEDC pre-catalyst exhaust gas temperature at 25°C ambient temperature 78

Figure 3.23, NEDC CO Light-off curve 79

Figure 3.24, The impact of biodiesel blend ratio and ambient temperature on the NEDC fuel consumption using AVL733 80

Figure 3.25, NEDC CO response 82

Figure 3.26, NEDC HC Response 83

Figure 3.27, NEDC NO_X Response 84

Figure 3.28, NEDC PM Response 85

Figure 3.29, NEDC fuel Consumption Response 86

Figure 3.30, The effect of the biodiesel blend ratio and ambient temperature on the maximum tractive Force in third gear at 30 km/h 88

Figure 3.31, The effect of the biodiesel blend ratio and ambient temperature on the maximum tractive Force in third gear at 50 km/h 88

Figure 3.32, The effect of the biodiesel blend ratio and ambient temperature on the maximum tractive Force in third gear at 80 km/h 89

Figure 3.33, Reduction in Tractive force with B50 Biodiesel blend relative to baseline diesel 90

Figure 3.34, Average boost pressure for B50 biodiesel and baseline diesel fuel at different ambient temperatures engine speeds 91

Figure 3.35, Average MAF for B50 biodiesel and baseline diesel fuel at different ambient temperatures and engine speeds 92

Figure 4.1, Fuel Editor Panel in WAVE Build 98

Figure 4.2, Specific heat capacity profile used in the WAVE model [118-126, and 140-144] 102

Figure 4.3, Vapour pressure profile used in the WAVE model [118-126, and 140-143] 102

Figure 4.4, Viscosity profile used in the WAVE model [120-126, 140-144] 103

Figure 4.5, Surface tension profile used in the WAVE model [121-124, and 144-143] 104

Figure 4.6, Basic Model for 2.0 l PUMA engine supplied by Ford 105

Figure 4.7, The DoE factors screen 109

Figure 4.8, The DoE response screen 109

Figure 4.9, DoE test plan 110

Figure 4.10, DoE Response, variations in DMD calculation 111

Figure 4.11, DoE Response, variations in SOC calculation 114

Figure 4.12, DoE response, variations in exhaust temperature 116

Figure 4.13, DoE response, variations in cylinder pressure 116

Figure 4.14, DoE response, variations in cylinder temperature 117

Figure 5.1, Layout of engine test cell 1 facility 122

Figure 5.2, Common Rail Injector adopted from Lucas [2] 127

Figure 5.3, Demanded Rail pressure for different fuel blends, matched engine load 130

Figure 5.4, Cylinder pressure vs. Crank angle at 1500 RPM and matched engine load 131

Figure 5.5, Cylinder pressure vs. Crank angle at 2250 RPM and matched engine load 132

Figure 5.6, Rate of Heat Release for 1500 RPM engine speed and (a) Low load (b) High Load 133

Figure 5.7, Rate of Heat Release for 2250 RPM engine speed and (a) Low load (b) High load .. 134

Figure 5.8, Engine out CO emissions with different fuel blends during both engine speeds, fixed engine load investigation 135

Figure 5.9, Engine out HC emissions with different fuel blends during both engine speeds, fixed engine load investigation 136

Figure 5.10, Engine out NO_X emissions with different fuel blends during both engine speeds, fixed engine load investigation 137

Figure 5.11, Cylinder pressure vs. Crank angle at 1500 RPM and fixed pedal position 138

Figure 5.12, Cylinder pressure vs. Crank angle at 2250 RPM and fixed pedal position 138

Figure 5.13, Rate of Heat Release for 1500 RPM engine speed at (a) 9% pedal (b) 17% pedal 140

Figure 5.14, Rate of Heat Release for 2250 RPM engine speed at (a) 15% pedal (b) 22% pedal 140

Figure 5.15, Average engine torque at all operating conditions, fixed pedal position 141

Figure 5.16, Engine out CO emissions with different fuel blends during both engine speeds, fixed pedal position investigation 142

Figure 5.17, Engine out HC emissions with different fuel blends during both engine speeds, fixed pedal position investigation 142

Figure 5.18, Engine out NO_X emissions with different fuel blends during both engine speeds, fixed pedal position investigation 143

Figure 5.19, Cylinder pressure vs. Crank angle at 1500 RPM, pilot off and fixed pedal position. 144

Figure 5.20, Cylinder pressure vs. Crank angle at 2250 RPM, pilot off and fixed pedal position. 145

Figure 5.21, Rate of Heat Release for 1500 RPM engine speed pilot off at (a) 9% pedal (b) 17% pedal 146

Figure 5.22, Rate of Heat Release for 2250 RPM engine speed pilot off at (a) 15% pedal (b) 22% pedal 147

Figure 5.23, Actual start of injection timing with different fuels and pedal position 148

Figure 5.24, Estimated ignition delay, pilot off fixed pedal position..... 150

Figure 5.25, percentage change in engine out emissions with deactivated pilot injection compared to the standard calibration..... 151

Figure 5.26, the reduction in engine power due to the deactivation of pilot injection for all fuel blends at all operating conditions..... 152

Figure 6.1, the effect of EGR swing on the engine torque and emissions for the 1500 RPM and 10% pedal position..... 158

Figure 6.2, the effect of EGR variation on (a) rate of heat release and (b) cylinder pressure at 1500 RPM and 10% pedal position..... 159

Figure 6.3, the effect of EGR swing on the engine torque and emissions for the 1500 RPM and 17% pedal position..... 161

Figure 6.4, the effect of EGR variation on (a) rate of heat release and (b) cylinder pressure at 1500 RPM and 17% pedal position..... 162

Figure 6.5, the effect of EGR swing on the engine torque and emissions for the 2250 RPM and 15% pedal position..... 163

Figure 6.6, the effect of EGR swing on the engine torque and emissions for the 2250 RPM and 22% pedal position..... 165

Figure 6.7, the effect of rail pressure swing on the engine torque and emissions for the 1500 RPM and 10% pedal position..... 167

Figure 6.8, the effect of rail pressure swing on fuel injection durations at the 1500 RPM and 10% pedal position..... 168

Figure 6.9, the effect of varying rail pressure on the engine torque and emissions for the 1500 RPM and 17% pedal position..... 169

Figure 6.10, effect of rail pressure variation on (a) rate of heat release and (b) cylinder pressure at 1500 RPM and 17% pedal position..... 170

Figure 6.11, the effect of rail pressure variation on the engine torque and emissions for the 2250 RPM and 15% pedal position..... 172

Figure 6.12, effect of rail pressure variation on (a) rate of heat release and (b) cylinder pressure at 2250 RPM and 15% pedal position..... 173

Figure 6.13, the effect of rail pressure variation on the engine torque and emissions for the 2250 RPM and 22% pedal position..... 174

Figure 6.14, the effect of main injection swing on fuel injection durations at the 1500 RPM and 10% pedal position..... 175

Figure 6.15, the effect of main injection timing variation on engine out emissions and performance at 1500RPM and 10% pedal 176

Figure 6.16, effect of main injection variation on (a) rate of heat release and (b) cylinder pressure at 1500 RPM and 10% pedal position 177

Figure 6.17, the effect of main injection timing swing on engine out emissions and performance at 1500RPM and 17% pedal 178

Figure 6.18, effect of main injection variation on (a) rate of heat release and (b) cylinder pressure at 1500 RPM and 17% pedal position 180

Figure 6.19, the effect of main injection timing swing on engine out emissions and performance at 2250RPM and 15% pedal 181

Figure 6.20, the effect of main injection timing variation on engine out emissions and performance at 2250RPM and 22% pedal 183

Figure 6.21, ECU demand injection signal with variations of pilot injection timing at the 1500 RPM and 10% pedal position 184

Figure 6.22, the effect of pilot injection timing variation on engine out emissions and performance at 1500RPM and 10% pedal 185

Figure 6.23, the effect of pilot injection timing variation on (a) rate of heat release and (b) cylinder pressure at 1500 RPM and 10% pedal position 186

Figure 6.24, the effect of pilot injection timing variation on engine out emissions and performance at 1500RPM and 17% pedal 188

Figure 6.25, the effect of pilot injection timing variation on engine out emissions and performance at 2250RPM and 15% pedal 189

Figure 6.26, the effect of injection timing variation on (a) rate of heat release and (b) cylinder pressure at the 2250 RPM and 15% pedal position 190

Figure 6.27, the effect of pilot injection timing variation on engine out emissions and performance at 2250RPM and 22% pedal 191

Figure 7.1, Diesel Particulate Filter combined with Oxidation Catalyst [132] 195

Figure 7.2, Schematic of thermocouple distribution inside the DOC catalyst, with broken ones coloured in pink 198

Figure 7.3, NEDC catalyst conversion efficiency 200

Figure 7.4, Total NEDC engine out and tailpipe CO and HC emissions for all fuel blends 201

Figure 7.5, NEDC engine out and tailpipe NO_X emission for all fuel blends 202

Figure 7.6, Engine out and average catalyst brick temperature for all fuel blends during NEDC 203

Figure 7.7, Temperature profile inside catalyst brick for all fuel blends during NEDC 205

Figure 7.8, Continuous catalyst CO conversion efficiency for all fuel blends 207

Figure 7.9, Continuous catalyst HC conversion efficiency for all fuel blends 208

Figure 7.10, Continuous catalyst NO_X passive conversion efficiency for all fuel blends 209

Figure 7.11, CO light-off curve during idle periods of the NEDC for all fuel blends 212

Figure 7.12, Averaged HC light-off curve during the idle periods of the NEDC for all fuel blends 213

Figure 7.13, Averaged NO_X light-off curve during the idle periods of the NEDC for all fuel blends 214

Figure 7.14, Effect of transient engine ramp on catalyst brich temperature and CO conversion efficiency 217

Figure 7.15, CO Light-off curve for baseline diesel and B50 in transient engine ramp condition. 218

Figure 7.16, HC Light-off curve for baseline diesel and B50 in transient engine ramp condition. 219

Figure 7.17, NO_X Light-off curve for baseline diesel and B50 in transient engine ramp condition 219

Figure 7.18, Engine out CO emissions during ramping up and down the pedal position, standard calibration..... 221

Figure 7.19, Engine out HC emissions during ramping up and down the pedal position, standard calibration..... 221

Figure 7.20, Engine out NOx emissions during ramping up and down the pedal position, standard calibration..... 221

Figure 7.21, Effect of EGR change with B50 RME fuel blend on engine MAF..... 223

Figure 7.22, Engine out CO emissions during ramp tests using modified engine calibration 224

Figure 7.23, Engine out HC emissions during ramp tests using modified engine calibration..... 224

Figure 7.24, Engine out NO_X emissions during ramp tests using modified engine calibration..... 225

Figure 7.25, Light-off curve for CO emissions for baseline diesel and B50, and with modified calibration..... 226

Figure 7.26, Light-off curve for HC emissions for baseline diesel and B50, and with modified calibration..... 227

Figure 7.27, Light-off curve for NO_X emissions for baseline diesel and B50, and with modified calibration..... 227

List of Tables

Table 1.1, EU Diesel emission standards for passenger cars (g/km) [3] 2

Table 2.1, Average Biodiesel emissions compared to conventional diesel, according to EPA [1] ... 8

Table 2.2, Main biodiesel feedstocks [6-11] 10

Table 2.3, The percentage FA composition in biodiesel fuel [7-9, 16, 24, 70, 71, 82-87, 93-97, 102] 13

Table 2.4, Fuel properties of different biodiesel feedstocks [7-9, 16, 24, 70, 71, 82-87, 93-97, 118] 14

Table 2.5, Fuel properties as a function of fuel composition [18] 17

Table 2.6, List of vehicle specifications cited 27

Table 2.7, List of cited engine specifications 32

Table 2.8, Emissions level at 2000 RPM and 12 bar BMEP [103] 46

Table 3.1, Vehicle Specification 52

Table 3.2, Summary table of Fuel Specification 53

Table 3.3, RME Fatty Acid Composition 54

Table 3.4, Vehicle Test Plan 60

Table 3.5, Percentage increase in FC compared to baseline diesel fuel during NEDC 81

Table 3.6, Reduction in tractive force with biodiesel blends relative to baseline diesel fuel 89

Table 4.1, Chemical composition value range used in the WAVE model [118-127] 100

Table 4.2, Fuel physical properties value range used in the WAVE model [118-127] 101

Table 4.3, Engine model specification 104

Table 4.4, Experimental data recorded for input into the WAVE model 107

Table 5.1, Ford Puma engine specification 126

Table 5.2, Fuel Specification 128

Table 5.3, Fatty acid composition 128

Table 5.4, Percentage increase in fuel demand relative to baseline diesel fuel 131

Table 5.5, Maximum cylinder pressure value, matched engine load 132

Table 5.6, Maximum cylinder pressure values at fixed pedal position 139

Table 5.7, Maximum in cylinder pressure values with corresponding crank angles 145

10.1, The student T test P values for baseline diesel and B50 fuel blends 251

Acknowledgments

I would like to express my gratitude to my supervisor Professor Gary Hawley for his clear direction and constructive suggestions throughout this work.

I would like to thank my co-supervisor Dr. Chris Bannister for his continuous support and guidance during all experimental procedures and writing up.

I would also like to thank all technical staff at University of Bath PVRC unit, with special mention going to Dr. Chris Brace, Dr. Sam Akehurst and Mr. Allan Cox for their assistance in managing the experimental work, Mr. Don Blake and Mr. Sam Hurley for their assistance in running chassis and engine dynamometers.

Many thanks to all of my colleagues for their support and contribution: Dr. Kai Zhang, Dr. Mitch Piddock, Dr. Shifei Ye, Richard Burke, Andy Lewis, Edward Chappel, Peter Dowell and Apiwat Suyabodha.

The final acknowledgments go to my family for giving me support and encouragement when I needed it, PAAET for financially supporting my entire PhD study.

Abstract

Biodiesel is an environmentally friendly alternative diesel fuel consisting of the alkyl esters of fatty acids which are expected to play a significant role in reducing overall CO_2 emissions. Biodiesel is produced commercially by a chemical reaction called transesterification which is a chemical process to lower the viscosity of the vegetable oils. Since Biodiesel is an oxygenated, sulfur free fuel, it typically reduces engine out emissions except for the oxides of nitrogen (NO_X). The chemical and physical properties of the fatty acids, as well as the effect of molecular structure, determine the overall properties of biodiesel fuel. Investigations into the impact of FAME properties on diesel engines are highly topical, as higher blends of biodiesel are introduced. The aim of this work is to perform a comprehensive study on the use of biodiesel fuel in production diesel engines, and its impact on emissions, performance and fuel consumption.

This thesis has shown that the use of biodiesel fuel reduces the engine out emissions of CO, HC and PM (except at sub-zero temperatures), and causes a slight increase in NO_X emissions and fuel consumption compared to baseline diesel fuel. However, the lower exhaust gas temperatures seen when using biodiesel blends leads to reduced catalyst conversion efficiency and an adverse effect on tailpipe emissions. The cylinder pressure and rate of heat release profiles of biodiesel blends are very similar to those of baseline diesel fuel when similar torque is demanded from the engine with relatively similar start of combustion for the main charge. Biodiesel blends show a slightly quicker rise in the rate of heat release and higher peak values compared to baseline diesel fuel. In the case of matched pedal positions, the ignition delay time decreases slightly with biodiesel use at lower engine load conditions compared to baseline diesel fuel. The sensitivity of engine performance and emissions with B25 is more pronounced for EGR rate, rail pressure, and main injection timing variations than for baseline diesel fuel. Finally, an adverse thermal impact of using biodiesel fuel on the performance of diesel oxidation catalyst was observed compared to baseline diesel however, no solid evidence of exhaust gas HC speciation effects was found.

List of Notations

Abbreviation	*Meaning & Units (if available)*
ATDC	After top dead centre
BTDC	Before top dead centre
BMEP	Break mean effective pressure
BPT	Balance point temperature (°C)
CA	Crank angle (°)
CBC	Carbonyl compound
CFD	Computational fluid dynamics
CFPP	Cold filter plugging point (°C)
CI	Compression ignition
CN	Cetane number
CO	Carbon monoxide
CO_2	Carbon dioxide
CP	Cloud point (°C)
CSO	Cottonseed oil
CVS	Constant volume sample
DI	Direct injection
DMD	Droplet mean diameter (m)
DOC	Diesel oxidation catalyst
DoE	Design of experiment
DPF	Diesel particulate filter
ECS	Emission control system
ECU	Electronic control unit
EGR	Exhaust gas recirculation
EPA	Environmental Protection Agency
ESC	European stationary cycle
EU	European Union
FA	Fatty acid
FAME	Fatty acid methyl ester
FC	Fuel consumption

HC	Hydrocarbon
ICE	Internal combustion engine
IDI	Indirect injection
JME	Jatropha methyl ester
LHV	Lower heating value (MJ/Kg)
MAF	Mass air flow (Kg/hour)
MBC	Model based calibration
NAC	NO_X adsorber catalyst
NEDC	New European drive cycle
NO_X	Nitrogen oxides
NPAH	Nitrated PAH
NSR	NO_X storage reduction
PAH	Polycyclic aromatic hydrocarbon
PKOME	Palm kernel oil methyl ester
P_{MAX}	Maximum cylinder pressure (bar)
PM	Particulate matter
PP	Pour point (°C)
RBME	Rice bran methyl ester
Re	Reynolds number
RME	Rapeseed methyl ester
ROH	Rate of heat release (J/° CA) or (J/second)
RPM	Revolution per minute
RSM	Response surface modelling
SCR	Selective catalytic reduction
SD	Standard deviation
SFC	Specific fuel consumption
SMD	Sauter mean diameter (m)
SME	Soybean methyl ester
SO_2	Sulphur dioxide
SO_X	Sulphur oxides
SOC	Start of combustion
SOF	Soluble organic fraction

SOI	Start of injection
THC	Total hydrocarbons
UFOME	Used frying oil methyl ester
ULSD	Ultra low sulphur diesel
VGT	Variable geometry turbocharging
VOC	Volatile organic compound
We	Weber number

Symbol	***Meaning & Units (if available)***
μ	Viscosity (mm^2/second)
σ	Surface tension (N/m)
ρ	Density (Kg/m^3)

Chapter 1 Introduction

1.1 Background

Global warming is considered to be one of the greatest environmental threats facing our planet today. Climate change has mainly been caused by the increase in atmospheric greenhouse gases due to human activities since the start of the industrial era [1]. When fuels are burnt, the exhaust products contain gaseous, solid, and liquid emissions. For internal combustion engines (ICE) there are just a few basic types of emissions to consider: oxides of nitrogen (NO_X), Carbon monoxide (CO), hydrocarbons (HC), Carbon dioxide (CO_2) and particulate matter (PM). In addition to these primary pollutants, reactions in the atmosphere generate secondary pollutants, namely acid rain, photochemical smog and tropospheric ozone [2]. Many of these pollutants have serious implications on human health and the environment. Consequently, many countries have established strict environmental regulations that must be met by all automobile manufacturers.

In the early 1990's, the European Union (EU) introduced legislation enforcing their own emission limits. The EU obligated all new light duty vehicles sold in the EU in 1993 to meet emission levels equivalent to 1987 U.S. standards. Subsequent reductions in emission levels were introduced over time becoming increasingly stringent [3]. To make this legislation more practical, and reflect the different modes of combustion, the EU introduced separate emission limits for diesel and gasoline vehicles. With advancements in emission reduction technologies and the use of alternative fuels, automobile manufacturers have been able to meet these standards. The current Euro 5 emission limits for diesel passenger cars are a substantial reduction from those introduced in 1992, as shown in Table 1.1.

Tier	Date	CO	HC	HC+NO	NO_X	PM
Euro 1	1992.07	2.72	-	0.97	-	0.14
Euro 2, IDI	1996.01	1.0	-	0.7	-	0.08
Euro 2, DI	1996.01	1.0	-	0.9	-	0.10
Euro 3	2000.01	0.64	-	0.56	0.50	0.05
Euro 4	2005.01	0.50	-	0.30	0.25	0.025
Euro 5	2009.09	0.50	-	0.23	0.18	0.005
Euro 6*	2014.09	0.50	-	0.17	0.08	0.005
*Proposed						

Table 1.1, EU Diesel emission standards for passenger cars (g/km) [3]

Legislation has driven research to satisfy increasingly stringent emission requirements such as improving the combustion process and utilizing advanced aftertreatment systems. Another approach has been to develop and popularise electrically powered vehicles and hybrids, and the use of alternative fuels.

The search for alternative fuels started when the pollution created by the burning of fossil fuels started to cause severe environmental damage [5]. Cars that run on electric power were also considered to be alternative fuel vehicles however, the limited range and recharging difficulties of electrical vehicles posed serious technical issues at that time, and thus greater attention was given to biofuels. Biofuels are expected to play a significant role in reducing overall CO_2 emissions [4]. Also, the possibility of substituting cleaner burning alternative fuels for gasoline and diesel has drawn increasing attention over the past decade. Biofuels produced from sugar cane, corn or other vegetable oils are attracting interest as renewable energy sources that do not increase CO_2 levels. Bioethanol is probably the most well known biofuel used in gasoline engines. Similarly, manufacturers have worked with biodiesel as it is the most common alternative fuel for traditional diesel engines.

Biodiesel is the general name for fatty acid alkyl esters and is the most common alternative fuel for traditional diesel engines, and fatty acid methyl ester (FAME) is more commercially produced due to its economic benefits. Biodiesel represents more than 80 % of the biofuel market share in Europe [1]. Since biodiesel is produced from vegetable oil, it does not contain any sulphur, aromatic hydrocarbons, metals or crude oil residues. The

absence of sulphur means a reduction in the formation of acid rain from sulphate emissions which generate sulphuric acid in the atmosphere.

1.2 Project Aims

The aim of this work was to perform a comprehensive investigation on the use of biodiesel fuel in production diesel engines, and its impact on emissions, performance and fuel consumption.

1.3 Project Objectives

To achieve the aim of this work, the following objectives were defined:

1. To conduct a review of published literature regarding biodiesel, in particular the environmental impact of using fatty acid methyl esters (FAME), variations in their feedstock and commercial production, and finally reviewing their physical and chemical properties and their impact on engine performance and emissions.

2. Undertake experimental vehicle work over a standard legislative drive cycle to assess the variations in performance and emissions when using several biodiesel blends at various ambient temperature conditions.

3. To asses the ability of the engine simulation software Ricardo WAVE, to predict the impact of biodiesel fuel on the combustion process of diesel engines by investigating the sensitivity of the software to changes in important fuel properties.

4. Undertake experimental work on an engine test bed to analyse the differences in combustion and emission characteristics of certain biodiesel blends compared to baseline diesel fuel.

5. To assess the sensitivity of a modern production diesel engine to calibration changes, when using a B25 blend compared to baseline diesel fuel.

6. Investigate the impact of different blends of biodiesel on the performance of a diesel oxidation catalyst, and assess its thermal and chemical effects.

1.4 Summary of Chapters

Chapter 1 Introduction

Contains background to the proposed subject, and states the aim and objectives of this work.

Chapter 2 Literature Review

Reviews recent published literature in the field of FAME physical and chemical properties and their affect on the engine and vehicle components, and their impact on diesel engine emissions and performance.

Chapter 3 Biodiesel Vehicle Trials

Investigates the effect of biodiesel blends on the fuel consumption, engine-out emissions, and tailpipe emissions of a standard diesel vehicle at multiple ambient temperatures, and quantifies the loss in vehicle power.

Chapter 4 Biodiesel Engine Simulation

Investigates the capability of the Ricardo WAVE software package to predict changes in engine performance caused by variations in fuel properties when simulating the use of biodiesel fuel. Properties investigated include the chemical composition, lower heating value, density, specific heat, heat of vaporization, vapour pressure, kinematic viscosity, surface tension, and cetane number.

Chapter 5 Biodiesel Engine Trials

Studies the combustion behaviour, engine out emissions, and performance of B25 and B50 biodiesel blends in a production calibration, Ford Puma 2.0 litre turbocharged diesel engine, equipped with a common rail fuel injection system, and compares the results to the baseline diesel fuel at two different engine loads and speeds.

Chapter 6 Biodiesel Engine Calibration Sensitivity

Assesses the sensitivity of a diesel engine to calibration changes such as EGR rate, rail pressure, and both main and pilot injection timing when the engine is fuelled with B25 biodiesel compared to baseline diesel fuel, by analysing its impact on performance and emissions.

Chapter 7 Biodiesel Oxidation Catalyst Performance

Investigates the effect of hydrocarbon species from RME exhaust on the catalyst light-off temperature of a diesel oxidation catalyst and compares it to baseline diesel fuel. The thermal impact of biodiesel blends on the catalyst performance using an instrumented catalyst is also investigated.

Chapter 8 Conclusions

Concludes the major findings from all previous chapters and makes recommendations for future work.

1.5 Papers Published From This Work

C. D. Bannister, J. G. Hawley, H. M. Ali, C. J. Chuck, P. Price, S. S. Chrysafi, A. Brown, and W. Pickford, 2009. "The impact of biodiesel blend ratio on vehicle performance and emissions", IMechE J. of Automobile Engineering Vol. 224 (3), part D, pp. 405-421

C. D. Bannister, J. G. Hawley, H. M. Ali, C. J. Chuck, P. Price, A. J. Brown, W. Pickford, "Quantifying the Effects of Biodiesel Blend Ratio, at Varying Ambient Temperatures, on Vehicle Performance and Emissions", *SAE Paper*, 2009, No. 2009-01-1893

Currently under review:

C. D. Bannister, H. M. Ali and J. G. Hawley, 2011. "Investigation into the impact of RME biodiesel on Diesel Oxidation Catalyst Performance", IMechE J. of Automobile Engineering, Part D

Chapter 2 Literature Review

2.1 Introduction

Vegetable oils have been the primary candidate as a substitute for diesel fuel since the early 1900s and this interest continued in various parts of the world during the Second World War due to insufficient supply and logistic difficulties of fossil fuel. The arrival of peace and smother flow of inexpensive fossil fuels, made research into diesel alternatives unnecessary. The control of oil production by OPEC and the subsequent rise in fuel prices refreshed the interest in alternative fuels, including vegetable oils as fuel for diesel engines. However, the high viscosity of vegetable oils, which results in poor fuel atomization and fuel injection problems, makes them best used when converted to esters which are commonly known as biodiesel.

In the past ten years more attention has been paid to alternative fuels especially biodiesel due to high inclination of the fossil fuel prices. Biodiesel, and more commonly fatty acid methyl ester (FAME), is becoming one of the faster growing alternative fuels in the global fuel market [5, and 6]. The successful introduction and commercialization of biodiesel in many countries around the world has been accompanied by the development of standards to ensure high product quality and user confidence. Some biodiesel standards are ASTM D6751 and the European standard EN 14214, which was developed from previously existing standards in individual European countries. In the mean time, researchers started investigating the wider aspects of using biodiesel fuel in diesel engines. Significant environmental benefits can be achieved by using biodiesel fuels as well as reduction in dependence on fossil fuel. Since biodiesel is produced from renewable biological sources, it can reduce the use of petroleum based fuels and possibly lower the overall emissions from diesel engines. The reasons for environmental benefits are that biodiesel is an oxygenated, Sulfur free, and a biodegradable fuel. The U.S environmental protection agency (EPA) has surveyed large numbers of biodiesel tailpipe emission results and reported their average as per Table 2.1. The table clearly shows the benefits of using biodiesel on exhaust emissions except for oxides of nitrogen (NO_X) [1]. The lower content of carbon (by weight) in biodiesel is the main contributor for tailpipe carbon

monoxide (CO) emission reduction. Biodiesel contains no aromatics and very small quantities of Sulfur, which will indeed reduce the production of Polycyclic Aromatic Hydrocarbons (PAH), Sulfur dioxide (SO_2), and many other toxic emissions. SO_2 contributes to respiratory illnesses and formation of acid rains. Biodiesel also contains higher concentrations of oxygen which will allow faster and more complete combustion compared to fossil diesel fuel [7]. This simply explains (at least in part) the reduction in unburned hydrocarbons (HC), particulate matter (PM), and CO [4, 8, and 9].

Emission Type	100% Biodiesel	20% Biodiesel
Regulated		
HC	**- 67%**	**- 20%**
CO	**- 48%**	**-12 %**
PM	**- 47%**	**-12 %**
NO_X	**+ 10%**	**+ 2%**
Non-Regulated		
Sulphates	**- 100%**	**- 20%**
Polycyclic Aromatic Hydrocarbons (PAH)	**- 80%**	**- 13%**
Nitrated PAH's (nPAH)	**- 90%**	**- 50%**
Ozone potential of Speciated HC	**- 50%**	**- 10%**

Table 2.1, Average Biodiesel emissions compared to conventional diesel, according to EPA [1]

Biodiesel is a nontoxic and biodegradable fuel; over 90% of biodiesel will degrade within 28 days in soil or water [10], and this biodegradability of biodiesel in natural environment makes it an attractive fuel. Many studies have been conducted to assess the energy balance, and life cycle costs of biodiesel and biodiesel blends compared to fossil diesel fuel [11]. This study compared findings for a comprehensive "cradle to grave" inventory of materials used; energy resources consumed; and air, water and solid waste emissions generated by fossil diesel fuels and biodiesel in order to compare the total "lifecycle" costs and benefits of each of the fuels. The total energy efficiency ratio (i.e. total fuel energy/total energy used in production, manufacture, transportation, and distribution) for fossil diesel fuel and biodiesel are 83.3% and 80.5% respectively. The report notes: "Biodiesel and petroleum diesel have very similar energy efficiencies." The study also compared the lifecycle emissions of many exhaust gases like, carbon dioxide, Carbon monoxide, and Sulfur oxides from biodiesel to fossil diesel fuel. Except for Nitrogen Oxides, all other lifecycle emissions were lower for biodiesel fuels. The major reduction is in the overall lifecycle emissions of carbon dioxide (a major greenhouse gas), which is

78% lower for biodiesel fuels. This reduction is a direct result of carbon recycling in plants [11].

Biodiesel can be used either as neat (100% - B100) or as blends at any proportion like 5, 10, and 20% (B5, B10, B20) by volume in baseline diesel fuel [12]. Blending is the preferred method so far to maximize the benefits of biodiesel and offsetting the cost differential with petroleum diesel [7]. To achieve consistent performance from biodiesel blends it is necessary that the biodiesel and diesel fractions are thoroughly mixed. A common method for blending fuels is very simple and known as the splash method where the biodiesel is added over the baseline diesel while maintaining a little agitation [10]. Currently, European car manufacturers approve up to 7% of biodiesel (B5) in diesel fuel to be used in their vehicles, which meets European fuel standards EN 14214 and EN 590. The guarantees afforded by manufacturers of vehicles, engines and equipment (catalysts, particulate filters, etc.) still remain very limited and prove to be one of the main difficulties in the use of biofuels. Fuels containing higher blends of biodiesel will become more popular in near future because it represents a good balance of cost, emissions, cold flow performance and material compatibility. Several methods have been used to reduce the viscosity of vegetable oil, including dilution, pyrolysis, micro-emulsion, and transesterification. Nowadays, transesterification is the current method which is used efficiently [7].

The aim of this review was to investigate the properties of biodiesel fuels and their impact on the performance and emissions of diesel engines. To achieve this aim, a literature survey of current publications regarding FAME production and the impact of their physical and chemical properties on engine performance was conducted. In addition, a review of the latest published studies on the impact of using biodiesel fuels on the actual performance and emissions of diesel engines is carried out.

2.2 FAME Production

2.2.1 Feedstock

The production of biodiesel is generally derived from plentiful biological sources such as, vegetable oils, animal fats, and recycled oils. During the last 20 years researchers have been carrying out extensive studies in the field of production and characterization of diesel fuel from multiple sources depending on climate and soil, different vegetable oil crops are used in biodiesel producing countries [7]. Predominantly rapeseed and sunflower oil are the main feedstocks in Europe, palm oil in tropical countries and soybean oil and animal fats in North America [10]. Table 2.2 presents main feedstocks currently used in biodiesel production [6-11].

Feedstock	Main Source Area	Notes
Soybean Oil	USA, China, South America	Edible
Rapeseed Oil	EU, China, India	Edible
Palm Oil	Indonesia, Malaysia	Edible
Sunflower Oil	Russian Federation, Ukraine, EU, Argentina	Edible
Cottonseed Oil	China, India, USA	Edible
Peanut Oil	China, India	Edible
Olive Oil	EU, Turkey	Edible
Jatropha Oil	India, Far East	Non-Edible
Algae Oil	USA, Others	Non-Edible
Beef Tallow	USA, Canada, Others	Animal waste
Pork Lard	All	Animal waste
Waste Cooking Oil	All	Non-Edible

Table 2.2, Main biodiesel feedstocks [6-11]

Mainly because of the high price of edible grade vegetable oils, investigations had begun to study the use of cheaper alternative feedstocks for biodiesel production such as used frying oil, animal fat and yellow grease. Beef tallow and pork lard, especially the inedible parts as a result of the meat packing process, are also used in the production of biodiesel. The advantages of animal feedstocks are their lower cost compared to vegetable oils; however an additional processing might be required to produce an acceptable biodiesel [7]. Waste yellow grease which is usually used frying oil has also been considered as a candidate for biodiesel production, and the selection is usually depends on geographic location and the quality of the feedstock.

The use of edible oils and animal fats for biodiesel production has recently been of great concern because they compete with food crops. Therefore, the contribution of non edible oils will be more significant and more justifiable for biodiesel production in the future especially in independent countries. Jatropha and Algae oils are the most mainstream alternatives for biofuel development, as they are easily available in many parts of the world and are very cheap compared to edible oils [10]. In addition, they have very similar characteristics to that of petroleum diesel which recommends them as a strong alternative for the diesel replacement.

2.2.2 Transesterification Process

Biodiesel is produced commercially by a chemical reaction called transesterification [4, 7, and 11] which is a chemical process to lower the viscosity of the vegetable oils by breaking up the triglyceride molecule, and then separate the fatty acid molecules from the glycerine molecule. This process brings the properties of the vegetable oils and animal fats closer to those of diesel fuel, solving the high viscosity problems of vegetable oils. The transesterification process involves mixing the feedstock oil (triacylglycerol) with an alcohol, usually methanol or ethanol, in the presence of a catalyst using a standard agitator or mixer [13, 14]. The reaction mixture is kept just above the boiling point of the alcohol (around 71°C) to speed up the reaction and the reaction takes place. In this reaction, the alcohol breaks up the triglyceride molecules into fatty acid (FA) and glycerine molecules, the FAME formation reaction is shown in Figure 2.1.

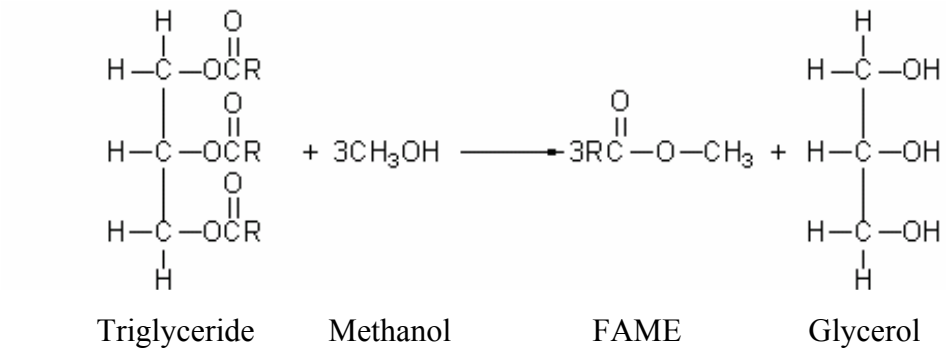

Figure 2.1, Formation of Methyl Ester from Triglycerides, adopted from [10]

Catalysts used in the transesterification process to speed up the reaction can be made from either base or acid metals and the choice depends on quality and cost of the process [10]. The usual reaction time varies from 1 to 8 hours and usually takes place at room temperature. The reaction products are methyl esters (if methanol is used) or ethyl esters (if ethanol is used) which is biodiesel and glycerol (type of sugar) as a by-product [7]. Once separated from the glycerol, the biodiesel is sometimes purified by washing gently with warm water to remove residual catalyst or soaps, dried, and sent to storage. Biodiesel has one-eighth the viscosity of the original vegetable oil. Each ester chain retains two oxygen atoms forming the "ester" and giving the product its unique combustion qualities as an oxygenated vegetable based fuel. The fact that alkyl (both methyl and ethyl) esters have the most similar properties to the petroleum diesel made it the optimum alternative fuel to be used in diesel engines.

2.3 FAME Properties

The fatty acid (FA) is turned into biodiesel mainly to lower its viscosity [15, 16], and the chemical composition of biodiesel is much simpler than fossil diesel fuel since it contains only six or seven different fatty acids, where fossil diesel fuel contains different length of hydrocarbon chains and aromatic compounds. The percentage of the different FA in fats or vegetable oils varies depending on the feedstock, which will have a direct impact on the properties of the fuel. The chemical and physical properties of the various individual FA, as well as the effect of molecular structure (branching of the chain) determine the overall properties of biodiesel fuel [4, 7, and 17]. The average FA composition of the main biodiesel feedstocks that were cited during this work are summarized in Table 2.3. The FA name is followed by number of carbon molecules and number of double bonds. The length of carbon chain and number of double bonds (un-saturation level) in the FAs will vary the physical and molecular properties, which will directly affect the overall performance of biodiesel within an engine and combustion system.

FA Composition	Soybean ME	Rapeseed ME	Palme Oil ME	Sunflower Oil ME	Cottonseed Oil ME	Jatropha Oil ME	Beef Tallow ME
Methyl Laurate C12:0	-	-	1.1	-	-	-	-
Methyl Myristate C14:0	-	-	1.2	-	-	-	3.2
Methyl Palmitate C16:0	10.3	3.7	43.0	6.1	26.3	14.7	26.0
Methyl Palmitoleic C16:1	0.4	-	-			1.0	2.8
Methyl Stearate C18:0	4.3	2.2	4.4	3.3	1.9	7.5	27.0
Methyl Oleate C18:1	23.5	62.8	41.0	19.7	15.8	40.0	38.0
Methyl Linoleate C18:2	53.5	22.3	8.3	70.3	55.5	36.0	1.8
Methyl Linolenate C18:3	7.5	8.5	-	-	-	-	-
Others	0.5	0.5	1.0	0.6	0.5	0.8	1.2

Table 2.3, The percentage FA composition in biodiesel fuel [7-9, 16, 24, 70, 71, 82-87, 93-97, 102]

The saturated fat is a fat that cannot chemically accept additional hydrogen and contains only single carbon-carbon bond. The degree of un-saturation is generally denoted by the iodine number, as the iodine number increases the un-saturation level increases [7]. The average fuel properties of major biodiesel feedstocks that were cited during this entire work are summarized in Table 2.4. These properties are the main factors that influence the combustion performance and emissions of diesel engines. Although, biodiesel has slightly higher density than petroleum diesel, it contains slightly less energy on a volumetric basis. This has been shown to result in a slight loss of engine power [4, 18, and 19]. On the other hand, the fuel consumption of vehicles running with biodiesel is expected to increase in order to compensate for the lower calorific value of biodiesel compared to baseline diesel fuel. It is also very noticeable from Table 2.4 that the flash point temperature of all biodiesel fuels, which is the lowest temperature where enough fluid can evaporate to form a combustible mixture [10], is much higher than baseline diesel fuel. This introduces a challenge when using biodiesel fuels in cold ambient environments.

Property	Diesel (D2)	Soybean ME	Rapeseed ME	Palme Oil ME	Sunflower Oil ME	Cottonseed Oil ME	Jatropha Oil ME	Beef Tallow ME	Waste cooking Oil ME
Cetane Number (CN)	52.8	53.3	53.7	59.6	52.6	52.1	55.6	57.8	53.6
Net Calorific Value (Mj/kg)	42.6	38.4	38.1	39.5	37.1	40.9	39.1	40.3	38.3
Density at 15°C (kg/m^3)	833	884	879	885	886	882	876	875	884
Kinematic Viscosity at 40°C (mm^2/s)	2.8	4.3	4.7	6.7	4.3	5.8	4.6	5.3	5.3
Flash Point (°C)	63	152	155	166	177	180	168	157	144
Oxygen Content (%)	0	10.8	10.6	12.2	10.9	*	11.3	*	11.1
Pour Point (°C)	-18.3	-2.8	-9.5	12.1	*	-4	3	12	-2.5

* Could not be obtained

Table 2.4, Fuel properties of different biodiesel feedstocks [7-9, 16, 24, 70, 71, 82-87, 93-97, 118]

Attempts have been made by various researchers to determine the best composition of biodiesel that would enhance the combustion process, and it was observed that the fuel properties of biodiesel play a significant role in the combustion process [7, 10, and 17]. The individual FAME properties and their effect on diesel engine's performance and emissions are discussed in details in the following sub-sections.

2.3.1 Cetane Number (CN)

CN is one of the main indicators of the ignition quality and combustion smoothness in diesel engines. It is a dimensionless descriptor for the ignition delay time of a fuel upon injection into the combustion chamber. The higher the CN, the shorter the ignition delay time and vice versa. It is an acceptable fact that the CN of biodiesel is generally higher than fossil diesel fuel due to the absence of aromatic compounds [20]. The European standard for biodiesel (EN 14214:2003) specifies the minimum requirements for CN to be 51, since too low CN might cause very rapid and incomplete combustion. Like other properties, CN number is affected by the molecular structure of the source material FA. The CN of biodiesel depends on the distribution of fatty acids in the original oil or fat from which it was produced. The longer the straight chain FA and the more saturated the molecules in the fuel, the higher the CN [7, 10, and 20].

A wide range review conducted by Gopinath et al. [21] on the influence of fatty acid structure and composition on cetane number, the author concluded that vast majority of studies acknowledged the fact that the CN increases with increase in the chain length and decreases with increase in the number of double bonds as presented in Figure 2.2.

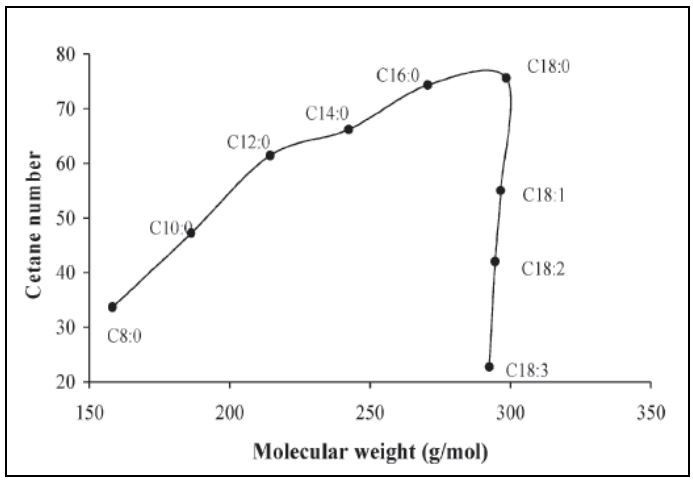

Figure 2.2, Cetane Number Trend Lines for Methyl Esters [21]

In a more specified study, Knothe et al. [22] studied the CNs of branched esters and compared them to those of straight chain esters, and the study conclusion was that the branching effect was not significant compared to the impact of the chain length and number of double bonds.

Higher CNs of the fuel was also correlated with reduced NO_X exhaust emissions for conventional diesel fuel as stated by Knothe [22], however this is not always true for all types of engine technologies, as modern engines that are equipped with more sophisticated injection systems that control the rate of injection are less sensitive to CN variations [20, 22]. This issue will be discussed in more details in the section related to FAME exhaust emissions. In addition to CN, several other properties of biodiesel are important for determining its suitability as an alternative to petroleum diesel fuel.

2.3.2 Heat of Combustion

The heat of combustion measures the energy released when a known quantity of a fuel is burned with oxygen under specific conditions; it is also referred to as the calorific value or heating value. The energy content in biodiesel molecules is about 10% lower than fossil diesel, as seen in Table 2.4, mainly due to the absence of aromatic hydrocarbons [15]. The petroleum diesel fuel contains 25-35% aromatics, which have greater energy per litre of fuel if compared to FAs. Therefore, it is generally known that biodiesel fuels have lower heat release values than petroleum diesel. The FA chain length is the most influential chemical property on biodiesel's calorific value, as reported by few authors that as the FA chain length increases the heat of combustion value increases [10, 20, and 23]. Fuel density and number of double bonds also have an effect on the fuel's calorific value but not significantly. A review conducted by Sinha et al. [23] concluded that the FAMEs have slightly higher combustion efficiency than baseline diesel fuel due to the structural oxygen content of the biodiesel which improves the combustion process, and similar observations were reported by Lapuerta et al. [4].

2.3.3 Density and Kinematic Viscosity

Both density and kinematic viscosity are very important properties of biodiesel since they affect the operation of fuel injection equipment, and consequently the combustion process. The density of biodiesel is always greater than petroleum diesel, as shown in Table 2.4, and density falls slightly as the chain length and saturation level increases [10, 24]. Similarly, biodiesel fuel has higher kinematic viscosity value than petroleum diesel, and it is directly proportion to the FA chain length and saturation levels [10, 15, and 24]. High viscosity leads to poorer atomization of the fuel spray of the fuel injectors as reported by many authors [19-26], and most of them agreed on the fact that biodiesel demonstrated poorer performance in low operation temperatures compared to fossil diesel because its viscosity and density increases more rapidly as temperature drops.

2.3.4 Cold Flow

In addition to biodiesel's viscosity as a measure of cold flow property, cloud point (CP) and pour point (PP) are more specified cold flow indication properties. The CP is the temperature at which wax first becomes visible when the fuel is cooled, and the PP is the lowest temperature at which the fuel can flow [7]. In addition to CP and PP, another property is also used in Europe for measuring the cold flow properties in biodiesel which is the cold filter plugging point (CFPP) [10]. It basically measures the highest temperature at which the fuel crystals fail to pass through a standard filter under standard conditions. One of the major drawbacks associated with the use of biodiesel is the poor low temperature performance due to their higher solidification temperatures, and engines fuelled with biodiesel may experience more fuel system plugging difficulties especially in cold weather conditions compared to baseline diesel fuel [25, 26]. Table 2.4 clearly shows the higher PP temperatures of biodiesel fuels compared to baseline diesel fuel, and this temperature varies significantly with different FAME feedstock.

In general, the crystallisation temperature for biodiesel increases as carbon chain length and saturation levels of the FA increases with saturation level being more influential factor [10, 20]. The saturated fatty compounds have significantly higher melting points than the un-saturated compounds which increases the crystallisation temperature of the fuel as reported by Knothe [20], and the relationship between some of the above mentioned fuel properties and fuel composition is summarized in Table 2.5.

	Saturated	Monounsaturated	Polyunsaturated
Fatty acid	12:0, 14:0, 16:0, 18:0, 20:0, 22:0	16:1, 18:1, 20:1, 22:1	18:2, 18:3
Cetane Number	High	Medium	Low
Cloud Point	High	Medium	Low
Stability	High	Medium	Low

Table 2.5, Fuel properties as a function of fuel composition [18]

The draw backs of biodiesel cold flow properties are usually minimized by using additive products to lower the CP temperatures [10]. Fuel winterisation is also used to improve the

cold flow properties of biodiesel fuel by reducing the total concentrations of saturated components [10, 20]. This method removes by filtration the solids formed during cooling of the FAMEs, leaving a mixture with higher content of unsaturated FA and thus with lower CP and PP. Complete reduction of saturated components is not recommended because it might affect the ignition quality of the biodiesel fuel [20].

2.3.5 Oxidation Stability

The oxidation stability is measured by its resistance to oxidation that may occur during storage, production, and use. The oxidation process is mostly influenced by the contact with oxygen in air and by other factors, such as elevated temperature, light exposure, and the presence of contaminants [20, 28, 29, 35]. Biodiesel is reported to be more susceptible to oxidation compared to fossil diesel due to its chemical nature [27], like all other vegetable oils, biodiesel has poor oxidation stability under both hot and cold temperatures compared to petroleum diesel, so understanding the factors affecting its degradation is very crucial. Oxidative stability is the major parameter for biodiesel in order to become a reliable automobile fuel and is a key characteristic in determining whether biodiesel is suitable for use as a replacement fuel in diesel engines [29].

FAMEs resistance to oxidation, polymerization, water absorption, and microbial activity are worse than fossil diesel due to the presence of unsaturated molecules, as reported by few authors [7, 20, 27, and 29-31]. The high degree of unsaturation is the most important factor that influences the stability of FAME, as it appears in Table 2.5, because double bonds are more susceptible to the attack from oxygen in air and to form mixtures of various products from polymers to short chain compounds [28, 35, and 36]. Further investigations in correlating oxidation stability to the total number of double bonds indicated that the position of the double bonds within the FA structure could also affect the oxidation stability of biodiesel fuel [28, 35, and 37].

Fuel oxidation could affect the physical and chemical properties, and also produce viscous collides and other impurities which have a tendency to polymerize and form species with higher molecular weights and increase the fuel viscosity [10, 29, 30, and 38-40].

Consequently, oxidized fuel could lead to microbial growths in fuel storage tank and sludge up fuel injection equipment, as reported by Ogawa et al. [40], and different combustion performance and emission characteristics than fresh biodiesel [32, 44]. In addition, corrosive products could also be produced during the oxidation process which makes biodiesel more reactive with other vehicle components such as engine lubricant, rubbers, plastics and even metallic components [31, 41-43]. The affect of biodiesel on engine components will be further discussed in the next section.

Depending on the storage conditions, biodiesel can be stored for a period of one year under normal storage conditions without significant change in quality parameters, and the long term storage could cause predominant oxidation instability [7]. Acceptable oxidative stability could be reached by appropriate addition of antioxidants with all different types of FAME fuels and their blends was extensively reviewed by Paligova et al. [32]. Similarly, Lin et al. [29] reported a significant retardation in the fuel property deterioration process with the addition of antioxidants to the Palm oil based biodiesel fuel.

2.4 FAME Performance in Diesel Engines

2.4.1 Compatibility

Material and equipment compatibility is always a concern for researchers whenever they plan for a fuel composition change. The difference in fuels physical and chemical properties will have a different effect on the engine and vehicle components, such as fuel system and engine's lubrication and after treatment systems. Biodiesel and biodiesel blends have shown that they might affect certain physical properties of some elastic materials used in hoses, gaskets and seal materials, as reported by Lamprecht [45]. The compatibility of seal and hose materials commonly used in automotive fuel systems using conventional diesel fuel has long been established however it is still undergoing research with biodiesel fuels [46].

The compatibility issue is only valid with certain polymers and rubbers found in hoses and gaskets that typically form part of the fuel system found in older vehicles and are not

found in many vehicles in use today according to national biodiesel board [47]. A study performed by Nakai et al. [48] evaluated the influence of biodiesel fuels on the automotive fuel-line rubber and plastic materials concluded that both B20 and B100 fuel blends did have an effect on the hose and liner materials, and only deterioration was observed when water and acid was added to the fuel to simulate oxidation of biodiesel. Similar observations were recorded in a technical report prepared by Terry et al. [49] when the authors examined the physical properties of five candidate elastomers commonly used in automotive fuel systems before and after immersion in the six test fuel blends under controlled conditions. The authors concluded their study by stating that all candidate materials tested exhibited good resistance to changes in physical properties of the test fuels at concentrations up to 20%. However, in a joint report issued in 2009, the fuel injection equipment (FIE) manufacturers stated that more extensive revisions will be required to facilitate biodiesel blends higher than 7% in order to reduce the risk of premature failure of the fuel system [50]. The effect of FAME on the lubrication and after treatment systems will be further explained in the following section.

2.4.2 Lubrication and Wear

Lubricity properties of fuel are very critical for reducing friction wear in engine components which are normally lubricated by the fuel rather than crankcase oil. Mechanical wear and fuel leaks can cause many problems in the engine fuelling system, as fuel pumps and injectors depend on the fuel for lubrication of moving parts. It has been known that biodiesel improves the lubricity of the diesel fuel, and it is a common practice among most of the diesel fuel producers to add 1-5% of biodiesel in the ultra low Sulfur diesel (ULSD) fuel to improve its lubrication quality [19, 51].

However, other concerns of using biodiesel are raised due to its effect on engine oil dilution, if an engine has a tendency to get unburned fuel into the crankcase, the situation will be more troublesome with biodiesel than with baseline diesel [52-56]. Different physical properties of FAMEs such as higher volatility, higher surface tension and higher specific gravity could lead to a larger fuel droplet size and thus more impingements on the cylinder wall from where it can be scraped into the crankcase oil by piston rings [57]. A

study by Fang et al. [58] reported that engine oil contaminations with biodiesel reduces the performance of lubricating oil because biodiesel fuels have higher flash points and hence will remain in the crankcase for longer periods of time than baseline diesel, which will also lead to a reduction in engine oil viscosity or sludge development caused by oxidation. Lower evaporation rates with biodiesel compared to ULSD was experimentally proven by Andreae et al. [52] leading to higher dilution rates over time.

On the other hand, few authors investigated the impact of biodiesel fuel on engine wear compared to baseline diesel, and no indication of excessive wear was observed when engine was fuelled with biodiesel fuel blends up to B20 [31, 34, and 59-61]. As a matter of fact, majority of the authors reported a reduction in wear rate with biodiesel and concluded their work by stating that the reduction in engine wear is a result of better lubricity properties of biodiesel fuel.

2.4.3 Fuel Injection System

The physical properties of fuel that have the most influential effect on the performance of injection systems are density, kinematic viscosity, and surface tension, as discussed previously, biodiesel fuels have higher density and kinematic viscosity than petroleum diesel, see Table 2.4. Also, the surface tensions of biodiesel fuels are slightly higher than baseline diesel fuel due to their difference in molecular structure [57, 62]. Higher fuel viscosity leads to poorer atomization of the fuel spray and higher surface tension values will produce larger average droplet size, therefore slower droplet vaporization and possibly a reduction in air and fuel mixing [7].

Several authors reported that the higher density values of biodiesel lead to its higher speed of sound and bulk modulus of compressibility, which will directly affect the injection timing settings particularly in case of pump-line-nozzle injection systems [4, 8, 24, 63-67]. The authors explained that higher bulk modulus of compressibility results in more rapid transferral of the pressure wave from the fuel pump to the injector needle and earlier injection in case of biodiesel fuels.

However, in case of engines equipped with an electronically controlled common rail fuel injector, several review studies reported no alteration to actual injection timings [4, 63, 64, 66, and 68]. Most of the studies indicated that no influence by differing biodiesel fuel properties on the injector needle response was observed when common rail fuel system is used due to the fact that in these systems the pump controls rail pressure for each individual injector rather than unit injectors pressurizing the fuel.

2.4.4 Exhaust After-Treatment System

The advancements in diesel engine technology have lead to an increase in light duty diesel powered vehicle popularity in Europe and the United States. The stringent emission standards for this vehicle class have lead to the necessity of emissions control systems on these vehicles, selective catalytic reduction (SCR) with urea and NO_X adsorber catalyst (NAC) are the leading technologies for meeting the new emission standards for the light duty diesel vehicles [2]. Extensive research has been conducted over the past years focusing on the performance and durability of these technologies in conjunction with conventional diesel fuels, however little research has been performed with the biodiesel fuels.

Most of the studies mainly concentrated on the impact of biodiesel fuel on diesel particulate filters (DPF) and to some extent on NO_X reduction systems. An investigation by Tatur et al. [69] reported faster soot regeneration rate in the DPF with B20 fuel blend compared to base diesel fuel. Few other studies also reported quicker soot oxidation process in the DPF with biodiesel fuel compared to baseline diesel fuel due to its lower balance point temperature (BPT), which indicates that the DPF inlet temperature at which the rate of particle oxidation approximately equals the rate of particle collection is much lower with biodiesel fuel blends [56, 60, 71-73]. The authors justified this improvement in DPF performance by changes in PM morphology and the addition of oxygen to the PM surface with biodiesel increased oxidation reactivity of the soot particles, yielding enhanced rate of soot oxidation. On the other hand, contradictory results were reported on the impact of biodiesel fuel on the performance of NO_X absorber catalyst (NAC) [69, and

70]. An improvement in the SCR system performance with biodiesel fuel was reported by Tatur et al. [60], due to lower exhaust temperature upstream of the NAC with biodiesel which is more favourable for NO_X adsorption efficiency compared to baseline diesel fuel, as the authors explained. On the other hand, Kawano et al. [70] reported a malfunction of NO_X storage reduction (NSR) catalyst when RME biodiesel was introduced to the engine due to the reduction in fuel rich spikes caused by higher distillation temperatures of biodiesel.

Despite an extensive search of published literature by the author, no investigations into the impact of biodiesel fuel on the performance of diesel oxidation catalysts (DOC) could be found.

2.4.5 Engine out Emissions

2.4.5.1 Particulate Matter (PM) and Smoke

The dry portion of PM is carbon (soot) and the liquid portion is a combination of unburned diesel fuel and lubricating oil, called soluble organic fractions (SOFs), which is adsorbed within the dry carbon particles [2]. PM emissions have been the most considerable concerns with the manufacturers of diesel engines, as it is very visible and often contains some carcinogenic aromatic hydrocarbons [1]. According to an EPA technical report issued in 2002 [1], the PM emissions of B100 and B20 are less than petroleum diesel by 47%, and 12% respectively (see Table 2.1). Biodiesel contains higher values of oxygen which will allow faster and more complete combustion compared to fossil diesel fuel [7, and 74], which explains (at least in part) the reduction in particulate matter (PM) emissions from biodiesel [4, 8]. The detailed process of the chemical mechanism involved in PM and soot reduction with FAMEs are still not very clear, but Pepiot et al. [75] speculated that the effect of the oxygen moieties contained in the molecules, and the dilution effect which forms various structural groups replaces highly sooting components of the baseline diesel fuel with cleaner HCs is the main factor in reducing sooting tendency.

The effect of biodiesel chemical composition on smoke opacity and PM emissions were investigated by few authors, as reported by Lapuerta et al. [4], their results did not show a solid correlation either with the chain length or with the unsaturation level. On the other hand, Schonborn et al. [17] reported an increase in PM with increasing number of double bonds in the FA and no significant impact FA chain length was observed.

2.4.5.2 Nitrogen Oxides (NO_X)

(Nitric oxide (NO) and nitrogen dioxide (NO_2), and are formed during the combustion of fuel at extremely high temperatures). The NO_X formation is also influenced by the oxygen concentration in the fuel, combustion duration, and the mixture richness in the combustion chamber [2]. Majority of cited literature in this work reported an increase in the NO_X emissions when using biodiesel fuels and the percentage increase is directly dependant on the physical and chemical properties of biodiesel. A few authors speculated that biodiesel fuel properties causes advancement in the start of fuel injection in the case of engines equipped with pump-line-nozzle injection system [4, 7, 10, 24, and 64] as explained in section 2.4.3. The advancement in injection timing resulted in a longer combustion period where temperatures are conducive to NO_X formation [76].

On the other hand, it was experimentally proven by Zhang et al. [64] and others [77, 78] that using biodiesel does not affect the start of injection if the engine is equipped with common rail fuel injection system. The higher adiabatic flame temperature caused by lower heat dissipation by soot due to its lower concentrations with biodiesel caused the increased in NO_X emissions in vehicles equipped with common rail injection systems [4, 24, and 64]. Similarly, an investigation by Cheng et al. [79] on the impact of biodiesel fuel on NO_X emissions concluded that the reduced soot radiative heat transfer with biodiesel could have played a significant role in increasing NO_X emissions.

The formation of NO_X emissions is also effected by fuel properties, such as cetane number, aromatics content and iodine number, Lapuerta et al. [24] reported that the use of

biodiesel fuels leads to a slight increase in NO_X emissions, especially in the case of highly un-saturated biodiesel fuels, see Figure 2.3.

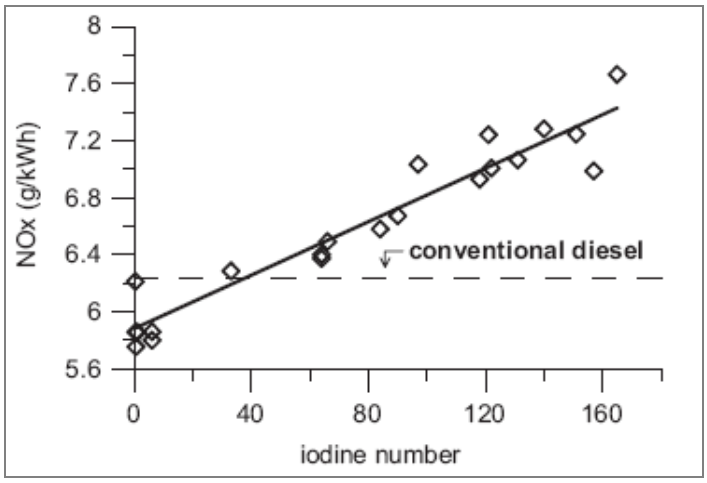

Figure 2.3, Effect of Iodine Number on NO_X Emissions [24]

Figure 2.3 clearly shows that as the iodine number of the fuel increases the NO_X emissions increases. Regarding the effect of molecular structure, few studies concluded that shorter chain length esters produce higher NO_X emissions [4, 10, 79, and 80], but the saturation level impact is more pronounced [79, 80]. In a unique explicit study, Schonborn et al. [17] investigated the influence of the FA chain length, number of double bonds on the combustion process and NO_X formation using several individual FA and the ability of fixing the injection timing, ignition timing, and ignition delay. The authors experimentally approved that longer chain FAMEs produce less NO_X compared to the shorter chain length mainly due to shorter ignition delay, which shifted the combustion towards diffusion control and reflected in a smoother heat release pattern of the fuel. Similarly, the NO_X emissions increased with increasing number of double bonds due to longer ignition delay periods associated with the un-saturated FAs. The effect of chain length and saturation level of FAs on the density and CN are the main contributors in altering the NOx emissions as reported by Knothe et al. [81]. However, McCormick et al. [82] reported that the saturation degree of biodiesel had a small effect on NO_X emissions in a common rail injection system, which indicates that the exact molecular structure affects of biodiesel fuels on the NO_X emissions are still open for speculations.

2.4.5.3 Hydrocarbons (HC)

It is the unburnt hydrocarbons (UBHC) leave the combustion chamber at the end of power stroke, and usually originate in the combustion zones were the mixture is not burnt completely [2]. The use of biodiesel reduces the amount of HC emissions, according to EPA report issued in 2002 [1] the HC emissions from B100 and B20 are less than petroleum diesel by 67%, and 20% respectively (see Table 2.1) and it reduces as the percentage of biodiesel increases in the fuel. This reduction in HC emissions is explained (at least in part) by the presence of oxygen in the fuel since it allows faster and more complete combustion compared to fossil diesel fuel [7]. The amount of UBHC increases with longer ignition delays that often lead to the formation of overly lean fuel and air mixtures which fails to undergo complete combustion [2]. Few authors investigated correlations between the FA molecular structures and HC emissions, but contradictory results were reported [4, 7, and 17].

2.4.5.4 Carbon Monoxide (CO)

CO emission concentrations increase as the combustible mixture becomes richer, as there will be incomplete combustion of the fuel, and diesel engines always produce negligible emissions of CO, since the air/fuel ratio is always lean [2]. Similar to HC, CO emissions can be easily oxidized in the diesel oxidation catalyst. According to EPA report issued in 2002 [1], the use of biodiesel further reduces the amount of CO emissions from diesel engines. A reduction of 48% and 12% with B100 and B20 respectively is reported (see Table 2.1), and it reduces as the percentage of biodiesel increases in the fuel. Similar to the UBHC, the amount of CO emissions increases with longer ignition delays that often lead to the formation of overly lean fuel and air mixtures which fails to undergo complete combustion [2], and no solid correlation between the FA molecular structures and CO emissions could be found in the literature as per author's knowledge.

2.5 Review of Vehicle Experiments with Biodiesel

In this section, recent published papers on vehicle trials with biodiesel are reviewed. Several studies are summarized regarding biodiesel's effect on engine performance and emissions. Vehicle trials on chassis dynamometer are the standard tool for legislatively prescribed emission tests, but vehicle testing with biodiesel had a small share in the research studies mostly for legislative and certification purposes. In this review, more attention will be paid to light-medium duty vehicle trials equipped with direct injection (DI) common rail fuel systems, although there are only a few papers published in the literature. In the mean time, papers on heavy duty vehicle testing will also be cited to provide an additional background to the review, and the review will be subdivided into sections according to each emission, a list of all cited publications on vehicle trials is presented in Table 2.6.

Vehicle Specifications	Experimental Method	Fuels	Reference & Publication Year
Mercedes C220, 2.2 CDI, Euro 3 calibration	On Road	B100 JME	[16] - 2005
International Truck, Cummins 250 HP	On Road	B100	[83] - 2004
Multiple, Medium - high duty	On Road	B20	[84] - 2004
Mitsubishi L-200, 2.4 DI Common Rail, Euro 4 calibration	NEDC, Chassis Dynamometer	B30 – B80 SME, PME, UFOME	[85] - 2010
Toyota Corolla, 2.0 IDI, Euro 2 calibration	Chassis Dynamometer	B5 – B20 SME	[86] - 2007
Audi, 1.9 TDI Common Rail	Chassis Dynamometer	B30 SME	[87] - 2003
1.4 DI Common Rail, Euro 4 calibration	Chassis Dynamometer	B5 – B30 RME	[92] - 2008
Toyota Avensis, 2.2 DI Common Rail, Euro 4 calibration	NEDC, Chassis Dynamometer	B30 RME	[88] - 2008
Renault Laguna, 1.9 DI Common Rail, Euro 3 calibration	Chassis Dynamometer	B10 Cottonseed Oil	[89] - 2007
2.0 DI, Euro 3 calibration	Chassis Dynamometer	B2 – B20 UFOME	[90] - 2007
Seat Altea, 2.0 TDI Common Rail, Euro 4 calibration	Chassis Dynamometer	B5 – B50 UFOME	[91] - 2007

Table 2.6, List of vehicle specifications cited

2.5.1 Particulate Matter (PM) and Smoke Opacity

A huge reduction in PM emissions (about 33%) was reported by Sanjeev et al. [16] when neat biodiesel (B100) from Jatropha methyl ester (JME) was used compared to baseline

diesel fuel. Similarly, Camden Council in Australia [83] reported a reduction of 91% in PM and 79% in smoke opacity emissions with B100 fuel compared to petroleum diesel, and Newcastle city council in Australia [84] also reported a 30% reduction in smoke and 39% in PM emissions. Karavalakis et al. [86] also reported a reduction of 18% and 24% in PM emissions with B5 and B20 from soybean oil methyl ester respectively compared to baseline diesel. Oak Ridge National Laboratory in the U.S reported 15-25% lower PM emissions with B30 than base line diesel fuel [87], which is generally attributed to the higher oxygen content of biodiesel fuels, as the authors explained. Bielaczyc et al [92] also reported a reduction in PM emissions by 5%, 10% and 21% with B5, B10 and B30 respectively; similarly, Yoshida et al. [88] reported a 16% reduction in PM emissions with B30 RME biodiesel.

On the other hand, Georgios et al. [89] did not observe any difference in PM emission from B10 cottonseed oil (CSO) compared to the baseline diesel fuel, and large reductions in PM emissions were achieved by Karavalakis et al. [85] with biodiesel blends up to B50, and this trend reversed with higher biodiesel concentrations. Arapaki et al. [90] used different blend ratios (B2, B5, B10, and B20) of used frying oil methyl esters (UFOME) in their study, the authors reported an unexpected increase of PM as the percentage of biodiesel increases in the fuel. The authors suspected that the highly saturated (low iodine number) and lower aromatic content of (UFOME) might be the reason for this result. When tested the same fuel on a different vehicle, Tzirakis et al. [91] reported that no significant differences in smoke opacity for the B5 and B20 blends compared to diesel fuel were observed; however with B50 a reduction 27% in smoke opacity was achieved which puts their previous findings under suspicious.

The average reduction in PM emission from Table 2.6 is about 24% for B20 fuel blends and about 58% for neat biodiesel. This result agrees with the general published literature, the reduction in PM emissions is more effective with lower concentrations of biodiesel in the fuel [4]. The majority of the authors emphasized that this reduction in PM is due to the higher values of oxygen availability in biodiesel which will allows faster and more complete combustion compared to fossil diesel fuel [7], several other reasons were proposed to explain the reductions of PM emissions with biodiesel, the absence of

aromatics and Sulfur in biodiesel fuel as well as the combustion advancement especially in pump-line-nozzle fuel injection systems [4, 7].

2.5.2 Nitrogen Oxides (NO_X)

Bielaczyc et al [92] reported an increase in NO_X emissions by 6% and 9% for B5 and B30 respectively compared to baseline diesel fuel over NEDC drive cycle, the authors attributed the results to higher oxygen concentrations and higher local combustion temperatures. A slight increase in NO_X emissions but not very significant was reported by McGill et al. [87] with the addition of SME biodiesel to the base fuel, which was also justified by the higher oxygen content of biodiesel fuels. Both authors speculated multiple causes for the increase in NO_X emissions with biodiesel, high oxygen content and higher density value of biodiesel, and the impact of physical and chemical properties of biodiesel on start of injection timing. Karavalakis et al. [85] also reported an increase in NO_X emissions with biodiesel blends over all driving conditions, and the authors also concluded that a strong correlation was found with both the degree of un-saturation and driving cycle, on the NO_X emissions. Further investigations into the affect of different biodiesel feed stocks on NO_X emissions were reported in section 2.4.5.2.

No significant change in NO_X emissions was reported by Yoshida et al. [88] when their vehicle was fuelled with B30 RME biodiesel and Georgios et al. [89] reported the same observations, and both authors reported that NO_X emissions were very close to the baseline values and below Euro 3 emission limits. Sanjeev et al. [16] also did not observe any increase in NO_X emissions with fresh B100 from Jatropha methyl Ester during normal load operating conditions. However, the maximum difference of NO_X emissions was only reported at full load due to higher combustion temperatures, the authors also investigated the impact of fuel aging on emissions and reported a slight increase in NO_X compared to fresh biodiesel.

In contrast to the most published literatures, Tzirakis et al. [91] reported a reduction trend in NO_X emissions as the percentage of biodiesel increased in the fuel with respect to diesel fuel, except in accelerating uphill conditions. The reductions ranged from 5.5% to 25%

with B5 to B50 fuel blends, and same authors reported similar observations using a different vehicle [90]. The authors justified this reduction in NO_X emissions by a reduction in the adiabatic flame temperature of combustion, and the use of highly saturated (low iodine number) methyl esters. This proposal, is however, disputed by a number of other studies [4, 24, and 64].

The majority of the published literature on vehicle trials in Table 2.6 reported a slight increase in NO_X emissions when biodiesel fuel was used as neat or blended with baseline diesel fuel. The average increase in NO_X emissions were in the range of 5% with low concentrations of biodiesel and reaches up to 10% with B100. Higher oxygen content and higher density of biodiesel were reported as the main factors for having higher NO_X emissions with biodiesel. Few authors speculated the alteration in the combustion process as a consequence effect of biodiesel's different chemical properties also a cause of higher NO_X emissions.

2.5.3 Hydrocarbons (HC)

A 25% reduction in HC emissions is reported by Sanjeev et al. [16] with B100, and similarly Arapaki et al. [90] achieved 55% reduction in HC with B20 UFOME. Yoshida et al. [88] also reported a 30% reduction in HC emissions with B30 RME biodiesel, and Karavalakis et al. [86] reported only 6% reduction in HC emissions with B20 SME.

On the other hand, no trend towards higher or lower HC emission levels was observed by Georgios et al. [89] when their vehicle was fuelled with biodiesel fuel. Karavalakis et al. [85] also reported a reduction in HC emissions with the addition of biodiesel, however the authors observed a trend towards higher emission levels over NEDC and speculated that the lower volatility of biodiesel blends and the cold start effect of the legislated NEDC were the main factors. Similarly, the reduction in HC emission was reported by Bielaczyc et al [92], but they also observed that the reduction in HC emissions started to reduce with higher blends of biodiesel and during the initial parts of NEDC.

The HC emission from diesel engines has not been an issue since the use of diesel oxidation catalysts, and the majority of authors show a reduction trend in HC emissions with the use of biodiesel fuel in their vehicles. The main factors reported by the authors were the oxygen content and higher CN of biodiesel compared to petroleum diesel. Higher oxygen content leads to more complete combustion and less unburnt HCs, and higher CN will also reduce the ignition delay which leads to less lean mixture zones [2].

2.5.4 Carbon monoxide (CO)

Karavalakis et al. [86] reported a 10% reduction in CO emissions with B20 SME compared to baseline diesel fuel. A higher reduction in CO emissions was reported by Arapaki et al [89] of 42% with B20 of UFOME, the authors also reported a reduction of 17% and 41% for B20 and B50 fuels respectively with a different vehicle [91]. Similarly Yoshida et al. [88] reported a reduction of 21% when their vehicle was fuelled with B30 RME biodiesel over NEDC drive cycle.

In contrast, Sanjeev et al. [16] reported unexpected increase in CO emissions, they observed a 50% increase in CO emissions with B100 from Jatropha methyl ester compared to fossil diesel. Similarly, Georgios et al. [89] tested B10 cottonseed oil and reported close values of CO emissions to the baseline values. Karavalakis et al. [85] also reported a reduction in CO emissions with the addition of biodiesel, however the authors observed a trend towards higher emission levels over NEDC and suspected lower catalyst efficiency during the cold start of the legislated NEDC. Bielaczyc et al [92] reported a reduction in CO emissions by 15% for B5, no changed for B20 and increased by 6% for B30. The authors concluded that not only the presence of oxygen but also other physical and chemical parameters of biodiesel fuels are of significant importance.

The percentage reduction in CO emissions depends on several factors, engine technology, engine load and speed, biodiesel type [4], and the additional oxygen content in biodiesel fuel is often used to explain the reason for lower CO emissions by most of the authors. The availability of extra oxygen enhances a complete combustion for the fuel, which reduces CO emissions [4, and 7].

2.5.5 Power and Fuel Consumption

Arapaki et al. [91] reported an increase in FC by 2%, 6%, and 9.5% for blends B5, B20, and B50 respectively, and also Yoshida et al. [88] reported an increase in FC by 3% with B30 RME biodiesel. The Camden Council [83] reported a reduction in the maximum power of the engine by about 17%, and an increase in FC by 2.4% with B100 due to the lower calorific value of methyl esters, and Karavalakis et al. [86] reported a maximum increase of 6.5% in FC when B20 was used compared to baseline diesel.

2.6 Review of Engine Experiments with Biodiesel

Engine testing is usually performed in laboratories over engine test stand (bench). This arrangement allows the engine to be operated in different operating regimes and offers measurement of several physical variables associated with the engine operation. Engine testing facilities are commonly used in engine development and catalyst performance research laboratories to achieve further emission reductions.

Engine Specification	Experimental Method	Fuels	Reference & Publication Year
Yanmar, Single Cylinder 0.5 DI	Steady State	B20 – B50 Palm Oil ME	[93] - 2007
Hino, 4 Cylinder 4.0 TDI with Common Rail, DOC + DPNR	JE05 Transient and Steady State	B5 – B100 RME	[94] - 2008
John Deere, 4 Cylinder 4.5 TDI with Common Rail	Steady State	B20, B100	[95] - 2008
Toyota, , 4 Cylinder 2.2 DI with Common Rail	Steady State	B30 RME	[88] - 2008
4 Cylinder 2.5 DI	Steady State	B10 – B100 RBOME	[23] - 2007
Cummins, 6 Cylinder 5.9 TDI	Steady State	B20, B100	[8] - 2006
VW, 4 Cylinder 2.5 TDI with Common Rail	Steady State	B20, B40	[64] - 2007
Mercedes, 4 Cylinder 2.2 CDI	Steady State	B100 JME	[16] - 2005
PSA, 4 Cylinder 2.2 TDI with Common Rail	NEDC, Other	B10 Cottonseed Oil	[89] - 2007
4 Cylinder 1.4 TDI with Common Rail, DOC	NEDC	B20 RME	[92] - 2008

Table 2.7, List of cited engine specifications

The current section summarizes few published studies on the impact of biodiesel fuel blends on the performance and emission of diesel engines. Table 2.7 lists engine specifications and few experimental details of the cited works.

2.6.1 Engine out Emissions

A reduction in smoke by 37% and 60% was reported by Lin. et al. [93] as well as an increase in NO_X emissions by 1.5% and 2.5% at 2400 rpm engine speed with B20 and B50 biodiesel blends respectively compared to petroleum diesel. The authors also reported a decrease in THC emissions by 15% and 22% with B20 and B50 respectively at 1200 rpm, and they stated that the combustion process was benefited by higher oxygen content, short carbon chain lengths, and numerous saturated carbon bonds as a result, smoke and THC emissions were significantly reduced.

The use of B5 and B20 blends reduced the PM emissions slightly relative to baseline diesel fuel, but with B80 and B100 was reversed as Kawano et al. [94] reported. The authors speculated that mixing oxygenated fuels in low concentrations is more effective in reducing PM emissions than high concentrations due low volatility of biodiesel. The engine out CO and HC emissions reduced and NO_X emission increased linearly with increasing percentage of biodiesel in the fuel.

Karra et al. [95] reported lower soot, HC, and CO emissions with B100 fuel, and increase in NO_X emissions with an increase in biodiesel concentration in the fuel. The change in NO_X emission was very little between baseline diesel and B20 fuels and considered to be statistically insignificant. The authors experimentally approved that both higher EGR levels and double injection strategies could reduce the soot and NO_X emissions of B100 fuel significantly, and the authors concluded that the increase in injection pressure resulted in an increase in NO_X emissions due to the fact that higher injection pressure creates better atomization and vaporization, which results in higher combustion temperature.

Similarly Yoshida et al. [88] reported no significant change in NO_X emissions with B30 compared to baseline diesel fuel, but the use of biodiesel fuel reduced HC, CO, and PM emissions. Also, no significant difference was found in fuel injection rates and spray penetration between both B30 blend and diesel fuels due to the benefits of common rail injection system, as the authors explained. In the mean time, the B30 fuel blend showed a tendency of slightly stronger penetration and longer injection duration under the main injection conditions which was speculated by the poor vaporization characteristics of biodiesel, but it was not great enough to have a negative impact on tailpipe emissions.

2.6.2 Combustion and Heat release

The combustion behaviour of Rice-bran oil methyl ester blends under different engine loads and speeds was investigated by Sinha et al. [23]. All tests were carried out under steady state engine conditions, and results were averaged in order to eliminate the effect of cycle to cycle variations. The main conclusions of this experimental study are summarized in the following points:

- The peak cylinder pressure is higher with biodiesel blends at no load but reverses at higher loads because it occurs near the TDC.
- The combustion starts earlier for all biodiesel blends due to shorter ignition delay and advanced injection timing effects of biodiesel, see Figure 2.4.

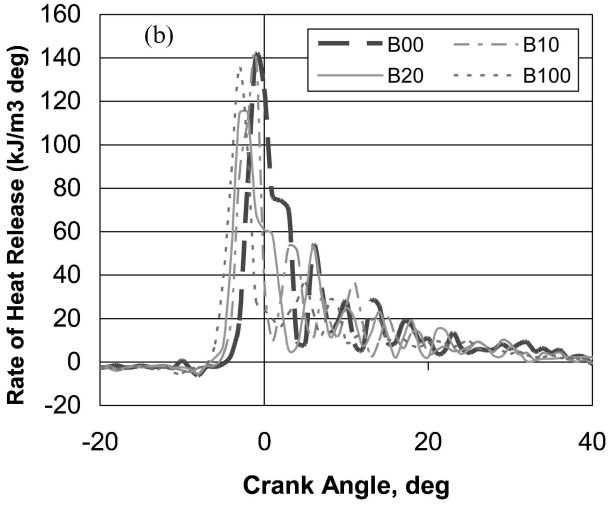

Figure 2.4, Instantaneous rate of heat release for 50 percent of rated engine load at 1400 RPM

- The premixed combustion heat release was higher for diesel fuel due to higher volatility and longer ignition delay of diesel, biodiesel tends to release energy earlier than diesel fuel especially in low loads.
- Cumulative heat release decreases as percentage of biodiesel increases in the blend due to lower heating value of the biodiesel, and the combustion duration reported to be higher for biodiesel blends than for diesel due to its slower rate of combustion.
- Satisfactory engine operation was observed with RBME blends, and no undesirable combustion features such as pre-ignition and knocking were observed.

In another study, Alam et al. [8] reported the response of a commercial engine to different oxygenated fuels, in terms of the injection timing, heat release, and flame structure. Five types of fuel were considered, ultralow sulphur diesel fuel (BP-15), B20 biodiesel, two blends of diglyme with diesel fuel (O-20 and O-95) and a neat biodiesel (B100). The results reported in this study, were obtained at 1800 r/min and 10% load. The experimental conclusions are summarized in the following points:

- The earliest start of injection occurred with biodiesel fuels relative to the base diesel due to the higher bulk modulus of compressibility of biodiesel, but earlier start of combustion occurred with B100 fuel, which might be due to earlier injection or shorter ignition delay, see Figure 2.5.

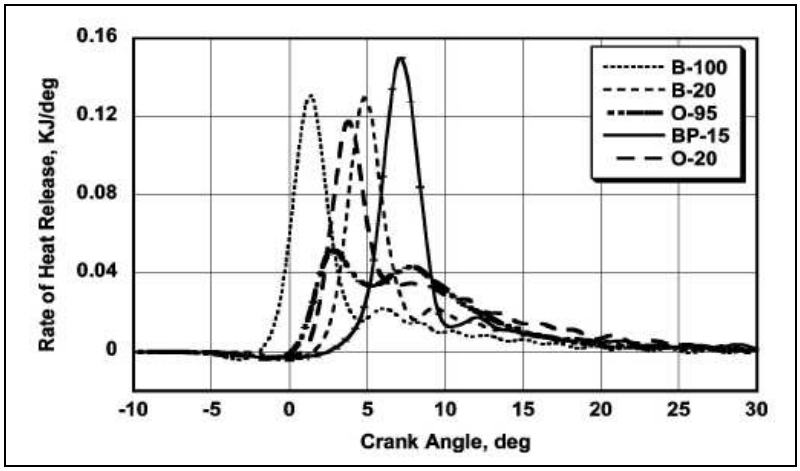

Figure 2.5, Rate of heat release analysis [8]

- The lowest premixed burn peak was observed with B100 and the highest with baseline diesel fuel, and the trend was consistent with the cetane number of the test fuels.
- Fuel properties, such as density, cetane number, and calorific value, had significant effects on the start of injection and combustion.

The impact of biodiesel on injection timing and heat release profiles was investigated by Zhang [64] and the study conclusions are summarized in the following points:

- During both high and low load conditions, the analysis of needle lift profiles and fuel injection line profiles showed that using biodiesel does not affect the start of injection with the common rail fuel injection system, and the actual fuel injection timing for all fuel blends well matched, see Figure 2.6.

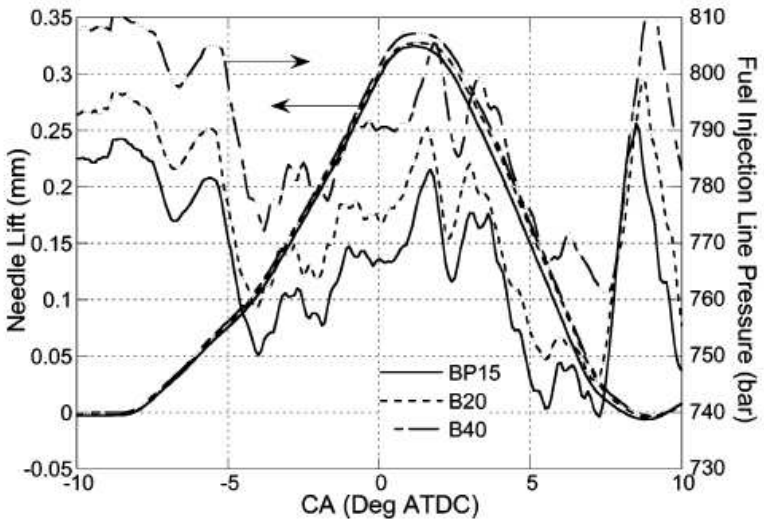

Figure 2.6, Needle lift and fuel injection line profiles [64]

- All three fuel blends had very similar heat release rate profiles under both single and double injection strategies, which showed that biodiesel did not significantly affect the combustion profile.

Similarly, Yoshida et al. [88] investigated the combustion characteristics of B30 RME biodiesel compared to baseline diesel fuel, and concluded the following points:

- Shorter ignition delays were observed with B30 fuel blend compared to baseline diesel fuel even though they had same cetane numbers, and the authors suggested that higher oxygen content in biodiesel under high EGR rates caused this active ignitability of B30 fuel blend.
- No significant difference in heat release rate was observed between both fuels under exactly the same conditions with double pilot injections, and the authors justified it by the moderate combustion resulted from pilot injections, which tends to make any difference in fuel properties difficult to observe, see Figure 2.7.

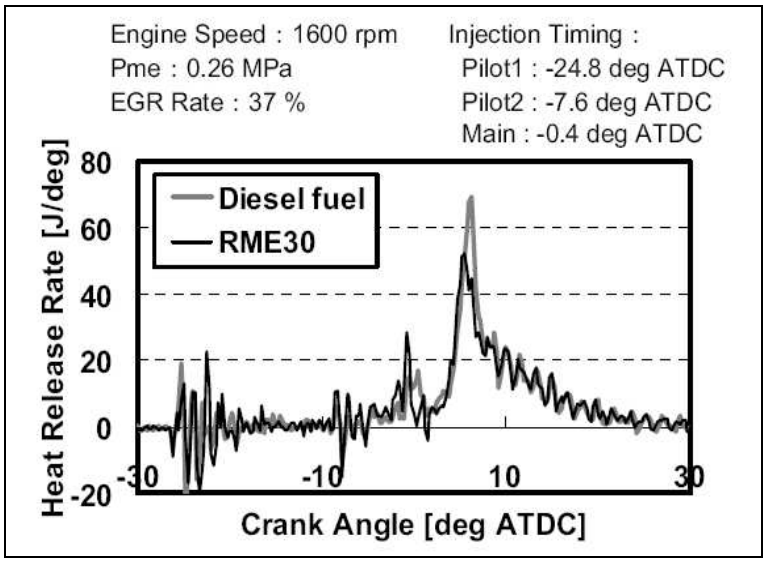

Figure 2.7, Heat Release Rates [88]

Also, Georgios et al. [89] reported no impact on the combustion process and in-cylinder pressures during all measured points except idle using a blend of 10% cottonseed oil with baseline diesel fuel.

The majority of published studies conclude a satisfactory engine operation with biodiesel fuel blends, and no undesirable combustion features such as pre-ignition and knocking were observed with biodiesel. They also reported that biodiesel fuel properties, such as

density, cetane number, and calorific value, had significant effects on combustion especially in engines equipped with conventional pump-line-nozzle fuelling system. On the other hand, using biodiesel does not affect the start of injection in the vehicles equipped with common rail fuel injection systems. Longer injection durations are experienced with biodiesel fuels to compensate for LHV in order to achieve the same power demand [94], however increasing the percentage of biodiesel causes, earlier start of combustion, quicker rise in the rate of heat release, and a higher peak of the rate of heat release [93].

2.6.3 Power and Fuel Consumption

A reduction in engine power by 3% was reported by Sanjeev et al. [16] with B100 biodiesel from Jatropha methyl ester. Also, Georgios et al. [89] reported minor effects on fuel consumption with 10% cottonseed oil blended with baseline diesel fuel, however during low engine speeds and idling conditions, the engine output power dropped by 14% compared to baseline diesel fuel.

Using B20 at high load conditions increased the fuel consumption of about 3.6-5.2% compared to baseline diesel, as Zhang et al. [64] reported. Similarly, Lin et al. [93] reported a reduction in engine power at full load with B50 blend of PKOME and diesel compared to pure diesel, and they also reported an increase in BSFC by 3.5% and 7.8% with B20 and B50 respectively due to LHV of biodiesel fuels due to its different chemical composition. In the medium size DI diesel engines, Kawano et al. [94] reported an increasing trend in BSFC with the addition of biodiesel to the fuel, it increased by 3.7%, 13%, and 18% for B20, B80, and B100 respectively. Similar results were reported by Karra et al. [95], the BSFC increased by 3.9% and 19.5% for B20 and B100 blends respectively.

Bielaczyc et al [92] reported an increase in the FC as the percentage of biodiesel increased in the fuel blend, and they also reported that the maximum engine power and maximum torque for B5 and B20 were comparable to the baseline diesel fuel. Yoshida et al. [88] also reported very minor increase in FC (less than 2%) with B30 biodiesel fuel.

With respect to FC and power output of biodiesel, most of the authors reported an increasing rate proportional to the biodiesel content in the blends. The average FC increase was in the range of 3.2% to 6.5% for B20. Most of the authors reported a power drop of 14% to 17% for B100 compared to diesel fuel. Others reported minor effects in both FC and output power with biodiesel blends. However, all authors agreed on a fact that the increase in FC and losses in power output is mainly caused by the lower heating value of biodiesel fuel.

2.7 Unregulated Emissions with Biodiesel

Besides the regulated emissions from diesel engines, a concern about the emissions of air toxics, carcinogenic and reactive hydrocarbon compounds is also increasing. The toxic emissions from diesel engines can be divided into two groups: Those in the HC portion of the gaseous emissions; and, the heavier hydrocarbons including Sulfates and some aromatic hydrocarbons found in PM [2]. According to EPA (table 2.2), by using B100 biodiesel fuel the reductions of Sulphates and PAH will reach up to 100% and 80% respectively. Very limited data on these emissions, while using biodiesels, are available, thus at the present time it is difficult to draw any conclusions on unregulated emissions and this area clearly needs more research in future.

Arapaki et al. [90] reported an increase in soluble organic fraction (SOF) emissions with addition of UFOME biodiesel to the fuel blend. An increase of 7% in SOF with B20 biodiesel fuel was reported, and the authors suggested that more attention should be paid at the unregulated emissions due to their direct impact on public health. Karavalakis et al. [86] also reported an increase in SOF emissions of biodiesel blends (about 2.5%) than those of petroleum diesel. The authors speculated that the fatty acid composition is the main reason for having higher SOF emissions.

On the hand, Camden Council [83] reported a significant reduction in PAH by 75% with B100 biodiesel compared to baseline diesel. Similarly, Sharp et al. [96] reported

substantial reduction in PAH and the use of B20 biodiesel fuel blend did not generate any new species that was not already present in diesel or biodiesel exhaust. A significant reduction in aromatic and oxygenated aromatic emissions was reported by Ballesteros et al. [97] with the use of biodiesel fuel blends compared to the conventional diesel fuel. McGill et al. [87] concluded their study by stating that the unregulated emissions did not seem to have much dependence on the fuel and the presence of an oxidation catalyst in the exhaust stream was very effective in reducing it, and similarly K. Yoshida et al. [88] reported the same SOF emissions from both B30 RME and baseline diesel fuels.

As discussed, few studies have evaluated the unregulated emissions from diesel engines. Many authors indicated that engine characteristics and the type of biodiesel fuel used are the major factors affecting the unregulated emissions from diesel engines. However, the scarcity and variability in the reported results make it very difficult to draw any solid conclusions on the impact of biodiesel on unregulated emissions and more research is required in this area.

2.8 Review of Engine Simulation with Biodiesel

2.8.1 Background

The simulation of internal combustion engine (ICE) has become very important in recent years due to the continuous higher stringent obligations from legislators on vehicle manufacturers. It becomes almost a necessity to assess the vehicles performance using both simulation studies and laboratory tests. Modelling an engine with proper software can lead to time and money savings, since the engine simulation results usually predict engine performance without going to the trouble of conducting the actual tests. Developing these tools not only will help the auto industry improve fuel efficiency, but also will help with optimising engine calibration for lower emissions. However, it should be noted that simulation in only a step prior to actual physical experimentation and the simulation results must be validated with experiment to establish a good reliability.

Combustion engines are complex, highly engineered systems and the traditional design methods will not suffice for the new complex systems, therefore the thermodynamic or fluid dynamic approaches have been developed as basic types of models. The thermodynamic approach is known as zero dimensional (0-D) [98], and for more realistic engine simulation, computational fluid dynamics (CFD) can be used, but the drawback is long computational time limiting its application. In addition to CFD packages, Matlab Simulink, Ricardo WAVE, AVL Fire, and Fluent are also commercially available softwares [99]. Modelling the compression ignition (CI) diesel engines represent a particular challenge due to the complex physics and mechanics of the heterogeneous combustion.

Theoretical models have been developed recently to analyze the performance characteristics of the CI engine fuelled by biodiesel and its blends due to its physical and chemical properties that may result in spray atomization differences. Atomization quality is influenced by the physical properties of the fuel, as discussed in section 2.4.3. Therefore, predicting the physical properties of biodiesel is a crucial step for the accurate prediction of the spray atomization and combustion processes. Next, a review of the recent published studies on engine simulation with biodiesel will be conducted.

2.8.2 Simulation Reviews

Brakora et al. [99] developed kinetic mechanisms to predict ignition timing and NO_X emissions over four engine loads with a use of soy bean based biodiesel and the authors modelled their single cylinder engine and biodiesel fuel using the KIVA-3V release. With 11% oxygen content in the fuel, the biodiesel was represented by $C_{19}H_{34}O_2$ chemical composition in the model and the simulation results of cylinder pressure and heat release rate are presented in Figure 2.8. The ignition timing and peak pressure were adequately predicted when compared to experimental values; however the NO_X emissions were under predicted at light load conditions compared to experimental results even though the general trend was similar to the experimental data.

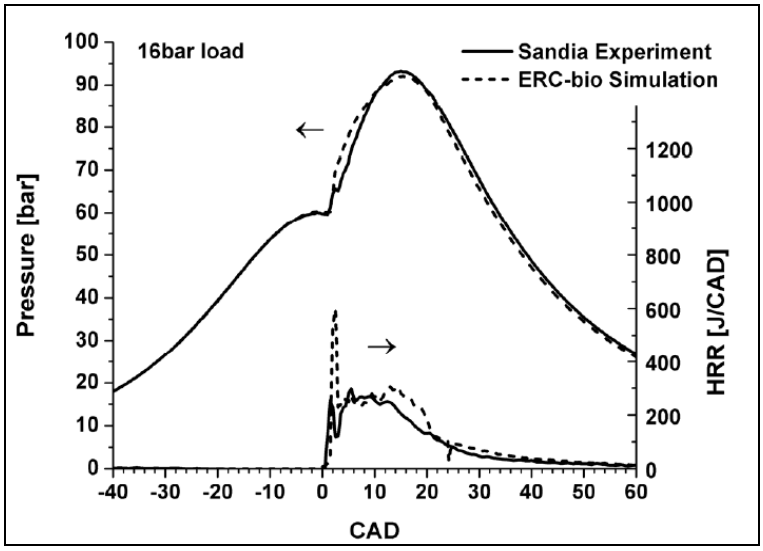

Figure 2.8, Simulation results of pressure and HRR [99]

Similarly, Szybist et al. [100] modelled their single cylinder engine using the CHEMKIN III package. The authors used n-heptane to simulate diesel fuel, and methyl butanoate to simulate soy based methyl ester biodiesel. The effect of altering the intake temperature on the HRR and combustion characteristics was correctly simulated by the model. However, the effect of different concentrations of biodiesel was not accurately simulated as engine out emissions. The authors concluded that the used model is not in the best position to simulate biodiesel combustion, due to the inability of the model to account for the physical properties of the fuel.

The combustion characteristics of Jatropha based biodiesel blends were investigated by Ali et al. [101] with the effect of altering the compression ratio of a single cylinder DI diesel engine. The authors used $C_{10}H_{22}$ and $C_7H_{10}O$ as the molecular formula for diesel and biodiesel fuels respectively in the combustion model and the simulation results showed that with increasing compression ratio, brake thermal efficiency increases, and both experimental and simulated results were in good agreement. Also, biodiesel fuel demonstrated lower brake thermal efficiency than that of diesel fuel, due to the fact that the calorific value of biodiesel is generally lower.

Ra et al. [62] investigated the effect of physical property differences between biodiesel and diesel fuels on CI engine operation in a multi dimensional CFD model that simulated the combustion in a 1.9 L light duty diesel engine by replacing the physical properties of diesel with those of biodiesel. The required physical properties of biodiesel were obtained from the literature and used in the model and includes, liquid density, vapour pressure, surface tension, and heat of vaporization plus several more profile properties were used, as they are very critical in fuel injection and combustion models. The model predicted a decrease in NO_X emissions and higher soot values with the use of biodiesel fuel. The authors justified these results by stating that differences in the chemical oxidation mechanisms between diesel and biodiesel fuels were not modelled in this simulation. The authors concluded that it is very important to accurately specify all of the physical properties of biodiesel fuel in the model, and appropriate chemistry mechanism needs to be incorporated for accurate prediction of emissions.

Cheng et al. [77] simulated the operation of a small bore high speed direct injection engine built by Ford. The authors used the three dimensional multi phase CFD package KIVA-3V release 2 which was modified to improve its compatibility with biodiesel simulation. The simulation is done in various injection schemes with soybean biodiesel ($C_{19}H_{35}O_2$) and low sulphur diesel fuel ($C_{14}H_{30}$). The authors reported an accurate prediction for petroleum based diesel and soybean biodiesel compared to the experimental measurements. The comparison showed accurate prediction of the combustion characteristics including ignition time, heat release rate and peak combustion pressure for all the injection cases. However, the predictions of NO_X emissions did not agree with the published literature.

Most of the developed simulation packages predicted the combustion profiles of biodiesel fuels to some extent; however contradictory results were reported with engine out emissions. As a result, further development is required in order to accurately model the CI engine when fuelled by biodiesel and its blends due to its physical and chemical properties that may result in spray atomization differences. Also, no studies could be found that used a single dimensional software package simulating biodiesel combustion in CI engines.

2.9 Engine Calibration with Biodiesel

2.9.1 Background

The standard diesel engine ECU is optimised to operate with baseline diesel fuel, so it is necessary to optimise the engine toward better emissions and performances when fuelled with biodiesel pure or blended than with baseline diesel fuel. Tuning the engine governing parameters by modifying the ECU mapping data could be possible to re-gain some of the power output gap and simultaneously reduce NO_X content in the exhausts by taking advantage of low CO emissions and the better combustion of biofuels [102]. This type of calibration is only possible when modern diesel engines are used due to the requirement of controlling the fuel pump and electronically controlling the injection timing. The most common practice for optimizing standard diesel engines for the use of biodiesel is to look for the best compromise between CO and NO_X emissions by modifying fuel injection strategy and EGR rate [7]. On the other hand, the deterioration of power is usually compensated by increasing the fuel quantity, because net energy release in biodiesel is less. The effect of biodiesel fuel on emissions depends not only on the fuel composition but also the operation modes and how the engine has been tuned. In this section, the experimental studies into diesel engine optimization with the use of biodiesel fuels are reviewed even though very little publications are available in this field.

2.9.2 Engine Optimization Reviews

Ireland et al. [102] investigated the possibility of improving the engine out NO_X emissions by modifying the main injection timing and EGR rate when the engine is fuelled with B20 RME biodiesel. The authors tested the sensitivity of the fuel consumption (FC), NO_X, and PM emissions to changes in a single parameter at a time, and then combined the calibration changes simultaneously to obtain optimized engine performance and emissions. Figure 2.9 shows the effect of changing engine parameters on emissions and FC, the best combination was one degree advance in main injection timing and 4% increase in EGR rate. Even though all four engine calibrations reduced both NO_X and fuel consumption for B20 below that of the stock calibration with B20, the selected combination reduced fuel consumption more than any of the other settings while resulting in emissions of NO_X approximately equal to that of baseline diesel with stock calibration.

Finally the authors concluded that, a simple calibration change could eliminate negative effects of B20 on NO_X emissions and fuel economy while preserving a significant reduction in PM emissions.

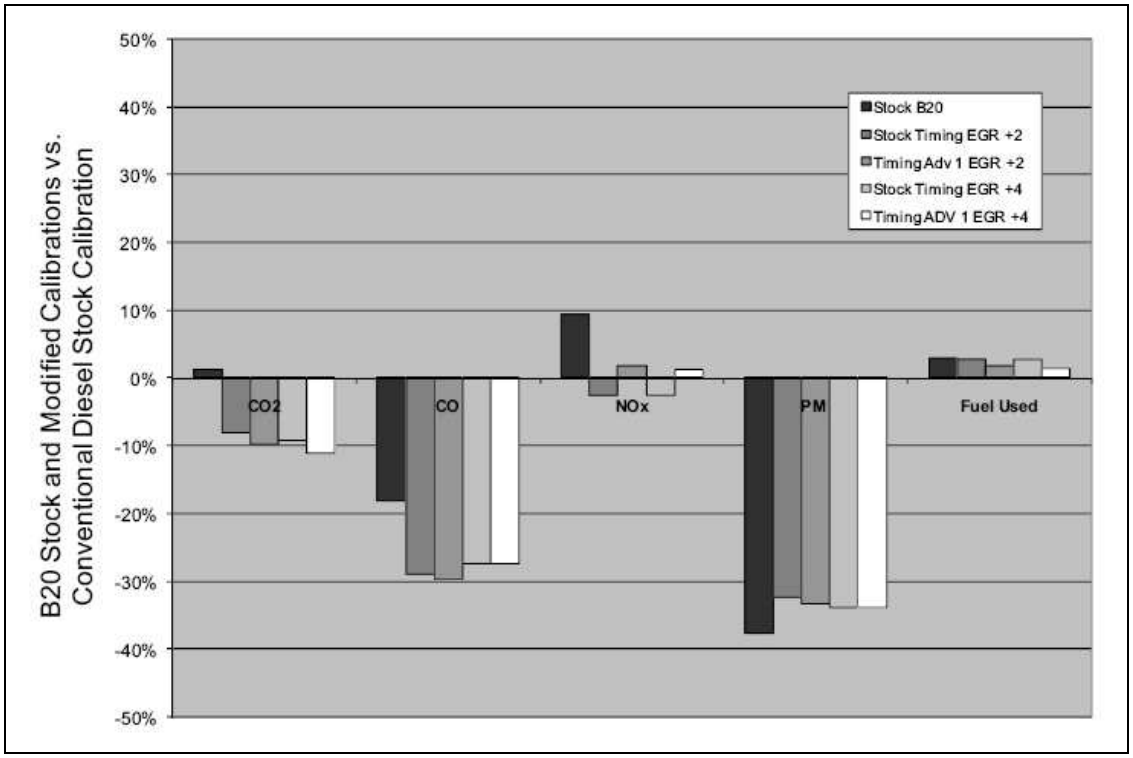

Figure 2.9, Effects on emissions and FC due to changes in engine Parameters [102]

Similarly, Senatore et al. [103] investigated the possibility of optimizing a commercial diesel engine with B100 biodiesel fuel by increasing the injected fuel mass to obtain the same engine power output, and tuning the EGR rate and fuel injection timing. The optimal calibration for the engine depended on engine speed/load, and biodiesel blend ratio used, Table 2.8 shows optimization results during 2000 RPM engine speed. By tuning the EGR rate and fuel injection timing, both CO and NO_X emissions closely matched up those of diesel fuel during the standard case.

	CO [ppm]	NOx [ppm]
B100 ECU std	71	1180
B100 ECU mod inj	97	830
B100 ECU mod egr	114	460
Diesel fuel	128	470

Table 2.8, Emissions level at 2000 RPM and 12 bar BMEP [103]

The authors also investigated the impact of engine calibration on rate of heat release; see Figure 2.10, the faster velocity of combustion process can be observed when biodiesel fuel is introduced to the engine compared to baseline diesel fuel. The figure clearly shows that by activating the EGR valve, the combustion velocity remains almost unchanged but the heat release peak decreases causing a lower value of mean gas temperature which probably caused the reduction in NO_X emissions.

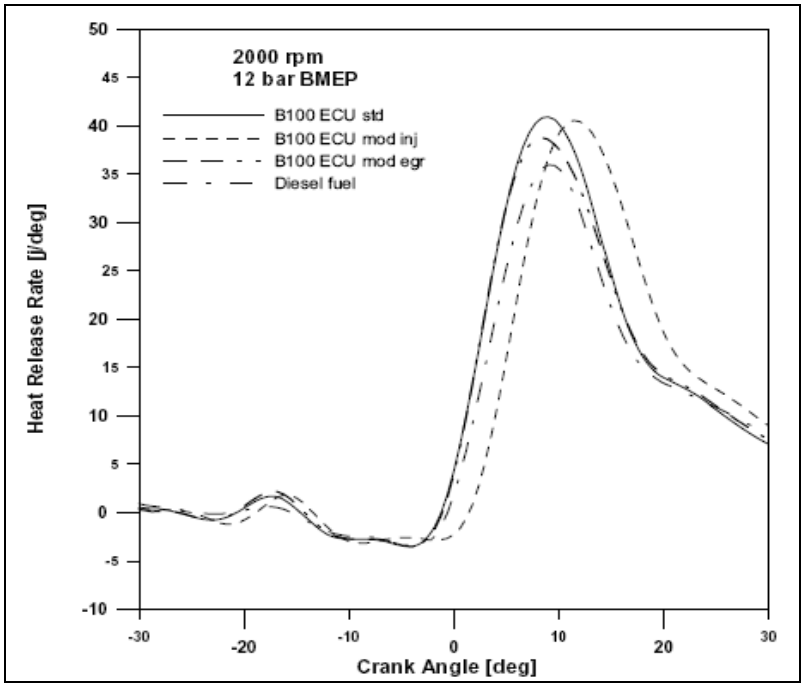

Figure 2.10, Heat Release Rate at 2000 RPM and 12 bar BMEP [103]

In a different study, Kawano et al. [70] achieved over 50% reduction in NO_X emissions when the EGR rate was optimized for RME biodiesel fuel without significantly effecting other emissions except a slight increase in FC of about 3%. The authors concluded that the ECU modifications are necessary to optimise the engine calibration for different type

of fuels, and are easily applicable to all commercial DI diesel engines equipped with a common rail injection system. Similar observations were obtained by Lujan et al. [104], Yoon et al. [105] and Zhang [106] when they modified the EGR rate to optimize the engine calibration for the introduction of biodiesel fuel. This calibration change has proved to be able to produce important benefits in terms of NO_X emissions without significant penalties on particulate emissions and FC. Moreover soot, HC, and CO emissions, maintained a lower level as compared to those obtained by baseline diesel fuel under the same EGR rate.

2.10 Conclusions

The aim of the literature survey was to perform a thorough review of current publications about FAME production, properties, and their impact on diesel engine emissions and performance. The following conclusions were drawn:

- The factors most affecting the physical and chemical properties of FAMEs are their carbon chain length and number of double bonds (un-saturation level). These factors will directly affect the fuel's performance in the fuel injection system as well as its combustion and emission characteristics.
- The cetane number, kinematic viscosity and crystallisation temperature of FAMEs increase as the chain length and saturation level increases in the fatty acid molecules, and its resistance to oxidation decreases with an increasing number of double bonds.
- FAMEs are compatible with most of the elastomers used in diesel engines and can improve fuel lubricity. Higher viscosity and surface tension of biodiesel fuels leads to poorer atomization of the fuel spray.
- The average fuel consumption increases with biodiesel use due to its lower calorific value compared to petroleum diesel fuel, and a reduction in engine out emissions of CO, HC and PM with biodiesel is reported by the majority of studies due to higher oxygen content which allows faster and more complete combustion of the fuel compared to petroleum diesel.

- An increase in NO_X emissions is reported with biodiesel use due to physical and chemical properties, such as cetane number and density. Studies suggest that increases in NO_X emissions could be linked to the molecular structure of the fatty acids with the level of un-saturation being most significant.
- Biodiesel fuel properties were found to have a significant effect on the combustion process especially in the case of pump-line-nozzle fuel injection systems, but the impact reduces significantly when common rail fuel injection systems are used.
- Simulation studies with biodiesel using CFD models reported contradictory results due to inability of the models to account for some biodiesel fuel properties. No literature could be found which examined the use of one-dimensional simulation packages to investigate the combustion of biodiesel fuels in compression ignition engines.
- Adjusting the EGR rate and injection timing can mitigate some of the negative effects of biodiesel use, such as an increase in NO_X emissions and fuel consumption, by optimising the combustion process.
- Whilst there have been studies investigating the impact of biodiesel use on diesel particulate filters, no published work could be found examining the impact of biodiesel fuel on the performance of diesel oxidation catalysts (DOC).
- All literature reviewed, discussed studies which examined biodiesel performance at room temperature (20-25°C approx.). The author could find no studies examining the interaction between ambient operating temperature and engine performance and emissions when using biodiesel fuels.
- Many studies discuss the impact of injection timing and EGR rate on engine emissions when using biodiesel, however, no literature could be found which examined the impact of other calibration parameters, such as rail pressure and pilot injection timing, on engine performance and emissions with biodiesel fuels.

In summary, many authors conclude their studies by requesting further investigations in order to achieve an improved understanding of the impact of FAME's cold flow properties on diesel engines, especially for fuel blends greater than 5%. This improved understanding

would provide engine manufacturers with information on the long-term impact of biodiesel use on engine operation and durability.

The lack of knowledge pertaining to the interactions between ambient temperature and vehicle performance when using biodiesel blends is addressed and discussed in the next chapter. An experimental programme will be conducted investigating the effect of biodiesel fuel blends on the fuel consumption, engine-out emissions, tailpipe emissions, and catalyst conversion efficiency of a standard diesel vehicle and compared to the results obtained from a reference diesel fuel when the vehicle is operated at different ambient temperatures.

Chapter 3 Biodiesel Vehicle Trials

3.1 Introduction

Vehicle testing over specified drive cycles is still used by the legislators to asses the compliance of vehicles with the emission standards since they provide a standardised means of measurement, and accurate comparison between vehicles running under tightly controlled test conditions. Although a large number of studies have investigated the effect of changing the biodiesel blend ratio on the vehicle fuel consumption and emissions, there are relatively little data pertaining to the interaction between the ambient operating temperature and these increases in the blend ratio.

3.1.1 Aims and Objectives

The aim of the work reported in this chapter, is to investigate the effect of biodiesel fuel blends, from a known feedstock, on the emissions and performance of a production vehicle with unmodified engine calibration when operated with various biodiesel blends at different ambient temperatures. To achieve this goal, the following objectives were set:

- Evaluate the impact of using various blends of RME biodiesel on fuel consumption, engine-out emissions, tailpipe emissions, and catalyst conversion efficiency at different ambient temperatures, and compare the results to a reference diesel fuel when the vehicle is driven over NEDC.
- Determine the presence and significance of the interactions between different blend ratios and ambient temperatures from total NEDC cycle results.
- Quantify the loss in vehicle power with increasing RME blend ratio and changes in ambient temperature when the vehicle is operated at full load.

3.1.2 Approach

The experimental work will be conducted using the chassis dynamometer facility at the University of Bath, which is described in section 3.2. The study required substantial planning in order to avoid any uncontrollable factors which could affect the validity of the experimental results. The following points were considered:

- With two variables in mind (blend ratio and cell temperature), a design of experiment (DoE) approach was used to plan the testing phase of this project.
- The test plan would cover several fuel blends of biodiesel and diesel to obtain clear trends of the effect of different ratios on diesel engine performance, emissions, and fuel consumption.
- The vehicle should be tested under different ambient conditions, -5°C and 25°C are reasonable conditions that simulate UK driving conditions. DoE suggested an interim temperature of 10°C in order to assess a non-linear relationship. With temperature as low as -5°C and different blend ratios, the effect of cold flow properties on a diesel combustion will be identified.
- The drive cycle should produce representative results which can be compared to other studies. The use of the NEDC provides this commonality.

3.2 Experimental Facility

3.2.1 Experimental Cell

The chassis dynamometer at the University of Bath can accommodate light duty; medium duty, front wheel, and rear wheel drive vehicles. It is climatically controlled with the capability of controlling the temperature from -10°C to 50°C. A photograph of the facility is shown in Figure 3.1.

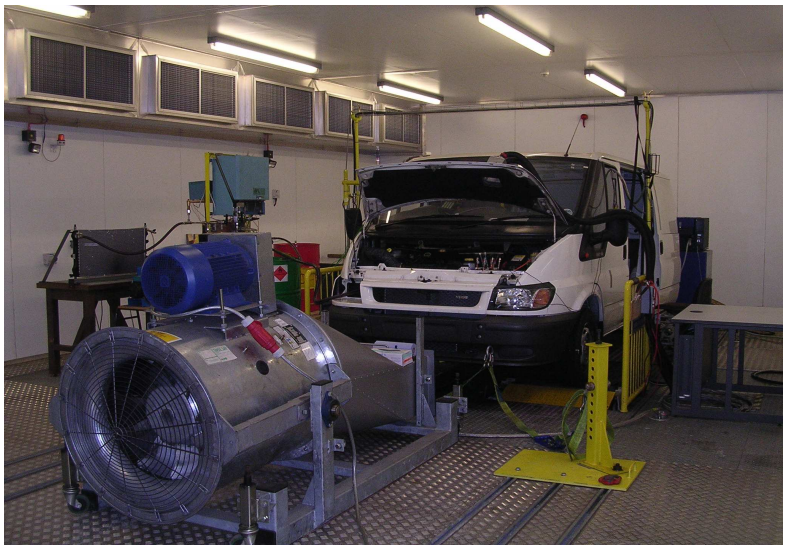

Figure 3.1, University of Bath chassis dynamometer testing facility

The vehicle testing facility is equipped with a Zollner 48" dynamometer with two independent 126 kW DC motors. A cooling fan is situated in the front of the vehicle to provide cooling air to the radiator, and the fan speed is automatically adjusted according to the vehicle speed.

3.2.2 Vehicle

A 2.0 litre Euro 3 compliant Ford Transit van, equipped with a direct injection common rail diesel engine operating on its standard production calibration was used in this study. The full specification of the vehicle is presented in Table 3.1.

Manufacturer	Ford Motor Company
Type	Transit Van 125 T260
Kerb weight	2455kg
Engine	Puma 2.0L production Spec (DuraTorq TDCi – 125PS)
Fuel Injection	Delphi Common Rail (production spec.)
Transmission	Front Wheel drive, five speed manual
Power train	Front wheel drive
ECU Module	DPC-801 (development/calibratable ECU)
Emissions Standard	EURO 3 (category N1 – III)
Year	2002

Table 3.1, Vehicle Specification

The vehicle was inspected prior to starting the experimental procedure, and the engine oil was changed. The vehicle was driven on the rollers for a period of 10 hours to age the new oil as well as ensuring its readiness for the testing program. A daily check sheet requesting vehicle and test parameters was prepared and completed to ensure repeatability of the tests on a daily basis, as well as preparing the vehicle for the next test.

3.2.3 Fuels

Baseline diesel fuel (B0) was supplied by Shell and a full specification sheet is given in Appendix A. The biodiesel fuel used in this study is rapeseed oil methyl ester (RME) supplied by BP and the specification table is given in Appendix B. The specifications of RME meet the European biodiesel standard EN 14214:2003 with a slightly lower cetane number (CN), which is not usually common in most of the biodiesel fuel types (see Table 3.2).

Property	Baseline Diesel (B0)	RME Biodiesel (B100)
Cetane Number (CN)	**52.8**	**49.5**
Net Calorific Value (Mj/kg)	**42.59**	**39.99**
Density at 15°C (kg/m^3)	**833**	**883.2**
Kinematic Viscosity at 40°C (mm^2/s)	**2.75**	**4.56**
Oxygen Content (%)	**0**	**11**
Water Content (mg/kg)	**68**	**210**

Table 3.2, Summary table of Fuel Specification

The CN of 49.5 for the RME fuel is slightly lower than the standard requirement of 51, which needed to be considered in the results analysis. The other properties follow similar trends to published biodiesel specifications. The summary Table 3.2 shows the RME fuel density, viscosity, and water content is higher than that of baseline diesel fuel. Also the net calorific value of RME fuel is lower by approximately 6% compared to baseline diesel fuel. Due to the extended duration of this study, the RME fuel drums were stored in a refrigerated location below 3°C to avoid possible oxidation or degradation of the fatty acids. The fatty acid break down for the RME fuel used in this project is presented in Table 3.3.

FA Structure	16 (0)	16 (1)	18 (0)	18 (1)	18 (2)	18 (3)	-
FA Name	Palmate	Palmitoleate	Stearate	Oleate	Linoleate	Linolenate	Others
(%)	2.05	0.31	1.66	62.82	20.41	9.15	3.60

Table 3.3, RME Fatty Acid Composition

Fuel blends of B5, B10, B20, B30, and B50 were prepared on site by splash blending the required volumetric ratios of baseline diesel and RME fuel in 50 litre barrels and connected directly to the vehicle's fuel system. Samples of each blend were taken at the beginning and end of the test program and analysed by nuclear magnetic resonance (NMR) to ensure the consistency of the blend ratio.

3.2.4 Facilities

3.2.4.1 Emissions Measurement

All gaseous emissions from the vehicle (NO_X, HC, CO, and CO_2) are collected in bags and analysed by MEXA-7400DETR analysers. Continuous second by second samples (modal) are also taken at engine out and post catalyst locations. The constant volume sampling (CVS) system and sample points are shown in Figure 3.2.

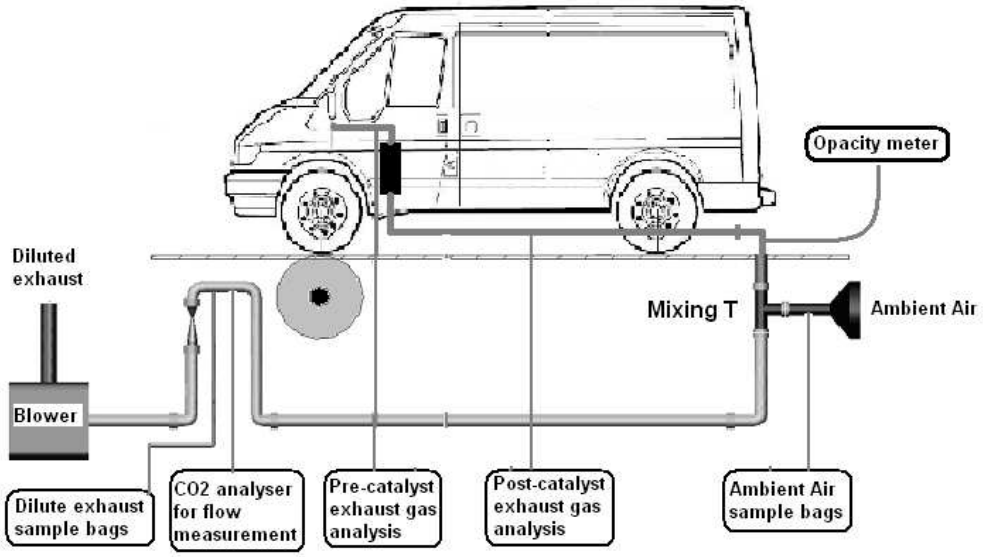

Figure 3.2, University of Bath chassis dynamometer and CVS system layout

In the CVS system the entire content of the vehicles exhaust is diluted with ambient air in the mixing T, and a pump or blower draws the diluted gasses at a constant flow rate defined by the in-line venturi. A small representative sample is subsequently drawn into bags for later analysis of each of the individual legislated gas species, while at the same time an additional set of sample bags are filled with ambient air to compensate for ambient air contamination. This technique, as explained by Hawley et al. [107], produces what are commonly termed as 'bag' results which provide a single overall result for the mass of each emission produced from the tailpipe over a legislative drive cycle. The CO_2 tracer technique is used to determine the modal exhaust gas volume flow rate in order to convert the volumetric emissions concentrations measured by the analysers into gravimetric values per unit time. The CO_2 tracer method requires measuring the CO_2 concentration in the raw exhaust gas at the tailpipe and the diluted sample in the mixing tunnel simultaneously, then the ratio of these two values are multiplied by the CVS flow to calculate the exhaust gas flow rate.

In addition to bag results, second-by-second emissions data was obtained to know when, and how much, exhaust pollutants are emitted in real-time, which can provide some useful information about the physical and chemical properties of the engine out gas, as well as allowing the determination of the emission conversion performance across the catalyst by simultaneous sampling before and after the catalyst. However, some difficulties arise when trying to align the actual magnitude of the pollutant mass measured with the magnitude produced by the engine. In other words, the time taken by the raw pollutant sample to travel from the combustion chamber to the analysers, and the analyser response delay time need to be accurately measured. The process of matching the instantaneous emissions measurement has been widely studied and resolved by Bannister et al. [108].

The PM and smoke was measured by the use of two separate methods. The AVL 439 opacity meter draws a sample from the exhaust stream for analysis (see Figure 3.2). The opacity measurements were only taken at 25°C and 10°C as the specified operational temperature range of the device is above 5°C. The second method measures the mass of PM in the exhaust by taking a sample from the exhaust and passing it through a paper

filter. The Horiba tapered element oscillating microbalance (TEOM) weighs the filtered carbon particles and reports it at the end of each test.

3.2.4.2 Fuel Consumption Measurement

The fuel consumption (FC) was measured by several methods in this experimental study. The carbon balance method uses emissions data (when the ratio of carbon to hydrogen (C:H) and carbon to oxygen (C:O) within the fuel is known) which allows the calculation of fuel consumption. In addition, a gravimetric weighing device (AVL 733S), Pierburg flow meter measurement, and ECU data is also used to measure fuel consumption.

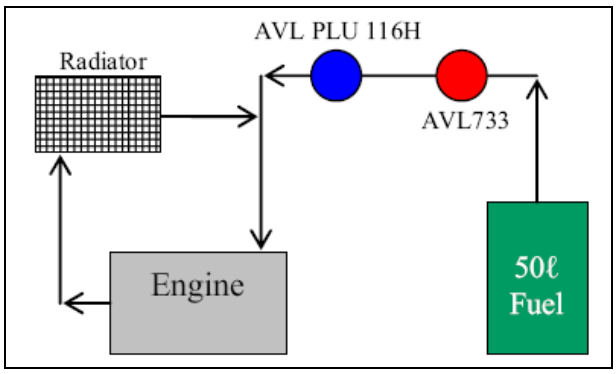

Figure 3.3, Fuel system layout

A schematic of the fuel feeding system used in this study is shown Figure 3.3. The fuel consumption is measured by weighing the 'beaker' within the AVL733 gravimetric fuel system, also as the fuel passes through the AVL PLU116H volumetric flow meter and into the engine. The system is equipped with a large air cooled radiator, to cool the return fuel back to the ambient cell temperature before feeding it back to the engine. The cooling of the hot return fuel from the engine ensured a consistent and repeatable fuel temperature was supplied to the engine throughout the drive cycle. When the testing of each blend batch was completed, the fuel system was totally drained and the next batch used to fill the system. In this change over, the vehicle was driven for more than 40 miles to ensure that the new fuel blend has passed through the entire system. The complete fuel system shown in Figure 3.3 was contained within the chassis dynamometer facility cell and therefore held and 'soaked' at the same ambient test temperature as the vehicle.

3.3 Experimental Program

3.3.1 NEDC

The European drive cycle was developed by the United Nations Economic Commission for Europe (ECE). The basic ECE cycle is an urban driving cycle, also known as the (Urban Drive Cycle). It was devised to represent city driving conditions and is characterized by low vehicle speed, low engine load, and low exhaust gas temperature. In order to account for more aggressive, high speed driving modes, an additional segment was added to the ECE cycle called the Extra Urban Driving Cycle (EUDC). The maximum speed of the EUDC cycle reaches up to 120 km/h. The combined (ECE+EUDC) is called the New European Drive Cycle (NEDC), it consists of four segments of ECE which takes 780 seconds and one segment of EUDC which takes 400 seconds, see Figure 3.4.

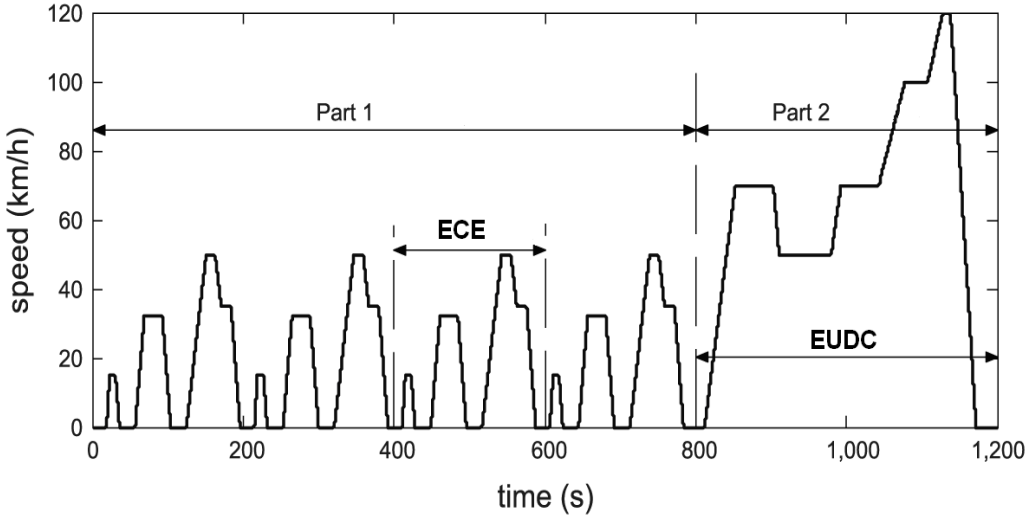

Figure 3.4, New European drive cycle (NEDC)

In order to investigate the effect of biodiesel fuel on a standard diesel vehicle and compare the results to a reference diesel fuel, the vehicle was tested over the NEDC. The NEDC was followed by a coast down cycle to ensure that the dynamometer settings and vehicle power train have not changed from test to test. In the coast down cycle, the dynamometer

drives the vehicle up to 120 kph while the engine is switched off and the gear box is in neutral. Then the vehicle is left to coast down from 120 kph to 20 kph and the time is recorded and compared to previous results.

3.3.2 Bath Full Load Cycle

A method developed at the University of Bath was used to investigate the effect of increasing biodiesel blends and changes in ambient temperature on vehicle's performance under 100% pedal (full load) engine conditions. Any potential loss in engine power will be clearly highlighted, since the driver will not be able to compensate for any loss in engine power by an increase in pedal position. Figure 3.5 shows the proposed full load testing method and the following steps will explain the cycle procedure:

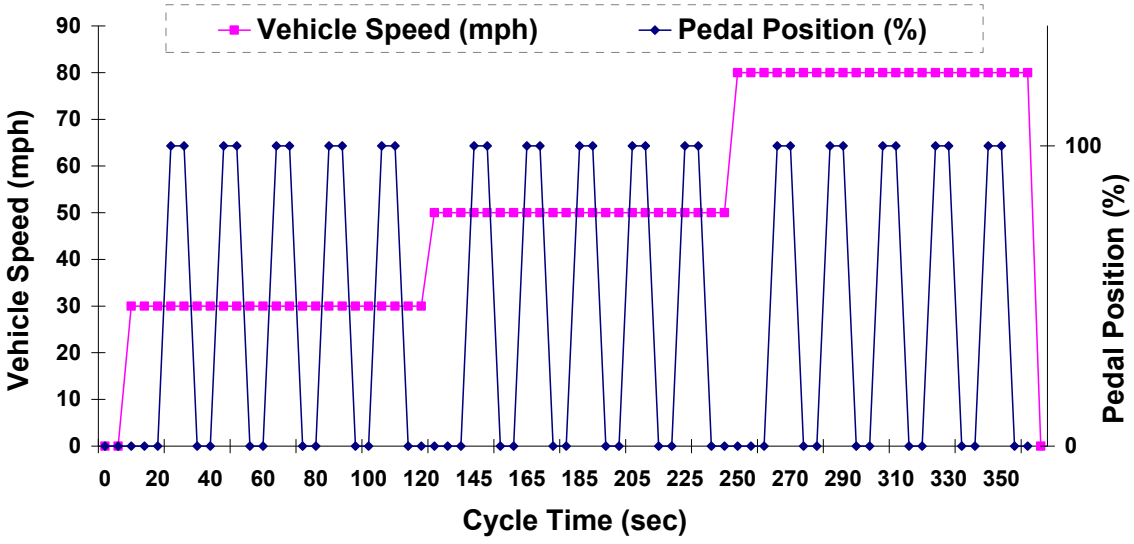

Figure 3.5, Full Load Method

1. The dynamometer rollers drive the vehicle at three different speeds, 30, 50, and 80 kilometres per hour in 3rd gear which corresponds to engine speeds of 1450, 2420, and 3870 RPM respectively. This provides data points at maximum engine torque at low, medium, and high engine speeds.
2. At each speed, 5 repetitions of 100% accelerator pedal steps are applied by the driver for 10 seconds. The vehicle and engine speed will rise slightly initially

before the dynamometer control can compensate and return the vehicle to the original speed regardless of the torque applied by the vehicle tyres.

3. The input force applied by the chassis dynamometer motors to bring the speed back to the set point can be directly recorded (this could be termed as maximum tractive force). The maximum tractive force was expected to vary according to the fuel blend used and ambient temperature.
4. Maximum tractive forces were averaged over five repeats only using data when the vehicle speed falls within ±1kph of the set point.

This high load test cycle was performed following a cold NEDC test each day according to the experimental plan. To ensure repeatability of test conditions, a conditioning cycle was performed after completing both testing cycles. This cycle also helped purged the catalyst of particulates left from previous tests. The design of experiments (DoE) approach was adopted as the experimental procedure since it provides a systematic method of vehicle testing as well as determining the significance and interactions of selected factors.

3.4 Design of Experiments (DoE)

DoE is an organized method to determine the relationship between the different factors affecting a process and the output of that process, which can produce more precise information in fewer experimental procedures [109]. With the rapidly increasing costs of laboratory experimental procedures, reducing their numbers without sacrificing the result quality becomes a very essential factor for all research organizations [110]. DoE is considered an efficient procedure for planning experiments so that the data obtained can be analyzed to yield valid and objective conclusions, and it is a multipurpose tool that can help in many experimental situations, and it is mostly used for two main objectives, first is to identify the important factors that has the most influential effect (Screening), second is to understand in more detail how the selected factors influence the response (Optimization) [109, and 110].

In this project, the screening method was used to determine if the blend ratio or the cell temperature was the most influential factor affecting the vehicle emissions. With the benefits of using a DoE approach, the experimental procedure was designed to ensure repeatability and consistent vehicle, fuel, and catalyst condition before each test, the designed test plan is presented in Table 3.4.

Test Number	Blend Ratio (B %)	Cell Temperature (°C)
1	0	25
2	0	25
3	0	10
4	0	-5
5	0	-5
6	5	25
7	5	25
8	5	10
9	5	10
10	5	-5
11	5	-5
12	10	25
13	10	10
14	10	10
15	10	-5
16	20	25
17	20	25
18	20	10
19	20	-5
20	20	-5
21	30	25
22	30	10
23	30	10
24	30	-5
25	50	25
26	50	25
27	50	10
28	50	-5
29	50	-5
30	0	25
31	0	10
32	0	10
33	0	-5
34	0	-5

Table 3.4, Vehicle Test Plan

The experimental matrix was designed using the Mathworks model based calibration (MBC) toolbox. A D-optimal quadratic design-of-experiments approach was adopted in order to minimize the number of test conditions while achieving good coverage of the

design space, as well as providing a detailed knowledge about the most influential factors affecting vehicle's emission, fuel consumption, and performance when biodiesel fuel is used. The baseline diesel fuel (B0) is repeated at the end of the experimental programme to ensure that there had been no gradual drift in the results over time.

In the next section, the effect of different RME fuel blends on the fuel consumption, engine-out emissions, tailpipe emissions, and catalyst conversion efficiency of a standard diesel vehicle will be discussed and compared to the results from the reference diesel fuel. The significance of any interactions between the blend ratio and ambient temperature over the New European Drive Cycle (NEDC) will be identified by plotting the response surface models (RSM) of the DoE. Finally, the variation in vehicle torque, when a production vehicle, with unmodified engine calibration, was run on various biodiesel blends over university of Bath full load cycle is presented.

3.5 NEDC Results

In this section, the emissions results over the NEDC cycle are presented and discussed in terms of each emission species and fuel consumption. In this analysis, the results from bag measurements will be used for comparison despite the continuous emissions measurements also being recorded. Only the average result graphs will be presented with error bars of ±2 standard deviation (±2 SD), representing a 95% confidence interval. The Student T test was used for the comparison of means of the two fuels baseline diesel and B50, to establish if the findings were statistically significant (the T results for all presented emission species and fuel consumption data are presented in Appendix C).

3.5.1 NEDC CO Emissions

The average tailpipe 'Bag' CO emission results over NEDC at three different cell temperatures are presented in Figure 3.6. Unlike most of the published literature, the tailpipe CO emissions showed an increasing trend as the percentage of biodiesel increased in the fuel. The highest amounts of CO emissions were produced during the -5°C ambient temperature which is probably due to the fact that at very cold temperatures, the air

density is very high and higher amounts of fuel will be required to make up a combustible mixture. Consequently, leads to poor combustion quality which will produce higher concentrations of CO in the exhaust. On the other hand, at lower ambient temperatures, the biodiesel fuel viscosity will increase which will lead to poor atomization and mixing quality thus cause local oxygen deficiency and incomplete combustion. The lowest CO emissions were produced during the 10°C ambient temperatures and it clearly shows the ambient temperature effect on the CO emissions. Further investigation is required to explain why the CO emissions produced during the 25°C ambient temperatures were higher than the 10°C ambient temperature experiments. This will be considered again in the engine strategy investigation section.

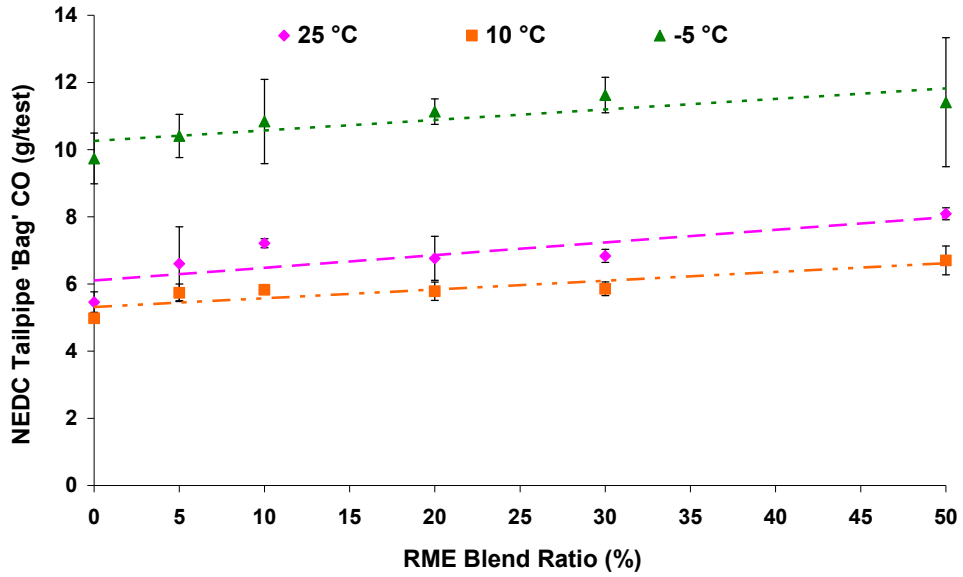

Figure 3.6, The impact of the biodiesel blend ratio and ambient temperature on the NEDC tailpipe bag CO emissions

The percentage increase in CO emissions for B50 fuel blend is about 30% at 25°C compared to baseline diesel fuel. Similarly, the increase in CO emissions for both 10° and -5°C experiments were about 20%, and 15% respectively with a greater than 95% confidence that the means of the baseline diesel and B50 data are statistically different at 25°C and 10°C and 90% confidence at -5°C. This is an unexpected result since oxygenated fuels are more likely to lead to complete combustion and a reduction in CO,

HC, and PM emissions. Even though the experiments at -5°C produced the highest amount of CO, the percentage increase as the biodiesel blend increases is the lowest.

At -5°C the spray atomization of the fuel will be much worse than at higher temperatures, due to higher kinematic viscosity, incomplete combustion of the fuel is more likely to occur causing higher CO emissions to form. On the other hand, to explain the general increasing trend of CO emissions with the addition of biodiesel in the fuel, a close look at the fuel specification is required. The CN of the RME is slightly lower than the baseline diesel (see Table 3.2), which may slightly affect the start of combustion as the concentration of RME in the fuel increases. The second possible reason can be related to the high concentration of unsaturated fatty acid composition of the RME fuel (see Table 3.3). The un-saturation levels will significantly affect the kinematic viscosity of the RME especially at low temperatures, and could cause poor atomization of the fuel in the combustion chamber. Poor atomization of the fuel can create more fuel rich zones in the cylinder leading to more incomplete combustion. Also, poor atomization could cause a rise in mean droplet diameter of the injected fuel (as discussed in the literature review), or an effective retardation of the injection timing by means of longer injection durations. This situation is caused by larger percentage pedal position from the driver necessary to compensate for lower calorific values of the biodiesel blended fuels and to achieve the required torque levels. The justifications related to the fuel specification might not be the main reasons for having higher tailpipe CO emissions with increasing biodiesel ratio in the fuel. Further investigations related to fuel combustion and engine strategies are required in order to explain this result.

The continuous second by second analyses of the CO emissions from the raw exhaust (pre-catalyst) was also investigated. A clear trend could not be seen from the pre-catalyst data, see Figure 3.7, but the pre-catalyst emissions show a slight decrease with increasing blend ratio although this decrease was not deemed to be statistically significant when analysed using a t test. The amount of CO emissions produced by the engine in both 25°C and 10°C ambient temperatures are very similar with all fuel blends, but the difference in the tailpipe emissions was very clear.

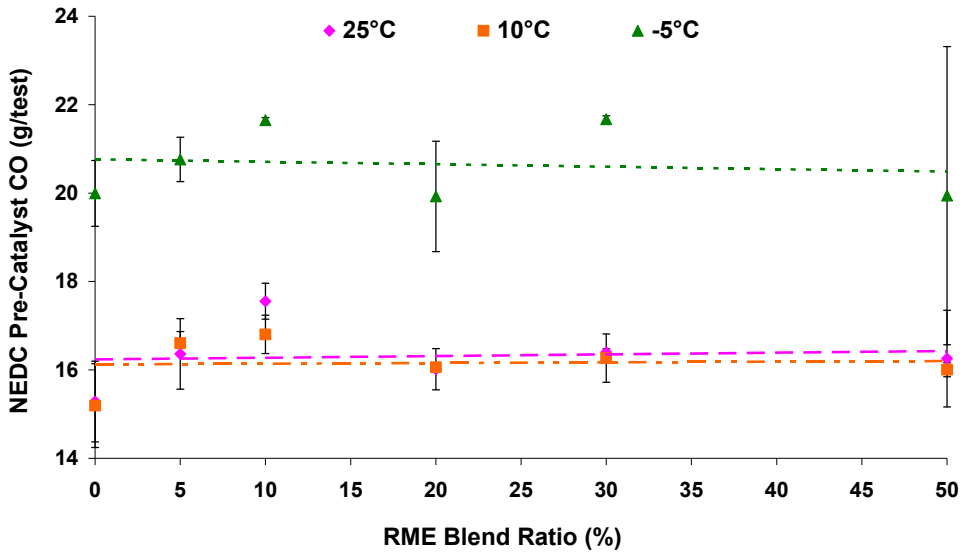

Figure 3.7, The impact of the biodiesel blend ratio and ambient temperature on the NEDC pre-catalyst CO emissions

To analyse the difference in pre-catalyst and tailpipe CO emissions, the average oxidation catalyst conversion efficiency needs to be investigated. This investigation will be discussed in the catalyst performance section 3.5.6.

3.5.2 NEDC THC Emissions

Figure 3.8 shows the THC emissions over the NEDC cycle for all different biodiesel fuel blends at all three ambient temperatures. As with tailpipe CO, HC emissions do not show a large reduction with increasing blend ratio and, on the contrary, at an ambient temperature of 25°C a slight increase is observed. The t test results, however, suggest that there is no statistically significant change in tailpipe THC emissions between baseline diesel and B50 fuel blend. The lowest THC emissions were recorded during the 25°C experiments and the highest during the -5°C. This statistically insignificant change might be due to the very low THC emissions of diesel engines, close to the lower detection limit of the analyser detectors.

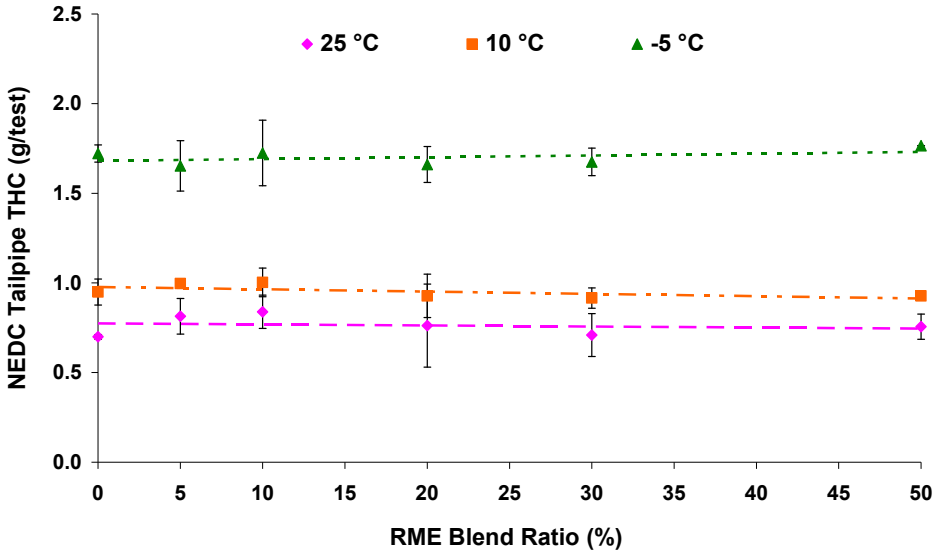

Figure 3.8, The impact of the biodiesel blend ratio and ambient temperature on the NEDC tailpipe THC emissions

Combustion pressure and heat release profiles would be very helpful to investigate the actual combustion difference with the use of biodiesel fuel blends in the vehicle, which unfortunately is not available. The pre-catalyst THC emissions were also investigated in Figure 3.9, as in the case of CO emissions, pre-catalyst THC emissions did not exhibit the same upward trend with increasing blend ratio seen at the tailpipe and, instead, a reduction trend was observed.

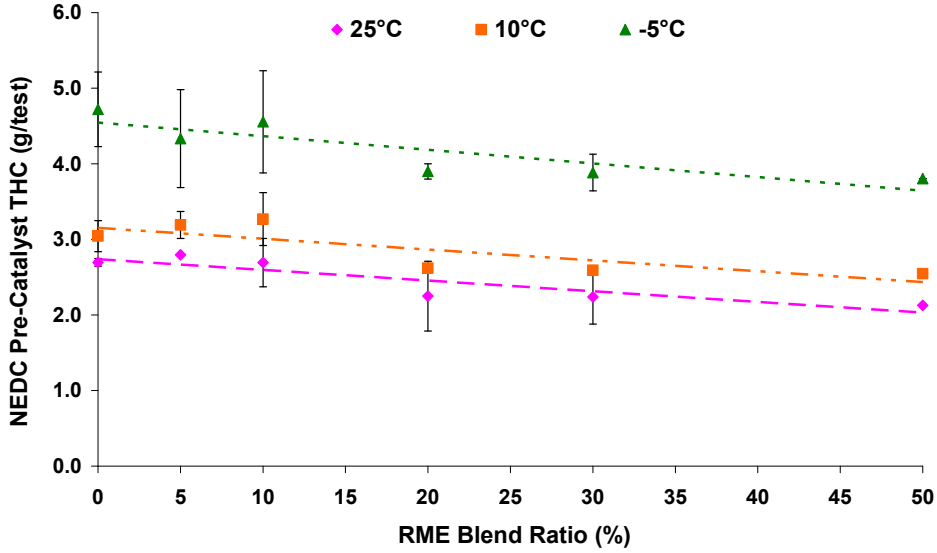

Figure 3.9, The impact of the biodiesel blend ratio and ambient temperature on the NEDC pre-catalyst THC emissions

The lower blends of biodiesel (B5 and B10) did not show significant change in engine out THC emissions at all ambient temperatures. However with higher blends, a reduction ranging from 20 to 25% in cycle THC mass was observed regardless of ambient temperature with a confidence level greater than 95%. The reduction in engine out THC emissions with increasing blend ratio was not reflected in the tailpipe emissions as seen in Figure 3.8. Again these observations will require more investigations into the catalyst performance which will be discussed in section 3.5.6.

3.5.3 NEDC NO_X Emissions

The tailpipe NO_X emissions for all fuel blends and ambient temperatures are plotted Figure 3.10. A slight increase in the NO_X emissions as the portion of biodiesel increases in the fuel blend is observed, and this generally agrees with most of the published literature. Also as the cell ambient temperature increases the amount of NO_X emissions produced increases.

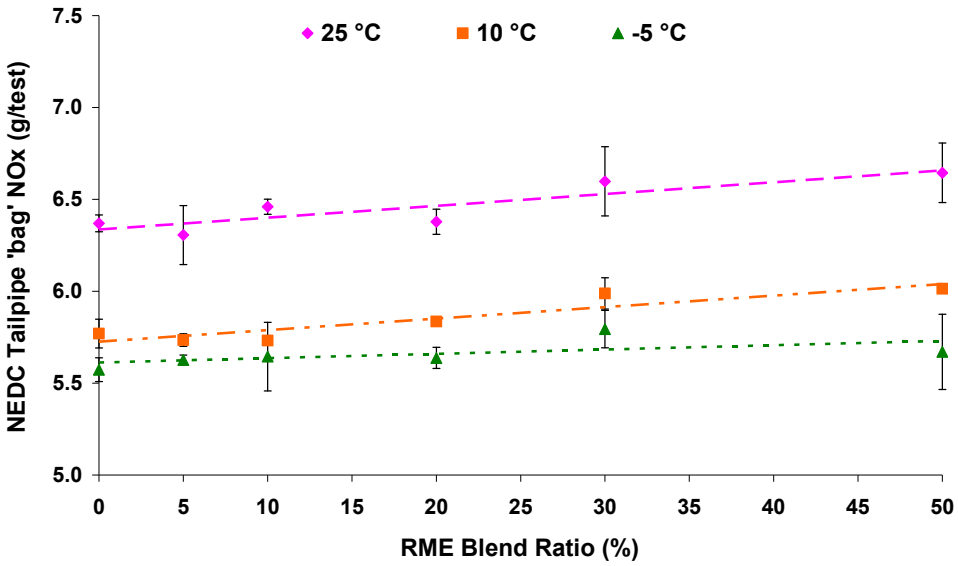

Figure 3.10, The impact of the biodiesel blend ratio and ambient temperature on the NEDC tailpipe bag NO_X emissions

The percentage increase in NO_X emissions compared to baseline diesel fuel is about 4% for B50 fuel at 25°C and 10°C ambient temperatures. At the -5°C ambient temperatures

the B50 fuel blend produced only 2% more NO_X compared to baseline diesel fuel, and statistical analysis confirmed 95% confidence in the increase in NO_X emissions at 25°C and 10°C between baseline diesel and B50; however, the increase at -5°C was not found to be significant. These results confirm that the NO_X formation is highly dependent on the in-cylinder temperature, and the ambient temperature is found to be more significant than increasing blend ratio. Furthermore, no significant change in NO_X emissions were observed with the low biodiesel blends (B5 and B10) during all ambient conditions. The main reason for higher NO_X emissions with biodiesel fuels is the higher oxygen content in the biodiesel fuel which increases the like hood of NO_X formation. Another explanation cited in the literature, is the lower heat transfer by the soot emitted from the use of biodiesel could lead to higher flame temperatures and more NO_X production during combustion. The percentage increase in NO_X emissions observed in this trial agrees with most of the published literature.

The engine out NO_X emissions showed very similar values and trends to the tailpipe 'bag' results (see Figure 3.11) since very little conversion by the diesel oxidation catalyst is expected.

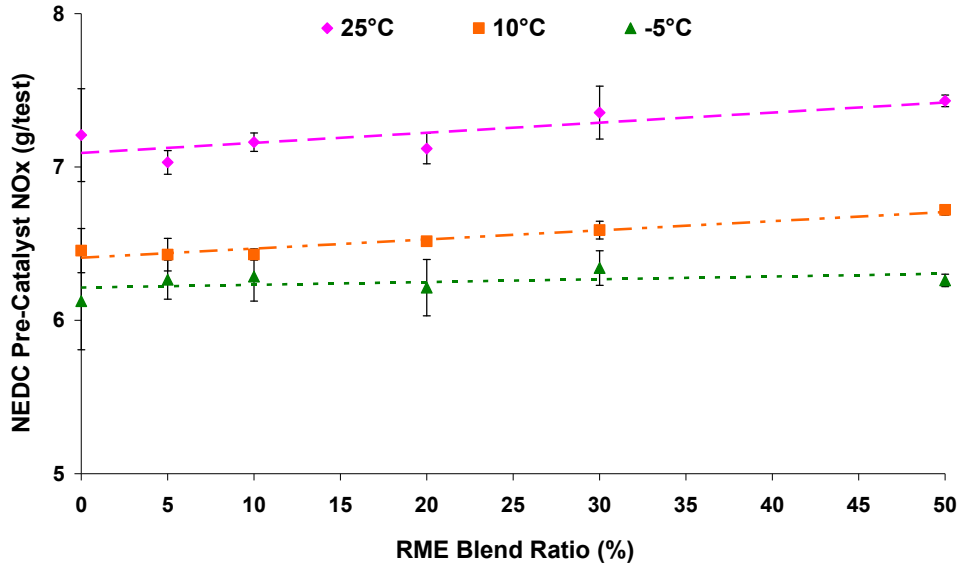

Figure 3.11, The impact of the biodiesel blend ratio and ambient temperature on the NEDC pre-catalyst NO_X emissions

A linear increase with increasing blend ratio (4.7% at 25°C and 10°C, with the t test confirming 95% confidence) was observed, but the impact becomes less significant at an ambient temperature of 25°C (0.5%, not deemed to be statistically significant). These percentage changes in NO_X emissions mirror those seen at the tailpipe as the catalyst is not designed for NOx conversion and instead relies on passive NO_X reduction and, as such, only small conversion efficiencies are observed.

3.5.4 NEDC PM Emissions

PM emissions were measured in this trial by two methods, gravimetrically by sampling a portion of tailpipe exhaust (TEOM) and by measuring the smoke opacity of the exhaust gas. It is generally reported in the literature that, as the percentage of biodiesel increases in the fuel, the amount of PM emissions decreases. This is because biodiesel contains more oxygen, which will allow faster and more complete combustion compared to fossil diesel fuel. Also, it does not contain any aromatics and Sulphur, which will reduce the production of Polycyclic Aromatic compounds.

Figure 3.12 describes the trend of tailpipe PM emissions measured using the TEOM. It is known that TEOM measurements are susceptible to moisture, leading to errors in the obtained results, and this is immediately noticeable by the larger scatter (and error bars) than were observed for other emissions species. A general downward trend is apparent at ambient temperatures of 25°C (16.5% reduction) and 10°C (3.3% reduction) for the B50 biodiesel blend compared to baseline diesel while a trend reversal occurs at -5°C, resulting in an increase in particulate mass (6.5% increase). A t test confirms 95% confidence in the reduction in PM at 25°C, but the changes at 10°C and -5°C were not found to be statistically significant.

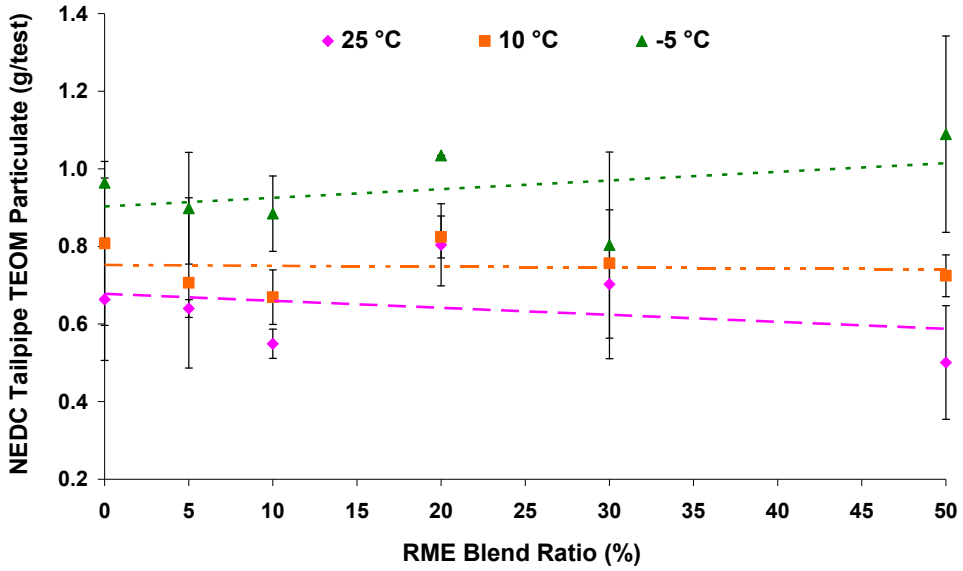

Figure 3.12, The impact of the biodiesel blend ratio and ambient temperature on the NEDC tailpipe PM emissions

The smoke opacity readings were integrated on a second-by-second basis in order to quantify any changes in smoke emissions. The accumulated smoke opacity with different RME blends are presented in Figure 3.13 and a general trend of smoke reduction can be clearly seen as the portion of biodiesel increases in the fuel.

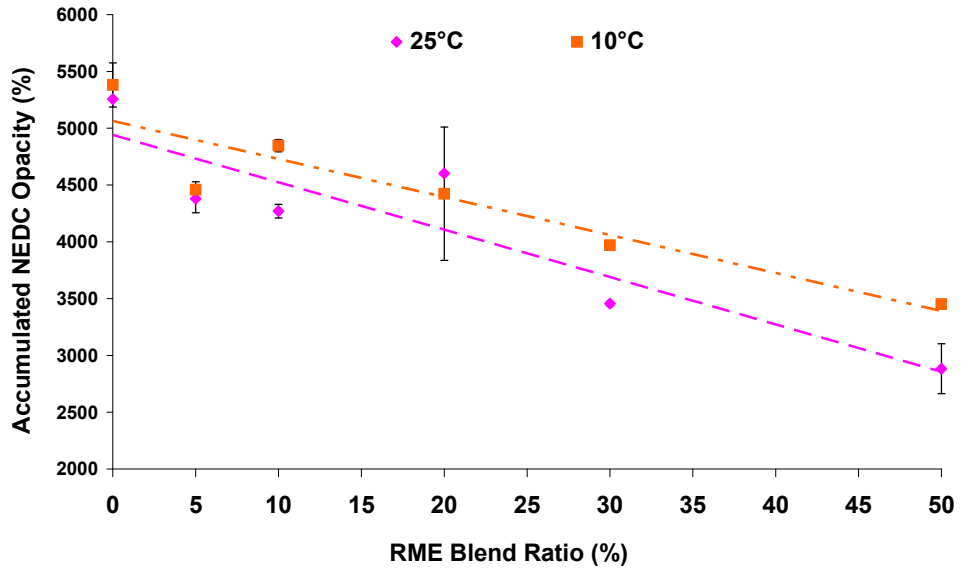

Figure 3.13, The impact of the biodiesel blend ratio and ambient temperature on the NEDC tailpipe opacity

The B50 fuel blend reduced the smoke opacity by 45% and 36% in the 25°C and 10°C ambient temperature experiments respectively. Unfortunately, the smoke opacity could not be measured during the -5°C ambient conditions due to equipment limitations.

The increase in PM emissions at the low ambient temperature and higher biodiesel concentrations are probably a result of the cold flow properties of biodiesel. The effect of higher viscosity and reduced atomization of biodiesel could be distinguished during these high concentration and low temperature experiments. At these conditions, even the higher oxygen content of biodiesel fuel could not overcome the reverse effects of cold flow properties. This observation needs to be further investigated and further experiments are required to have more confidence in these results since no published work could be cited which examined very low experimental ambient temperatures.

3.5.5 Engine Strategy Investigations

To closely visualise the combustion process, the cylinder pressure and heat release profiles are required. However, further information can be drawn by looking at the engine map transition for both baseline diesel and B50 fuels (see Figure 3.14). The plot shows clearly that the engine is warming up slightly faster in the case of B50 fuel blend compared to the baseline diesel fuel.

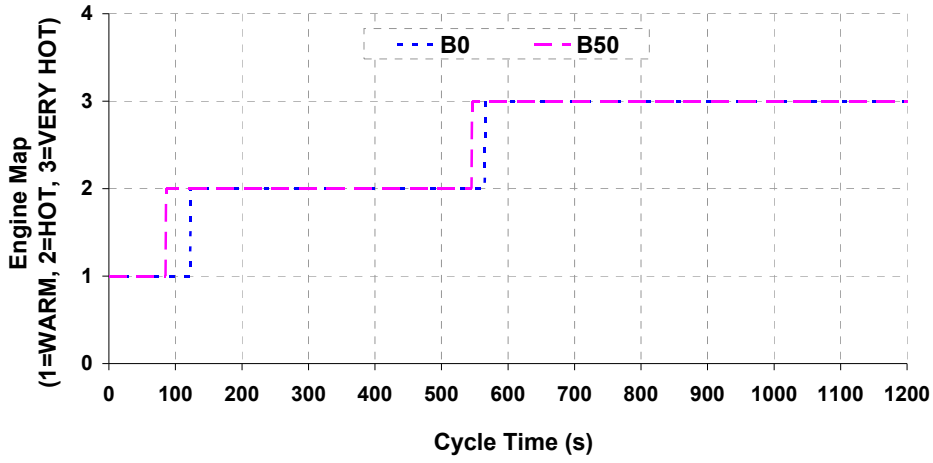

Figure 3.14, Impact of B50 biodiesel on Engine Map Transition (NEDC 25°C ambient Temperature)

The quicker engine warm up is probably due to slightly retarded combustion caused by reduced atomization and slightly lower CN of the RME. In addition there was likely to be increased combustion duration as the portion of biodiesel increases in the fuel due to a larger volume of fuel needing to be injected to compensate for the reduced energy content.

The retarded combustion could not be caused by a change in injection timing delay resulting from higher kinematic viscosity of RME, since the vehicle is equipped with a common rail fuel injection system. However, with higher fuel viscosity, longer injection duration is required to deliver the higher demanded mass of fuel. Figure 3.15 demonstrates the effect of B50 biodiesel on integrated pedal position (as with smoke opacity measurement, second-by-second data was integrated to quantify differences).

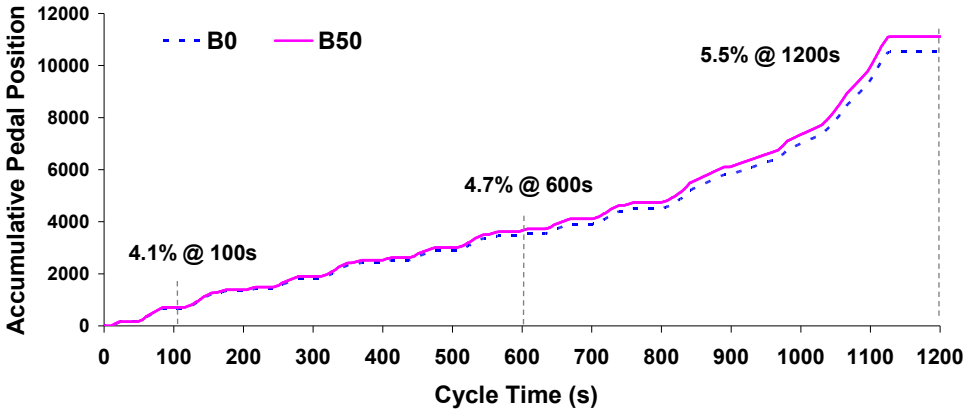

Figure 3.15, Impact of B50 Effect RME on Cumulative Pedal Position (NEDC 25°C ambient Temperature)

The increase in the accumulative pedal position with B50 blend is an indication of longer duration of fuel injection. With B50 fuel blend, a 5.5% increase in pedal position was required compared to baseline diesel fuel in order to inject the required amount of fuel.

The expected slightly retarded combustion and increased injection duration could lead to an increase in the emissions of HC and CO, since it reduces the time available for completing the combustion. This explanation can also be used to explain the earlier discussion about the unexpected increase in CO emissions with increasing RME in the

fuel. This increase in injection duration might be the reason behind the quicker map transition with B50 biodiesel fuel blend in figure 4.15. The timing of both pilot and main injections was also investigated, but it was difficult to see any change or trend when biodiesel fuel was introduced, due to transient nature of the drive cycle.

On the other hand, the effect of varying only the ambient temperature on the engine map transition is investigated; Figure 3.16 shows the impact of ambient temperature on engine map transition for baseline diesel fuel. During both 10°C and -5°C ambient temperatures the engine started in the COLD map strategy but at 25°C the engine started in the WARM map. The largest portion of the cycle time is spent in the HOT map for the 10°C ambient temperatures, while at the 25°C conditions the majority was in the VERY_HOT map. Cold-start strategies incorporating temperature-dependent engine maps dictate injection timings (pilot and main injection) as well as EGR rates and, as a result, increasing ambient temperature does not necessarily lead to a reduction in CO emissions. This may explain why, during this study, the engine calibration resulted in the lowest measured CO mass over the drive cycle being recorded at 10°C and not 25°C.

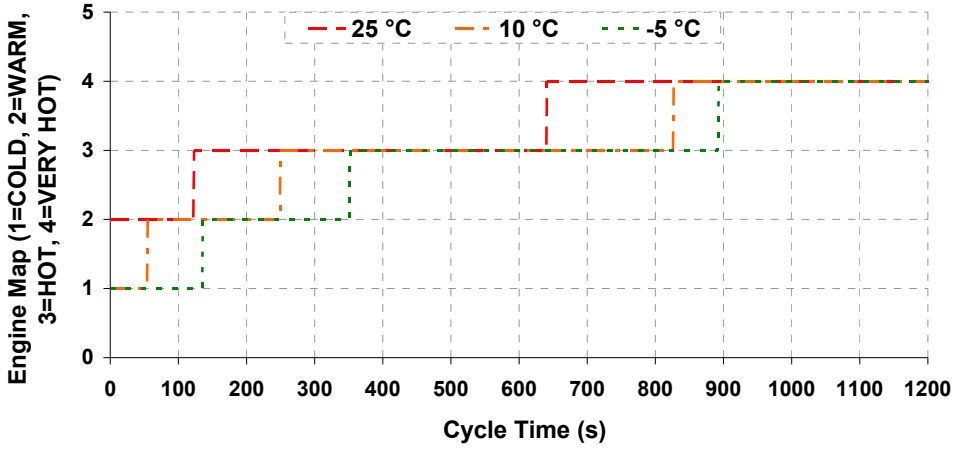

Figure 3.16, Impact of Ambient Temperature on Engine ECU Map Transition

3.5.6 Catalyst Performance Investigations

3.5.6.1 Catalyst Conversion Efficiency

The oxidation catalyst used with diesel engines can achieve a significant reduction of CO and HC emissions but the pure oxidizing environment of the exhaust gas suppresses the possibility of efficient NO_X removal [133]. However, limited NO_X conversion efficiency can be achieved within a narrow catalyst temperature range dependant on the availability of sufficient HC concentrations in the exhaust gas to act as a reducing agent (often defined in terms of the HC/NO_X ratio) in a process called passive de-NO_X [134-136]. The principle of passive de-NO_X is based on NO_X reacting with HCs on the catalyst surface instead of oxygen in locally rich regions, and this mutual annihilation offers removal of these two emission components [137].

By comparison of continuous pre-catalyst and tailpipe emissions concentrations, the instantaneous catalyst conversion efficiency was calculated and compared for different blend ratios and ambient temperatures over the complete NEDC. The NEDC catalyst conversion for CO emissions of all blend ratios and ambient temperatures are presented in Figure 3.17, where a general decreasing trend as percentage of biodiesel increases in the blend can be clearly seen.

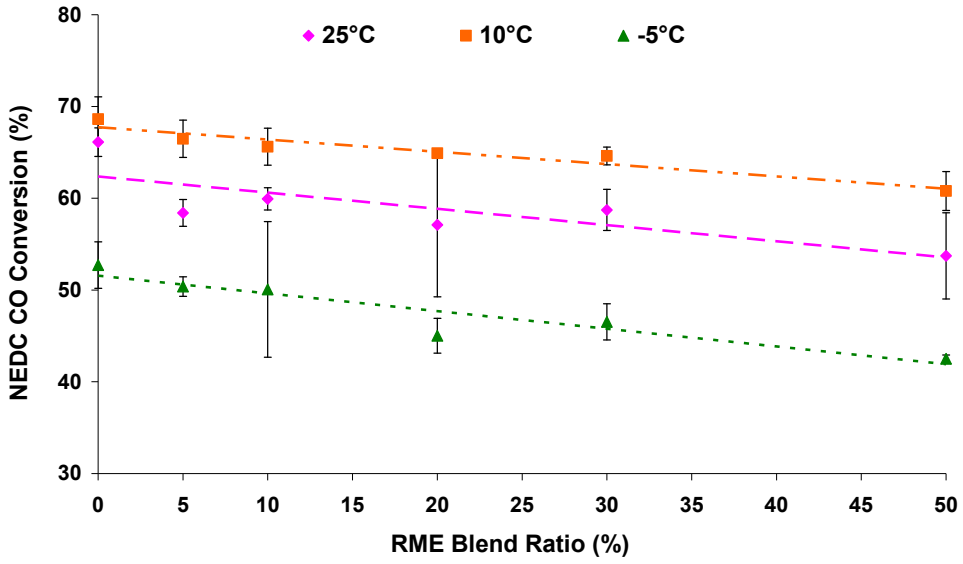

Figure 3.17, NEDC CO Catalyst Conversion Efficiency

When comparing the baseline diesel and B50 fuel blends, the average CO conversion efficiency dropped by 14%, 10%, and 18% at 25°C, 10°C, and -5°C ambient temperatures respectively. The highest conversion efficiency was recorded during the 10°C ambient temperature experiments. This explains the lower tailpipe CO emissions from the 10°C ambient temperatures even though the engine out CO emissions was similar to those of the 25°C ambient temperatures (see Figure 3.7). To further investigate the reason for having higher CO conversion efficiency during the 10°C ambient experiments, engine strategy transition with varying ambient temperatures was investigated.

During all 25°C ambient temperature experiments, the engine transits to the very hot strategy slightly quicker than the 10°C experiments. The very hot strategy adjusts the engine calibration towards lower NO_X emissions by retarding the injection and increasing EGR rate, which could lead to an increase in the CO emissions. Also, quicker transition when the catalyst is not hot enough, might lead to a higher percentage of CO break through in the case of the 25°C ambient temperature tests. A relatively cold catalyst will not oxidize engine out emissions efficiency, and so CO, THC, and NO_X to some extent will all be emitted from the exhaust pipe in significant amounts and cause the well known (cold start) problem.

Similarly Figure 3.18 shows decreases in NEDC THC catalyst conversion efficiency of 10%, 9%, and 18% at 25°C, 10°C, and -5°C respectively. NO_X conversion efficiency did not show and changes or trends with different fuel blends and ambient temperatures. The average NO_X Conversion efficiency ranged between 10-12% in this experimental procedure. The results obtained from this study indicate that the average catalyst performance efficiency dropped as the percentage of biodiesel increases in the fuel and as the ambient temperature reduces. These values represent the average conversion efficiency over the entire drive cycle. Further break down of the CO conversion efficiency relative to cycle time was investigated for baseline diesel and B50 fuels at 25°C ambient conditions.

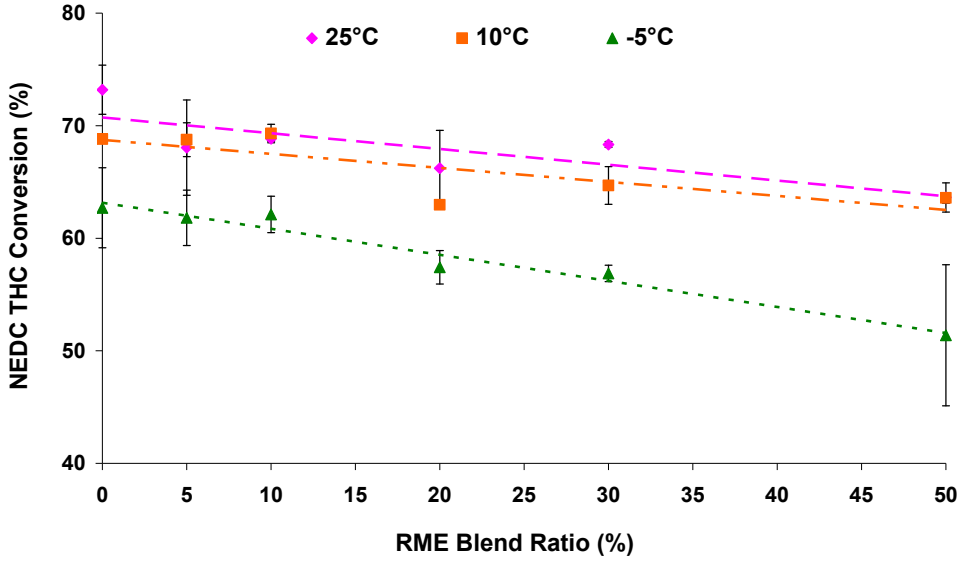

Figure 3.18, NEDC THC Catalyst Conversion Efficiency

Figure 3.19 shows histograms describing the proportion of cycle time spent at different CO conversion efficiencies for baseline diesel and B50 at 25°C. The use of B50 biodiesel reduced the proportion of the drive cycle where the catalyst was operating at greater than 50% efficiency compared with baseline diesel, however its proportion of time where the catalyst was operating at lower than 50% efficiency increased.

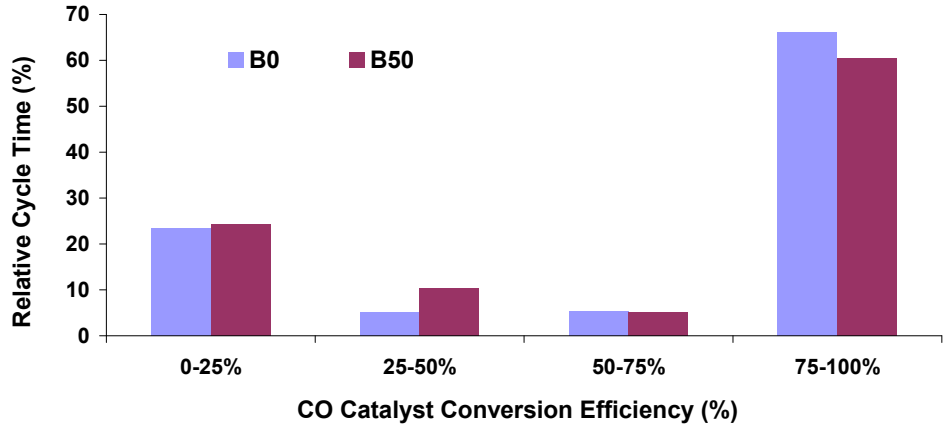

Figure 3.19, Catalyst CO conversion efficiency relative to cycle time

The distribution for both fuel types is biased towards the extremes of catalyst performance with the catalyst either almost fully converting and converting more than 75% of engine-out emissions or the catalyst is too cold to achieve any significant conversion, converting less than 25% of the CO to CO_2. Examination of the second-by-second CO conversion data suggested that for increasing biodiesel blends the catalyst achieved high conversion later in the drive cycle and periodically the conversion reduces down again during low power portions of the cycle. For baseline diesel the catalyst, once it started to convert, did not light down, suggesting that the heat transfer from the exhaust together with the heat released in the catalyst was sufficient to allow conversion to continue.

Similar to CO, the THC catalyst conversion efficiency operates for a lower proportion of cycle time at high conversion efficiencies for B50 blend compared to baseline diesel fuel. However, the distribution for THC shown in Figure 3.20 is significantly different from that seen for CO.

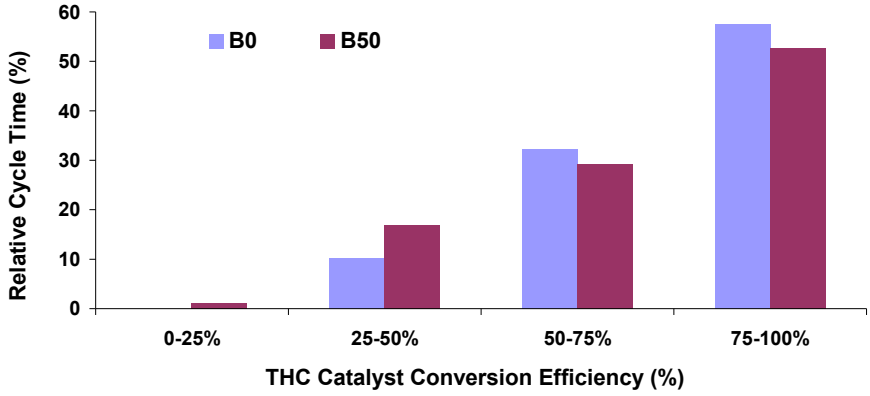

Figure 3.20, Catalyst THC conversion efficiency relative to cycle time

The THC conversion profile is heavily skewed towards the higher conversion efficiencies with relatively little time spent at lower conversion efficiencies. The diesel oxidation catalyst (DOC) is known to have the capability of storing HC emissions on the catalyst surface when cold until it is hot enough to evaporate all HCs [111]. When B50 is used, this trend is less marked, the proportion of time where conversion efficiency was high (50-100%) is reduced and operating time at lower efficiency (less than 50%) was increased

compared with baseline diesel. Further, for baseline diesel, THC conversion was always above 25%, and only fell below 50% conversion for 10% of the cycle. By comparison, 20% of the cycle had a conversion of less than 50% for B50.

The reduced catalyst performance efficiencies observed for CO and THC could be attributed to a change in the exhaust gas component concentrations and speciation, leading to a less favourable oxidation environment within the catalyst, or a reduction in the catalyst monolith temperature, but further work would be needed to establish the relative impact.

3.5.6.2 Exhaust Temperature Investigations

As discussed in section 3.5.6.1, the average catalyst performance efficiency reduced as the percentage of RME increases in the fuel. The second-by-second pre-catalyst gas temperature, for both baseline diesel and B50 biodiesel blend at the 25°C ambient temperature, is presented in Figure 3.21.

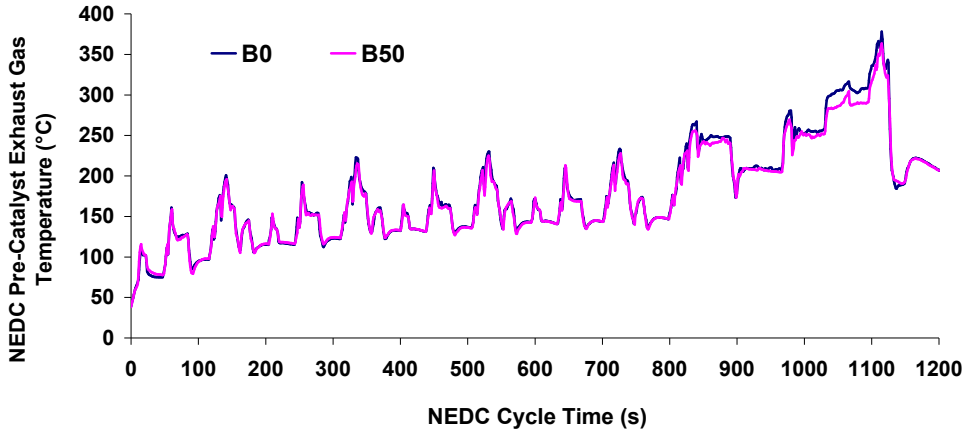

Figure 3.21, The impact of B50 biodiesel on NEDC engine-out exhaust gas temperature at 25°C ambient temperature

Figure 3.21 clearly shows that the exhaust gas temperature is always lower when the vehicle is running with B50 fuel blend compared to baseline diesel fuel. The variation in exhaust gas temperature marginally increases as the vehicle moves towards the higher load

portion of the cycle and the difference become even clearer. This reduction in exhaust temperatures is most likely caused by the lower calorific value of biodiesel fuel as discussed earlier, and it becomes more significant when higher power is demanded. The impact of all biodiesel blend ratios on the average NEDC pre-catalyst exhaust gas temperature in the 25°C ambient conditions was also investigated (see Figure 3.22).

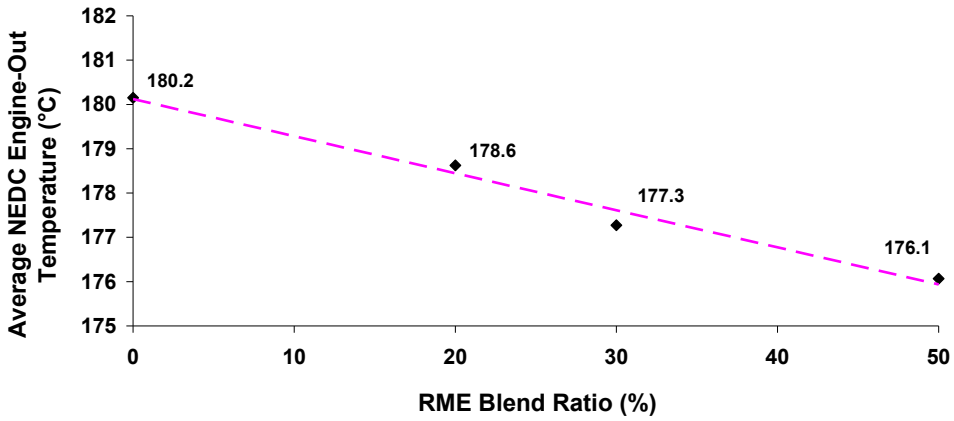

Figure 3.22, The impact of the biodiesel blend ratio on the average NEDC pre-catalyst exhaust gas temperature at 25°C ambient temperature

Figure 3.22 shows the variation in the average exhaust gas temperature at the catalyst inlet with increasing blend ratio for tests run under 25°C ambient conditions. It can be seen that increasing the blend ratio from 0% to 50% resulted in a 2.3% reduction in the average gas temperature. A reduction in energy available in the exhaust gas (manifesting as lower gas temperatures) with increasing blend ratio could account for the extended catalyst light-off times and reduced catalyst performance observed over the NEDC when using biodiesel. Furthermore, lower exhaust temperatures might have an effect on the performance of the variable geometry turbo charger which will be investigated in the full load experimental testing.

3.5.6.3 HC Speciation Investigations

Even though the conversion efficiency of the catalyst is mostly affected by the exhaust gas temperature, other factors such as the effect of different hydrocarbon species were

reported by several authors that might have an impact on the catalyst performance due to variations in light-off temperature [97, 111-115]. In this vehicle trial, an attempt to investigate the effect of different HC species from RME fuel on the catalyst performance will be performed by producing catalyst light-off curves.

The catalyst light-off curve is produced by plotting the continuous conversion efficiency of each emission species against catalyst temperature, by doing so any variations in the exhaust temperatures will be eliminated. However the transient nature of NEDC introduces a lot of challenges into performing this investigation, therefore only engine idling conditions were selected in order to ensure consistent exhaust flow values and gas residence times within the catalyst. Furthermore, the actual catalyst brick temperature could not be recorded during this experimental procedure but was approximated by the post catalyst temperatures which certainly introduces an additional error in the light-off temperature obtained, however this error should be consistent or still allow a comparison between blends. Figure 3.23 shows the CO catalyst light-off curves for both baseline diesel and B50 fuels.

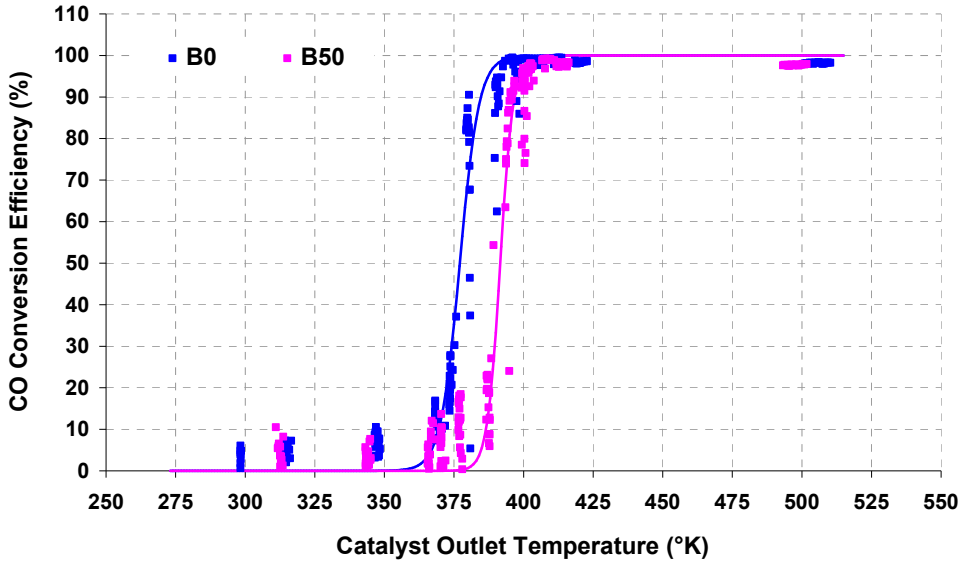

Figure 3.23, NEDC CO Light-off curve

A sigmoid function is used to fit the best curve, it can be seen that the rise in conversion for B50 fuel is delayed compared to baseline diesel, and the curve shift implies that the catalyst is influenced by different HC species. 50% CO conversion efficiency is reached at a temperature of about 380°K and 390°K for baseline diesel and B50 fuels respectively. In other words, at the same temperature, baseline diesel and B50 fuels will have different conversion rates when the gas temperature is between 373°K and 423°K (between 100°C and 150°C). This increase in catalyst light-off temperature with B50 biodiesel might explain the overall lower emission conversion efficiency when biodiesel fuel blends were used in the vehicle; however it requires more detailed and accurate investigations in order to draw solid conclusions.

3.5.7 Fuel Consumption (FC)

The AVL733 gravimetric fuel consumption results are presented, as these results were the most accurate with the lowest error range compared to other methods. Figure 3.24 demonstrates the impact of the blend ratio and ambient temperature on the total mass of fuel burnt during the NEDC compared to the baseline diesel fuel.

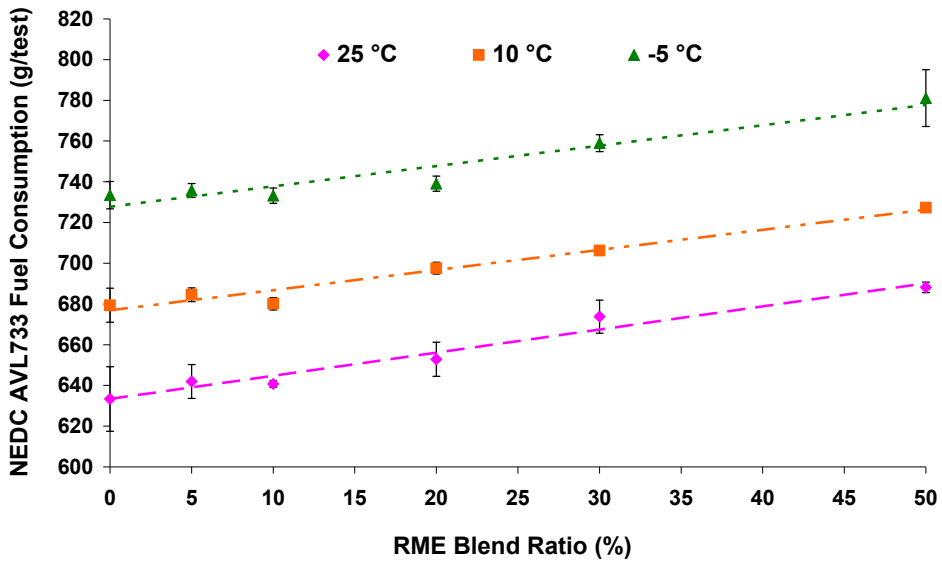

Figure 3.24, The impact of biodiesel blend ratio and ambient temperature on the NEDC fuel consumption using AVL733

The fuel consumption results were consistent at all temperatures and increased as the percentage of biodiesel was increasing in the fuel blend. The FC was measured by several methods in this experimental study, but the AVL733 gravimetric fuel consumption results were used in the discussion as it produced the most accurate results. The percentage increase in FC recorded with all measuring methods for all biodiesel blend ratios compared to baseline diesel fuel is presented in Table 3.5.

FC Measuring Method	RME Blend Ratio (%)				
	5	10	20	30	50
	Percentage Increase During 25°C Ambient Temperature				
AVL733	1.3	1.2	3.1	6.4	8.7
ECU Data	0.7	0.0	2.3	4.0	5.9
Pierburg Flow meter	1.5	-0.3	3.9	5.0	5.8
Carbon Balance (Bag)	1.1	3.7	3.8	6.0	7.9
	Percentage Increase During 10°C Ambient Temperature				
AVL733	0.8	0.1	2.7	4.0	7.0
ECU Data	0.9	-0.5	2.8	3.3	3.2
Pierburg Flow meter	1.5	1.2	3.3	2.1	3.3
Carbon Balance (Bag)	2.8	3.5	3.8	5.8	7.4
	Percentage Increase During -5°C Ambient Temperature				
AVL733	0.3	0.0	0.8	3.5	6.5
ECU Data	-0.8	-0.4	1.6	3.3	4.0
Pierburg Flow meter	-0.8	-1.2	-2.0	-0.2	3.3
Carbon Balance (Bag)	2.5	3.2	2.3	5.7	7.3

Table 3.5, Percentage increase in FC compared to baseline diesel fuel during NEDC

The low biodiesel fuel blends, B5 and B10, showed a negligible 1% increase in FC compared to the baseline diesel fuel in all ambient temperatures. The percentage increase in FC was within 1-3% for B20, and 3-7% for B30 fuel blends. It can be seen that the use of B50 fuel resulted in about 6%, 7%, and 9% increases in fuel consumption at -5°C, 10°C, and 25°C respectively (a t test confirmed 95% confidence that the differences were statistically significant). These increases in fuel consumption were substantially higher than would be expected on the basis of the calorific value of the fuels alone. The net calorific value of B100 used in this study is approximately 6% lower than the baseline diesel fuel (see Table 3.2). Therefore, only 3% reduction in calorific value is expected from the B50 fuel blend, other factors such as the physical properties of the biodiesel fuel accounting for the additional FC penalty. Poor atomization of the biodiesel fuel and larger Sauter mean diameter (SMD) due higher kinematic viscosity could lead to lower

combustion efficiency. This result generally agrees with most of the published literature about a slight increase in FC with the use of biodiesel fuel due to its lower calorific value, and improvements in fuel consumption could potentially be made via the optimization of the engine calibration as it will discussed during the full-load tests.

Next, the presence and significance of the interactions with different blend ratios and ambient temperatures from total NEDC cycle results were investigated, which is the second objective of this work.

3.5.8 NEDC Surface Response Model

In this section the significance of any interactions between the blend ratio and ambient temperature over the New European Drive Cycle (NEDC) will be identified by plotting a response surface model (RSM) of the DoE. The response models are based on the effect of biodiesel on tailpipe (bag) emissions and thus environmental impact. Figure 3.25 shows a response surface for CO in relation to ambient temperature and blend ratio derived from the experimental data.

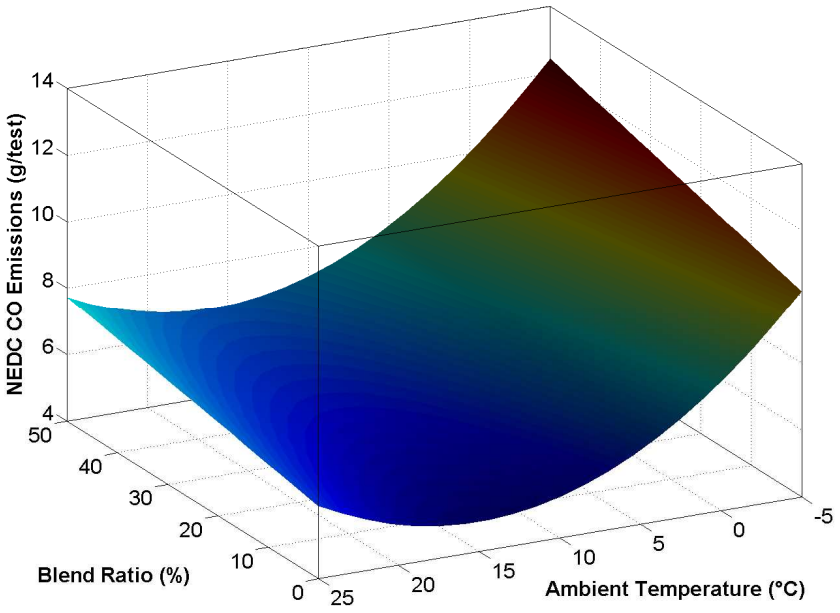

Figure 3.25, NEDC CO response

It can be seen that temperature is clearly the most dominant factor with cold start strategies, incorporating temperature dependant engine maps, impacting on measured CO mass emission over the drive cycle. Contrary to some other studies, CO was found to increase by more than 25% at 25°C with B50 fuel compared to baseline diesel. The higher adiabatic flame temperatures and the higher oxygen content present within methyl esters would be more likely to lead to complete oxidation of the fuel in the combustion process. The percentage increase in CO with blend ratio is similar across the temperature range with no significant compounded interaction between the inputs. Regardless of blend ratio, CO emissions were found to be lowest at an ambient temperature of 10°C.

Figure 3.26 shows the response surface for NEDC HC emissions. As with CO emissions, ambient temperature was found to be the most significant factor with blend ratio having minimal effect on total cycle HC emissions. At an ambient temperature of 25°C, there is a slight downward trend in HC with increasing blend ratio, however no significant impact is observed at 10 or -5°C.

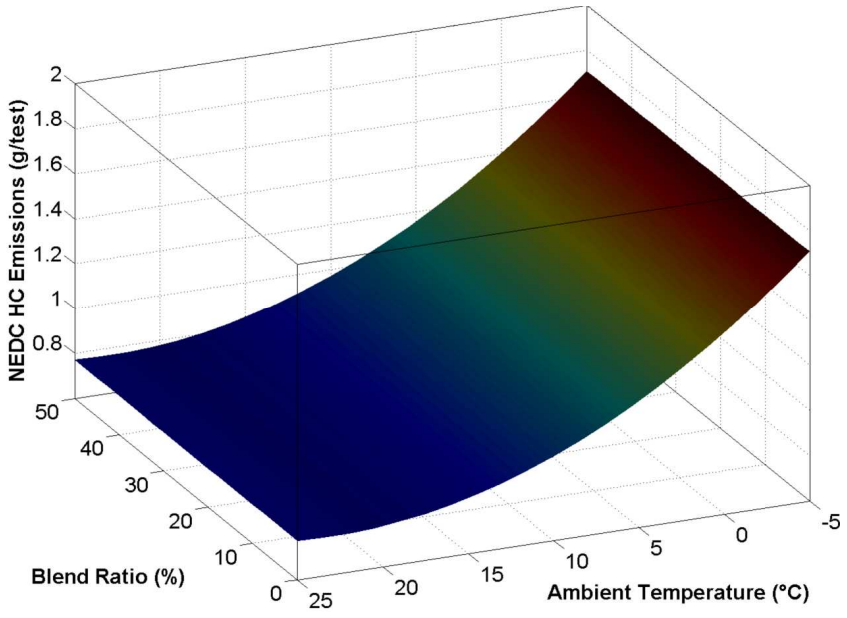

Figure 3.26, NEDC HC Response

Figure 3.27 shows the impact of temperature and blend ratio on NEDC cycle NO_X emissions. As observed in other studies, NO_X generally increases with increasing blend

ratio however; at low ambient temperatures this increase is very modest. The recorded increase in NO_X emissions with B50 is 5.5% at 25°C, and 1.2% at -5°C which is not statistically significant. The trend is far more pronounced at temperatures of 10 and 25°C, probably due to higher maximum cylinder temperatures under these ambient conditions.

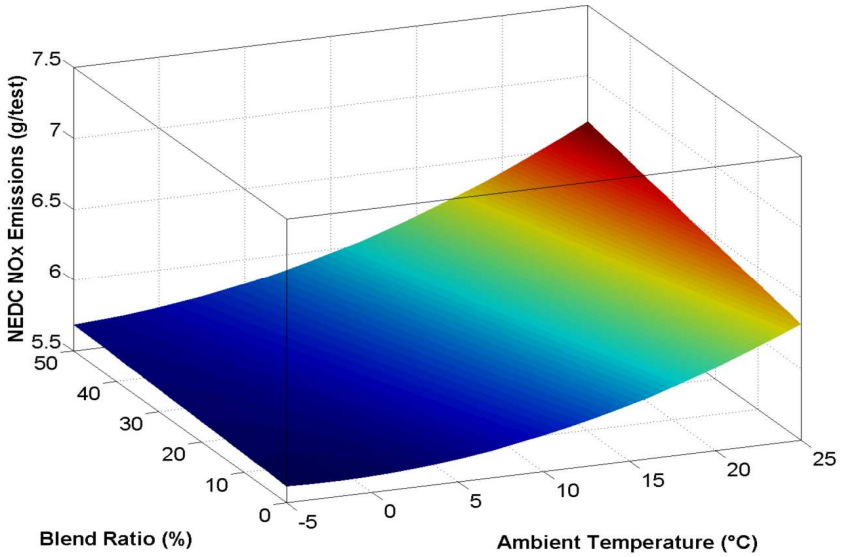

Figure 3.27, NEDC NO_X Response

The response surface for gravimetric particulate emissions (measure by TEOM) over NEDC is plotted in Figure 3.28. Unlike with some of the other emissions species responses, PM has a strong interaction between blend ratio and ambient temperature. Regardless of blend ratio, a decrease in ambient temperature leads to a large increase in particulates over NEDC cycle. However, this trend is most significant at higher biodiesel blend ratios.

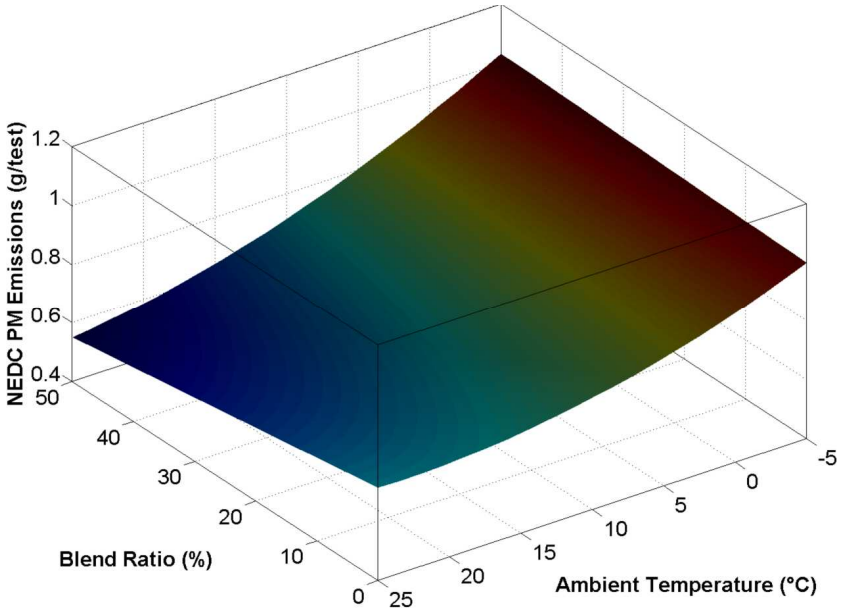

Figure 3.28, NEDC PM Response

At an ambient temperature of 25°C it can be seen that increasing the blend ratio leads to a decrease in PM emissions by 30%, however at 10° C blend ratio is observed to have very little effect and at -5°C the trend is reversed with an increase in blend ratio up to B50 resulted in a 3.5% increase in particulate emissions compared to baseline diesel fuel. Many factors affect the generation of PM within the combustion chamber such as fuel droplet size and degree of mixing between the injected fuel and the available air. Within common rail fuel injection systems the fuel is injected at very high pressure causing good atomization, and thus smaller droplet size and effective in-cylinder mixing. However, biodiesel has higher kinematic viscosity than conventional diesel fuel and it increases as the ambient temperature drops. At 25°C the additional oxygen contained within the biodiesel leads to more complete combustion of the fuel and reduces particulates with increasing blend ratio however, as the ambient temperature decreases this benefit is offset against significantly higher fuel viscosity leading to larger fuel droplet size and decreased atomization/mixing and increase in PM emissions.

Figure 3.29 shows how fuel consumption varies over the NEDC cycle. As was expected, ambient temperature has a substantial effect on fuel consumption at all blend ratios.

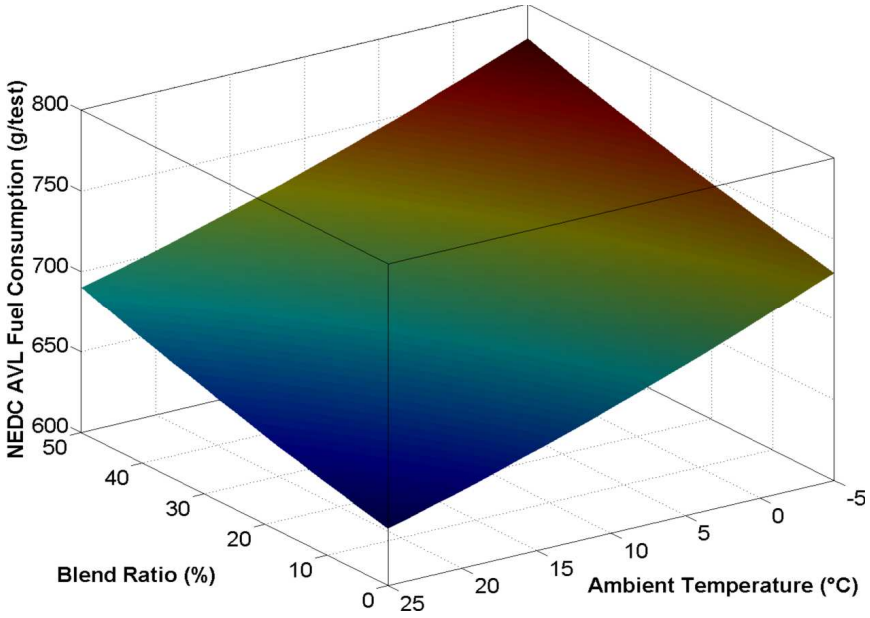

Figure 3.29, NEDC fuel Consumption Response

Also as the blend ratio increases so does the fuel consumption consistent with the lower calorific value of the biodiesel compared to conventional petroleum diesel leading the driver to demand higher pedal positions and larger fuel quantities in order to achieve the required torque. There appears to be no significant interaction between blend ratio and temperature with similar percentage change observed at 25 and -5°C. The expected fuel consumption penalty due to lower calorific value for B50 fuel is 3% compared to baseline diesel, however the actual measured increase was 5.1% for B50 suggesting other fuel specific factors must contributed to a loss in engine power rather than calorific value alone.

In section 3.6, the loss in vehicle power with increasing biodiesel blend ratio and changes in ambient temperature when the vehicle is operated under full load conditions is discussed.

3.6 Full Load Results

The developed full load method described in section 3.3.2 was used to investigate the effect of biodiesel on vehicle performance at high engine load conditions. The change in tractive force at different engine speeds when the vehicle is fuelled with varying blends of biodiesel and baseline diesel is quantified, and a preliminary investigation is conducted in order to offer explanations of the observed trends.

3.6.1 Dynamometer Tractive Force

The calorific value of the biodiesel used in this study is approximately 6% lower and the kinematic viscosity is 65% higher than the baseline diesel fuel. As the blend ratio was increased, the energy available per unit volume of fuel decreased; thus, under the full-load operating conditions experienced during this cycle, where injection durations are fixed (100% pedal), less energy was available per injection event.

The impact of biodiesel blend ratio on the measured dynamometer tractive force at 30 km/h, 50 km/h, and 80 km/h are given in Figure 3.30, Figure 3.31, and Figure 3.32 respectively. As would be expected, an increase in the blend ratio leads to an approximately linear reduction in the maximum tractive force at any given vehicle speed or temperature, with this trend exaggerated for the higher vehicle speed condition. At each vehicle speed, the absolute value of the tractive force decreases with increasing ambient temperature potentially because of an increase in the air and fuel density and improved intercooler efficiency at lower temperatures. Therefore, the 25°C ambient temperature trials always have the lowest measured tractive force even though the effect of physical properties of RME biodiesel should be less significant at this temperature compared to the other colder conditions. Also, it can be seen that the decreasing trend in tractive force during the -5°C ambient temperature tests with increasing blend ratio is slightly more pronounced especially 30 and 50 km/h.

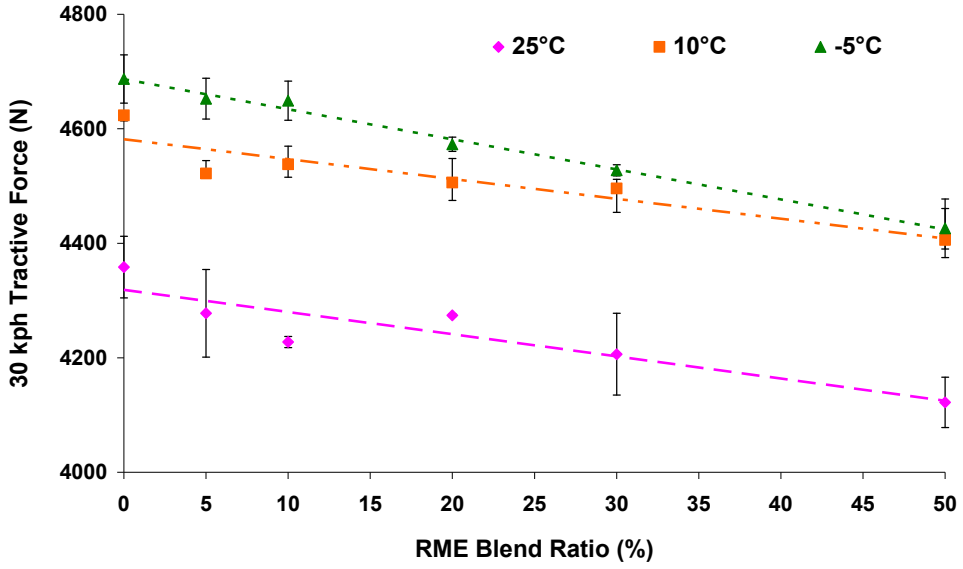

Figure 3.30, The effect of the biodiesel blend ratio and ambient temperature on the maximum tractive Force in third gear at 30 km/h

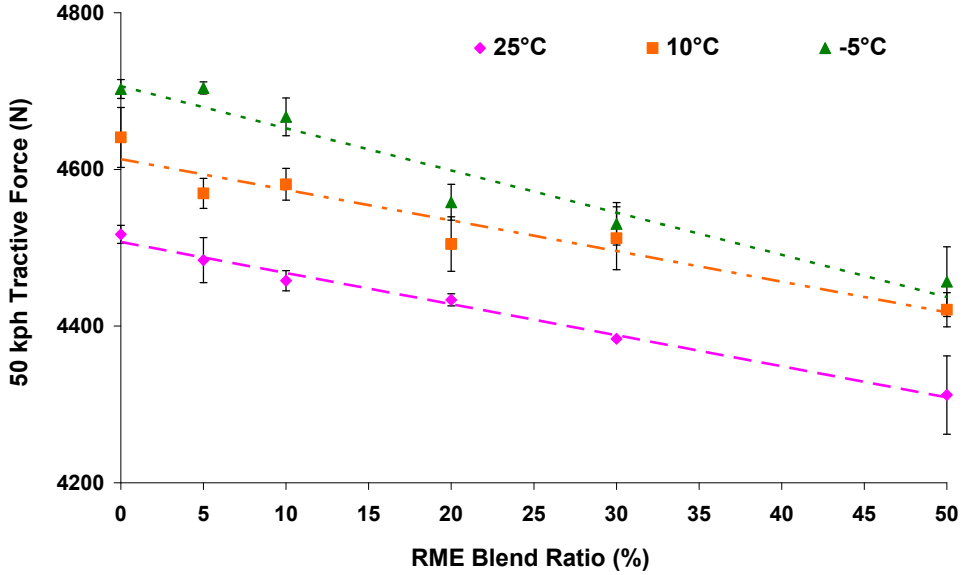

Figure 3.31, The effect of the biodiesel blend ratio and ambient temperature on the maximum tractive Force in third gear at 50 km/h

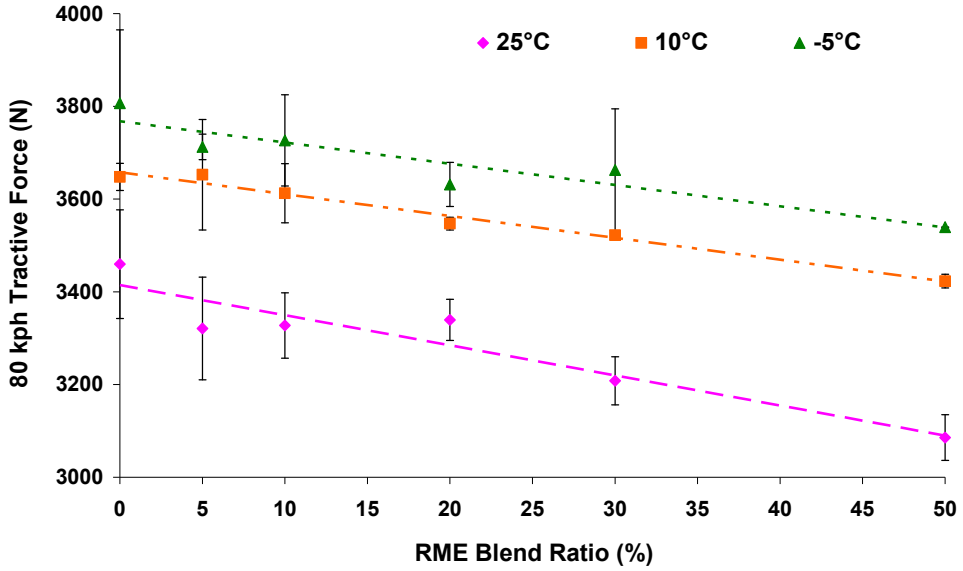

Figure 3.32, The effect of the biodiesel blend ratio and ambient temperature on the maximum tractive Force in third gear at 80 km/h

To further analyse the results, the percentage reduction in dynamometer tractive force for all biodiesel blends relative to the baseline diesel fuel has been investigated and tabulated in Table 3.6. During the lower vehicle speeds of 30 km/h and 50 km/h, the percentage reduction in tractive force shows linear trend with increasing blend ratio and ambient temperature relative to baseline diesel fuel; however step change is shown for the 80 km/h speeds.

Tractive Force Reduction (%)						
30 kph	**B0**	**B5**	**B10**	**B20**	**B30**	**B50**
25°C	0.0	-1.9	-3.0	-1.9	-3.5	-5.4
10°C	0.0	-2.2	-1.8	-2.5	-2.8	-4.7
-5°C	0.0	-0.7	-0.8	-2.4	-3.4	-5.6
50 kph						
25°C	0.0	-0.7	-1.3	-1.9	-3.0	-4.5
10°C	0.0	-1.5	-1.3	-2.9	-2.8	-4.7
-5°C	0.0	0.0	-0.8	-3.1	-3.7	-5.2
80 kph						
25°C	0.0	-4.0	-3.8	-3.5	-7.3	-10.8
10°C	0.0	0.1	-1.0	-2.8	-3.4	-6.2
-5°C	0.0	-2.5	-2.1	-4.6	-3.8	-7.0

Table 3.6, Reduction in tractive force with biodiesel blends relative to baseline diesel fuel

As the reduction in the vehicle's tractive force is linear with increasing biodiesel blend ratio, the B50 results will be used for further discussion. Figure 3.33 clearly shows that the percentage reduction in tractive force with B50 biodiesel is highest at the 80 km/h vehicle speed and similar during both lower speed conditions. Also, varying the ambient temperature becomes far more significant at the 80 km/h vehicle speeds, which requires further investigation.

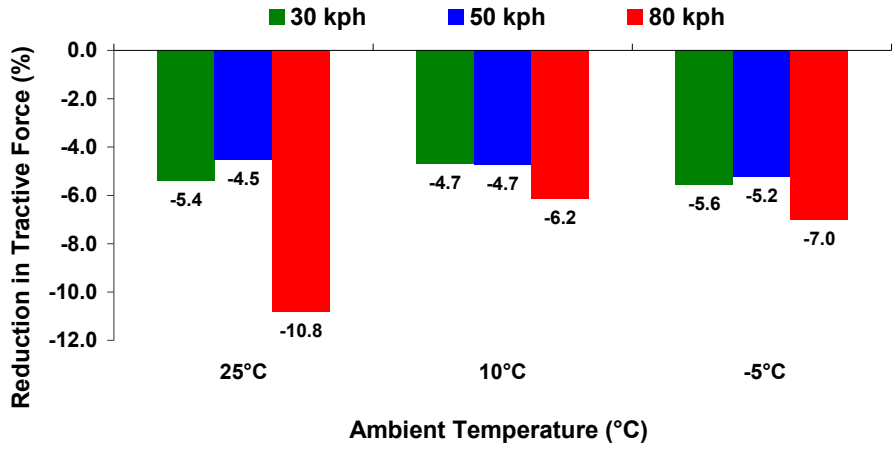

Figure 3.33, Reduction in Tractive force with B50 Biodiesel blend relative to baseline diesel

Further investigation revealed that the significant temperature dependant reduction in tractive force with increasing blend ratio observed at 80 km/h is attributed to a reduction in boost pressure (between baseline diesel and B50), and hence similar reductions in mass air flow and possibly fuel quantity. These issues will be further investigated in the next section.

3.6.2 Power Drop Investigation

With the lower calorific value of the B100 RME, it is expected that the B50 fuel will produce 3% less power compared to baseline diesel fuel. However, the drop in vehicle tractive force is more than 5% at lower speeds and reached more than 10% during the higher vehicle speed conditions and higher ambient temperatures. This suggests that, other than the LHV of biodiesel, some engine related factors are also affecting the overall

performance of the vehicle and causing larger reductions in tractive force as the load and ambient temperature increases.

The boost pressure of the variable geometry turbo-charger (VGT) was investigated for any variations with changing engine speed, biodiesel blend, and ambient temperature. Figure 3.34 plots the variations in boost pressure with respect to vehicle speed and ambient condition for baseline diesel, and B50 fuels. The 30 km/h, 50 km/h, and 80 km/h vehicle speeds correspond to engine speeds of 1450 RPM, 2420 RPM, and 3870 RPM respectively.

Figure 3.34 shows that the actual boost pressure achieved decreased with B50 biodiesel despite the fact that identical boost pressures are demanded by the VGT, and the differences are more exaggerated at higher engine speeds.

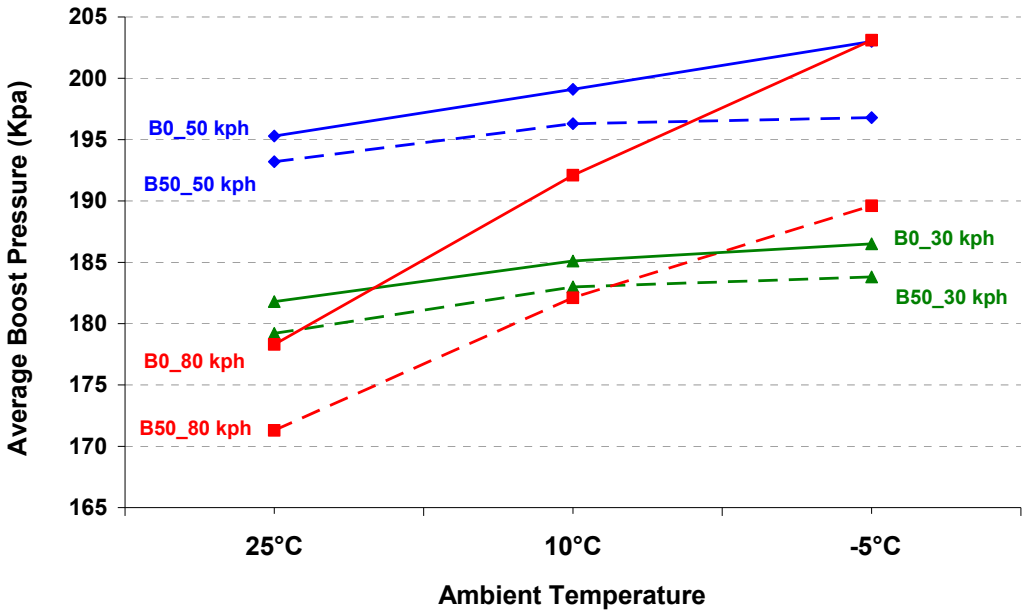

Figure 3.34, Average boost pressure for B50 biodiesel and baseline diesel fuel at different ambient temperatures engine speeds

The cause of the reduced boost pressure is unclear but it is speculated that the lower exhaust gas temperatures seen with biodiesel fuel could be a significant factor. The reduction in boost pressure with increasing ambient temperatures is probably caused by

the reduction in air density and consequently lower exhaust pressures which explains their lower average tractive force in Figure 3.33. Furthermore, reduced boost pressures will lead to a reduction in the amount of added fuel due to the engine control unit compensating for lower air density. This, in turn, explains the lower average tractive force as the ambient temperature and RME blend ratio increases. The effect of different ambient temperatures on the boost pressure is more significant during the higher speed conditions as is shows by the increased gradient of the line. The 50 km/h vehicle speed shows the highest boost pressure, which is probably because the engine speed of 2420 RPM is in the better efficiency region of the VGT performance compared to other engine speeds. This might explains the similar percentage reduction in tractive force to the lower speed conditions.

In addition to variations in VGT boost pressures, the mass air flow (MAF) is expected to vary with changing ambient temperature and fuel blend. The average MAF values with respect to vehicle speed and ambient temperature for all conditions for baseline diesel, and B50 fuels are presented in Figure 3.35.

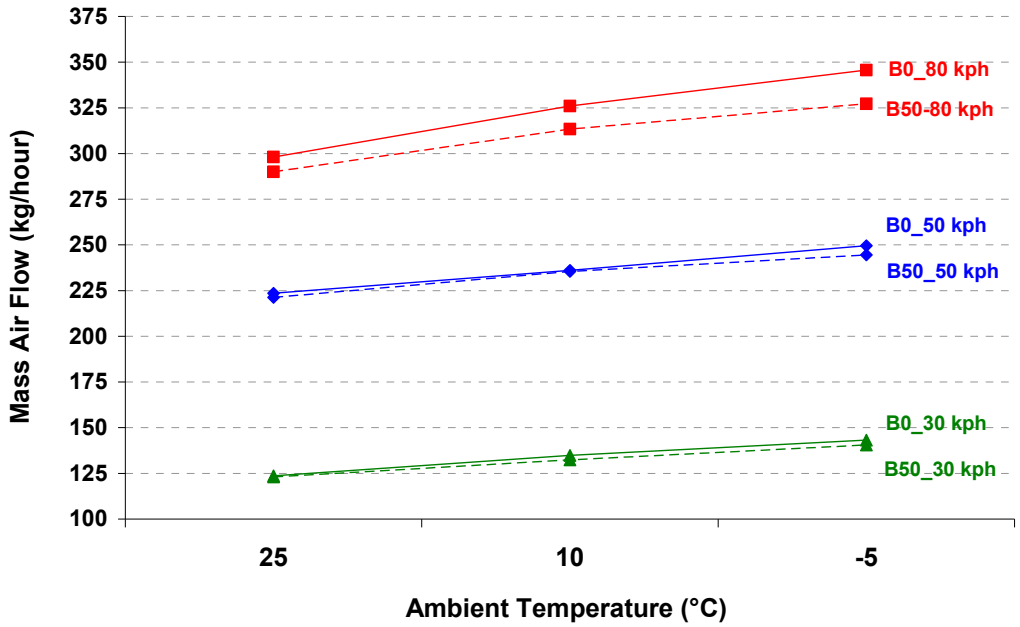

Figure 3.35, Average MAF for B50 biodiesel and baseline diesel fuel at different ambient temperatures and engine speeds

The MAF values increased as the ambient temperature reduced which explains the higher boost pressures during the -5°C ambient temperatures. The average MAF values for the biodiesel fuel blend is very similar to the baseline diesel fuel at 30 km/h and 50 km/h vehicle speeds. However during the 80 km/h vehicle speed, the difference in MAF values between both fuels becomes more significant which is caused by higher variations in boost pressure at this operating condition, see Figure 3.34.

In summary, as well as the lower calorific value of biodiesel fuel, the combustion characteristics also had a significant impact on engine performance. This effect highlights the complexity of engine calibration and the unexpected impacts and interactions which result from changes in fuel properties, as well as demonstrating the potential need for revised engine calibration strategies when using biodiesel.

3.7 Conclusions

A comprehensive vehicle trial with biodiesel and diesel blends was performed at the Chassis Dynamometer facility. The aim of the work was to investigate the effect of biodiesel fuel blends, from a known feedstock, on the emissions and performance of a production vehicle, with unmodified engine calibration, when operated with various biodiesel blends at different ambient temperatures. The following conclusions can be drawn from this work:

- The engine out (pre-catalyst) CO emissions reduced slightly with increasing biodiesel blend ratio at all ambient temperatures and THC emissions were found to reduce by 20–25% when then engine was operated on higher RME blends. Engine out NO_X emissions were observed to increase by approximately 4% at ambient temperatures of 25°C and 10°C but, at -5°C, the blend ratio becomes less significant and only a 0.5% increase was recorded.
- The tailpipe (post-catalyst) emissions of CO were found to increase with increasing RME blend ratio at all ambient temperatures, increasing by 15–30% for

B50 compared to baseline diesel fuel. No significant change was observed for tailpipe THC, despite the reductions in pre-catalyst emissions levels. This was attributed to the reduction in catalyst conversion efficiency with increasing blend ratio. The reduction in the catalyst performance is probably due to the decrease in the exhaust gas temperatures and an expected change in exhaust gas THC speciation as the blend ratio increases.

- The engine out exhaust gas temperature was found to be lower when the vehicle was running with biodiesel blends compared to baseline diesel fuel, demonstrating an inversely proportional relationship with the blend ratio. The average NEDC exhaust gas temperature for B50 reduced by approximately 4°C compared to baseline diesel fuel for tests run at 25°C ambient conditions.

- Tailpipe PM emissions were found to decrease with increasing blend ratio, reducing by 16.5% at 25°C and by 3.3% at 10°C when using B50 however, PM emissions increased by 6.5% at -5°C possibly because higher fuel viscosity led to larger injected droplet diameters and reduced spray atomization. Statistical analysis of PM emissions data suggested that variations observed at 10°C and -5°C fell within the range of experimental uncertainty,

- The B50 fuel blend reduced the smoke opacity by 45% and 36% at 25°C and 10°C ambient temperatures respectively.

- The fuel consumption was found to increase with increasing blend ratio at all ambient temperatures. B5 and B10 showed very little increase compared to baseline diesel, however the percentage increase ranged from 1-3% for B20, 3-7% for B30 and from 7-9% for B50 blends.

- Ambient temperature had the most significant impact on total NEDC emissions and fuel consumption, and no significant interactions between blend ratios and ambient temperatures with similar percentage change was observed except for the PM, which showed a strong interaction between blend ratio and ambient temperature.

- Increasing the blend ratio and ambient temperature decreased the test vehicle's maximum tractive force. This reduction was in the order of 5% for the B50 blend at low vehicle speeds and 6–10% at higher speeds compared to baseline diesel fuel.

However, it was noted that, under certain engine operating conditions, increasing the blend ratio had an impact on turbocharger performance, leading to a reduction in the boost pressure and corresponding decreases in the engine power and tractive force.

Discussion of this study suggested several additional areas which could be investigated in order to shed more light on the observed trends. The availability of cylinder pressure data could have provided substantial information to explain the impact of biodiesel fuel on the combustion process caused by fuel property variations which could explain emissions and temperature variations. Actual catalyst brick temperature could be measured to produce more accurate catalyst light-off curves in order to investigate HC speciation impact of biodiesel fuel on catalyst performance. Finally, the ability to modify the engine calibration could provide insights into the optimal engine calibration strategies when using biodiesel. The time requirements and expense of actual experimental programs promotes the use of simulation. It is unclear however if current simulation tools are capable of predicting the effects of biodiesel use on performance and emissions, therefore in the next chapter, the sensitivity of Ricardo WAVE software to changes in fuel properties and the subsequent effect on the combustion performance is reported.

Chapter 4 Biodiesel Engine Simulation

4.1 Introduction

Simulating the operation of internal combustion engines has become a key process in assessing new enabling technology and benchmarking performance in relation to emissions and fuel economy. Simulation reduces the amount of testing required to assess aspects of engine performance and is a critical tool in assisting design engineers to safeguard base engine durability as a result of new platform changes.

The aim of this work is to investigate the potential of engine simulation packages such as the Ricardo WAVE software package (WAVE Build 8.1) to asses the impact of changes in fuel properties, for biodiesel, on simulated combustion performance. To achieve the aim of this study, the following steps were followed:

- Determine the relevant fuel properties which are used in the WAVE combustion model and identify the combustion quality factors.
- Obtain from literature, the required biodiesel fuel properties to be inputted into the model.
- Set up the Ricardo WAVE simulation using a pre-validated Ford 2.0 l engine model with engine experimental parameters.
- Design a DoE plan to asses the sensitivity of the combustion model to changes in the fuel properties.
- Plot the response models and identify the fuel properties that are most significant.

4.2 Ricardo WAVE Software

Ricardo wave software is a 1-D gas dynamics simulation package used worldwide in automotive industry, the ability to model diesel combustion processes in a robust and reliable manner within WAVE is particularly useful since it characterises most engines

very well [139]. WAVE is capable of analyzing the dynamics of pressure waves, mass flows, and energy losses in various components of internal combustion engine flow network, and it is provided with a user friendly interface that allows users to build models of the entire engine flow system by selecting the appropriate components from a toolbox and connecting them by piping elements [116]. It has three combustion models as standard: "Wiebe", "Diesel Jet" and "Profile" in addition to an emissions prediction model.

WAVE operates by running through three primary programs, pre-processors, solvers, and post-processors [141]. The pre-processors are programs used to set up the simulation by using relevant input values, and then it converts the data into a format suitable for the solver, the solvers then analyse the data provided by the pre-processors. Post processors are programs used to view and interpret the results provided by the solvers [116]. In the next section, the relevant fuel properties which influence the combustion model in Ricardo WAVE will be investigated.

4.3 WAVE Model Sensitivity to Fuel Properties

As discussed in the FAME properties section 2.3 of chapter 2, the chemical and physical properties of biodiesel are totally different to baseline diesel fuel. The length of the carbon chain and number of double bonds (un-saturation level) of the fatty acids will vary the physical and molecular properties, which will directly affect the overall combustion performance of biodiesel and subsequently overall performance and emissions. In order to assess the sensitivity of the Ricardo WAVE diesel engine model to the biodiesel fuel properties, several combustion and fuel evaporation factors were selected that were expected to be most affected by these properties.

Fuel Evaporation Process

The droplet mean diameter (DMD) of fuel leaving the injectors is a measure of fuel evaporation and atomization. In fuel combustion applications, Sauter Mean Diameter (SMD) became the most common measure in fluid dynamics as a way to estimate the

average droplet size. It was originally developed by the German scientist, J. Sauter in the late 1920s. It is defined as the diameter of a sphere that has the same volume, surface area ratio as a particle of interest [117]. This factor was selected to investigate the sensitivity of WAVE's evaporation models on different fuel properties.

Fuel Combustion Process Quality

The factors selected to represent the combustion quality are start of combustion (SOC), exhaust temperature (T_{exh}), maximum cylinder pressure (P_{max}), maximum cylinder pressure angle (P_{maxA}), maximum cylinder temperature (T_{max}), and maximum cylinder temperature angle (T_{maxA}). These are the most common factors generally used in the majority of diesel studies to describe a simplified combustion process. In the next section, the required fuel properties are identified with selected values.

4.3.1 Fuel properties

4.3.1.1 Selecting Fuel Properties

Several fuel properties are used by WAVE to create custom fuel types in addition to the air composition and the ability to select multiple fuels to create a blended fuel mixture. These properties are listed in the programmes fuel editor panel (see Figure 4.1).

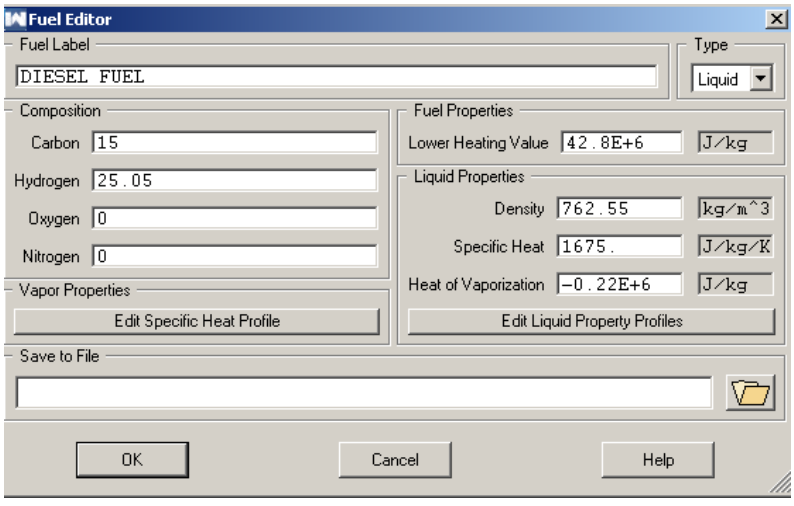

Figure 4.1, Fuel Editor Panel in WAVE Build

The selected fuel properties that were varied in this study are listed below:

1. The chemical composition of the fuel in terms of Carbon, Hydrogen, Oxygen and Nitrogen content
2. Lower heating value (LHV)
3. Density
4. Specific heat
5. Heat of vaporization
6. The cetane number

In addition to a single value entry at the simulation ambient temperature, values for the following properties with varying temperature were required:

7. Specific heat
8. Vapour pressure
9. Kinematic Viscosity
10. Surface tension

4.3.1.2 Fuel Property Values

The selection of fuel property values was based on the idea of covering the entire range of fuel types by including both the low end and the high end of diesel and biodiesel fuels. This scenario was defined to emphasise the sensitivity of the WAVE model to any of the selected fuel properties. Properties of various biofuel types are not as readily available in open literature as those of baseline diesel fuels; therefore, a great deal of literature was investigated in order to determine a range of properties that covers the vast majority of biodiesel types (see section 2.3 of chapter 2).

4.3.1.2.1 Chemical Composition Values

The selection of the range of values was based on the literature survey conducted in chapter 2, such that most of the known diesel and biodiesel fuels chemical composition should fall within this range [7]. The atomic composition of baseline diesel fuels contains

a mixture of hydrocarbons depending on the method of production. Most of the molecules in No.2 diesel fuel have between 10 and 22 carbon atoms per molecule and often the average molecular composition is used in combustion models. The average molecular composition for No.2 diesel fuels varies between 14-16 carbons, 20-34 hydrogen atoms, and zero oxygen atoms [121-123].

In the case of biodiesel fuel, the composition depends on the fatty acid (FA) profile of the fuel. The discrepancies seen in engine performance tests from various researchers are, in part, a result of variations in physical properties of different biodiesel fuels [7]. The chemical composition of biodiesel is far simpler than baseline diesel fuel since it contains only five or six different FA, whereas fossil diesel fuel contains variously long hydrocarbon chains and aromatic compounds. The percentage of the different FA in fats or vegetable oils varies depending on the feedstock, which will have a direct impact on the properties of the fuel. The chemical and physical properties of the various individual FA, as well as the effect of molecular structure will determine the overall properties of biodiesel fuel. The values chosen to represent both the low end and the high end of diesel and biodiesel fuels chemical compositions are presented in Table 2.1.

Atoms	Lower	Higher
Carbon (C)	12	18
Hydrogen (H)	20	40
Oxygen (O)	0	2

Table 4.1, Chemical composition value range used in the WAVE model [118-127]

4.3.1.2.2 Physical Properties Values

Similar to the chemical composition, the fuel's physical property values were selected to cover the lowest and the highest possible values of both diesel and biodiesel fuels. The adopted range of values are based on the literature survey, given in section 2.3 of chapter 2 and [118-127], are presented in Table 4.2.

Property	Lower	Higher
LHV (J/kg)	35	45
Density (kg/m^3)	800	900
Specific Heat Capacity (J/kgK)	1500	2200
Heat of Vaporization (J/kg)	-0.2E^6	-0.35E^6
Cetane Number	46	60

Table 4.2, Fuel physical properties value range used in the WAVE model [118-127]

4.3.1.2.3 Temperature Profiles

Obtaining a single property value at ambient simulation conditions, such as those given in Table 4.2 was not particularly challenging compared to obtaining an array of data at varying temperatures. As discussed in the literature review, the properties of all fuel types, more specifically biodiesel, vary significantly as the temperature changes. Furthermore, the fuel property variation among each biodiesel fuel type is also very significant. These properties are usually required for fuel combustion modelling, but the wide range of temperatures required for these properties makes the data difficult to obtain. A comprehensive literature survey was conducted in order to obtain data profiles of liquid fuel properties, such as, specific heat, vapour pressure, viscosity, and surface tension with varying test temperature [118-126, 140-144]. An average profile was developed to represent the lower and higher limit values for diesel and biodiesel fuel properties.

1. **Specific Heat Capacity**

It is generally known that the specific heat of biodiesel fuels is higher than baseline diesel fuels, and there is a progressive increase in specific heat as the temperature rises [143]. The specific heat capacity profile used in this study with varying temperature is given in Figure 4.2, only the first two points of specific heat capacity of biodiesel could be obtained from literature [144]. The rest of the trend profile was estimated proposing a linear increase with temperature.

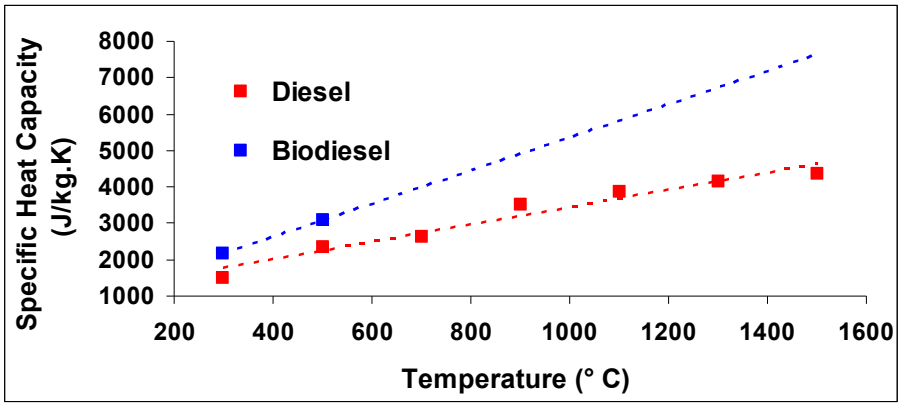

Figure 4.2, Specific heat capacity profile used in the WAVE model [118-126, and 140-144]

2. Vapour Pressure

The vapour pressure increased with raising temperature and it is generally higher for diesel fuels compared to biodiesel [124]. Unlike baseline diesel fuel, only four points of vapour pressure with varying temperature for biodiesel fuel could be obtained from literature [120-124] see Figure 4.3. The variation in vapour pressure becomes more noticeable as the fuel temperature increases above 373 K (100°C) as reported by Chakravarthy et al. [143], therefore the first two points in the graph corresponding to temperature range between 400-500 K were estimated closely to follow the actual trend.

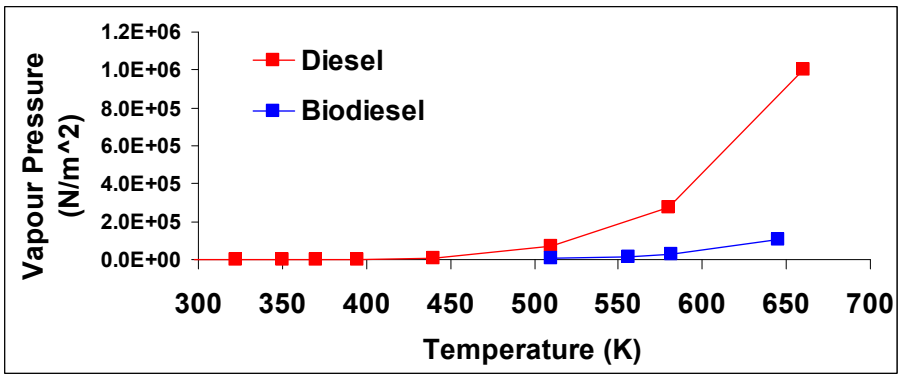

Figure 4.3, Vapour pressure profile used in the WAVE model [118-126, and 140-143]

3. Viscosity

The third fuel property profile required by the WAVE model is viscosity. Viscosity is a measure of internal friction between liquid molecules [120]. As discussed in the literature review section 2.3 of chapter 2, biodiesel fuels have higher viscosity than baseline diesel.

Not like other fuel properties, viscosity values of biodiesel fuels with varying temperature were reported in several studies [120-126, 140-144]. Figure 4.4 shows the average viscosity profiles of diesel and biodiesel types and clearly shows that variations in fuel viscosity is an issue since most of the engine fuelling systems operate within 300-400 K temperature range depending on climatic conditions.

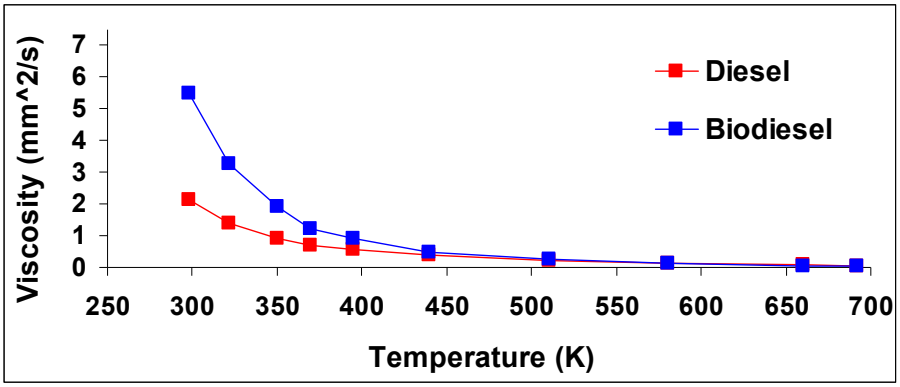

Figure 4.4, Viscosity profile used in the WAVE model [120-126, 140-144]

4. Surface Tension

It is generally known that biodiesel fuels have slightly higher surface tension values than baseline diesel fuel, and it decreases with increasing temperature [124]. The surface tension profile used in this study with varying temperature is given in Figure 4.5, similar to specific heat capacity only few points could be obtained from literature [121-124, and 144-143]. The rest of profile was fitted with a linear curve that estimates the variation in surface tension with temperature.

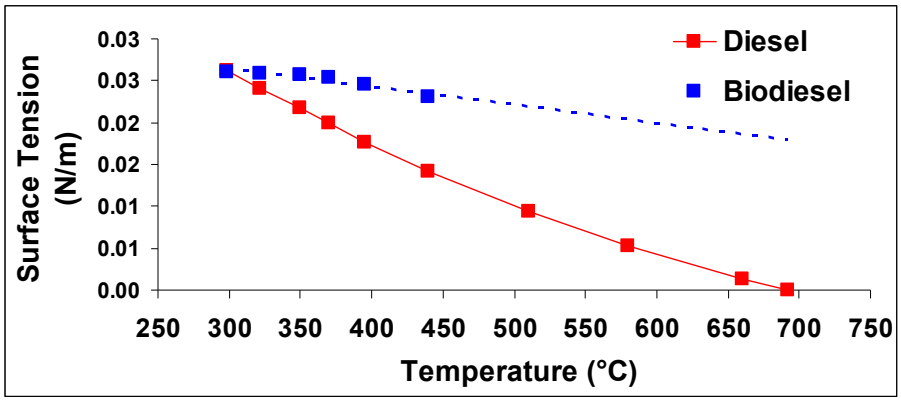

Figure 4.5, Surface tension profile used in the WAVE model [121-124, and 144-143]

4.3.2 Simulation Set Up

4.3.2.1 Engine Model

The engine model used for this study represents Ford 2.0 litre, four cylinder compression ignition engine. This engine model had already been experimentally validated with an existing Ford PUMA 2.0 litre engine using baseline diesel fuel by the Ford Motor Company at the University of Bath. The only change applied to this model is the removal of the variable geometry turbocharger and compressor units in order to simplify the simulation and reduce the running time but to compensate, inlet and exhaust conditions were set to match experimental data as if the turbocharger was fitted. To reduce the effect of residual gas content and temperature, the exhaust gas recirculation (EGR) ratio was set to zero value. The full engine specifications are listed in Table 4.3.

Specification	Value
Bore x Stroke (mm)	86.0 x 86.0
Number of Cylinders	4
Total Displacement (cm^3)	1998.23
Compression Ratio	16.0
Engine Type	Diesel
Fuel Injection system	Common Rail DI
Clearance Height (mm)	1.0

Table 4.3, Engine model specification

The procedure to setup the simulation for the purpose of this work was straightforward since the model had already been constructed. The basic model used in this study is presented in Figure 4.6.

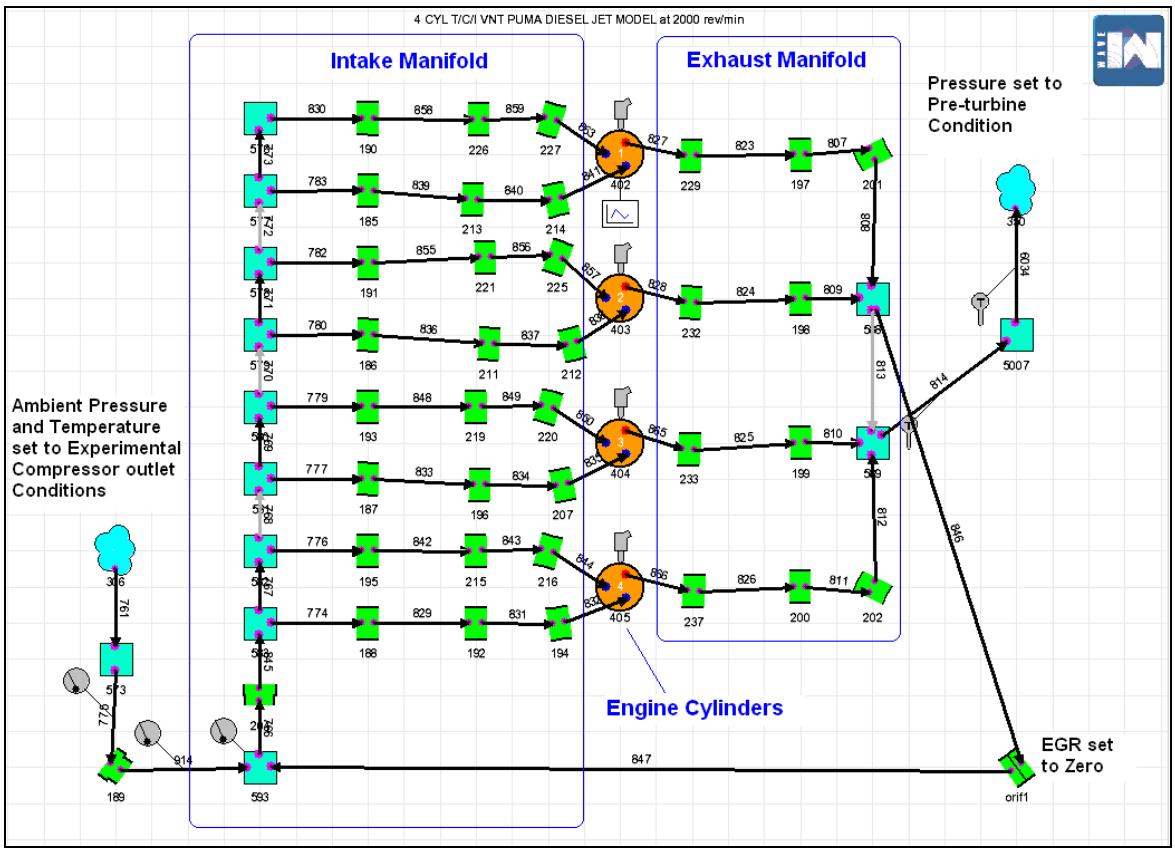

Figure 4.6, Basic Model for 2.0 l PUMA engine supplied by Ford

Figure 4.6 shows a complete engine model in WAVE build which consists of a series of icons which represent engine components. These icons are linked together by a series of ducts and junctions which represent sections of the intake and exhaust manifolds, and all specifications and physical properties are entered directly into the modules. The middle part of the model indicates the four cylinders and fuel injectors attached. The left side icons show the ambient air and the air intake system through the intake manifold. Exhaust gas is pumped into the exhaust ducts and combined in the exhaust manifold as shown on the right side of the cylinders.

The objective of this work was to asses the sensitivity of the Ricardo WAVE software package to changes in fuel properties, so steady state engine conditions were selected at two different engine speeds and loads. The first simulation condition was set at 2000 RPM engine speed and 147.5 Nm load, which represents a low-mid engine speed with medium load conditions. The second condition of 3000 RPM and 230 Nm represents a mid-high engine speed and high engine load condition. The next step was to create the fuel files for the different fuels under investigation to be inputted into the WAVE model.

4.3.2.2 Creating Fuel Files

The fuel properties obtained earlier in section 4.3.1 were inputted into the WAVE model by creating custom fuel files. The first step of creating the fuel files was to specify the ambient air composition in the "fuel and air properties" panel [117]. Then the custom created fuel files for each fuel under investigation are called, to retrieve the fuel property data, for the engine combustion model via the general parameters panel in the main WAVE input file. The remainder of the engine combustion parameters required to run the WAVE model were obtained experimentally on the engine test bed, and these are discussed.

4.3.2.3 Experimentally Obtained Data

Several operating parameters are required before running the WAVE combustion model, such as fuel injected quantity, start of injection timing, injection pressure and duration, intake and exhaust pressures and temperatures. Therefore, it was necessary to operate the engine at specified steady state conditions in order to obtain the required data. The engine was operated with baseline diesel fuel until reaching normal operating temperature and the required data were collected, see Table 4.4. Other inputs, which were also derived experimentally, for input into WAVE, are included in the following table:

Testing Condition	2000 RPM 147.5 Nm	3000 RPM 230 Nm
Fuel Demand (mg)	25.63	44.1
Start of Injection (° ATDC)	1.31	-3.73
Injection Duration (deg)	7.6	20.5
Injection Pressure (bar)	1131	1320
Intake Temperature (K)	336	334.2
Intake Pressure (bar)	1.72	2.56
Exhaust Pressure (bar)	1.95	2.73

Table 4.4, Experimental data recorded for input into the WAVE model

4.3.2.4 Running the WAVE model

Requesting output plots

After setting up the model and loading all fuel properties and profiles, the simulation was run and the results obtained from the WAVE output files. WAVE incorporates a post processor for all WAVE simulations and enables visualization and report generation. In this study, the output plots selected from this simulation are listed below:

1. Heat release rate
2. Accumulated heat release
3. Cylinder pressure
4. Cylinder temperature

Inputting fuel Injection parameters

All injector specifications were supplied with the validated model and no changes were necessary. The fuel injector type selected for this work delivers a specified amount of fuel per injection event, following a user defined flow profile [127]. The mean fuel drop diameter is set to "Auto" to allow automatic calculation within the combustion model. The initial fuel injection velocity was set to "Auto" allowing WAVE to calculate the instantaneous injection velocity from injection rate and nozzle size. The user defined profiles of injection rate and pressure can be loaded through the profiles tab of the cylinder injector type editor. An injection profile vs. crank angle is required as input, and then WAVE scales these profiles to match the experimental load and conditions. The injection profiles for the steady state simulation were developed based on the engine experimental data analysis. The injection pressure profile is a constant value since the engine is

equipped with common rail fuel injection system. Finally, the injected mass and start of injection timing were inputted to the model through the injector editor window.

After preparing the WAVE model for the combustion simulation of fuels with different properties, an experimental procedure needed to be designed to achieve the objectives of this project efficiently. With many variables in mind, using a design of experiments approach becomes crucial, and it is discussed in next section.

4.4 Experimental Approach

4.4.1 MODDE 7 Software Package

MODDE 7 design of experiments (DoE) software package is a window based modelling and design software tool for the generation and evaluation of statistical experimental designs. DoE helps to extract the maximum amount of information from the collected data in the fewest number of experimental runs by varying all relevant factors simultaneously over a set of planned experiments, and then connect the results by means of a mathematical model. The main objective of using the DoE software package is to achieve the aim of this study efficiently and with the least possible simulation numbers.

Generally, most DoE software packages fulfil two main objectives, firstly is to identify the important factors that have the most influential effect (screening), second is to understand in more detail how the selected factors influence the response (response surface modelling (RSM)) [109]. For the purpose of this study, a screening design was used to identify the most influential fuel property factors which cause substantial changes in the combustion performance and fuel evaporation. The screening design uses simple models such as, linear or linear with interactions, and experimental designs that allow the identification of the factors with the largest effects in the fewest possible experimental runs.

4.4.2 Experimental Design Process

With twelve fuel property variables (factors) and seven combustion quality responses that were identified in the previous section, the simulation screening program was planned in the MODDE 7 DoE software package and the effect of these fuel properties on the combustion process was investigated and variations recorded. The factors and responses were inputted into the model with their abbreviations and units identified, as shown in Figure 4.7 and Figure 4.8.

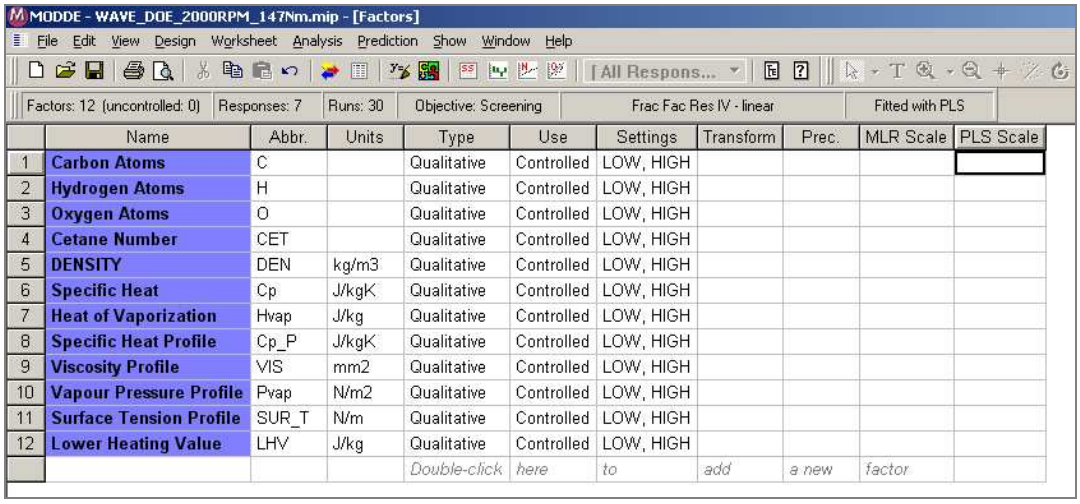

	Name	Abbr.	Units	Type	Use	Settings	Transform	Prec.	MLR Scale	PLS Scale
1	**Carbon Atoms**	C		Qualitative	Controlled	LOW, HIGH				
2	**Hydrogen Atoms**	H		Qualitative	Controlled	LOW, HIGH				
3	**Oxygen Atoms**	O		Qualitative	Controlled	LOW, HIGH				
4	**Cetane Number**	CET		Qualitative	Controlled	LOW, HIGH				
5	**DENSITY**	DEN	kg/m3	Qualitative	Controlled	LOW, HIGH				
6	**Specific Heat**	Cp	J/kgK	Qualitative	Controlled	LOW, HIGH				
7	**Heat of Vaporization**	Hvap	J/kg	Qualitative	Controlled	LOW, HIGH				
8	**Specific Heat Profile**	Cp_P	J/kgK	Qualitative	Controlled	LOW, HIGH				
9	**Viscosity Profile**	VIS	mm2	Qualitative	Controlled	LOW, HIGH				
10	**Vapour Pressure Profile**	Pvap	N/m2	Qualitative	Controlled	LOW, HIGH				
11	**Surface Tension Profile**	SUR_T	N/m	Qualitative	Controlled	LOW, HIGH				
12	**Lower Heating Value**	LHV	J/kg	Qualitative	Controlled	LOW, HIGH				
				Double-click	*here*	*to*	*add*	*a new*	*factor*	

Figure 4.7, The DoE factors screen

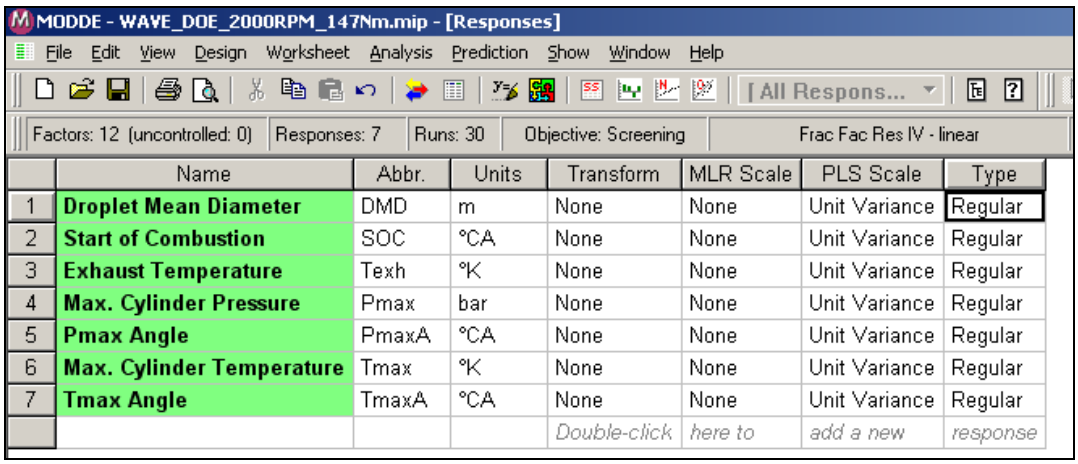

	Name	Abbr.	Units	Transform	MLR Scale	PLS Scale	Type
1	**Droplet Mean Diameter**	DMD	m	None	None	Unit Variance	Regular
2	**Start of Combustion**	SOC	°CA	None	None	Unit Variance	Regular
3	**Exhaust Temperature**	Texh	°K	None	None	Unit Variance	Regular
4	**Max. Cylinder Pressure**	Pmax	bar	None	None	Unit Variance	Regular
5	**Pmax Angle**	PmaxA	°CA	None	None	Unit Variance	Regular
6	**Max. Cylinder Temperature**	Tmax	°K	None	None	Unit Variance	Regular
7	**Tmax Angle**	TmaxA	°CA	None	None	Unit Variance	Regular
				Double-click	*here to*	*add a new*	*response*

Figure 4.8, The DoE response screen

After feeding all variables into the model, MODDE generated the simulation test plan in randomized order. The test plan generated for the current investigation is shown in Figure 4.9.

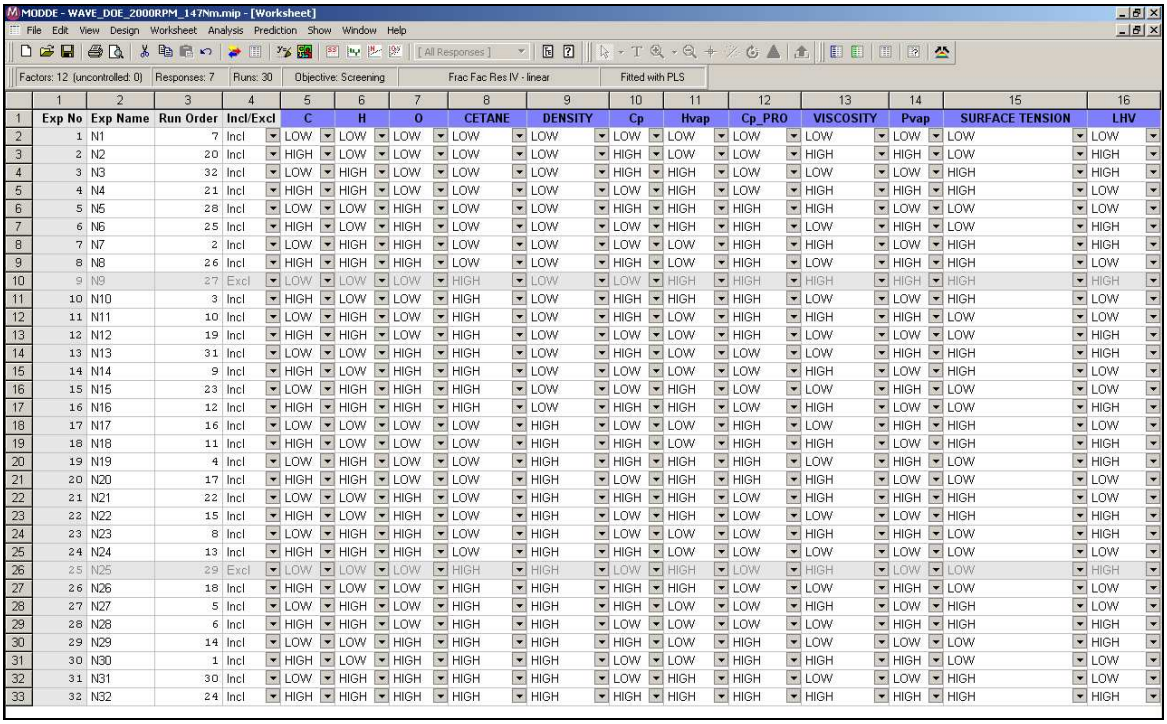

MODDE - WAVE_DOE_2000RPM_147Nm.mip - [Worksheet]

File Edit View Design Worksheet Analysis Prediction Show Window Help

Factors: 12 (uncontrolled: 0) | Responses: 7 | Runs: 30 | Objective: Screening | Frac Fac Res IV - linear | Fitted with PLS

	1	2	3	4	5	6	7	8	9	10	11	12	13	14	15	16
1	Exp No	Exp Name	Run Order	Incl/Excl	C	H	O	CETANE	DENSITY	Cp	Hvap	Cp_PRO	VISCOSITY	Pvap	SURFACE TENSION	LHV
2	1	N1	7	Incl	LOW	LOW	LOW	LOW	LOW	LOW	LOW	LOW	LOW	LOW	LOW	LOW
3	2	N2	20	Incl	HIGH	LOW	LOW	LOW	LOW	HIGH	LOW	LOW	HIGH	HIGH	LOW	HIGH
4	3	N3	32	Incl	LOW	HIGH	LOW	LOW	LOW	HIGH	HIGH	LOW	LOW	LOW	HIGH	HIGH
5	4	N4	21	Incl	HIGH	HIGH	LOW	LOW	LOW	LOW	HIGH	LOW	HIGH	HIGH	HIGH	LOW
6	5	N5	28	Incl	LOW	LOW	HIGH	LOW	LOW	HIGH	HIGH	HIGH	HIGH	LOW	LOW	LOW
7	6	N6	25	Incl	HIGH	LOW	HIGH	LOW	LOW	LOW	HIGH	HIGH	LOW	HIGH	LOW	HIGH
8	7	N7	2	Incl	LOW	HIGH	HIGH	LOW	LOW	LOW	LOW	HIGH	HIGH	LOW	HIGH	HIGH
9	8	N8	26	Incl	HIGH	HIGH	HIGH	LOW	LOW	HIGH	LOW	HIGH	LOW	HIGH	HIGH	LOW
10	9	N9	27	Excl	LOW	LOW	LOW	HIGH	LOW	LOW	HIGH	HIGH	HIGH	HIGH	HIGH	HIGH
11	10	N10	3	Incl	HIGH	LOW	LOW	HIGH	LOW	HIGH	HIGH	HIGH	LOW	LOW	HIGH	LOW
12	11	N11	10	Incl	LOW	HIGH	LOW	HIGH	LOW	HIGH	LOW	HIGH	HIGH	HIGH	LOW	LOW
13	12	N12	19	Incl	HIGH	HIGH	LOW	HIGH	LOW	LOW	LOW	HIGH	LOW	LOW	LOW	HIGH
14	13	N13	31	Incl	LOW	LOW	HIGH	HIGH	LOW	HIGH	LOW	LOW	LOW	HIGH	HIGH	HIGH
15	14	N14	9	Incl	HIGH	LOW	HIGH	HIGH	LOW	LOW	LOW	LOW	HIGH	LOW	HIGH	LOW
16	15	N15	23	Incl	LOW	HIGH	HIGH	HIGH	LOW	LOW	HIGH	LOW	LOW	HIGH	LOW	LOW
17	16	N16	12	Incl	HIGH	HIGH	HIGH	HIGH	LOW	HIGH	HIGH	LOW	HIGH	LOW	LOW	HIGH
18	17	N17	16	Incl	LOW	LOW	LOW	LOW	HIGH	LOW	LOW	HIGH	LOW	HIGH	HIGH	LOW
19	18	N18	11	Incl	HIGH	LOW	LOW	LOW	HIGH	HIGH	LOW	HIGH	HIGH	LOW	HIGH	HIGH
20	19	N19	4	Incl	LOW	HIGH	LOW	LOW	HIGH	HIGH	HIGH	HIGH	LOW	HIGH	LOW	HIGH
21	20	N20	17	Incl	HIGH	HIGH	LOW	LOW	HIGH	LOW	HIGH	HIGH	HIGH	LOW	LOW	LOW
22	21	N21	22	Incl	LOW	LOW	HIGH	LOW	HIGH	HIGH	HIGH	LOW	HIGH	HIGH	HIGH	LOW
23	22	N22	15	Incl	HIGH	LOW	HIGH	LOW	HIGH	LOW	HIGH	LOW	LOW	LOW	HIGH	HIGH
24	23	N23	8	Incl	LOW	HIGH	HIGH	LOW	HIGH	LOW	LOW	LOW	HIGH	HIGH	LOW	HIGH
25	24	N24	13	Incl	HIGH	HIGH	HIGH	LOW	HIGH	HIGH	LOW	LOW	LOW	LOW	LOW	LOW
26	25	N25	29	Excl	LOW	LOW	LOW	HIGH	HIGH	LOW	HIGH	LOW	HIGH	LOW	LOW	HIGH
27	26	N26	18	Incl	HIGH	LOW	LOW	HIGH	HIGH	HIGH	HIGH	LOW	LOW	HIGH	LOW	LOW
28	27	N27	5	Incl	LOW	HIGH	LOW	HIGH	HIGH	HIGH	LOW	LOW	HIGH	LOW	HIGH	LOW
29	28	N28	6	Incl	HIGH	HIGH	LOW	HIGH	HIGH	LOW	LOW	LOW	LOW	HIGH	HIGH	HIGH
30	29	N29	14	Incl	LOW	LOW	HIGH	HIGH	HIGH	HIGH	LOW	HIGH	LOW	LOW	LOW	HIGH
31	30	N30	1	Incl	HIGH	LOW	HIGH	HIGH	HIGH	LOW	LOW	HIGH	HIGH	HIGH	LOW	LOW
32	31	N31	30	Incl	LOW	HIGH	HIGH	HIGH	HIGH	LOW	HIGH	HIGH	LOW	LOW	HIGH	LOW
33	32	N32	24	Incl	HIGH	HIGH	HIGH	HIGH	HIGH	HIGH	HIGH	HIGH	HIGH	HIGH	HIGH	HIGH

Figure 4.9, DoE test plan

The test plan was performed for both engine conditions (2000 RPM speed 147.5 Nm load, and 3000 RPM 230 Nm) as given in Figure 4.9. The required response values were collected from the each simulation run and entered to populate the model. The model fitted the regression equation which was specified earlier to link the experimental factors to the responses which will be discussed in the next section.

4.5 Results and Discussion

4.5.1 Effect of Fuel properties on the Fuel Evaporation

The mean droplet diameter of liquid fuels is expected to be directly proportional to most of the physical properties, more specifically surface tension and kinematic viscosity. The

DoE response of the fuel evaporation sub model for the 3000 RPM 230Nm simulation experiments is presented in Figure 4.10 which shows the variations from the mean value.

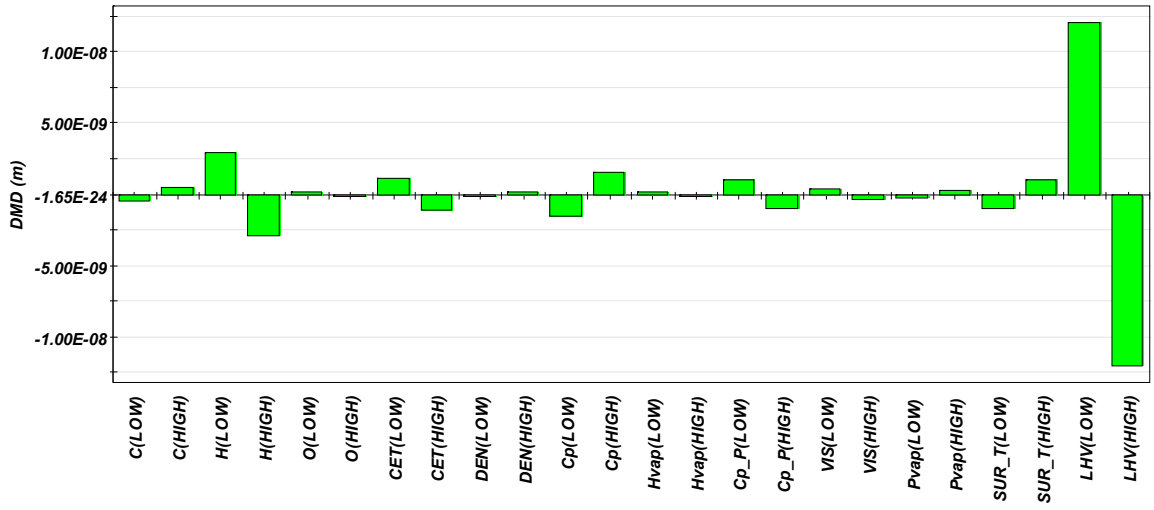

Figure 4.10, DoE Response, variations in DMD calculation

At the first glance, it can be noticed that the LHV, and hydrogen content, respectively are the most influential fuel properties affecting DMD calculation. Other properties such as specific heat capacity, cetane number, surface tension, and the rest of physical properties respectively have very minor effect on the DMD calculation. This result suggests that the factors expected to be the most critical are irrelevant in calculating DMD in the in-cylinder fuel evaporation sub model of WAVE.

Further investigations indicated that the calculation of the Sauter mean diameter (SMD) in the in-cylinder evaporation model [128] is based on the correlation by Hiroyasu et al [129]. The equation is shown below:

$$SMD = 0.38 D_n * \mathrm{Re}^{0.25} * We^{-0.32} \left(\frac{\mu_l}{\mu_a}\right)^{0.37} \left(\frac{\rho_l}{\rho_a}\right)^{-0.47}$$

Equation 4.1

Where,

D_n = Nozzle diameter (m)

Re = Reynolds number (non-dimensional)

We = Weber number (non-dimensional)

μ_l= Viscosity of liquid fuel (cSt)

μ_a = Viscosity of air (cSt)

ρ_l = Density of liquid fuel (kg/m^3)

ρ_a = Density of air (kg/m^3)

And Weber & Reynolds numbers are calculated by:

$$\mathrm{Re} = \frac{\rho_i V_d D_n}{\mu_i}$$

Equation 4.2

$$We = \frac{\rho_i V_d^2 D_n}{\sigma_i}$$

Equation 4.3

Where,

(σ_i) = Surface tension of liquid fuel (N/m)

And V_d is characteristic velocity of the droplets and is calculated by:

$$V_d = \sqrt{\frac{\left(P_{inj} - P_{cyl}\right)}{\rho_l}}$$

Equation 4.4

Where,

P_{inj} = is the user input injection pressure (N/m^2)

P_{cyl} = Instantaneous cylinder pressure (N/m^2)

According to Equation 4.1, the SMD values depend on four main factors:

- Injector nozzle diameter

- Reynolds number
- Weber number
- Fuel density and viscosity with respect to air

The injector nozzle diameter is directly proportional to the calculated SMD and it is constant for all simulation experiments. The Reynolds number determines the fluid dynamic properties and can vary greatly depending on the temperature of fluids, and viscosity. The Weber number is a measure of the relative importance of the fluid's inertia compared to its surface tension and it is used in analyzing thin film flows and the formation of droplets. Both Reynolds and Webber numbers are calculated based on the fuel's density, viscosity, and surface tension in addition to the droplet velocity (V_d). Their values are directly proportional to the droplet velocity which is determined by the instantaneous cylinder pressure. The influence of cylinder pressure may explain why the LHV of the fuel affects the DMD calculation where the LHV is used as an input to determine the heat of formation of the fuel. Lower calorific value fuels will have, in general, lower combustion temperatures and pressures which will significantly affect the calculations of Reynolds and Weber numbers since the fuel injection duration is often extended to after the start of combustion. The ratios of fuel density and viscosity with respect to air have a minor effect on the overall calculations because it is raised to a very small exponent, but it will be affected by the instantaneous cylinder temperature. Even though fuel density and viscosity is used in calculating the SMD value, and the surface tension is used in calculating Weber number, their significance is very minor on the overall results. The most significant factor affecting the SMD calculation seems to be the injector nozzle diameter as it appears in the equation while other physical properties will not have insignificant effects, which suggests that the current fuel evaporation model is unsuitable for predicting the spray evaporation of biodiesel. The response of the 2000 RPM 147.5Nm simulation experiments were very similar, so the engine speed and load did not have an effect the evaporation model response.

4.5.2 Effect of Fuel properties on the Combustion Process

The combustion model's sensitivity to changes in fuel properties was widely examined by considering several factors. The criteria of selecting these factors were to understand the combustion characteristics of different fuels. The first investigation into the combustion

performance of the model was the effect of fuel properties on the start of combustion (SOC). In most combustion model simulations, the SOC is predicted based on the calculation of the ignition delay which is the time between the start of injection and the start of detectable heat release. The DoE response to the simulation results of SOC crank angles for 3000 RPM 230 Nm experiments are presented below in Figure 4.11.

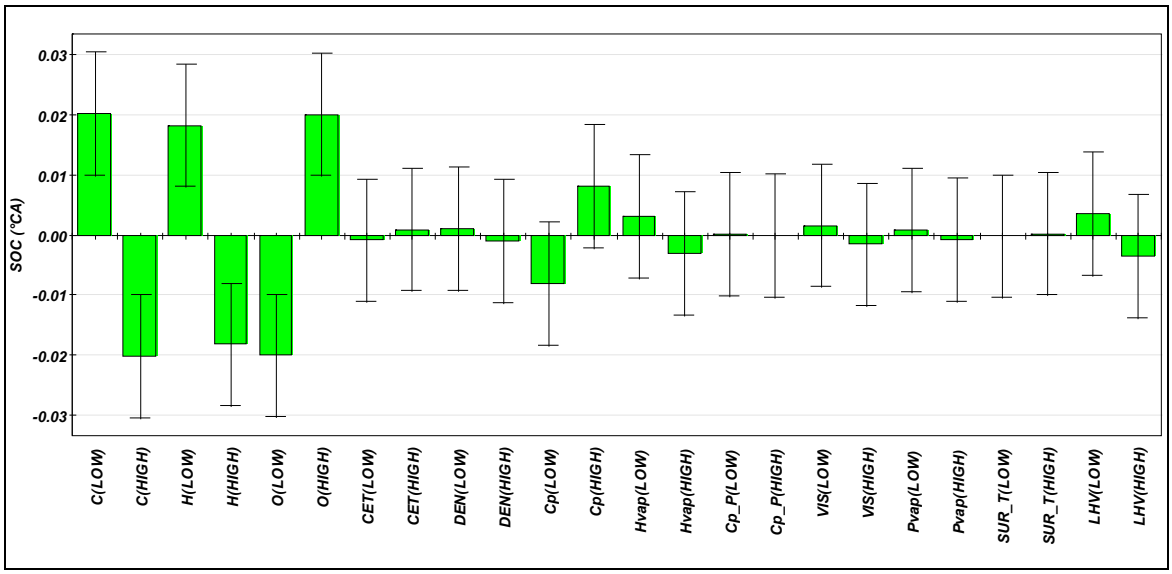

Figure 4.11, DoE Response, variations in SOC calculation

The most influential factors affecting the simulated SOC are oxygen, carbon, and hydrogen composition of the fuel respectively. Due to the large error bars of all other fuel properties (factors), it is mainly the chemical composition that is affecting the calculation of the SOC in the WAVE model with good statistical confidence levels, where the error bars shown represent a ± 95% confidence interval in the responses. To understand these results, a closer look at the calculation method used in this model needs to be undertaken.

In the combustion model, the ignition delay predictions are obtained from the diesel Wiebe combustion sub-model based on the work by Watson *et al* [127]. This model has the capability of predicting the ignition delay and responds to changes in the trapped mixture conditions as well as engine operating speed [117]. The heat release profile represented by the Wiebe function includes premix, diffusion and tail burning phases. The ignition delay is calculated using the in-cylinder temperature and pressure (averaged over

the delay period). In addition to the in-cylinder temperature and pressure histories, this extended correlation includes an additional dependency on the fuel CN. The ignition delay is determined by the following equation:

$$\Delta\theta_{delay} = 323\exp^{(2100*C/T_{sum,80.0})/P_{sum}}$$

Equation 4.5

Where:

$$C = \frac{67}{25 + CN}$$

Equation 4.6

(And cetane is the fuel's specific cetane number as per fuel specification data)

$$T_{sum} = \sum_n \frac{T_c^n + T_c^0}{2} * \frac{\Delta\theta_n}{\theta_{n+1} - \theta_0}$$

Equation 4.7

Also (T_c^n, and T_c^0) are cylinder temperatures, current and at the start of injection respectively. $\Delta\theta_n$ and θ_n are time step size in degrees, and crank angle at start of injection respectively.

$$P_{sum} = \sum_n \frac{P_c^n + P_c^0}{2} * \frac{\Delta\theta_n}{\theta_{n+1} - \theta_0}$$

Equation 4.8

Similarly, (P_c^n, and P_c^0) are cylinder pressures, current and at the start of injection respectively.

According to Equation 4.5, the ignition delay is calculated using the in-cylinder temperature and pressure plus a dependency on the fuel CN. Apparently the effect of the fuel's chemical composition is the most influential in calculating the SOC, and the CN of the fuel has a negligible effect on the SOC. Similar results were observed in the lower

speed and load experiments (2000 RPM 147.5 Nm), which shows poor sensitivity of the WAVE combustion model to any changes in fuel CN.

Similar results were observed in the responses of all other combustion factors. DoE responses to the exhaust temperature, cylinder pressure, and cylinder temperatures are presented in Figure 4.12, Figure 4.13, and Figure 4.14 respectively.

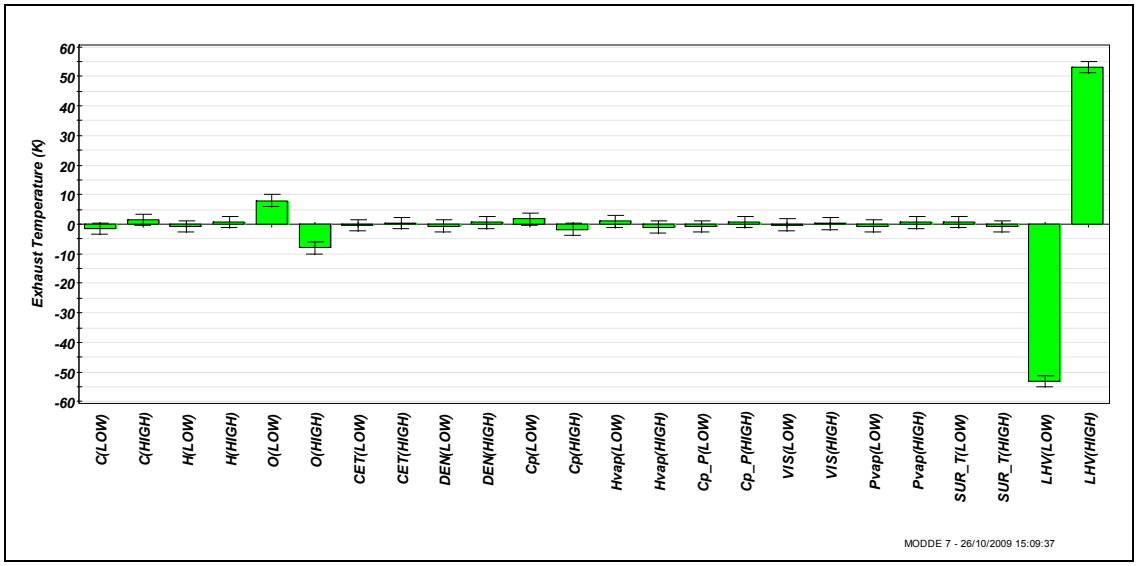

Figure 4.12, DoE response, variations in exhaust temperature

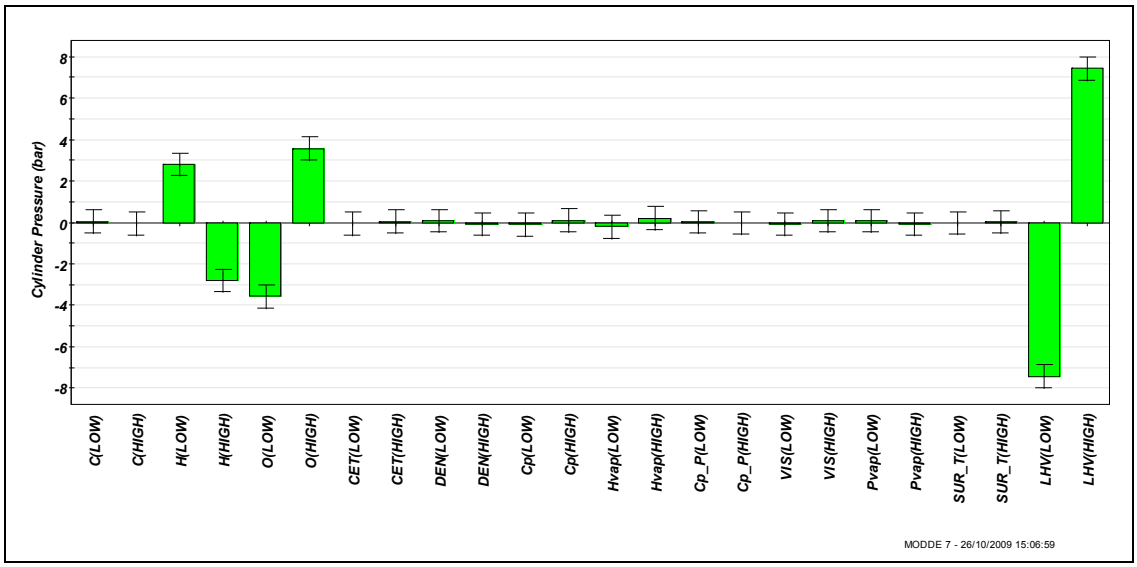

Figure 4.13, DoE response, variations in cylinder pressure

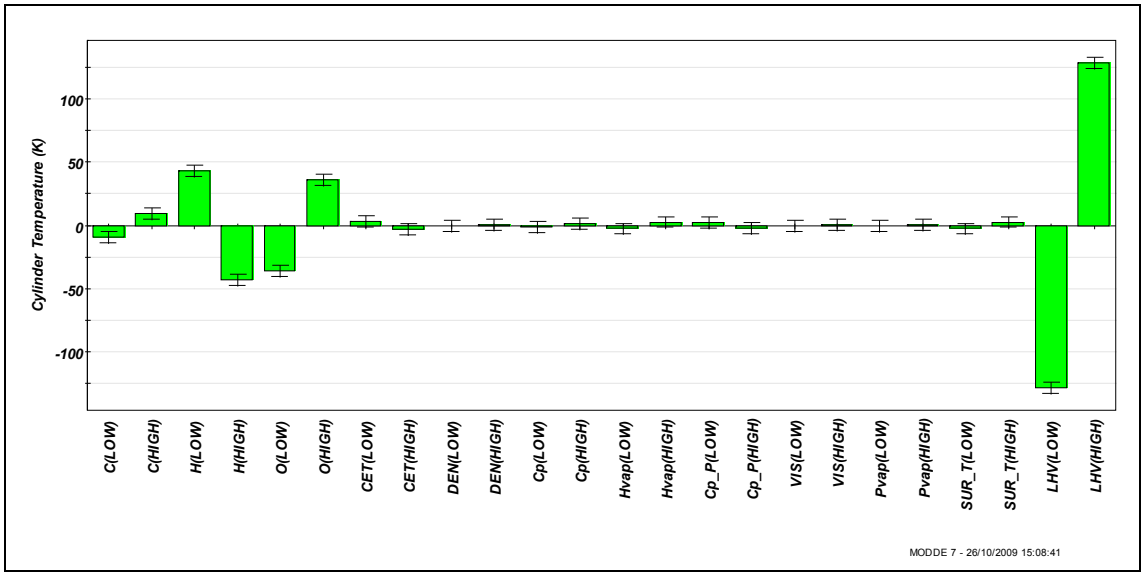

Figure 4.14, DoE response, variations in cylinder temperature

Mainly the fuel's LHV is the most significant property in altering the responses of the combustion factors in the WAVE model. The chemical composition of the fuel is the second property that has an effect on the combustion parameters, and the effect of all other fuel properties is negligible as shown in the DoE model responses. The combustion factors under investigation are calculated by the 'Diesel Jet' secondary combustion sub model used by the Ricardo WAVE software package. The 'Diesel Jet' combustion sub model is more advanced than other standard diesel combustion models which can be used in conjunction with the other combustion models such as diesel Wiebe [117]. It requires that a primary diesel combustion sub-model must first be applied to the cylinder of interest. It has the ability to predict combustion heat release rate from user specified fuel injection rate and injector geometry.

The heat transfer is calculated using the Woschni [131] equation which is based on the convective heat transfer concept and has been used frequently in heat transfer studies. The instantaneous heat transfer coefficient calculations are mainly dependant on two contributions. The first contribution is scaled with mean piston motion and geometry, and the second contribution is related to turbulence effects and differential pressure and temperature rises resulting from combustion. This explains the depending of the above

combustion predictions on the fuel's calorific value and oxygen composition since these factors are directly proportional to the combustion temperature and pressure. Further more, the 'Diesel Jet' combustion model is influenced by several factors with droplet evaporation being the main one [128] which is not effected significantly by any of the fuel's physical properties as discussed earlier. In actual experimental work, it is expected that some fuel properties such as CN, density, and viscosity would have a noticeable impact on the combustion process. These properties would shift the combustion process either forward (retarding) or backward (advancing) which will, in turn, alter the peak cylinder temperature, pressure and exhaust temperature. This topic was widely investigated and discussed in the literature review (chapter 2).

4.6 Conclusions

The aim of this study was to investigate the potential of engine simulation packages such as the Ricardo WAVE to asses the impact of changes in fuel properties, such as those for biodiesel, on simulated combustion performance. The following conclusions could be drawn:

- The lower heating value and hydrogen content respectively were the most influential fuel properties affecting the calculation of SMD in this WAVE model. Other properties such as specific heat capacity, cetane number and surface tension had only a very minor effect.
- This study suggests that the physical properties of biodiesel expected to be most significant are irrelevant in calculating SMD using WAVE. Limitations in the application range of the empirical equation used in the fuel evaporation model might explain the poor response of the model to the changes in the physical properties of the fuel.
- The most influential factors affecting the predicted SOC were found to be oxygen, carbon, and hydrogen composition. In spite of the fact that the ignition delay is calculated using the in-cylinder temperature and pressure plus a dependency on the fuel CN, the CN of the fuel has a negligible effect on the predicted SOC.

- Overall, the LHV and the chemical composition of the fuel are the most significant properties affecting the WAVE combustion models. The basic combustion models appear to be too simplistic to consider the fuel's physical properties in the calculation. The predicted heat release when using the more sophisticated 'Diesel Jet' model was also found to be insensitive to changes in fuel properties.
- WAVE's basic combustion models were not suitable for accurately predicting the impact of the different physical and chemical properties of biodiesel.

Chapter 5 Biodiesel Engine Trials

5.1 Introduction

Combustion in a diesel engine is a complicated physical and chemical process, starting with injecting the fuel into the combustion chamber to exhausting the burnt gases. Diesel combustion depends on many different parameters such as charge mixing, injection timing and pressure in addition to critical fuel properties. The physical and chemical properties of the fuel play a significant roll since they directly affect the vaporization process and the self ignition of the fuel vapour in the combustion chamber. Differences in the chemical properties between petroleum diesel and biodiesel fuels lead to differences in their physical properties which will have direct impact on the combustion process. The effect of biodiesel on emissions and performance is specific for each engine type, and depends on the engine speed and load conditions in addition to the ambient conditions and biodiesel feedstock and quality.

In the vehicle trial study reported in Chapter 3, the impact of various biodiesel fuel blends on the diesel engine's performance and emissions during different ambient temperatures was investigated. However, the impact of biodiesel fuel on the actual combustion process could not be determined because the cylinder pressure data could not be measured. The availability of cylinder pressure data could have provided substantial information regarding the impact of biodiesel fuel on the combustion process. The impact of biodiesel fuel blends on the combustion behaviour in a modern high speed diesel engine is presented in this chapter.

5.2 Aims and Objectives

The aim of this experimental phase was to investigate the combustion behaviour of two different blends of biodiesel (B25 and B50) compared to baseline diesel fuel when the engine is operated at different load and speed conditions. To achieve the aim, the following objectives were set:

- Evaluate the impact of biodiesel fuel on the combustion process analysing cylinder pressure and heat release data at defined operating conditions while running the "production" engine calibration.
- Determine the impact of biodiesel fuel properties on the combustion process when compared to baseline diesel fuel by operating the engine and fixed pedal positions in order to minimize ECU calibration issues.
- Investigate the impact of biodiesel fuel on the start of injection and ignition delay, by operating the engine with deactivated pilot injection. The impact of pilot deactivation on the engine performance and emissions to be quantified.
- Compare engine out emissions between biodiesel and the baseline diesel fuel.

5.3 Experimental Facility

The experimental work was carried out in test cell within the Powertrain and Vehicle Research Centre (PVRC) in the Department of Mechanical Engineering at the University of Bath. This test cell (PVRC-cell 1) is capable of performing full drive cycle and transient test schedules with emission measurement, fuel supply and high speed in-cylinder pressure measurement. The layout of this experimental facility is shown in Figure 5.1.

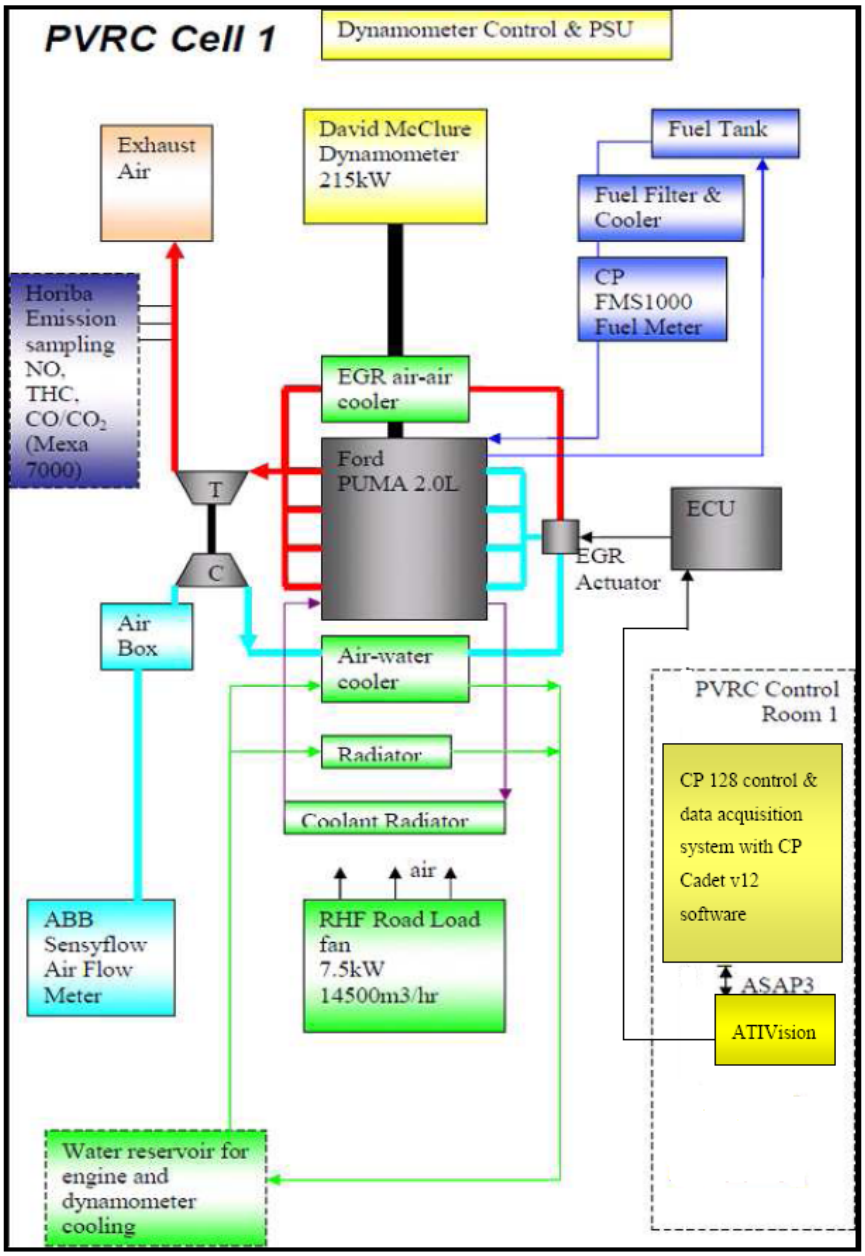

Figure 5.1, Layout of engine test cell 1 facility

5.3.1 Measuring equipment

This state of the art engine test cell is equipped with CP CADET V12 control and data acquisition system, CP Combustion Analysis System (CAS) and a Horiba MEXA 7000 series emission analyser.

5.3.1.1 Engine dynamometer

The engine used in this experiment was coupled to a 215kW AC dynamometer, which is capable of running steady state tests, as well as transient schedules with modelled gear shifts.

5.3.1.2 CP CADET V12

The CP Cadet V12 software is installed on two remote PCs to remotely control the engine testing facilities, and the data acquisition system connecting with the sensors and sending signals to communicate with other controllers. The software contains real time multi-tasking direct digital control functions which interface with the dynamometer, ECU ASAP3 connection, fuel weighers, sensors and controllers. The CP128 system capture cards are capable of sampling data at rates of up to 80Hz at 16 bit resolution and at up to 160Hz at 8 bit resolution. The Combustion Analysis System (CAS, further details later) is also connected to CP CADET V12. The ECU and its calibration tool (ATI vision) are connected with two CP CADET PCs via the CAN bus. Therefore the data from the engine test facilities, ECU and CAS are able to be collected in one CP CADET PC acquisition system.

5.3.1.3 ATI Vision

For fast sampling of engine response, data is logged using ATI Vision 2006 sp2 which is installed on the PC as the calibration tool in the engine test cell. ATI vision is an integrated calibration and data acquisition tool that collects signals from the ECU and external sources. It samples engine response such as speed, fuel injection, mass air flow, EGR mass and start of injection timing during a transient at a rate of 50Hz (0.02s). The fuel demand measurement from ATI vision was calibrated against CP gravimetric fuel weigher for accuracy before the experimental tests.

5.3.1.4 CAS System

The combustion analysis system (CAS) was developed by D2T for internal combustion engine research and design. The crank angle based data capture and acquisition system allows the engine parameters to be measured in real time, such as the cylinder pressure analysis, rate of heat release calculation, combustion noise detection, mass fraction of fuel burned calculation, needle lift, etc.

5.3.1.5 MEXA Analysers

This experimental facility is equipped with two Horiba MEXA 7100 DEGR gas analysers for simultaneous emission measuring at the inlet and outlet of the diesel exhaust catalytic converter. The analysers are designed to measure exhaust emissions from diesel or gasoline engines, and they are capable of measuring CO, CO_2, NO_X, THCs and O_2. They are also capable of second by second emission measurements which are ideal for driving cycle and steady-state testing. To ensure repeatability of the experimental procedure, a scheduled purging and calibration procedure were followed before each batch of experiments. In addition, the analyser filters were changed on daily basis or even more frequently depending on the test frequency.

5.3.1.6 In-Cylinder Pressure Measurement

A Kistler 4045A pressure transducer was used to measure in-cylinder pressure which is positioned in the place of the glow plugs. The pressure change in the engine cylinder acts on the diaphragm and the force is transmitted to the quartz, which under loading yields an electrostatic charge. This charge is conditioned to be recorded on the measurement system (in this project, CP combustion analysis system). The advantage of this transducer is its rapid response to changes in cylinder pressure. The high sensitivity and low thermal shock error properties of the piezoelectric crystal make it an ideal candidate for use in engine testing. The maximum pressure that the sensor can measure is 250 bar while the maximum allowed in-cylinder pressure of this particular engine is 160 bar. The amplitude of the signal from the pressure sensor is very small and hence this signal is passed through

a charge amplifier in order to convert it into a measurable voltage and this is then processed into the crank angle domain as provided by the crank shaft encoder.

5.3.1.7 Crank Shaft Encoder

The crank angle encoder used is a Kistler 2613B encoder and it provides a crank angle degree domain for measurements. The crank angle encoder is mounted on the free end of the crankshaft and can measure 360 individual degree marks. These marks are scanned by a photoelectric cell which gives an electrical output which is picked up by the pulse converter in the encoder. The encoder has a high resolution of 0.1˚ CA.

5.3.1.8 Temperature Measurement

Temperature measurements are made using K-type thermocouples which operate on the principle of Seebeck effect where the junction of two different conductors creates a voltage dependant upon temperature at that junction. The two alloys that are used are Nickel-Chromium and Nickel-Aluminium alloys. The grounds for the selection of this type of thermocouple are their ability to operate over a wide operating range coupled with a sensible accuracy of 1°C. They thermal inertia of the thermocouples is relatively low due to a small diameter of 1.5mm. The thermocouples are calibrated with the aid of the CP Software, and the temperature range for a typical type K thermocouple is between -200°C to +1350°C which is suitable for engine diagnostics.

5.3.2 Engine Specification

The baseline engine investigated in the experimental work is a Ford Puma 2.0 litre turbocharged diesel engine, the engine specification is summarised in Table 5.1. Further details of the fuel injection system are given in the next section.

Engine Details	Notes
Engine Type	Compression Ignition
Number of Cylinders	4
Engine Displacement (cc)	1998
Cylinder Bore (mm)	86
Cylinder Stroke (mm)	86
Compression Ratio	16
Fuel Injection System	High pressure Common Rail Direct Injection
Injection Pressure (bar)	1400
EGR	Mass Flow Controlled
Turbocharger	Garrett variable geometry
Max Torque (Nm)	310 at 1800-2500 RPM
Max Power (kW)	96 at 3800 RPM

Table 5.1, Ford Puma engine specification

5.3.3 Fuel Injection System

The engine used in this investigation is equipped with a common rail fuel injection system as detailed above. The main advantages of theses systems over the traditional pump-line-nozzle are their high pressure capabilities and the independent control of the injection pressure with engine speed changes. In addition, these systems are very flexible in adjusting pressures for different conditions to determine the best injection pressure required to optimize engine performance. This independent control of pressure generation and injection in common rail systems is accomplished by the high-pressure accumulator, this consists of the rail and the high pressure fuel lines to the nozzles. The modern common rail fuel injection systems are usually offered with electronic control injectors (ECI) with capabilities of multiple injections per stroke and very quick response injection timing. The introduction of ECIs made it possible to control both pressure and flow area of the fuel into the combustion chamber. The key component of these injectors is the solenoid valve which controls the opening and closing of the injector by means of needle vertical motion. A schematic drawing of a typical solenoid driven common rail fuel injectors are presented in Figure 5.2.

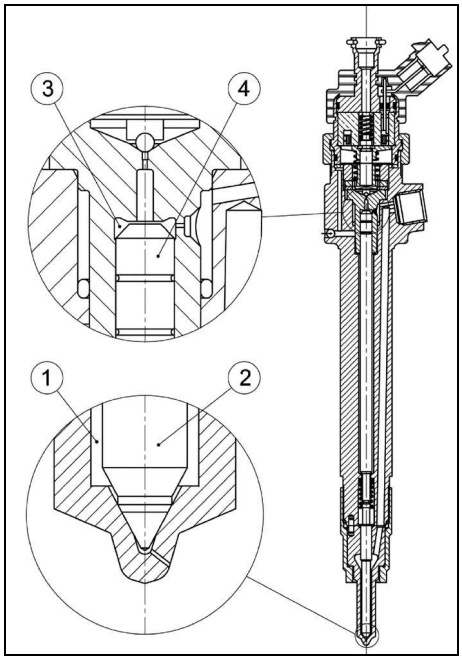

Figure 5.2, Common Rail Injector adopted from Lucas [2]

The operating principles of the electronic fuel injectors controlled by solenoid valves can be summarised as follows: In order to control the opening and closing time of the needle (2), a small chamber of pressurised fuel (3) is present at the top of the needle's control piston (4). This controlled volume is connected to the rail through a small orifice that assures that same pressure between the nozzle and the chamber when the valve is closed. When injection is required, the solenoid valve, on the top area of the injector, is energised by the engine management system which will lift the piston's control valve and the pressure in the control volume will reduce rapidly, thus creating a pressure drop. This will result in a negative net force on the valve needle, and the injection is initiated through the delivery chamber (1). As soon as the solenoid closes, the pressure in this chamber will increase again resulting in the closure of the needle.

5.3.4 Fuels

The fuels used in this experimental work are the same fuel used in the previous vehicle testing work. The baseline diesel fuel (B0) is supplied by Shell, and the biodiesel fuel used in this study is rapeseed oil methyl ester (RME) supplied by BP and the full specification sheets are attached in appendix 2, and 3. The specifications of RME meets

the European biodiesel standard EN 14214:2003 with slightly lower cetane number (CN), which is not usually common in most of the biodiesel fuel types (see Table 5.2), and the fatty acid composition in Table 5.3.

Property	Baseline Diesel (B0)	RME Biodiesel (B100)
Cetane Number (CN)	**52.8**	**49.5**
Net Calorific Value (MJ/kg)	**42.59**	**39.99**
Density at 15°C (kg/m3)	**833**	**883.2**
Kinematic Viscosity at 40°C (mm^2/s)	**2.75**	**4.56**
Flash Point (°C)	**55**	**182**
Water Content (mg/kg)	**68**	**210**
Oxygen Content (%)	**0**	**11**

Table 5.2, Fuel Specification

FA Structure	16 (0)	16 (1)	18 (0)	18 (1)	18 (2)	18 (3)	-
FA Name	**Palmate**	**Palmitoleate**	**Stearate**	**Oleate**	**Linoleate**	**Linolenate**	**Others**
(%)	**2.05**	**0.31**	**1.66**	**62.82**	**20.41**	**9.15**	**3.60**

Table 5.3, Fatty acid composition

The RME fuel drums were stored in a refrigerated location below 3°C to avoid any possible oxidation or degradation of the fatty acids. Prior to this experimental procedure, a sample of the B100 RME fuel was sent to the Ford Motor Company Fuels and Lubricants laboratory for oxidation stability analysis. It appeared that the B100 sample was still at 8.3 hrs induction period (current EN14214 limit is 6hrs), and approved to be well within specification for oxidation stability.

Fuel blends of B25, and B50 were prepared on site by physically mixing the required volumetric ratios of baseline diesel and RME fuels. Samples of each blend prepared were evaluated in the chemistry department of at the University of Bath to ensure the consistency of the blend ratio. The samples were analysed and the results were calculated by nuclear magnetic resonance (1 HNMR), the calculated ratios came to 25.4, and 48.7 for the B25, and B50 fuel blends respectively.

5.4 Approach

A detailed study of the combustion behaviour, engine out emissions, and performance of B25 and B50 biodiesel fuel blends in comparison with baseline diesel fuel was carried out. The engine was started and warmed up until reaching its 'VERY_HOT' ECU strategy before any data collection was attempted. The engine out emission analysers were prepared and calibrated prior to any experimental run. The studies were conducted on the standard calibration engine at the following conditions:

- Fixed Engine Load: The engine was operated using all three fuel blends at 1500 RPM and 2250 RPM with two fixed loads representing low and mid-high loads for each engine speed.
- Fixed Pedal Position: The engine was operated using all three fuel blends at 1500 RPM and two fixed pedal positions of 9% and 17%. Similarly at the 2250 RPM with two fixed pedal positions of 15% and 22% representing low and mid-high loads.
- Fixed Pedal position (pilot injection off): Similar to the previous experiment but with deactivating of the pilot injection in order to reduce the disturbance in the rail pressure and take a more detailed evaluation of the main combustion process, combustion duration, and mass fraction of fuel burned.

5.5 In Cylinder Investigation: Fixed Engine Load

Evaluating combustion stages and events are not an easy task especially with the complexity associated with diesel combustion. However, with the availability of the high speed data acquisition systems, sensitive pressure transducers, and precision crank shaft encoders, acquiring data from the combustion chamber of diesel engines becomes manageable. Information is analysed in the form of instantaneous cylinder pressures and heat release rates. In this experiment, all the instantaneous data were recorded for 100 consecutive cycles and then averaged out in order to eliminate the effect of cycle to cycle variations.

In this experimental work, the engine will be operated with biodiesel fuel blends and the engine out torque will be matched with that of baseline diesel fuel. Demanding the

required power from the engine is obtained via pressing the accelerator is what actually happens in real live, regardless of fuel being used. The impact of biodiesel fuel on the fuel injection system was also investigated and compared to the baseline diesel fuel.

5.5.1 Fuel Injection Process

Investigating the demand injection timing did not show any variations with biodiesel fuel during all the operating conditions. An attempt was made to identify the actual start of injection (SOI) timing by analysing the variations in continuous rail pressure, but this was impossible due to the presence of pilot injection. The pilot injection disturbs the stability of rail pressure line and makes it very difficult to estimate the SOI of the main charge. The demanded rail pressures in this experimental study when the engine was operated with different fuel blends at standard calibration and different engine speed and load conditions are plotted in Figure 5.3. The figure shows a slight increase in rail pressure demand with biodiesel fuel blends, which is most likely attributed to the higher pedal demand by the engine ECU to match baseline diesel fuel power. The average increase in rail pressure demand is about 5% with B50 biodiesel compared to baseline diesel fuel, and the percentage increase in rail pressure dropped with engine speed and load.

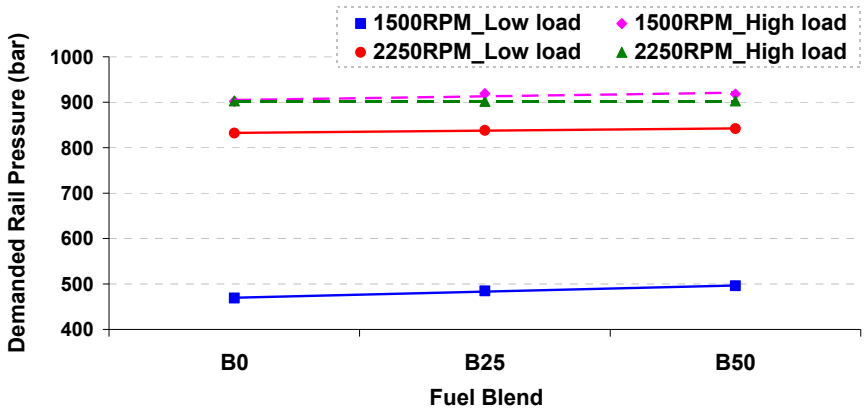

Figure 5.3, Demanded Rail pressure for different fuel blends, matched engine load

Increasing the rail pressure and occasionally fuel injection duration is the common response from the ECU to increase fuel amounts injected into the combustion chamber to overcome the lower energy content of biodiesel fuel. The actual fuel demanded by the engine ECU is increased as the percentage of biodiesel increases during all experimental

conditions to overcome the LHV of biodiesel fuel. The percentage increase in fuel demand with biodiesel fuel blends compared to the baseline diesel fuel is summarized in Table 5.4.

RPM	1500		2250	
Load	Low	High	Low	High
B25	9	4	5	6
B50	16	6	10	8

Table 5.4, Percentage increase in fuel demand relative to baseline diesel fuel

The percentage increase in fuel demand during the lower load conditions is higher than during the higher load conditions with biodiesel fuel blends. This is probably a consequence of lower atomization and evaporation of biodiesel fuels during lower operating conditions which was also reported by [94], in addition to lower calorific value which the majority of studies report [64, 83, 86, 88, 91, and 95]. Whereas during the higher load operating conditions the draw back of higher viscosity and flash point diminishes, as the cylinder pressure and temperatures increase.

5.5.2 Combustion Analysis

To investigate the actual combustion process, the in cylinder pressure profiles and rate of heat release were analysed. The in cylinder pressure profile with crank angle for all fuel blends at different engine operating conditions is shown in Figure 5.4, and Figure 5.5.

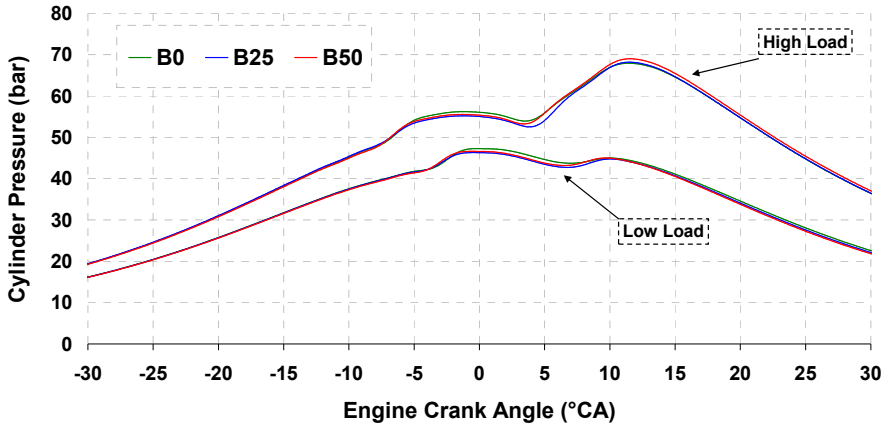

Figure 5.4, Cylinder pressure vs. Crank angle at 1500 RPM and matched engine load

Figure 5.4 shows that the cylinder pressure profiles for all three fuels are pretty similar during both engine load conditions for the speed of 1500 RPM. The variations in maximum cylinder pressure ($P_{Max.}$) are very small and cannot be considered significant; the P_{Max} values with the corresponding engine crank angles is presented in Table 5.5. Similar trends are observed from the 2250 RPM engine speed experiments (see Figure 5.5). Both figures show that the peak pressures increase as the engine load increases, and it does not vary significantly with increasing engine speed.

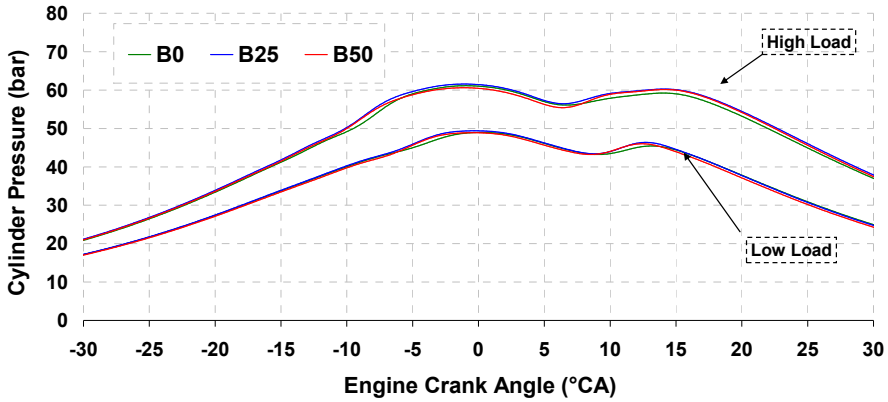

Figure 5.5, Cylinder pressure vs. Crank angle at 2250 RPM and matched engine load

RPM	1500				2250			
Load	Low Load		High Load		Low Load		High Load	
P_{Max}	bar	°CA	bar	°CA	bar	°CA	bar	°CA
B0	45.1	10.0	67.9	11.4	45.5	13.1	59.2	14.0
B25	45.1	10.1	68.2	11.5	46.4	12.7	60.2	14.1
B50	45.2	10.1	69.0	11.5	46.0	12.4	60.2	14.2

Table 5.5, Maximum cylinder pressure value, matched engine load

Both cylinder pressure curves and maximum pressure values for both biodiesel blends are very similar to the baseline diesel fuel which was also reported by Kawano et al. [94]. The peak pressure value usually depends on the burn rate after the start of ignition during the rapid combustion stage. In order to further investigate the difference in combustion characteristics between diesel and biodiesel fuels, the rate of heat release per second for all fuel blends was investigated and shown in Figure 5.6, and Figure 5.7.

The combustion stages inside the cylinder can be visualized by the rate of heat release calculation as the fuel burns inside the combustion chamber, as shown in Figure 5.6 and Figure 5.7. The initial drop in the heat release rate which can be observed directly after SOI is due to the energy requirement to evaporate the fuel accumulated during ignition delay period, and it starts to increase as combustion is initiated.

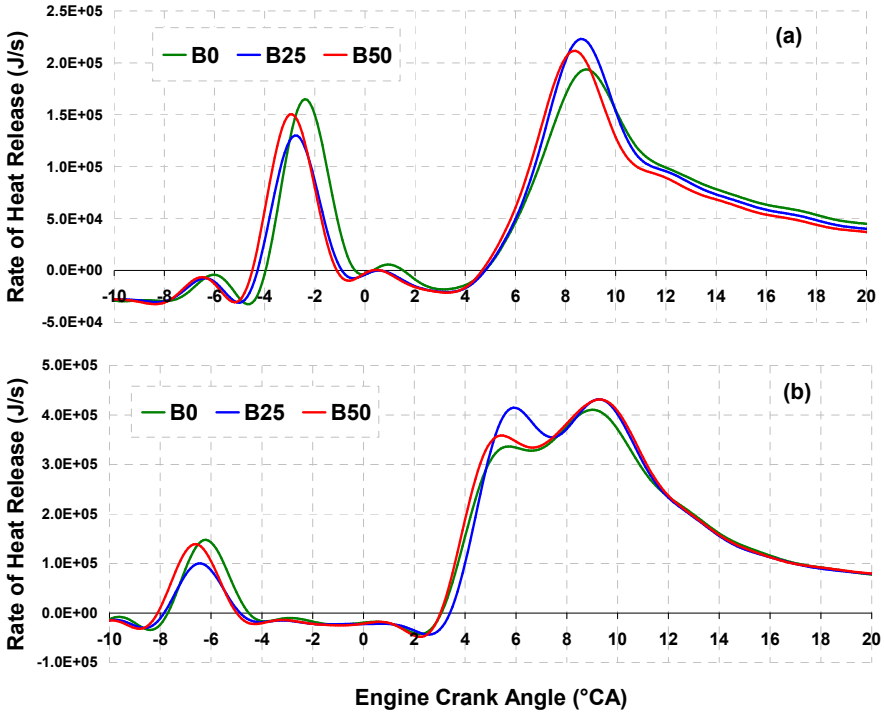

Figure 5.6, Rate of Heat Release for 1500 RPM engine speed and (a) Low load (b) High Load

The first smaller rise in the rate of heat release is caused by the pilot injection and the second one is when the main injection kicks in. Generally, both plots follow similar heat release profiles for all three fuels during the low pedal and high pedal conditions, which basically indicate that both B25 and B50 blends experience very similar combustion phases, or stages, as the baseline diesel fuel.

The initial combustion associated with pilot injection fuel burn for biodiesel fuel blends appear to be slightly earlier under both operating conditions, and this observation can be more distinguished during the higher engine speed conditions (see Figure 5.7), where it

clearly shows an earlier rise in the rate of heat release due to pilot injection. The variation in the start of pilot fuel burn ranges from 0.5 to 1.0°CA earlier with B50 biodiesel compared to baseline diesel fuel. However, this does not seem to affect the start of combustion (SOC) of the main charge with all fuel blends. It can also be observed that the rise in the rate of heat release curve is quicker and the peak values are higher with biodiesel blends compared to baseline diesel fuel during most of the engine operating conditions.

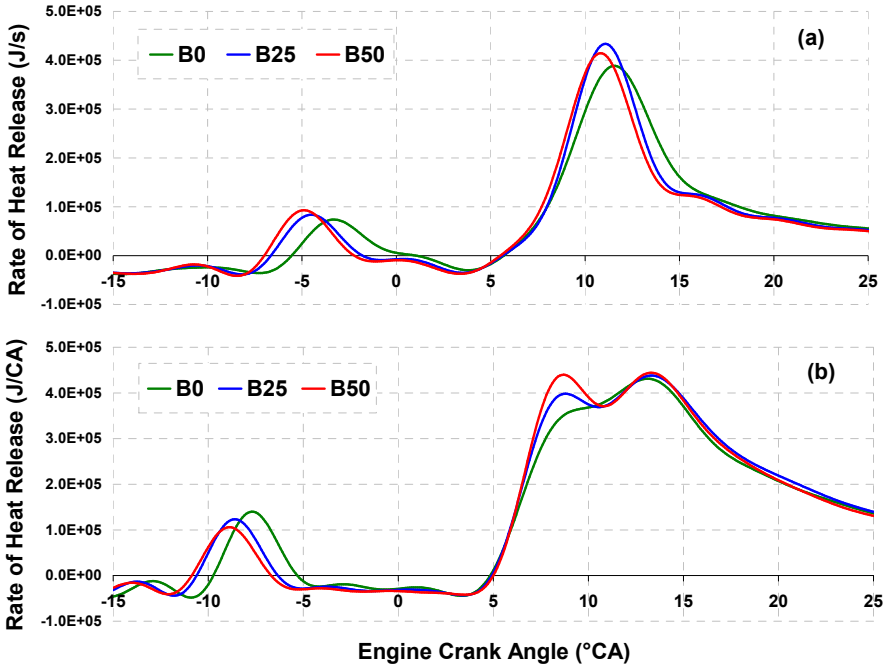

Figure 5.7, Rate of Heat Release for 2250 RPM engine speed and (a) Low load (b) High load

The earlier start of pilot fuel burn and quicker rise in the rate of the heat release curve and higher peak values with biodiesel fuel is probably attributed to their higher oxygen content compared to baseline diesel fuel, as the demand start of injection should be very similar (refer to section 5.5.1). The earlier start of pilot fuel burn can also be attributed to the higher rail pressures, since the CN is slightly lower compared to baseline diesel fuel, see Table 5.2. These observations suggests that quicker start of combustion and higher burn rate is more likely to happen with biodiesel fuel blend compared to the baseline diesel fuel during these operating conditions.

On the other hand, increasing pedal with biodiesel fuel to match the engine power of baseline diesel fuel will also correspond to other changes in engine calibration parameters such as EGR value and VGT speed which directly affects the amount of mass air flow (MAF) into the engine due to variations in boost pressure and the exhaust gas temperature. This is a logic response from engine ECU to overcome the deficiency in calorific value in biodiesel fuel by altering operating parameters. Next, the impact of biodiesel fuel on the engine out emissions compared to baseline diesel fuel is reported.

5.5.3 Emissions Analysis

The engine out emissions of CO, HC, and NO_X for all fuel blends and different engine operating conditions are presented in Figure 5.8, Figure 5.9, and Figure 5.10 respectively.

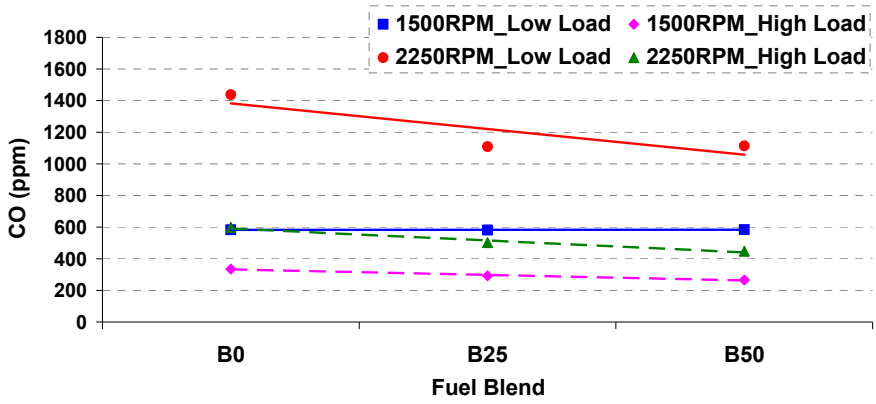

Figure 5.8, Engine out CO emissions with different fuel blends during both engine speeds, fixed engine load investigation

The average engine out CO emissions shows general reduction trend as the percentage of biodiesel increases at all engine operating conditions, however the reduction varies according to engine operating condition (see Figure 5.8). The highest amount of CO emissions produced during the high speed and low load conditions, and the lowest during the low speed high load conditions. Generally, the reduction in CO emissions increases as the engine load and speed increases, and it can be observed by steeper reduction curves of the higher speed and load conditions. The CO decreases by 21%, 23%, and 25% when B50 fuel blend is used during 1500 RPM high load, 2250 RPM low load, and 2250 RPM high load conditions respectively compared to baseline diesel fuel and no significant

difference in CO emissions could be observed at 1500 RPM low load condition. The reported reason for the reduction of CO emissions with biodiesel is the additional oxygen content in the fuel, which enhances more complete combustion of the fuel leading to CO emissions reduction which agrees with most of the published studies [86-89, 91, and 94].

The total hydrocarbon emissions showed more dependency on the engine operating conditions as it appears in Figure 5.9, where the percentage reduction varies significantly with engine operating conditions.

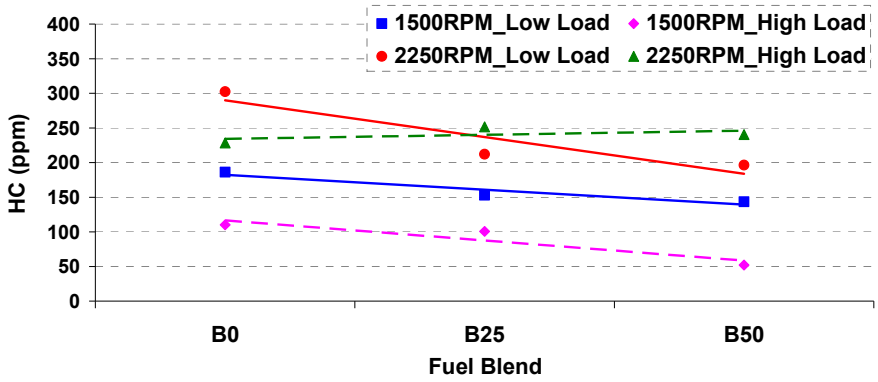

Figure 5.9, Engine out HC emissions with different fuel blends during both engine speeds, fixed engine load investigation

Similar to CO emissions, the lowest amount of HC emissions were recorded from the low speed high load conditions and the highest during high speed low load conditions. The engine out HC emissions reduced with biodiesel fuel blend for all engine operating conditions except for the high speed and high load condition where no significant change was observed. Using B50 fuel blend reduced the HC emissions by 23%, 53%, and 35% during 1500 RPM low load, 1500 high load, and 2250 RPM low load conditions respectively compared to baseline diesel fuel. It is generally known that using biodiesel fuel reduces the amount of HC emissions compared to the conventional diesel fuel due to the oxygen content in the biodiesel molecule, which leads to a more complete and cleaner combustion, which agrees with most of the published studies [16, 86, 88, and 90]. The results obtained in this work suggest that the percentage reduction in HC emissions is extremely dependant on engine operating conditions.

Figure 5.10 shows a clear increasing trend of engine out NO_X emissions as the percentage of biodiesel increases in the fuel blend at all engine operating conditions except at low speed low load condition.

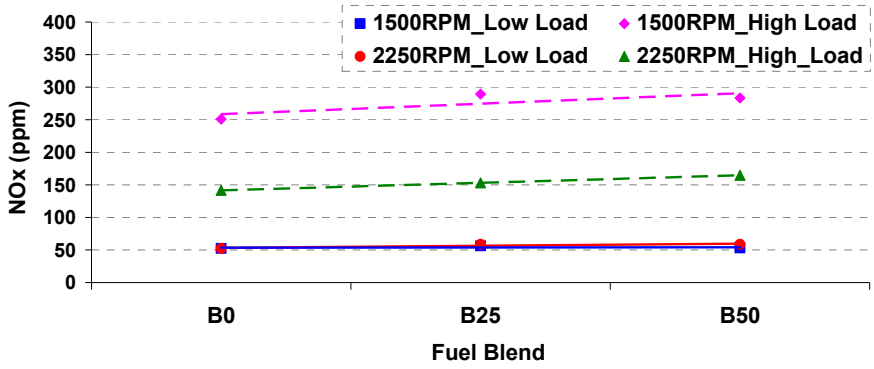

Figure 5.10, Engine out NO_X emissions with different fuel blends during both engine speeds, fixed engine load investigation

The percentage increase in NO_X emissions with B50 fuel blend is about 13% during all operating conditions compared to baseline diesel fuel, except at 1500 RPM low load condition, were it shows no significant change. The low speed high load conditions produce the highest amounts of NO_X emissions as a trade off for lower CO and HC emissions as a result of more efficient combustion as seen in Figure 5.8 and Figure 5.9. However, during the low speed low load condition the engine out NO_X emissions did not show any significant change with B50 fuel blend. Most of the published literature in this field indicated a slight increase in NO_X emissions with biodiesel, and the percentage increase depends significantly on engine type, engine technology, and its operating conditions, refer to sections 2.5.2 and 2.6.1 of chapter 2.

To match the engine power of diesel fuel, the engine ECU increased the pedal demand when operated with biodiesel fuel, which corresponded in other changes in engine calibration. Next, an investigation into the impact of biodiesel fuel on the combustion process by operating the engine at fixed pedal positions is reported, and the results compared to those of baseline diesel fuel.

5.6 In Cylinder Investigation: Fixed Pedal position

This section reports variation in the combustion process with biodiesel fuel blends when the engine is operated with similar pedal demand to that of baseline diesel fuel. This procedure will minimize the impact of pedal demand variations on engine calibration parameters such as EGR value and VGT speed discussed in the previous section. In this study, the demanded rail pressure and the injected quantity of fuel are kept the same with all fuel blends for a fixed pedal position.

5.6.1 Combustion Analysis

Figure 5.11 and Figure 5.12 show the cylinder pressure profiles for the fixed pedal position experiments against engine crank angles engine speeds.

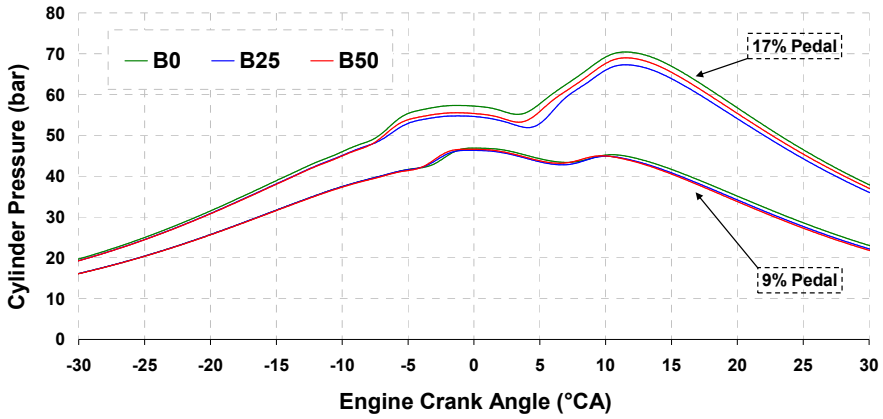

Figure 5.11, Cylinder pressure vs. Crank angle at 1500 RPM and fixed pedal position

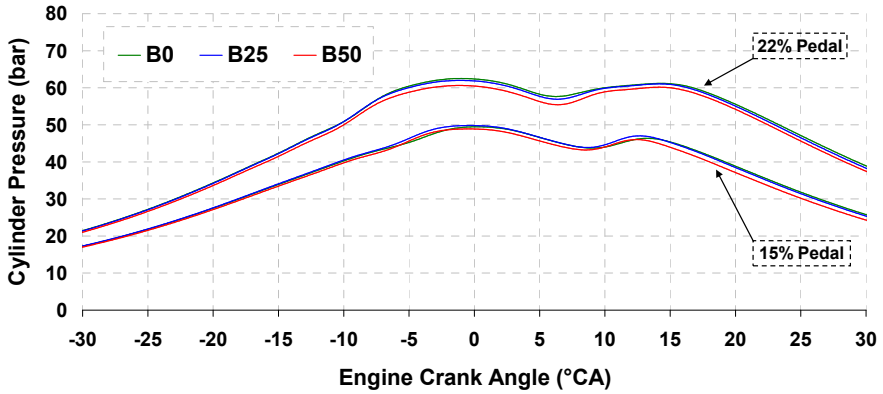

Figure 5.12, Cylinder pressure vs. Crank angle at 2250 RPM and fixed pedal position

Both figures show that the cylinder pressure profiles for all three fuels are very similar during both engine load conditions and for both engine speeds. The pressure curves follow similar paths and no indications of earlier start of combustion can be seen. The maximum cylinder pressure ($P_{Max.}$) values are presented in Table 5.6.

RPM	1500				2250			
Pedal	9%		17%		15%		22%	
$P_{Max.}$	bar	°CA	bar	°CA	bar	°CA	bar	°CA
B0	45.3	10.5	70.4	11.5	46.4	13.2	61.2	14.3
B25	44.9	10.1	67.3	11.5	47.0	12.7	61.0	14.2
B50	44.9	9.7	69.0	11.5	46.0	12.4	60.2	14.2

Table 5.6, Maximum cylinder pressure values at fixed pedal position

The maximum cylinder pressure values show a very slight decreasing trend as the percentage of biodiesel increases especially in the case of higher pedal position conditions. Generally ($P_{Max.}$) values occur at very similar crank angles for all fuel blends during the higher pedal conditions, and slightly earlier for biodiesel fuel blends during the lower pedal conditions.

The rate of heat release curves show similar observations as discussed in the previous section, see Figure 5.13 and Figure 5.14. The rate of heat release associated with pilot injection shows slightly earlier rise with biodiesel fuels during all operating conditions compared to the baseline diesel fuel. However, the main combustion always starts at very similar crank angle with all fuel blends during all engine operating conditions, except for B25, where it shows an unexpected trend during the 1500 RPM 17% pedal position which is probably due to an experimental error.

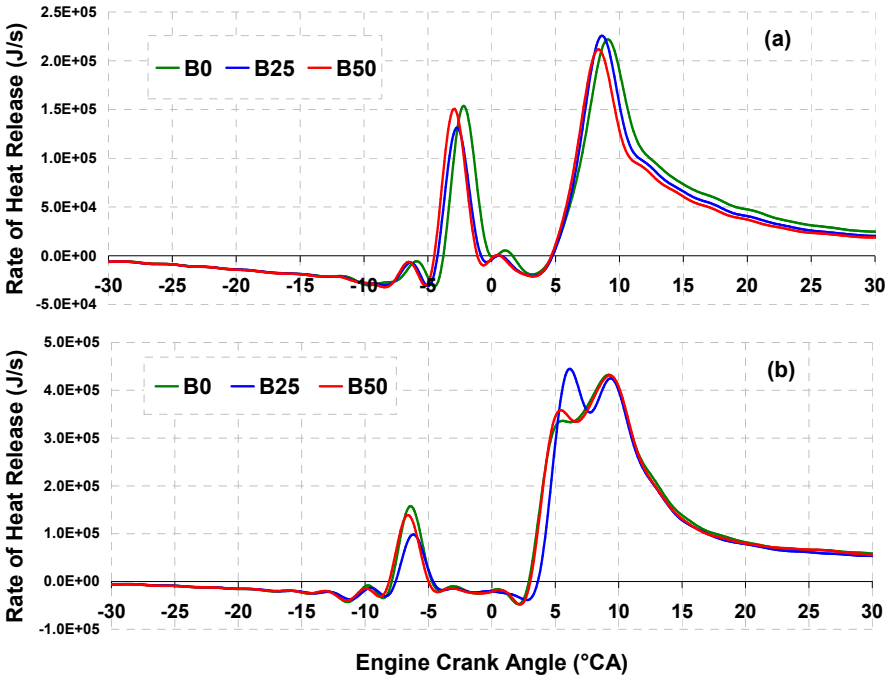

Figure 5.13, Rate of Heat Release for 1500 RPM engine speed at (a) 9% pedal (b) 17% pedal

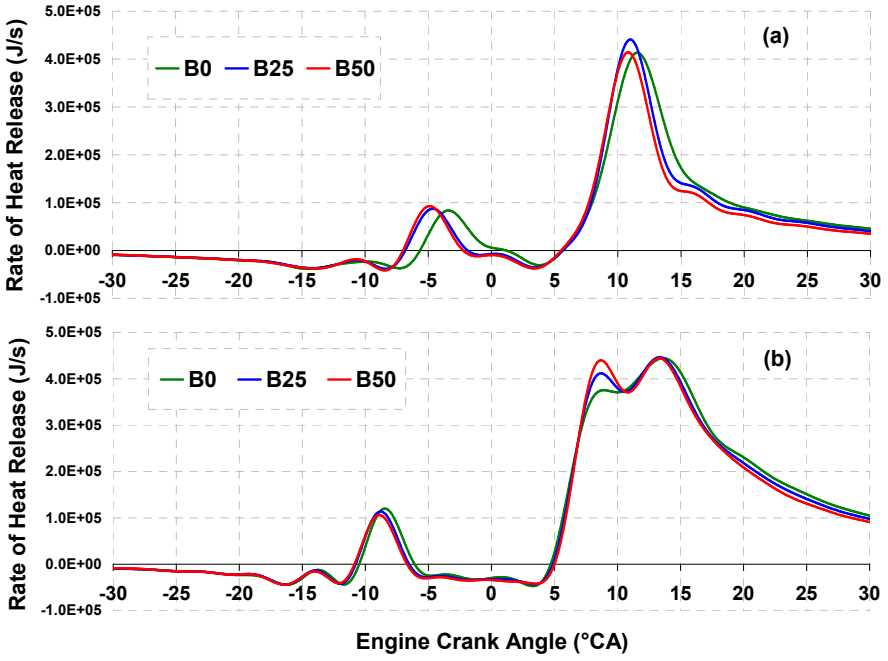

Figure 5.14, Rate of Heat Release for 2250 RPM engine speed at (a) 15% pedal (b) 22% pedal

Even though the demanded rail pressures are constant during this experimental work, the initial combustion of the pilot fuel starts slightly earlier in case of biodiesel fuel blends,

and the quicker rise in heat release rate is also visible. This result indicates the previous suggestion of higher burn rate of biodiesel fuel blends compared to the baseline diesel fuel, which is most likely attributed to the higher oxygen content of biodiesel fuel.

The use of biodiesel fuel blends reduces the engine output power compared to baseline diesel fuel, Figure 5.15. Using B50 biodiesel fuel reduced the engine power by 14% and 4% during the lower and higher pedal positions respectively of the 1500 RPM engine speed, and during the 2250 RPM engine speed, it reduced by 12% and 8%. This is probably due to very low engine outputs during the lower pedal conditions, and any reduction in engine power will have significant impact on the percentage reduction.

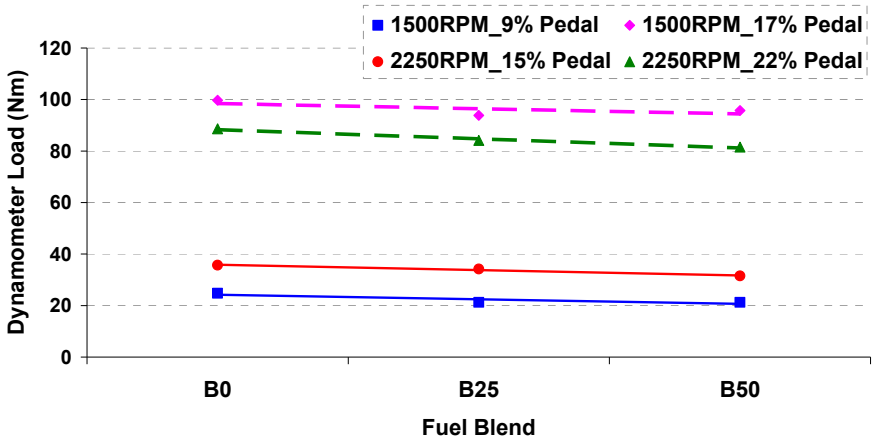

Figure 5.15, Average engine torque at all operating conditions, fixed pedal position

5.6.2 Emissions Analysis

The engine out emission results showed very similar trends and values to the fixed load results, and these are presented in Figure 5.16, Figure 5.17, and Figure 5.18. The CO emissions reduced with biodiesel fuel at all engine operating conditions, and the percentage reduction increased as the engine speed and pedal position increased, the reduction of CO emissions with B50 fuel blend ranged between 14% to 25% compared to baseline diesel fuel.

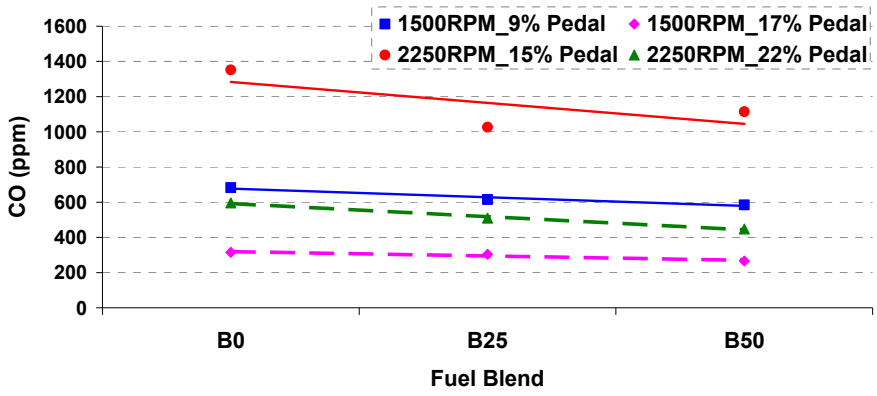

Figure 5.16, Engine out CO emissions with different fuel blends during both engine speeds, fixed pedal position investigation

The lowest amount of HC emissions were produced from the low speed high pedal engine operating condition, and the highest was during high speed high pedal conditions. The engine out HC emissions reduced with increasing biodiesel fuel blend for all engine operating conditions. The percentage reduction in HC emissions with B50 was the highest during the 1500 RPM 17% condition with 59% reduction, and the lowest during the 2250 RPM 22% pedal with 14% compared to baseline diesel fuel. During the lower pedal conditions of both speeds, the reduction was 29% with B50 biodiesel compared to baseline diesel fuel.

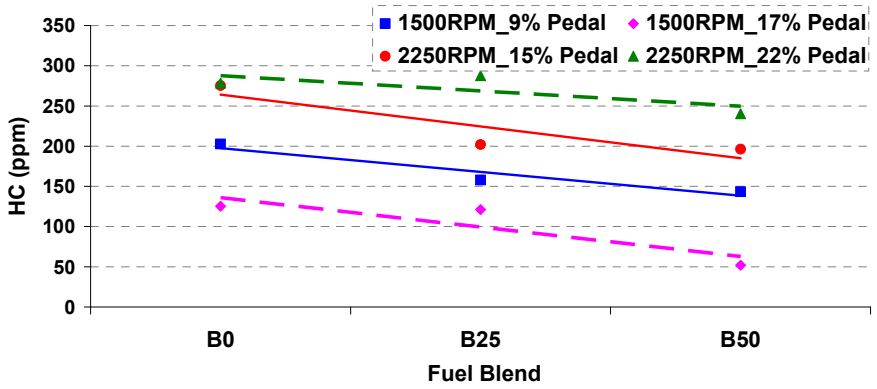

Figure 5.17, Engine out HC emissions with different fuel blends during both engine speeds, fixed pedal position investigation

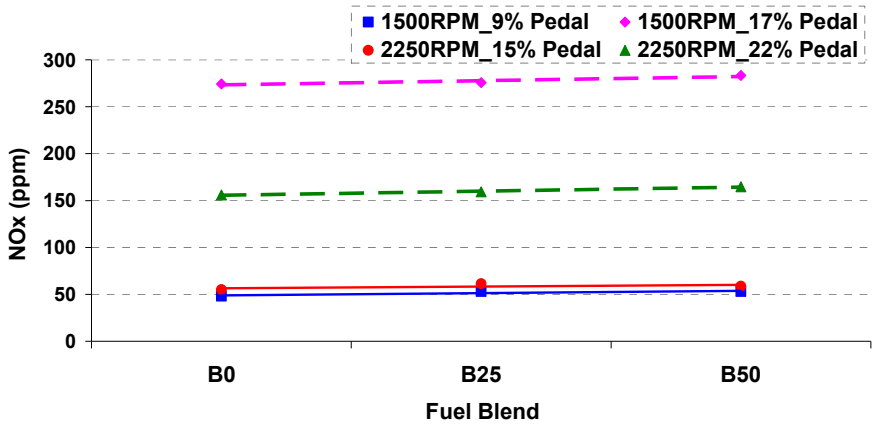

Figure 5.18, Engine out NO_X emissions with different fuel blends during both engine speeds, fixed pedal position investigation

The engine out NO_X emissions showed the typical increase as the percentage of biodiesel increases in the fuel blend at all engine operating conditions (Figure 5.18). The percentage increase with B50 fuel blend during the lower pedal conditions is about 8.5 %, and during the higher pedal conditions is about 4.5 % compared to baseline diesel fuel. The low speed high pedal condition produce the highest amount of NO_X emissions as a trade of higher combustion efficiency and a consequence lower CO and HC emissions observed in Figure 5.16 and Figure 5.17.

The ability to estimate the actual injection timing would be very helpful in order to determine the impact of biodiesel fuel on certain combustion parameters such as ignition delay and combustion duration. An attempt was made in (section 5.5.1) of the current chapter to identify the actual start of injection (SOI) timing by analysing the variations in continuous rail pressure, but the presence of pilot injection disturbed the stability of rail pressure line and makes it very difficult to estimate it.

5.7 In Cylinder Investigation: Fixed Pedal position and deactivated Pilot injection

To investigate the impact of biodiesel fuel on certain combustion parameters such as ignition delay and combustion duration, the engine was operated without the pilot injection in an attempt to identify the actual start of injection (SOI) timing by analysing the variations in continuous rail pressure. Deactivating the pilot injection is not a common practice in a real operating engine due to various benefits of this early pre injection process, since it can be effective in decreasing the ignition delay of the main injection and thus reducing the rate of heat release and consequently in cylinder pressure rise [2]. Also, it is known that the use of pilot injection can reduce engine noise effectively with a penalty of slight increase in soot emissions [130]. The pilot injection was disabled in this part of experimental procedure from the engine calibration map through the ECU calibration tool (ATI vision) in order to explore the difference in combustion process of biodiesel fuels. The disturbance in the engine operation was noticeable upon deactivation of pilot injection especially during the lower pedal conditions; the engine experienced a dramatic noise increase and large rise in engine out emissions as an indication of a compromised combustion process.

5.7.1 Combustion Analysis

The cylinder pressure profiles are plotted in Figure 5.19 and Figure 5.20 for both engine speeds, and the ($P_{Max.}$) values in Table 5.7.

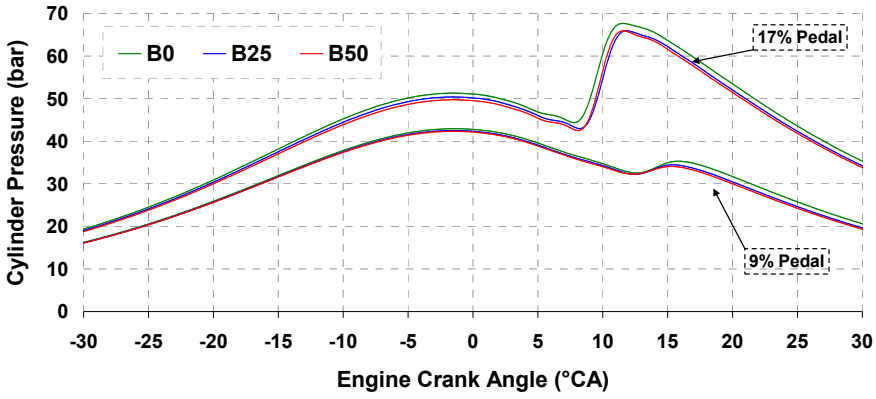

Figure 5.19, Cylinder pressure vs. Crank angle at 1500 RPM, pilot off and fixed pedal position

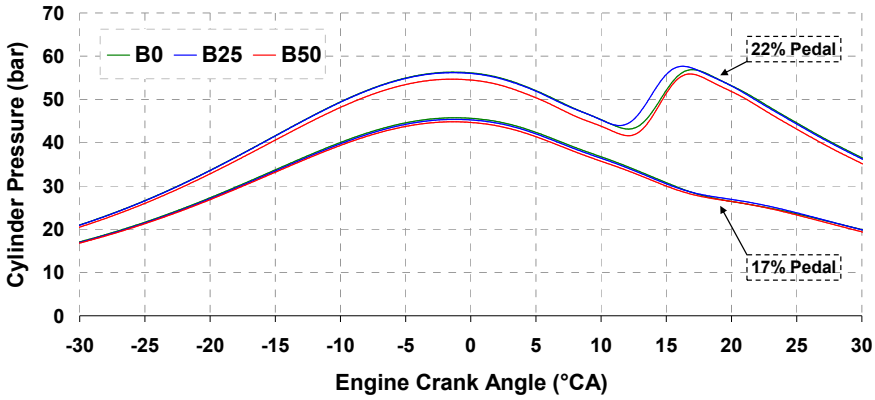

Figure 5.20, Cylinder pressure vs. Crank angle at 2250 RPM, pilot off and fixed pedal position

The pressure curve profiles are very similar with all fuels used, and it is slightly higher in case of baseline diesel fuel during the 1500 RPM engine speed. However, during the higher engine speed the B25 shows slightly higher pressure values than the baseline diesel fuel during the 22% pedal condition. The demanded injection timing by ECU is 3.5° after top dead centre (ATDC) for both pedal positions during the 1500 RPM engine speed, and during the higher engine speed conditions it is 4° ATDC and 3.8° ATDC for the low pedal and high pedal conditions respectively. As appears in Figure 5.19 and Figure 5.20, the rise in pressure curve due to fuel combustion is very low during the lower pedal conditions and more specifically during 2250 RPM engine speed which is an indication of deterioration in the combustion process. This will probably impact the overall performance of the engine during these conditions which will be further investigated in the emissions and engine power analysis. The combustion pressure ($P_{Max.}$) values does not show any significant change with all fuel blends as shown in Table 5.7.

RPM	1500				2250			
Pedal	9%		17%		15%		22%	
$P_{Max.}$	bar	°CA	bar	°CA	bar	°CA	bar	°CA
B0	35.3	15.8	67.6	11.6	28.5	17	56.9	17.0
B25	34.5	15.4	66.0	11.8	24.4	17	57.7	16.3
B50	34.0	15.3	65.9	11.6	28.0	17	55.9	16.8

Table 5.7, Maximum in cylinder pressure values with corresponding crank angles

In general, the maximum cylinder pressure values are much lower and further delayed away from TDC compared to the previous experiments where the pilot injection was active, and combustion deterioration due to pilot injection loss is probably what has caused this reduction in cylinder pressure.

The rate of heat release diagrams for all fuels at different engine operating conditions are shown in Figure 5.21 and Figure 5.22. Figure 5.21 shows that the rate of heat release starts increasing slightly earlier with B50 biodiesel fuel blend during the low pedal condition and with baseline diesel fuel during the higher pedal condition. Higher peaks of heat release rates can be seen with baseline diesel fuel compared to biodiesel during the lower pedal condition, which is probably owing to higher volatility and better mixing of diesel with air at such low speed low load conditions. During the higher pedal condition of 1500 RPM engine speed, the trend reverses as the SOC of baseline diesel fuel picks up earlier than biodiesel fuel blends.

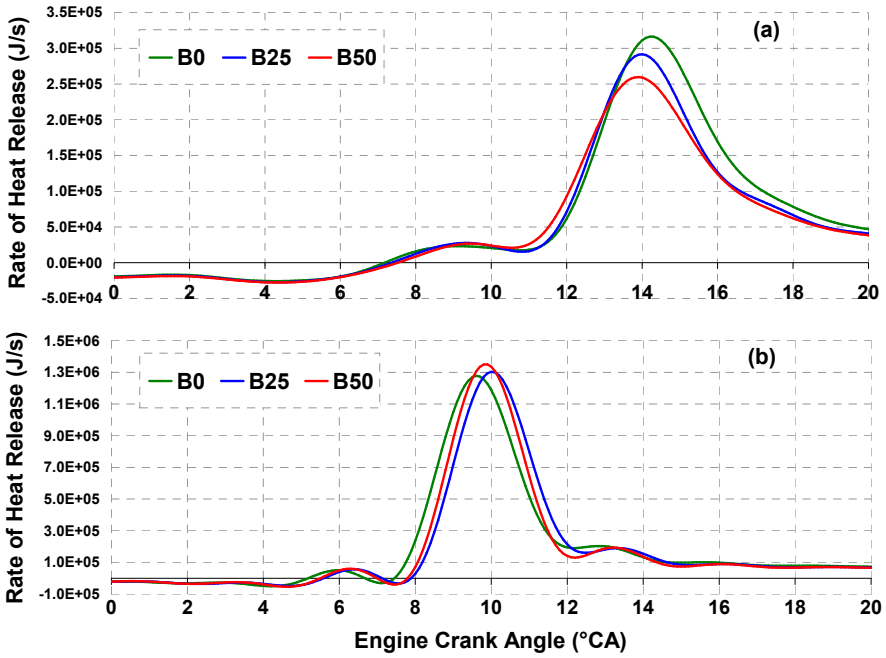

Figure 5.21, Rate of Heat Release for 1500 RPM engine speed pilot off at (a) 9% pedal (b) 17% pedal

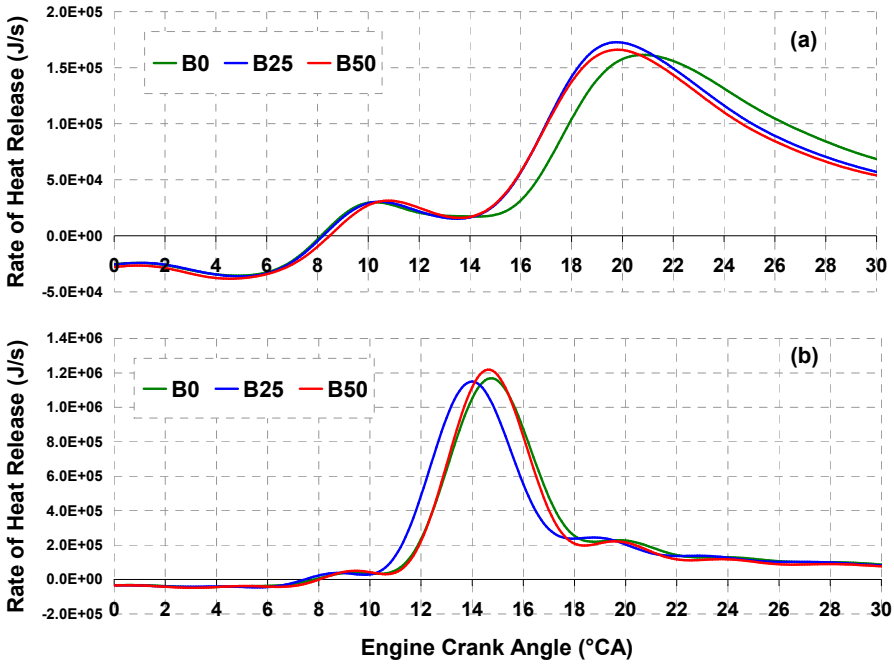

Figure 5.22, Rate of Heat Release for 2250 RPM engine speed pilot off at (a) 15% pedal (b) 22% pedal

Figure 5.22 shows earlier SOC with biodiesel blends during the 2250 RPM engine speed compared to baseline diesel fuel. Overall, the rate of heat release results does not show an obvious trend with biodiesel fuel blends compared to diesel, which is most likely caused by instability of the combustion process when pilot injection is deactivated.

5.7.2 Fuel Injection Process

The actual start of injection (SOI) was investigated in order to indentify any adverse effects of biodiesel fuel properties on the injection system. The start of injection was identified as the first infinitesimal reduction in rail pressure other than the normal line pressure fluctuations. This small reduction in rail pressure is normally caused by releasing the fuel into the combustion chamber and it indicates that the fuel is flowing through injector channels. Since there is a delay period between the start of injection signal from the ECU requesting fuel and the actual nozzle needle lift, the demanded time by ECU is not the most accurate indication of the actual start of injection. Furthermore, the actual physical drop in rail pressure is a better and more realistic indication for the start of injection since the response of the nozzle needle solenoid valve might vary slightly from case to case, and previous researchers have based their conclusions about fuel injection

timing with biodiesel based on fuelling pressure as reported by Szybist et al. [67]. These results confirm the generally accepted idea that the fuel line pressure is a good indication of the fuel injection timing [68, 78]. While this is an accurate way to measure the comparative SOI, it is difficult to estimate the injection duration from the fuel pressure line.

Figure 5.23 shows the actual SOI timing for all experimental conditions with all three fuel blends. The results show that the SOI slightly retards with the increase biodiesel percentage in the blend during the lower load conditions of both speeds, and this variation is very small as it does not exceed 0.3°CA retardation with B50 compared to baseline diesel, and during the higher engine load conditions no significant change in SOI can be observed with all fuel blends.

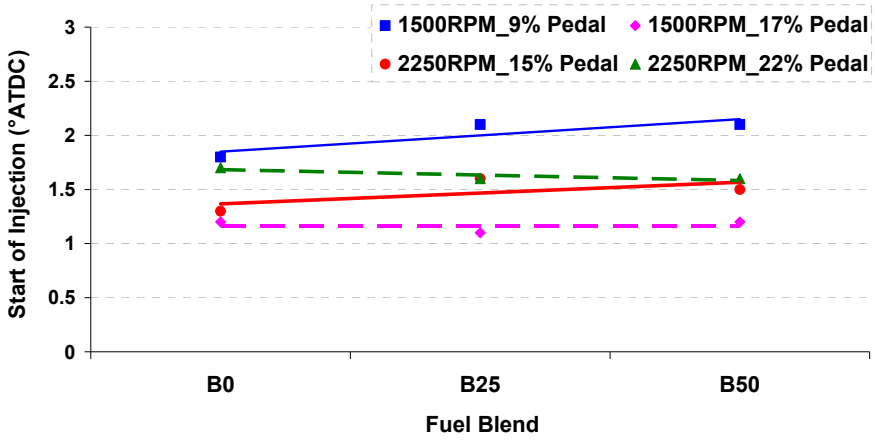

Figure 5.23, Actual start of injection timing with different fuels and pedal position

The little advancement in SOI in the case of baseline diesel fuel during lower load conditions is probably attributed to its lower viscosity and density compared to biodiesel fuel. As discussed in section 5.3.3 of this chapter, the operation of electronic fuel injectors are mainly dependant on balancing forces on the injection needle by means of pressure drops through precise valve seats and orifices. The fuel's kinematic viscosity will have an impact on the response of the fuel injector by either quicker or slower passage through the injector channels.

From these results, it can be concluded that the impact of biodiesel fuel on SOI can not be considered as significant which agrees with most of the published literature with common rail fuel injection system, refer to section 2.4.3 of chapter 2, and the difference in physical and chemical properties of biodiesel does not seem to have a significant effect on the performance of the common rail fuel injection system.

5.7.3 Ignition Delay Investigation

The ignition delay is the time or crank degrees between the start of injection and start of combustion. The parameters that most affect ignition delay is temperature and pressure of the air during the delay period in addition to the CN of the fuel used [2]. Long ignition delays are not desirable due to the fact that large amounts vaporized fuel mixes with air during this period and burns rapidly giving a high rate of pressure rise. As discussed in the literature review chapter 2 section 2.3.1, it is commonly known that the CN of biodiesel is generally higher than fossil diesel fuel due to the un-presence of aromatic compounds, which proposes that shorter ignition delay periods are expected with biodiesel fuels and its blends.

In this experiment the ignition delay was determined by calculating the crank angle difference of the instantaneous rise in the heat release rate and the actual SOI value determined in the previous section. The calculated crank angle degrees were then converted to milliseconds in order to account for engine speed. The estimated ignition delay periods (crank angle and time) for all fuel blends during all engine operating conditions are plotted in Figure 5.24. The ignition delay period is shorter during the higher load conditions due to the availability of higher amounts of fuel and consequently higher cylinder pressures and temperatures.

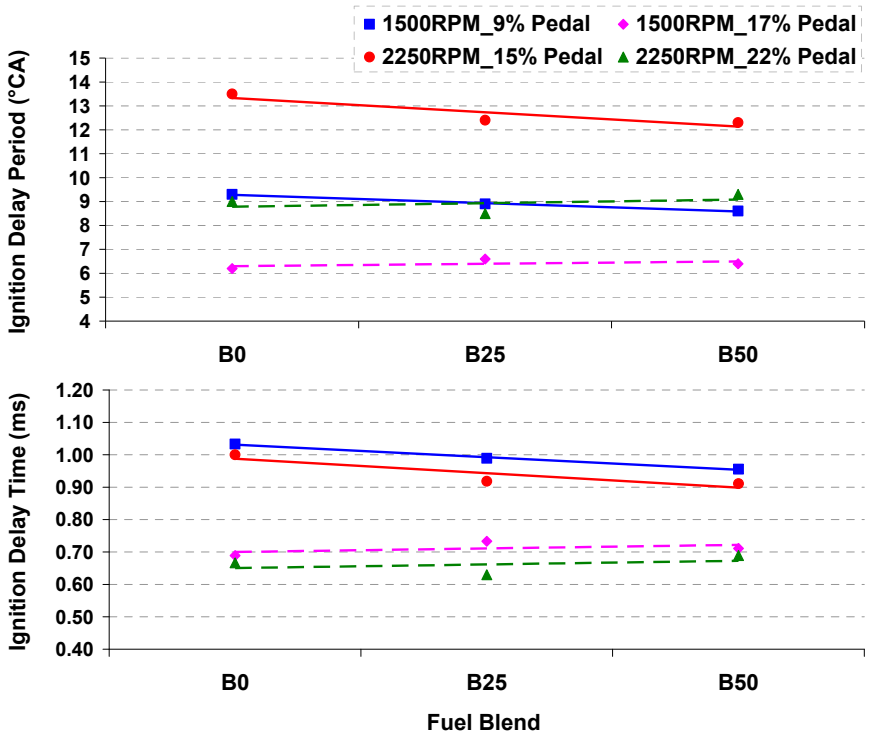

Figure 5.24, Estimated ignition delay, pilot off fixed pedal position

Figure 5.24 also shows that the ignition delay time decreases slightly with increasing biodiesel blend during the lower pedal conditions, whereas it does not show any significant change during the higher pedal conditions. The reduction in the ignition delay time in the lower pedal conditions corresponds to about 1° CA with B50 biodiesel compared to baseline diesel fuel, see Figure 5.24 top. Even though the RME fuel used in this experiment does not have higher CN than baseline diesel fuel (CN of RME is 49.5 and for baseline diesel is 52.8, see Table 5.2), but it produces a shorter ignition delays. This reduction in ignition delay with biodiesel is mostly attributed to better ignition quality of biodiesel as a result of its higher oxygen content compared to baseline diesel fuel, which became very beneficial during lower engine load conditions [17].

From the combustion analysis of this section, it was noticed that the effect of deactivating the pilot injection was significant on the combustion performance during all engine operating conditions. The percentage change in engine out emissions and performance when the pilot injection is deactivated is presented in the next section.

5.7.4 Effect of Deactivation of Pilot Injection

The impact of deactivating the pilot injection is more significant on biodiesel fuel compared to baseline diesel fuel, Figure 5.25.

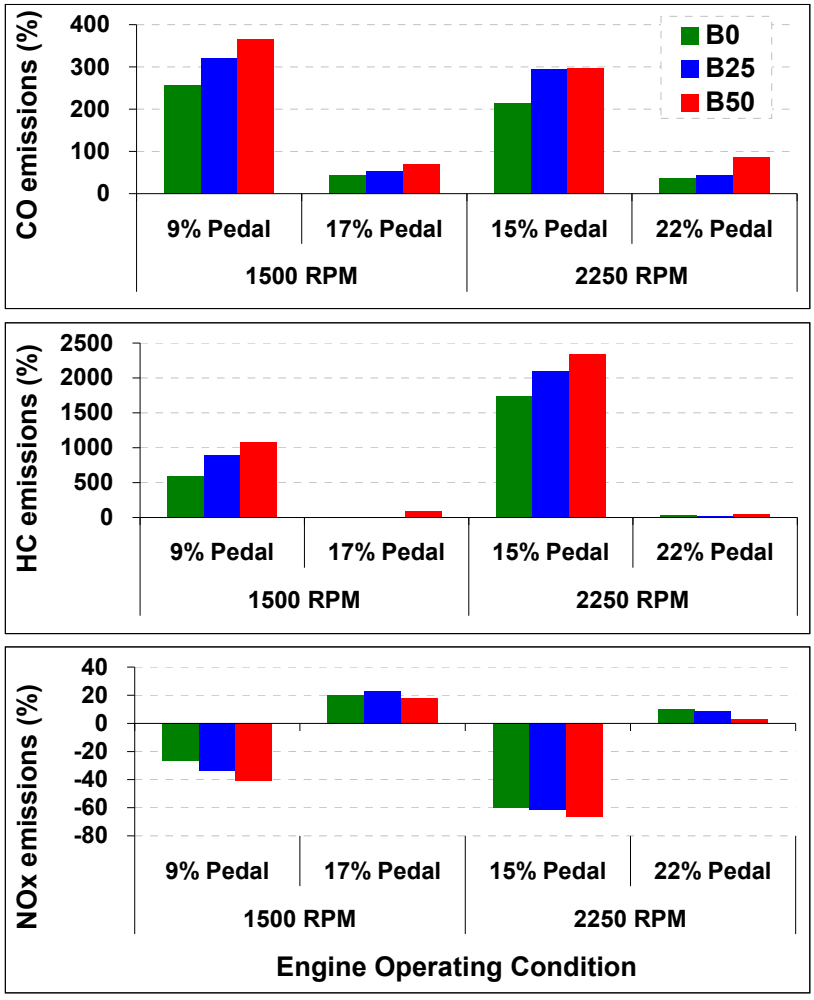

Figure 5.25, percentage change in engine out emissions with deactivated pilot injection compared to the standard calibration

The emissions of CO and HC significantly increases by deactivating pilot injection, but with higher percentages in case of biodiesel fuel blends especially during lower load conditions due to the deterioration in the combustion process. Even during the higher load conditions where the combustion process was more efficient, the engine produced higher

amounts of CO and HC emissions with B25 and B50 blends compared to baseline diesel fuel. These results really emphasise that losing the pilot injection has more impact on the combustion process with biodiesel especially when the engine is operated at lower load conditions. The combustion of the fuel injected in the pilot injection process contributes very strongly to the overall combustion strategy, because it does effectively "warm up" the combustion chamber so the main injection vaporizes more quickly and decreases the ignition delay. As a result, losing the pilot injection will slow down the vaporization process of the fuel and the impact will be even more significant on higher viscosity and slower atomized biodiesel fuel blends.

The analysis of the engine output power also revealed that by deactivating the pilot injection, the power produced by the engine dropped dramatically with all fuels and higher reduction is seen with biodiesel blends, see Figure 5.26. This bar chart clearly shows the huge impact of deactivating the pilot injection on the engine power during lower load (low pedal) operating conditions, however the impact is much lower during higher load conditions.

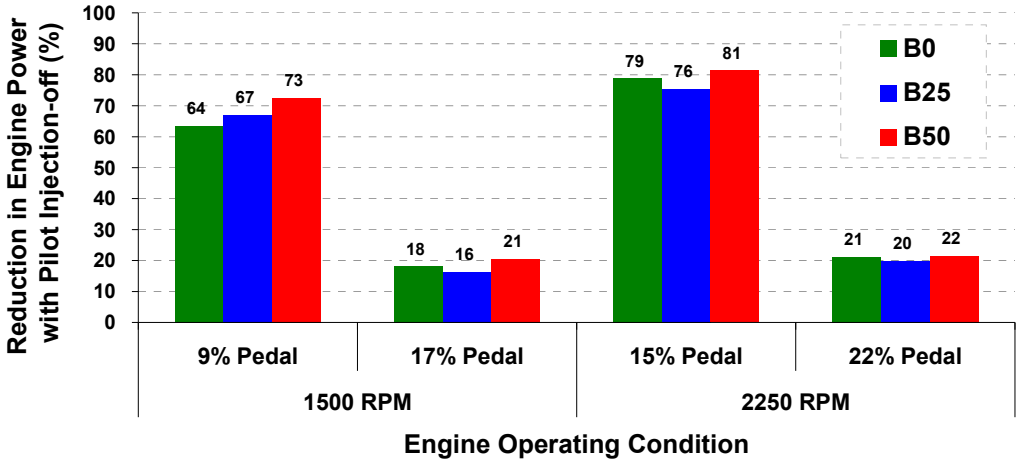

Figure 5.26, the reduction in engine power due to the deactivation of pilot injection for all fuel blends at all operating conditions

The highest drop in engine power was during 2250 RPM and 15% pedal conditions, where it dropped by an average of 80% for all fuel blends. This is probably due to the vital role of pilot injection in conditioning the cylinder by raising its temperature and pressure

before the main injection for quicker and more complete combustion which is more significant during higher engine speeds. Also the amount of fuel volume lost, as a proportional to the total volume, by deactivating the pilot is more significant at 15% pedal and 2250 RPM engine speed conditions due to higher engine power produced at this speed compared to the 1500 RPM and 9% pedal.

During the 1500 RPM and 9% pedal, the drop in engine power was the worse for B50 compared to the baseline diesel fuel because this low temperature and pressure condition creates the worst case scenario for the higher flash point B50 biodiesel. In addition the recorded rail pressure at this speed and load is around 500 bars only compared to all other engine operating conditions, which are around 900 bars. The lower rail pressure will have more negative impact on more viscose biodiesel fuels as a result of lower atomization efficiency. However, at the higher load conditions the impact of losing the pilot injection is less significant due to the already higher pressure and temperatures conditions of the cylinder in, addition to the fact that the fuel volume lost is considered a very little portion to the total volume of fuel at these high load conditions.

Several factors might be attributing to this reduction in engine power and deterioration in the combustion process when the pilot injection is deactivated. The first factor is the reduction in total amount of fuel injected during each stroke, even though the amount of fuel injected by the pilot is very little but its ratio to the total amount will be significant during lower load conditions. Secondly loosing the benefits of pilot injection which is raising the cylinder pressure slightly due to the combustion of the fuel and therefore the heat within the cylinder also rises, and again this will have higher impact during lower load conditions. The third possible factor might be that the engine is not optimized to operate without pilot injection, and further modification of engine map could improve the situation.

5.8 Conclusions

The aim of this experimental work was to investigate the combustion behaviour of two different blends of biodiesel (B25 and B50) compared to the baseline diesel fuel when the engine is operated at two different load and speed conditions. The following conclusions are drawn from this study:

- The cylinder pressure profiles of the biodiesel blends are very similar to the baseline diesel fuel, and both biodiesel blends experience very similar combustion phases or stages as the baseline diesel fuel when similar loads are demanded from a standard calibration diesel engine. Earlier SOC of the pilot fuel by 0.5-1.0° CA with B50 biodiesel compared to baseline diesel fuel is observed, but the SOC of the main charge did not show any significant variations for all fuel blends.
- A slightly quicker rise in the rate of heat release and higher peak values were observed with biodiesel blends compared to baseline diesel fuel at most of the engine operating conditions, most likely caused by improved ignitability of biodiesel due to increased oxygen content and higher rail pressures seen with biodiesel fuels.
- The fuel demand increased with increasing blend ratio at all experimental conditions to compensate for the reduced LHV of biodiesel. The percentage increase in fuel demand at the lower load conditions was 10-16% and during the higher load conditions was 6-8% for a B50 blend. This fuel consumption penalty was greater than would be expected due to calorific value alone and is likely as a consequence of reduced atomization and evaporation of biodiesel fuels during lower operating conditions.
- The maximum cylinder pressure decreased slightly (1-2%) with biodiesel when the engine was operated at pedal positions matched to those for diesel fuel. The SOC did not show any significant variations with biodiesel compared to baseline diesel.
- The use of biodiesel blends reduced the engine output power compared to baseline diesel fuel. Using B50 reduced the engine power by up to 14% and 8% during the lower and higher pedal positions respectively.

- By deactivating the pilot injection the actual SOI was determined; it slightly retarded with biodiesel during the lower load conditions with both speeds, and the variation was very small and did not exceed 0.3° CA with B50 compared to baseline diesel, during the higher engine load conditions no significant change in SOI could be observed. The ignition delay time decreased slightly with biodiesel during the lower pedal conditions, whereas it did not show any significant change during the higher pedal conditions. The reduction in the ignition delay time corresponded to about 1° CA with B50 biodiesel compared to baseline diesel fuel which most likely attributed to better ignition quality of biodiesel as a result of its higher oxygen content compared to baseline diesel fuel. This investigation also emphasised that deactivating the pilot injection had more adverse impact on the engine performance and emissions with biodiesel fuel especially when the engine is operated at lower load conditions due to the critical role of the pilot injection on the overall combustion strategy.

- In general, the engine out CO emissions reduced with biodiesel at all engine operating conditions, with the reduction varying according to engine speed and load. On average, the CO reduction with B50 fuel was approximately 23% compared to the baseline diesel fuel. Similarly, the engine out HC emissions reduced with biodiesel use at all engine operating conditions except for the high speed and high load condition where no significant change was observed. The variation in HC emissions was significantly influenced by engine speed and load, with the average reduction in HC emissions, with a B50 blend, being approximately 35% compared to the baseline diesel fuel. The NO_X emissions showed an increasing trend as the percentage of biodiesel increased in the blend at all engine operating conditions. The average percentage increase in NO_X emissions for B50 was approximately 13% compared to baseline diesel fuel.

Chapter 6 Biodiesel Engine Calibration Sensitivity

6.1 Introduction

Engine calibration is the method that is used to optimise engine performance, durability and emissions. This is undertaken by tuning the engine governing parameters by modifying the ECU mapping data. Work reported in chapters three and five has shown that biodiesel fuel has, in certain cases, a negative effect on power, fuel economy and emissions. The aim of the work reported in this chapter is to assess the sensitivity of the Ford Puma 2.0 litre turbocharged diesel engine, equipped with common rail fuel injection system to calibration changes with a B25 biodiesel and compare it with the results for baseline fuel. Understanding the effect of changes on the performance and emissions may aid engineers to optimize the engine for biodiesel use. This study has been performed by adjusting a number of the main engine parameters such as EGR value, fuel line rail pressure, and both main and pilot injection timing.

6.2 Approach

This work was carried out within the Powertrain and Vehicle Research Centre (PVRC) in the Department of Mechanical Engineering at the University of Bath. The approach to determine the sensitivity of the diesel engine to calibration changes with B25 was to operate the engine whilst adjusting a number of the main parameters compares the results with the standard calibration. The engine was operated with both B25 and baseline diesel fuel at 1500 RPM and two fixed pedal positions of 10% and 17%, and at the 2250 RPM with two fixed pedal positions of 15% and 22% representing low and mid-high loads. The investigation was carried out with the following calibration adjustments:

- Perform a wide range swing in EGR compared the standard calibration plus setting it zero value.
- Vary the fuel system rail pressure by a factor of ± 10% compared to the standard calibration.

- Swing the main injection timing demand by advancing and retarding the standard demand time by 2° CA.
- Finally, vary the pilot injection timing by advancing and retarding it from the main calibration by a factor of 2° CA.

6.3 Varying the EGR Rate

Recirculation of the exhaust gas into the engine involves the replacement of oxygen and nitrogen with mainly carbon dioxide from the engine exhaust. As a result, it reduces the oxygen concentration of the intake mixture, which results in lower NO_X due to lower combustion temperature, but excess rates of EGR could reduce the combustion efficiency and increase CO and HC emissions [2]. However, biodiesel is an oxygenated fuel and it undergoes improved combustion in the engine due to the presence of molecular oxygen which also leads to higher NO_X emissions [4, 7, 10, 24, and 64]. Thus, using EGR with biodiesel could be more beneficial in reducing NO_X emissions without or less emission penalties as reported by a number of studies [70, 102-106]. The pedal position was fixed for all fuel blends during all operating conditions and the EGR value fraction passing into the combustion chamber was controlled by both adjusting the EGR valve position and altering the rate of mass air flow (MAF) through the ECU calibration tool (ATI vision). The variations in EGR percentage investigated were around 10% higher and 10% lower than the standard calibration in addition to setting the EGR value to zero for both fuel blends during all engine operating conditions.

6.3.1 1500 RPM 10% pedal

The effect of EGR swings on engine performance and emissions during the 1500 RPM and 10% pedal position are shown in Figure 6.1. The standard calibration calls for an EGR value of 47% for this operating condition, and increasing the EGR rate increases the engine out emissions of both CO and HC significantly in addition to a reduction in engine torque and NO_X emissions.

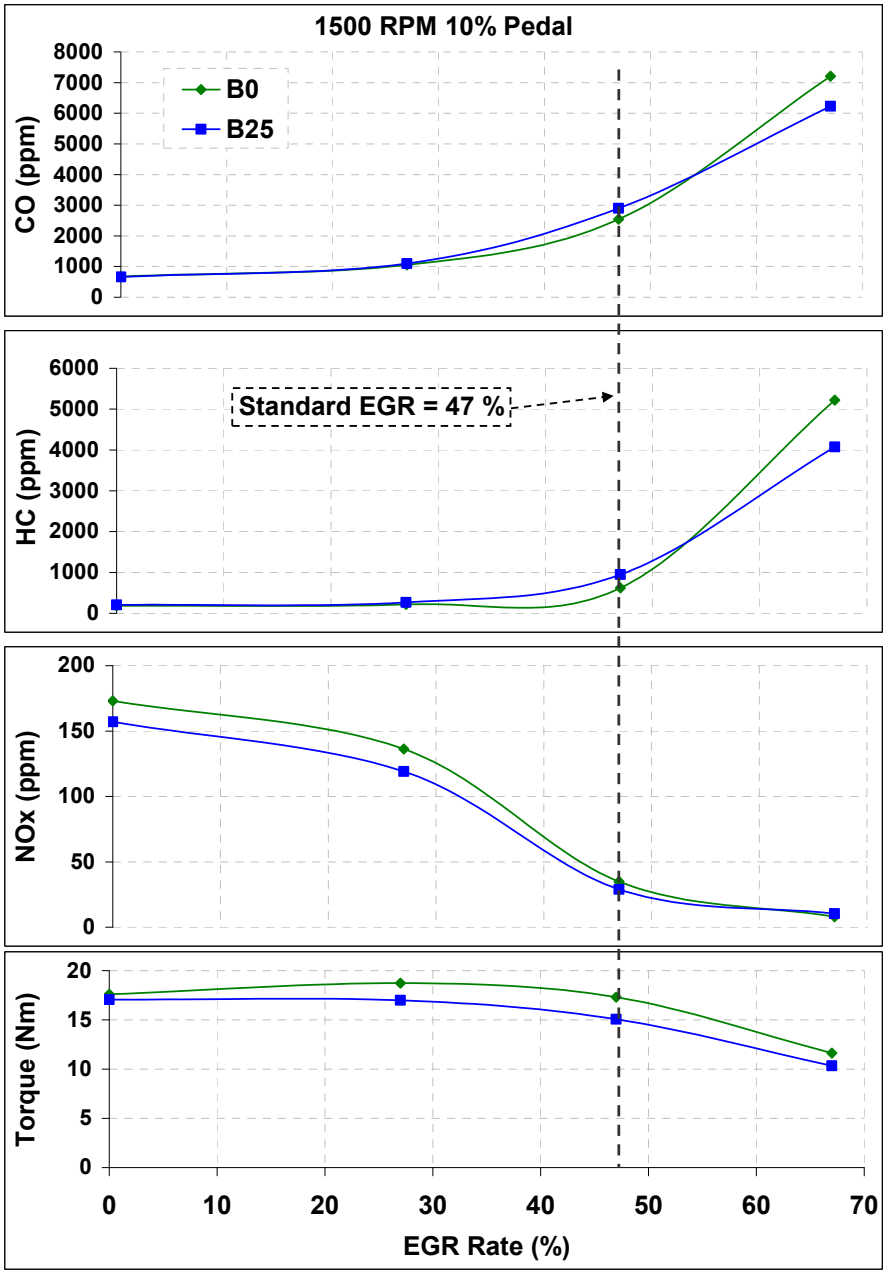

Figure 6.1, the effect of EGR swing on the engine torque and emissions for the 1500 RPM and 10% pedal position

This indicates a possibility of further deterioration in the combustion process by increasing the EGR rate. This is caused by a further compromise reduction of oxygen inside the combustion chamber due to very high amount of EGR being re-circulated which contains a great deal of unburned hydrocarbons and products of partial combustion, and this excessive amount of EGR might also lead to extremely unstable combustion and even misfiring. Even though increasing the EGR amount deteriorates the combustion and

reduces engine torque by 32 % with both fuels at the condition, but the engine out emissions show slightly lower sensitivity with B25 compared to the baseline diesel fuel, which is most probably caused by higher oxygen content of biodiesel fuels.

The deterioration of the combustion with increasing EGR amount is clearly evident by analysing both the rate of heat release and cylinder pressure curves plotted in Figure 6.2.

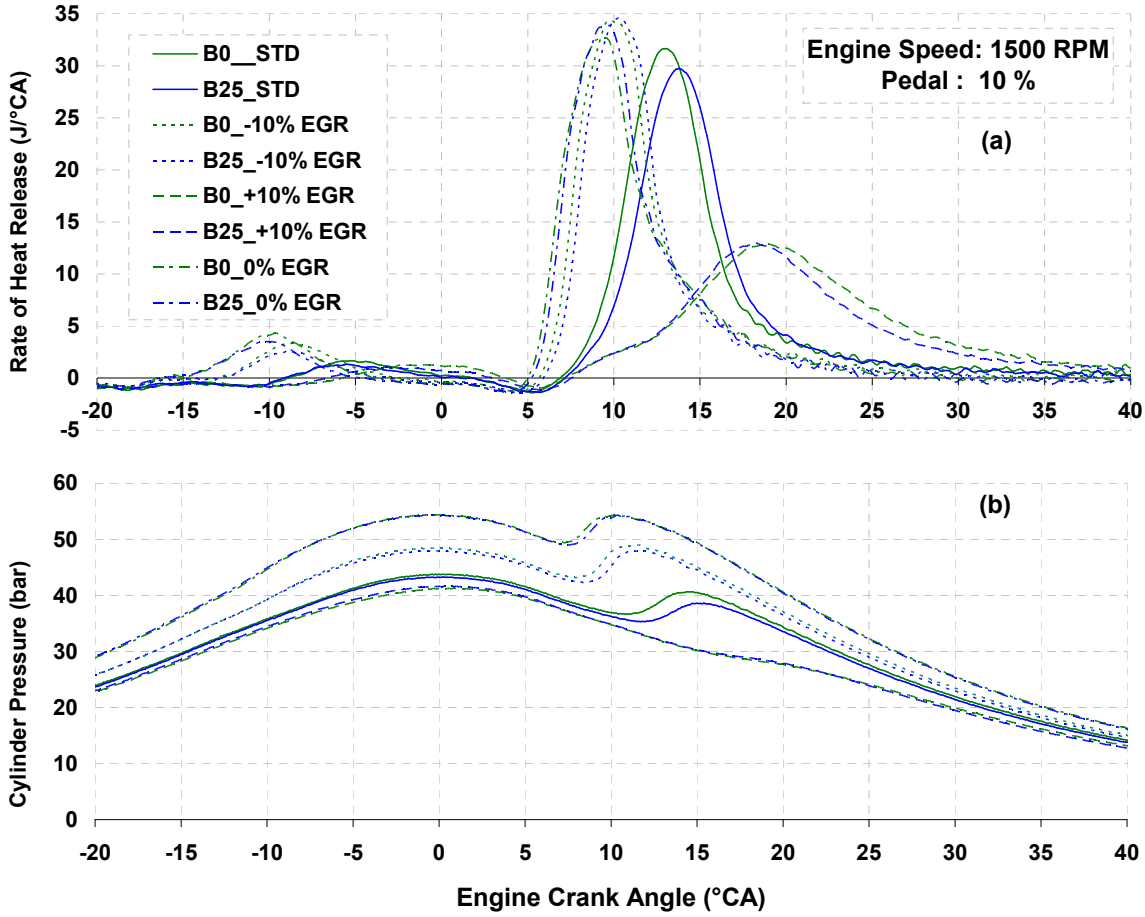

Figure 6.2, the effect of EGR variation on (a) rate of heat release and (b) cylinder pressure at 1500 RPM and 10% pedal position

Only in the case of EGR increase, the rate of heat release starts earlier with B25 compared to the baseline diesel fuel whereas during the standard condition and when EGR is reduced, the B25 fuel shows a more delayed trend. Also with increasing EGR, the cylinder pressure curve of B25 matches the baseline diesel fuel curve.

However, with the EGR value tuned to a lower rate, the engine output performance and emissions of CO and HC improved for both fuel blends with a penalty of increase in NO_X emission resulted from higher combustion efficiency and higher cylinder pressure and temperature compared to the standard calibration, with slightly lower response from B25. In the mean time, the engine out performance and emission response to EGR reduction shows very similar sensitivity with both fuels compared to the standard calibration. Finally, shutting the EGR valve completely improved the combustion efficiency significantly by reducing both CO and HC emissions for both fuels, and the higher combustion pressures and temperatures also caused significant increase in NO_X emissions. However, closing the EGR valve completely improved the engine output torque very slightly which might be attributed to loosing a great amount of thermal heat energy which is very effective during such a low operating condition. The engine performance and emissions response to closing the EGR valve was very similar with B25 and the baseline diesel fuels.

6.3.2 1500 RPM 17% pedal

The investigation results of the higher pedal position of the 1500 RPM engine speed versus EGR variations are shown in Figure 6.3. The standard EGR rate during this operating condition was about 16% and the impact of EGR variation shows very similar trends to the 10% pedal condition. Increasing the EGR value over the standard calibration increases the engine out emission of CO with both fuels however; the percentage increase was 70% lower with B25 compared to baseline diesel fuel. Similarly, higher percentage reduction of HC emissions (10% higher) were observed with B25 compared to the baseline diesel fuel. The engine out NO_X emission shows slightly higher percentage reduction in case of the baseline diesel fuel when the EGR rate was increased compared to B25, and the engine out torque reduced by 3.5% with baseline diesel fuel whereas it does not show any change with B25. This indicates that the impact of increasing the EGR value is less significant on the combustion process in case of B25 compared to the baseline diesel with a benefit of significant reduction in HC and NO_X emissions, which is most probably caused by higher oxygen content of biodiesel fuels.

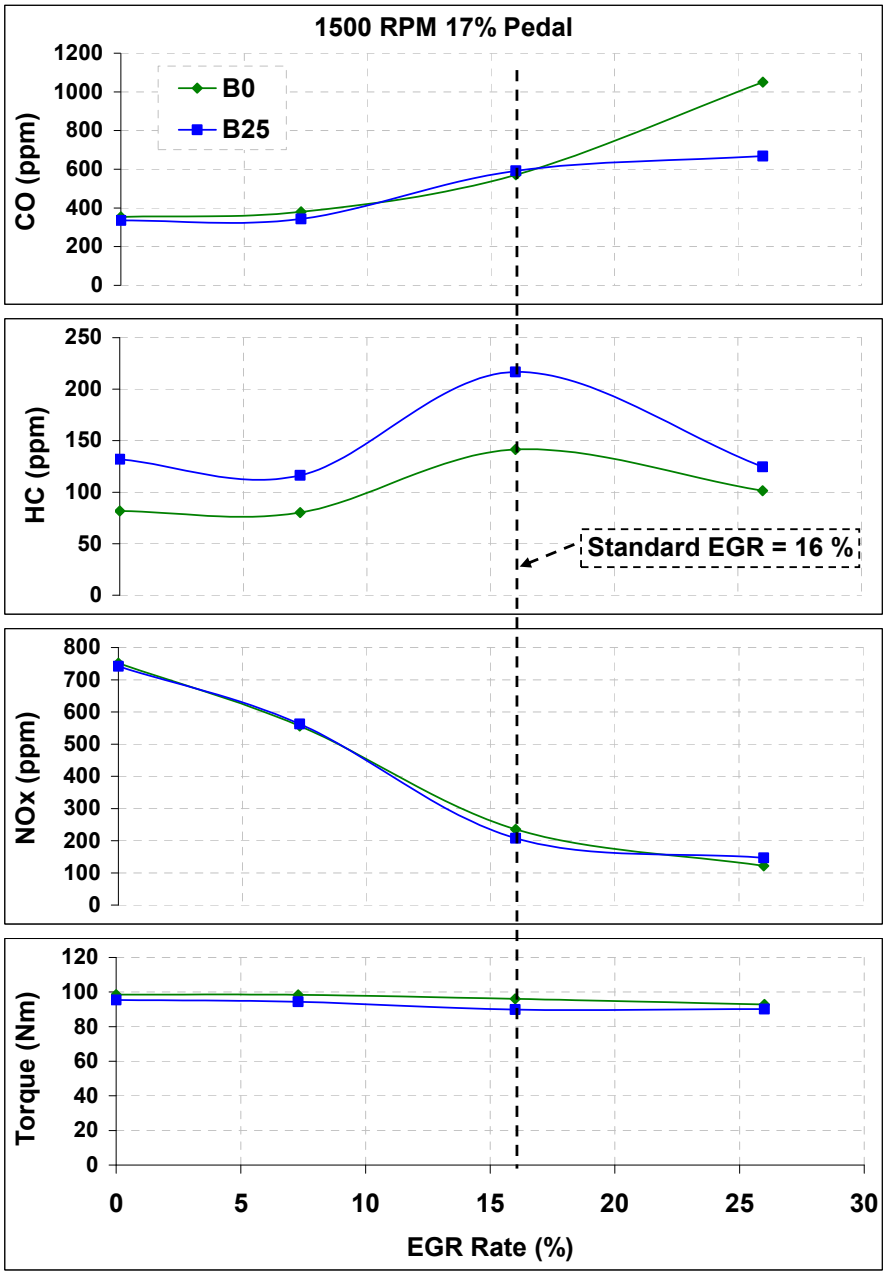

Figure 6.3, the effect of EGR swing on the engine torque and emissions for the 1500 RPM and 17% pedal position

Increasing the EGR rate generally reduced the combustion pressure and reduced the peak cylinder temperature and rate of heat release as shown in Figure 6.4. The rate of heat release shows earlier rise with baseline diesel fuel when EGR is increased, but the curve corresponds to B25 quickly catches up and reaches higher peak values compared to

baseline diesel fuel which probably explains the higher percentage increase in NO_X emissions.

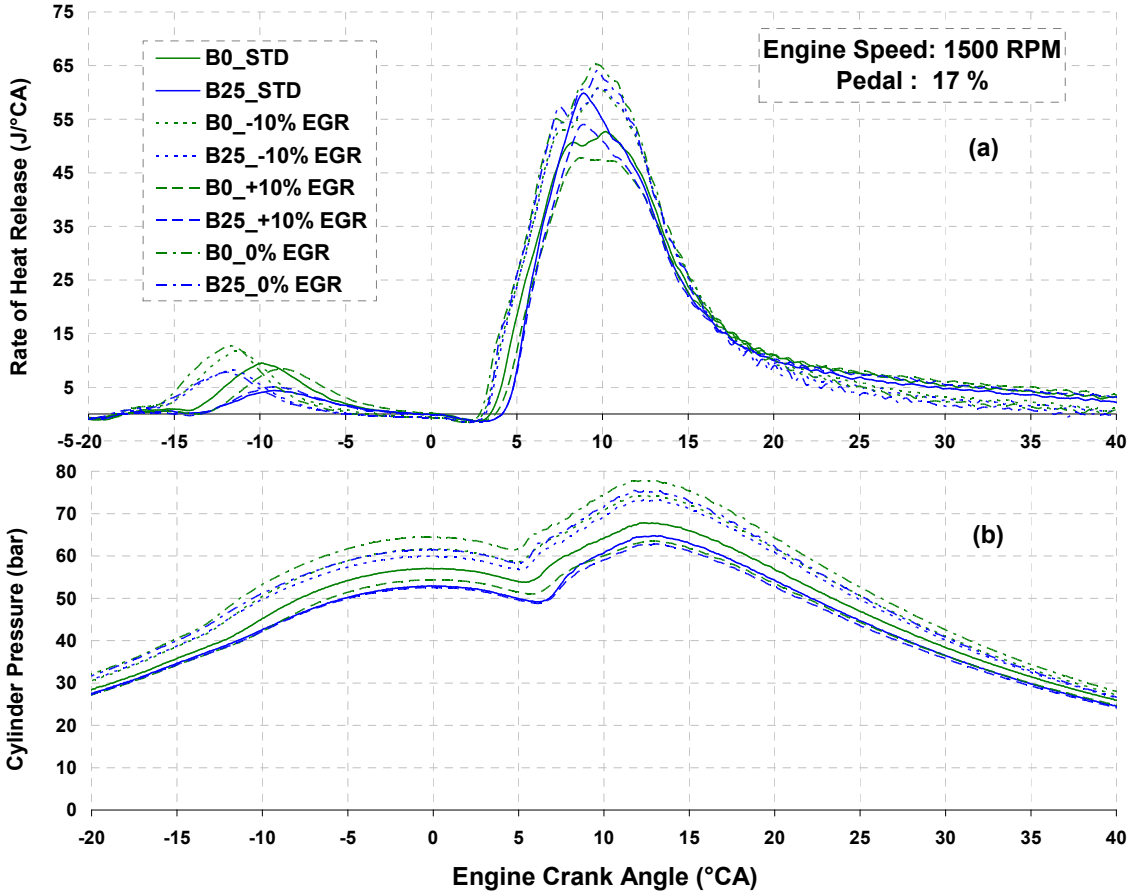

Figure 6.4, the effect of EGR variation on (a) rate of heat release and (b) cylinder pressure at 1500 RPM and 17% pedal position

On the other hand, reducing the EGR rate shows similar impact on engine out performance and emissions seen in the previous condition, and it is very similar with both fuels. The engine output emissions of CO and HC improved with both fuels with a penalty of significant increase in NO_X emission probably resulted from higher combustion cylinder pressure and temperature compared to the standard calibration. In the mean time, the improvement in engine out performance with EGR reduction is very low compared to the standard calibration. Finally, closing the EGR valve completely had very similar impact on the engine out emissions when engine was running with both fuels with hardly any benefits on engine out torque very similar to the previous engine operating condition with further increase in NO_X emissions.

6.3.3 2250 RPM 15% pedal

The effect of adjusting the EGR rate on engine out emissions and performance during this higher engine speed and 15% pedal condition are shown in Figure 6.5.

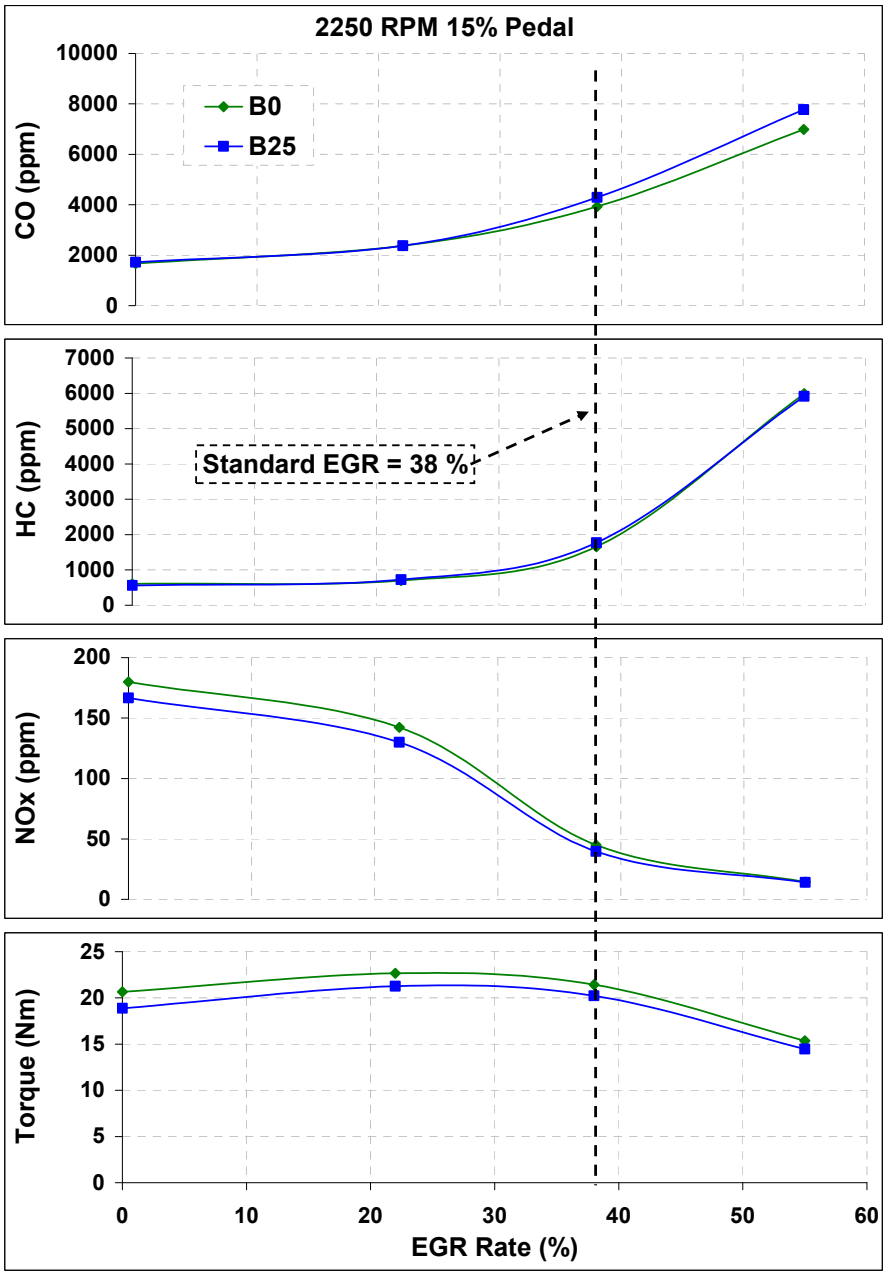

Figure 6.5, the effect of EGR swing on the engine torque and emissions for the 2250 RPM and 15% pedal position

The standard calibration for the lower pedal condition calls for 38% EGR to be recycled back to the inlet manifold. Increasing the EGR rate leads to significant increase in both CO and HC emissions in addition, to a steep reduction engine out torque with both fuels. This indicates further deterioration in the combustion process with a slight benefit of NO_X reduction due to the expected declination in combustion pressures and temperatures. The impact of increasing the EGR is almost the same with both fuels compared to the standard calibration.

Decreasing the EGR rate shows similar response to the lower engine speed condition, and same the impact for both fuels. Finally, shutting off the EGR valve completely slightly improved the combustion efficiency by reducing both CO and HC emissions with an addition increase in NO_X emission without any benefits in engine output torque. As a matter of fact, the engine output torque reduces slightly with both fuel blends in spite of the expected better combustion efficiency which could be attributed the loss of thermal heat energy from EGR during this low power engine operating condition.

6.3.4 2250 RPM 22% pedal

The investigations of the higher pedal position of the 2250 RPM engine speed versus EGR variations are shown in Figure 6.6. The standard EGR value during this operating condition was about 14%, and an increase in EGR value resulted in a slight increase in the CO emissions. The HC emissions showed a little drop with both fuels with slightly higher percentage decrease in case of B25 compared to the standard calibration. The NO_X emissions and engine output torque showed a similar percentage decrease with both fuels compared to the results from the standard EGR rate.

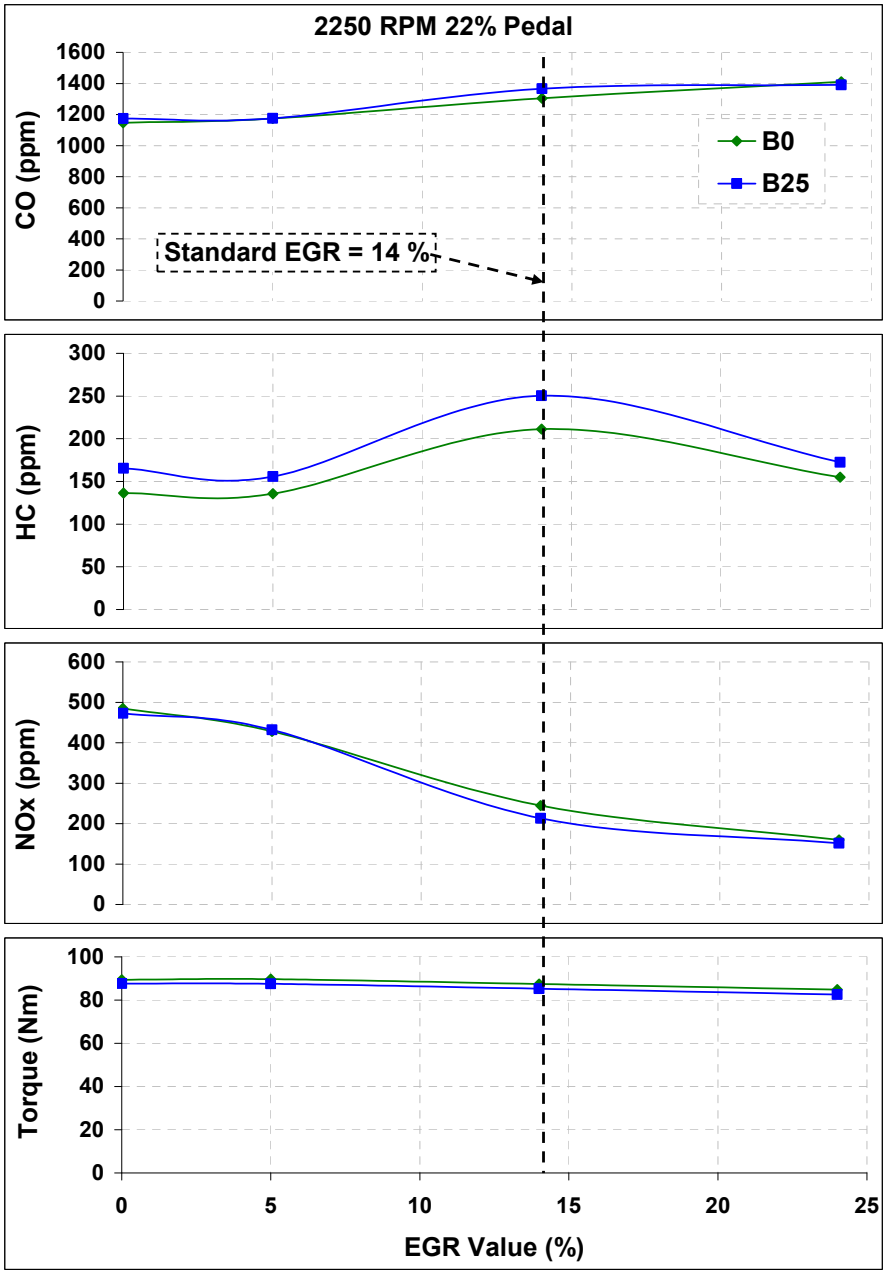

Figure 6.6, the effect of EGR swing on the engine torque and emissions for the 2250 RPM and 22% pedal position

On the other hand, reducing the EGR rate does not seem to produce any advantages of B25 over the baseline diesel fuel, since both fuels show very similar impacts on the engine performance and emissions compared to the standard calibration, and similar results were obtained when the EGR rate was set to zero.

6.4 Varying Rail Pressure

The fuel injection equipment (FIE) used in this investigation is a common rail fuel injection system as detailed in the previous chapter. The main advantage of theses systems is the flexibility in adjusting the rail pressures for different operating conditions to achieve optimum fuel/air mixing and engine performance and emissions. Altering the injection pressure is expected to effect the spray atomization and penetration of the injected fuel depending on the fuel's chemical and physical properties such as viscosity and surface tension. In this experimental procedure, the rail pressure was varied by changing the value of the multiplier in the engine ECU through the ECU calibration tool (ATI vision). The variations in rail pressures investigated were 10% higher and 10% lower than the standard calibration for both fuel blends during all engine operating conditions.

6.4.1 1500 RPM 10% pedal

The effect of varying the rail pressure on the engine out emissions and performance during the 1500 RPM and low pedal condition are shown in Figure 6.7, and the standard rail pressure demanded by engine ECU is around 550 bar. Increasing the rail pressure causes the CO and HC emissions to increase for both the baseline and B25 fuels compared to the standard rail pressure, also a reduction in NO_X emissions can be clearly observed as the rail pressure increases. However, it is clearly noticeable that the impact of increasing the rail pressure is less significant on engine out emissions in case of B25 compared to the baseline diesel fuel. The percentage increase in CO and HC emissions is significantly lower with B25 compared to baseline diesel fuel, in addition to lower reductions in NO_X emissions. However, the percentage increase in engine torque is slightly higher with B25 compared to baseline diesel fuel when rail pressure increased by 10%.

Increasing the rail pressure improves the fuel atomization process in the case of the higher viscosity biodiesel fuel which was also reported by Karra et al. [95]; this is more pronounced with the effect on baseline diesel fuel less significant. On the other hand, the engine out torque shows a slight increase as the rail pressure increases with both fuels

which is what anticipated due to the better fuel atomization process leading to more efficient combustion.

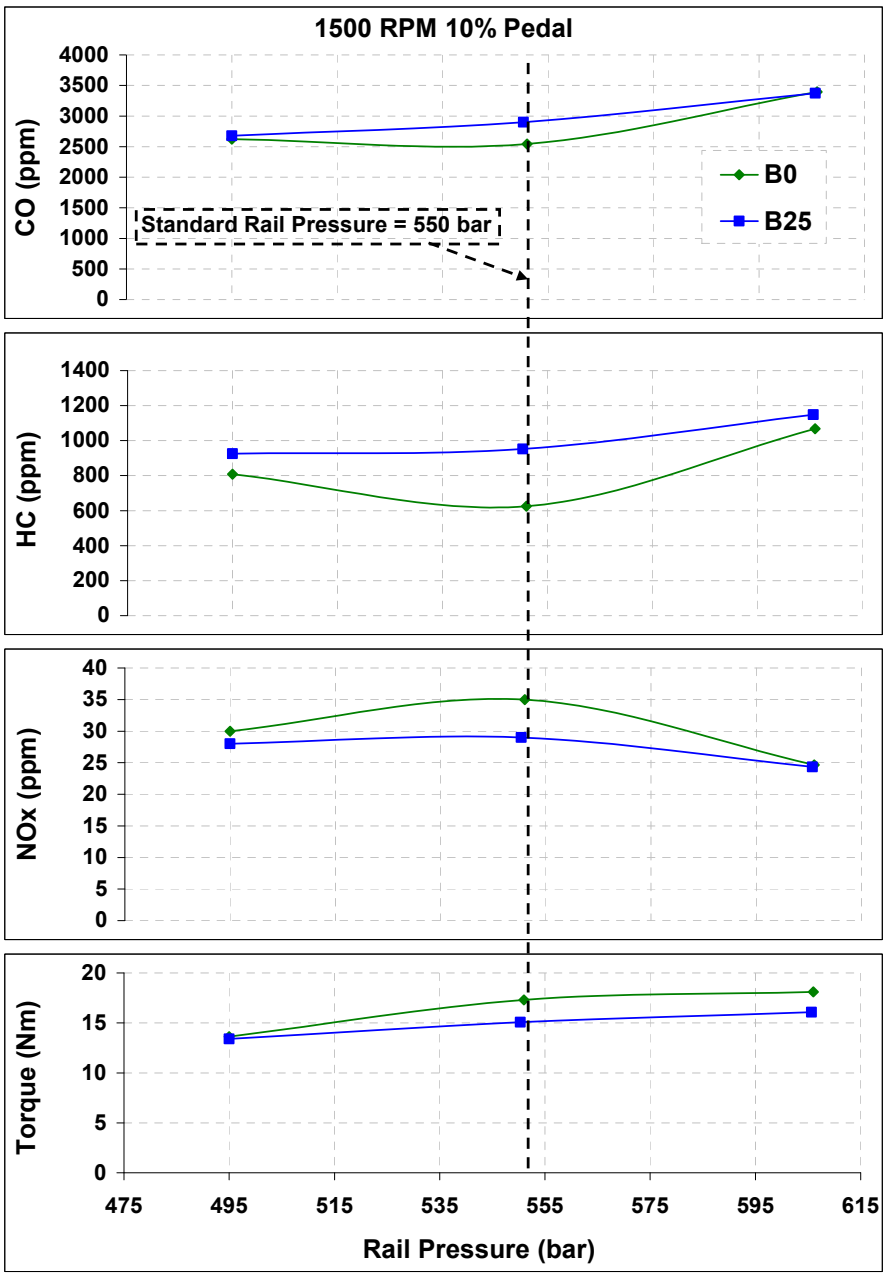

Figure 6.7, the effect of rail pressure swing on the engine torque and emissions for the 1500 RPM and 10% pedal position

Varying the rail pressure value will subsequently cause the engine ECU to recalculate the injection duration in order to maintain the same fuel quantity delivered. The ECU adjusts

the injection duration by controlling the current passing through the injector solenoid valve. The demanded injection duration is shown by plotting the solenoid valve voltage versus cycle crank angle. Figure 6.8 shows the variations in injection duration with adjusting rail pressures. The variations in the voltage values between baseline diesel and B25 fuels are due to different current clamp range settings, and are only used to define injection timing and duration. The magnitude of the signal does not impact on these parameters.

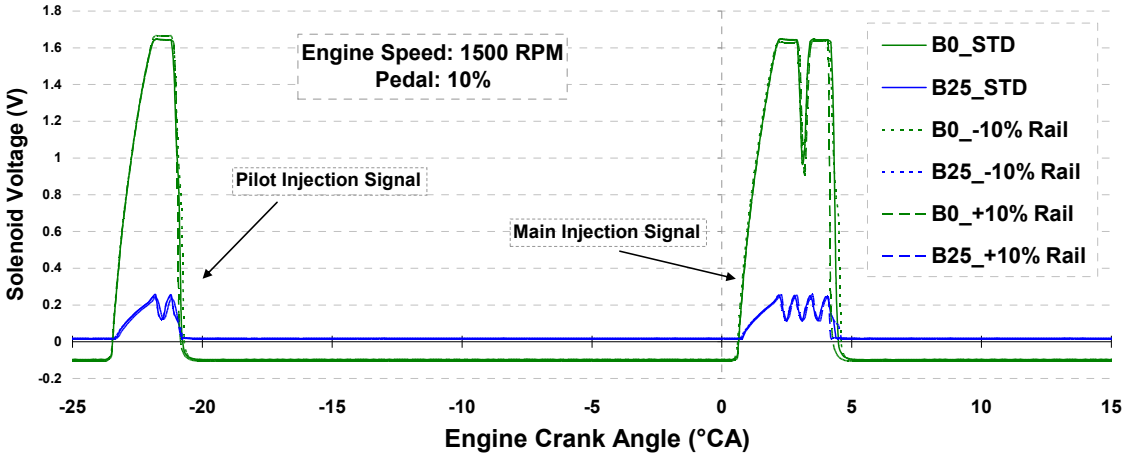

Figure 6.8, the effect of rail pressure swing on fuel injection durations at the 1500 RPM and 10% pedal position

Thus higher quantities of fuel are injected in shorter periods of time when rail pressure is increased to keep the total amount injected similar to the standard fuel quantity calculated by the ECU which also explains, at least in part, the slight increase in the engine out torque. On the other hand, higher injection rates could also increase the CO and HC emissions due to either the effect of charge cooling during such a low load and speed conditions, or the effect of cylinder wall wetting caused by higher spray penetration [130].

Finally reducing the rail pressure causes further deterioration in the combustion process since it reduces the fuel atomization and evaporation process inside the combustion chamber for both fuel blends. Surprisingly, the B25 was less affected by this reduction in the rail pressure.

6.4.2 1500 RPM 17% pedal

During the higher pedal condition of 1500 RPM engine speed, increasing the rail pressure improved the combustion process for both fuels with an expected increase in NO_X emissions as a trade off, see Figure 6.9.

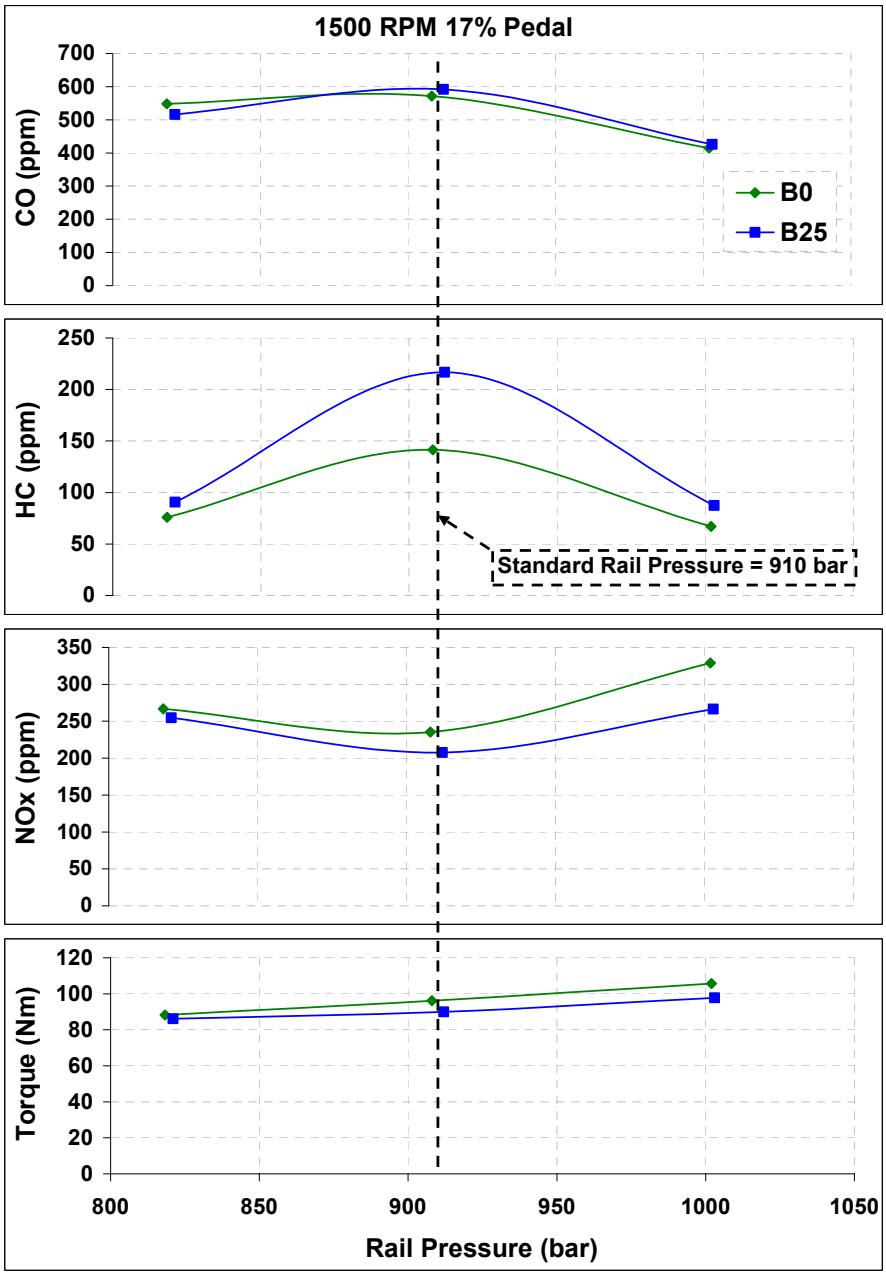

Figure 6.9, the effect of varying rail pressure on the engine torque and emissions for the 1500 RPM and 17% pedal position

Increasing the rail pressure at this condition benefits the B25 fuel, where the percentage reduction in HC emission is higher compared to the baseline diesel fuel in addition to lower percentage increase in NO_X emissions. The percentage increase in engine out torque is very similar with both fuels when the rail pressure is increased by 10% compared to the standard calibration. The improvement in the combustion process is clearly evident in Figure 6.10, which shows higher cylinder pressure curves and earlier start of combustion as the rail pressure increases with both fuels. The higher injection pressure achieves a high degree of atomization which enables sufficient evaporation to help reduce the higher viscosity draw back of biodiesel fuel blends.

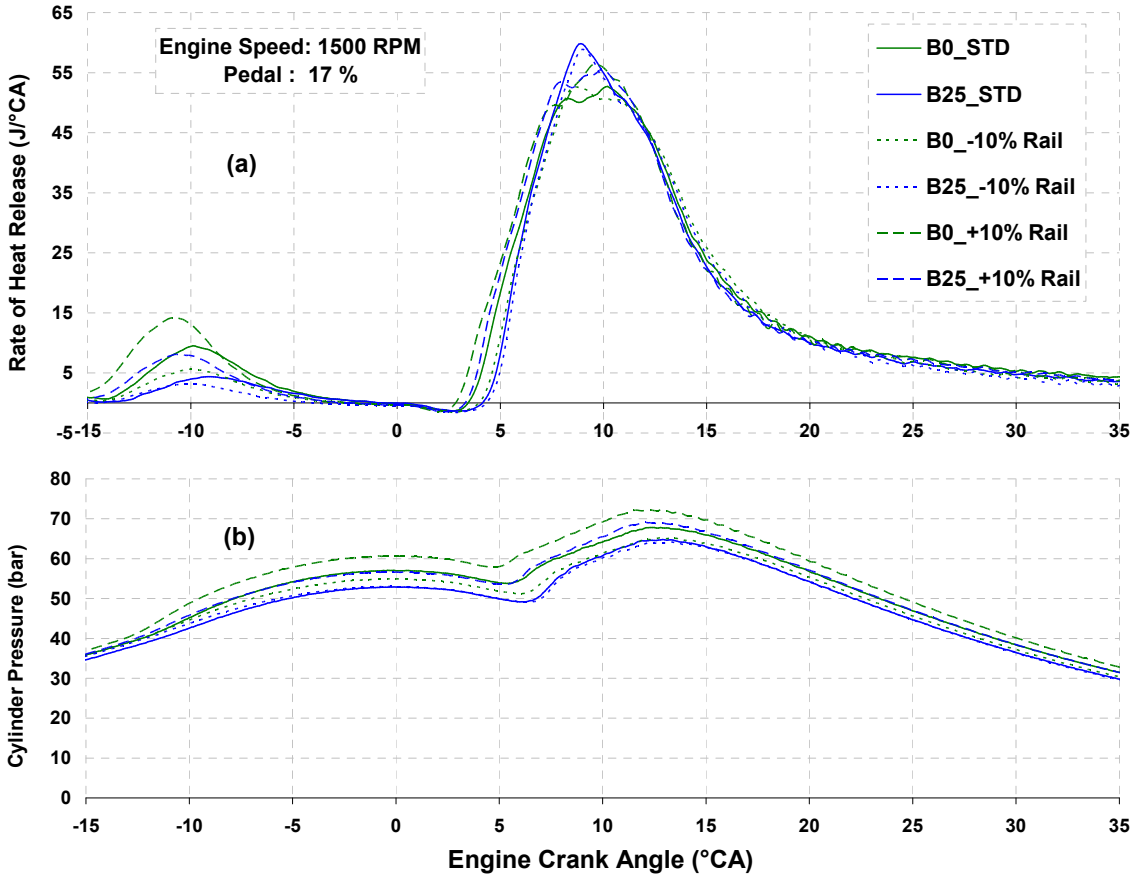

Figure 6.10, effect of rail pressure variation on (a) rate of heat release and (b) cylinder pressure at 1500 RPM and 17% pedal position

Reducing the rail pressure caused a reduction in CO and HC emissions and increased the NO_X emissions with both fuels. Also, it appears from Figure 6.9 that the reduction in engine power is less significant when the engine is fuelled with B25 compared to the baseline diesel fuel, since reducing the rail pressure lowers cylinder pressure and slows the burn rate as in Figure 6.10.

6.4.3 2250 RPM 15% pedal

The effect of rail pressure swing on the engine torque and emissions during the 2250 RPM and 15% pedal position are shown in Figure 6.11. Increasing the rail pressure caused the CO emissions to increase by 7% in case of baseline diesel, and decrease by 1% with B25 compared to the standard rail pressure. Similarly, the HC emissions increased by 8% in case of baseline diesel and decrease by 10% with B25 when rail pressure increased, and the NO_X emissions dropped by 7% and increased by 4% with baseline diesel and B25 fuels respectively. The engine output torque was increased by 15% with both fuels by increasing the rail pressure compared to the standard calibration. These results suggest that increasing the rail pressure improved the combustion efficiency of the engine when fuelled with B25 and suffered the lowest emission impact compared to baseline diesel fuel.

Increasing the rail pressure advances the start of combustion and produces higher pressure curve with B25 compared to baseline diesel, Figure 6.12. The higher injection pressure at this higher engine speed condition is more critical to achieve higher degree of atomization to enable quicker fuel evaporation especially in case of B25, in addition to the oxygen content which enables quicker start of combustion.

The sensitivity of the engine performance and emissions to the reduction in rail pressure is very similar to the first operating condition of 1500 RPM and 10% pedal condition. It shows further deterioration in the combustion process since it reduces the fuel atomization and evaporation process inside the combustion chamber for both fuels, and surprisingly the B25 is less affected by this reduction in the rail pressure.

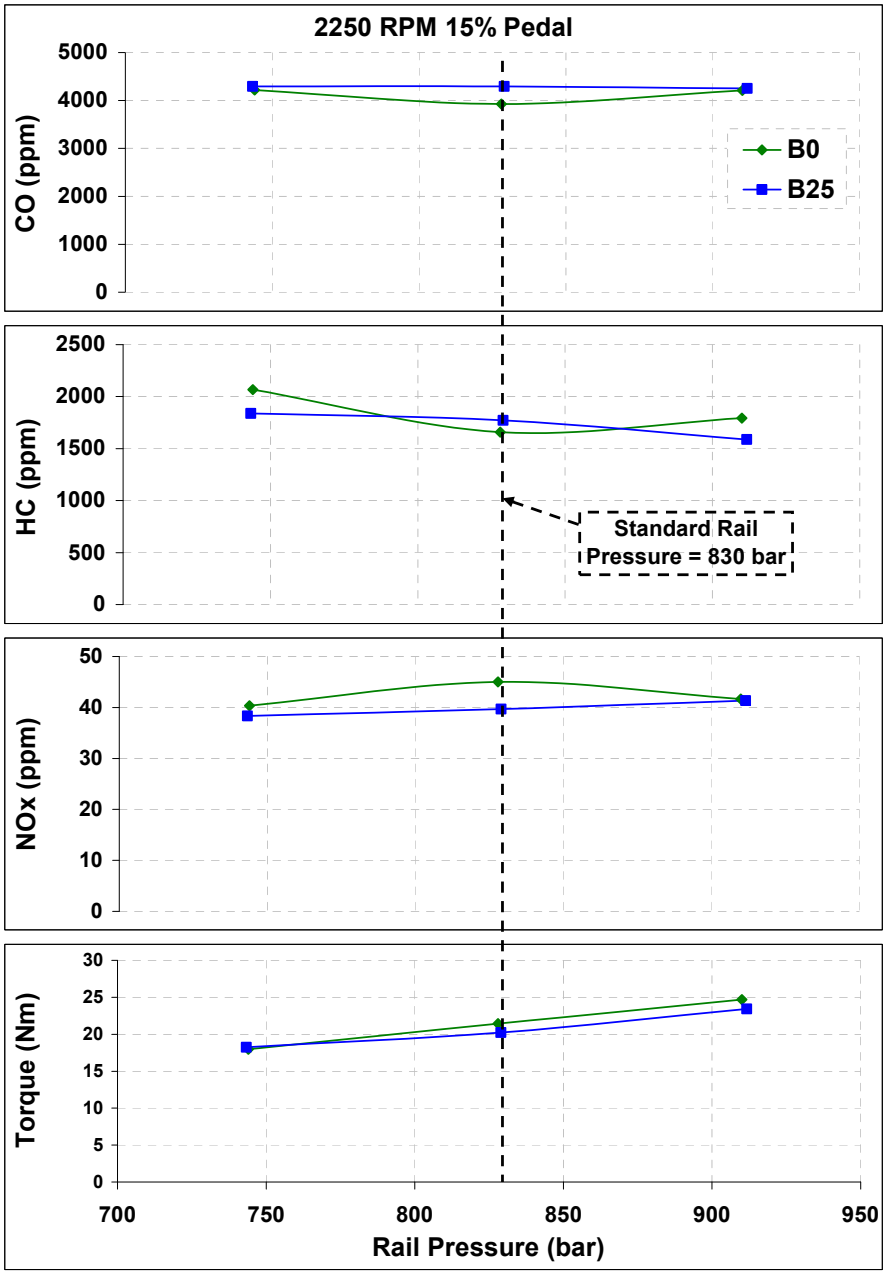

Figure 6.11, the effect of rail pressure variation on the engine torque and emissions for the 2250 RPM and 15% pedal position

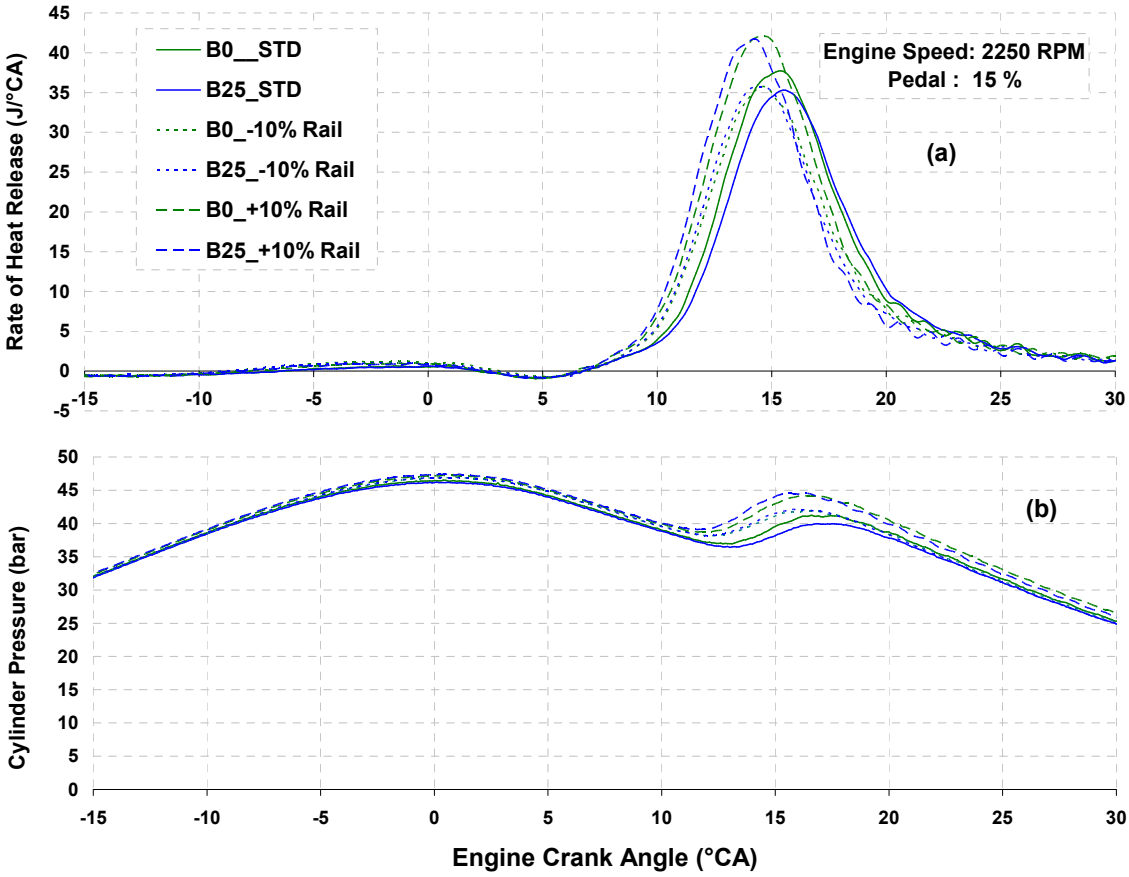

Figure 6.12, effect of rail pressure variation on (a) rate of heat release and (b) cylinder pressure at 2250 RPM and 15% pedal position

6.4.4 2250 RPM 22% pedal

During this operating condition, increasing the rail pressure improved the combustion process for both fuel blends with a slight increase in NO_X emissions, Figure 6.13. The sensitivity impact of increasing the rail pressure during this operating condition is very similar with both fuels in terms of engine out emissions and performance compared to the standard calibration. The same discussion for the lower speed condition is valid here as an explanation of the effect of rail pressure increase on the engine out performance and emissions. The CO emissions reduced by about 5%, the HC emissions reduced by 35% and the NO_X emission was increased by 20% with both fuels by increasing the rail pressure compared to the standard calibration. The percentage increase in engine output torque was also very close for both fuels compared to the standard calibration. These results suggest that increasing the rail pressure benefited the engine performance exactly the same with both fuels. Also reducing the rail pressure had very similar impact with

fuels compared to the standard calibration as a result of expected lower fuel atomization and slower fuel burn rate.

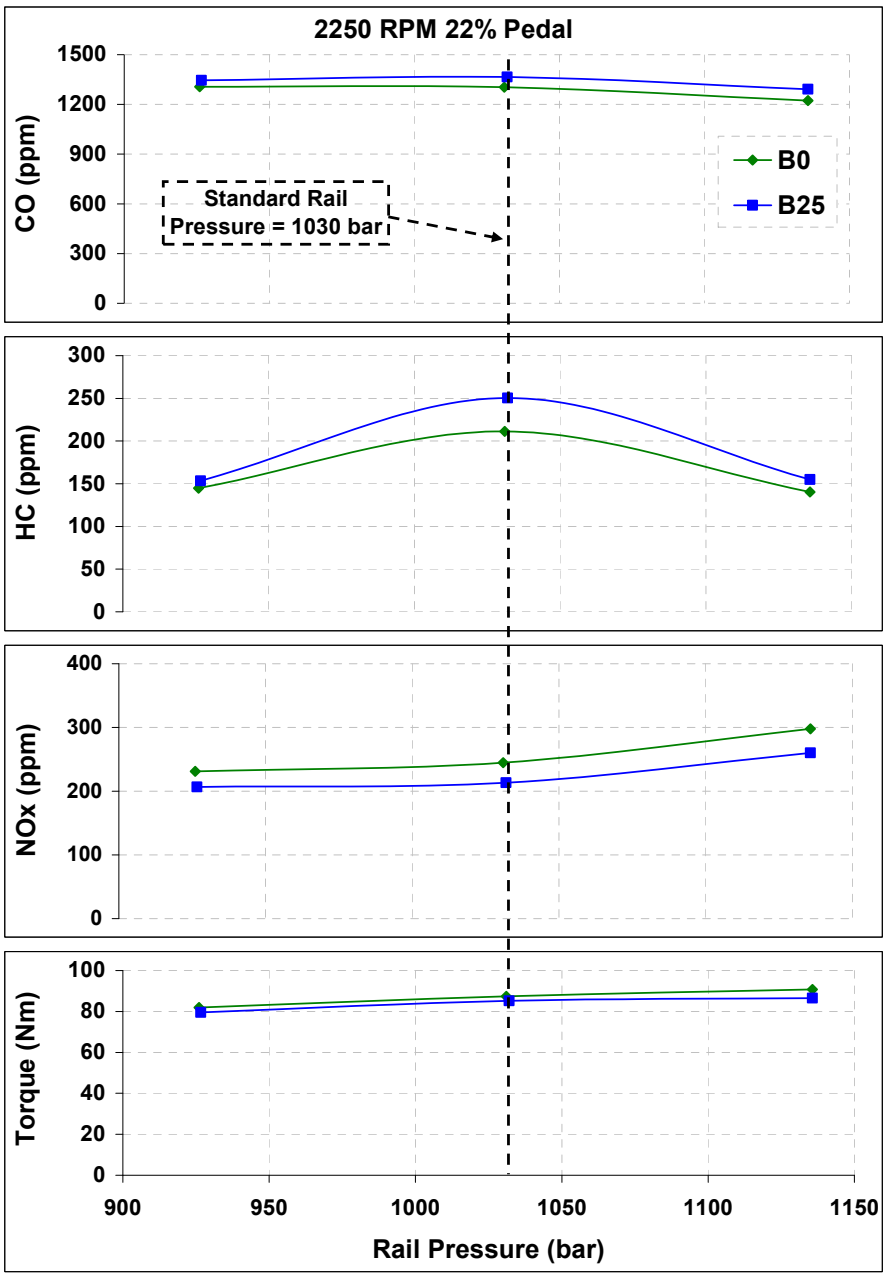

Figure 6.13, the effect of rail pressure variation on the engine torque and emissions for the 2250 RPM and 22% pedal position

6.5 Varying Main Injection Timing

The objective of this part of the investigation was to understand the effect of varying the main fuel injection timing on the engine performance and exhaust emissions when the engine is operated with B25 and compare it to the baseline diesel fuel. Fuel injection timing is considered one of the major parameters that affect the combustion and exhaust emissions of diesel engines. The main injection timing was varied by directly changing the value of the adder corresponds to the injection timing in the engine ECU map input. The injection timing was advanced and retarded by 2° CA relative to the standard calibration for all fuel blends during all the selected engine operating conditions.

6.5.1 1500 RPM 10% pedal

The standard calibration calls for injection timing of 4.1° CA after top dead centre (ATDC) during this operating condition, and the advanced and retarded injection timings were set at 2.1° ATDC, and 6.1° ATDC respectively.

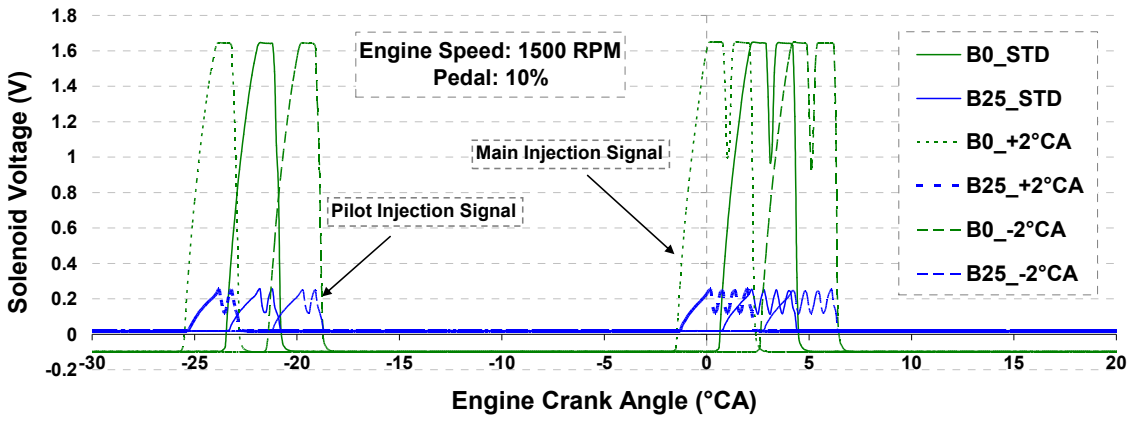

Figure 6.14, the effect of main injection swing on fuel injection durations at the 1500 RPM and 10% pedal position

Swinging the main injection timing adjusts the pilot injection timing at the same time with similar crank angle degrees as shown in Figure 6.14, keeping the duration angle between them the same all the time. The effects of swinging the injection timing on engine out emissions and performance for the 10% pedal position are shown in Figure 6.15.

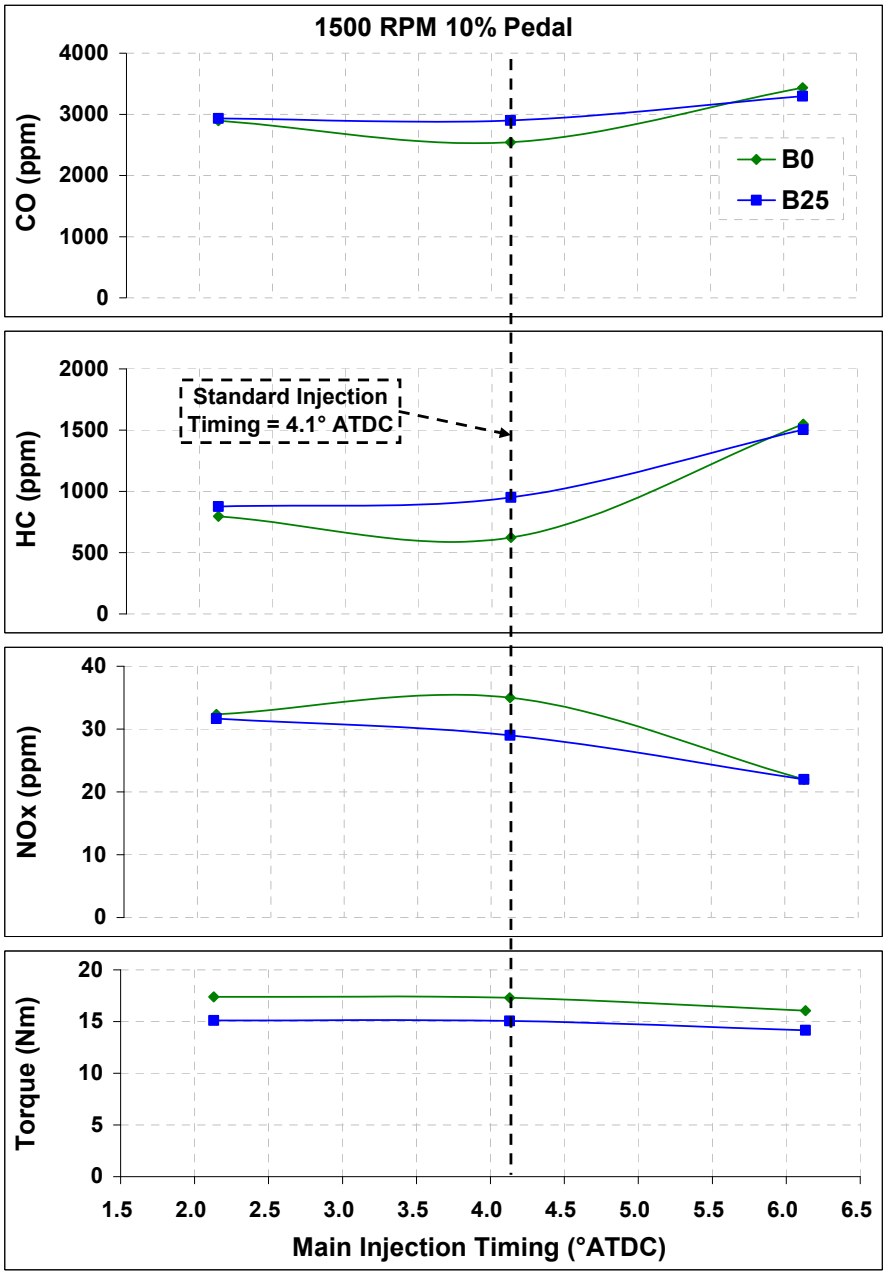

Figure 6.15, the effect of main injection timing variation on engine out emissions and performance at 1500RPM and 10% pedal

Advancing the injection timing to 2.1° ATDC, in other words earlier injection, has brought the engine out emissions of B25 to match those of baseline diesel fuel. The CO emissions increased by 14% in case of baseline diesel and on the other hand did not show any difference in case of B25. Similarly, advancing the main injection timing increased the HC emission by 27% for the baseline diesel and was reduced by 8% for B25 compared

to the standard calibration. Whereas the NO_X emissions showed a slight increase with B25 and a slight reduction with baseline diesel compared to the standard calibration when the injection was advanced, and did not show a significant impact on the engine output torque with both fuels. The cylinder pressure and rate of heat release curves for this operating condition are shown in Figure 6.16.

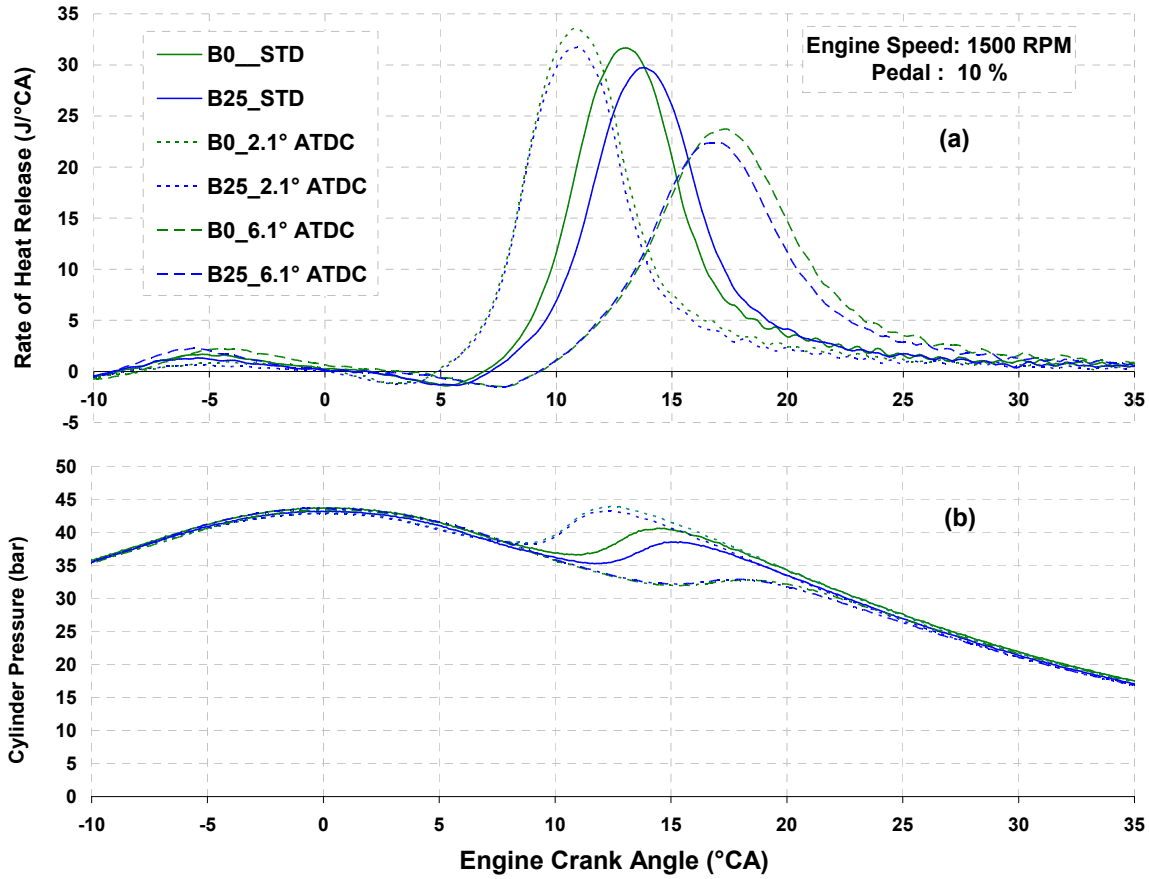

Figure 6.16, effect of main injection variation on (a) rate of heat release and (b) cylinder pressure at 1500 RPM and 10% pedal position

Figure 6.16 shows that advancing the injection timing to 2.1° ATDC, has advanced the SOC closer to the TDC which is probably what have caused the improvement in the combustion process. It has also matched the SOC of both fuels which probably accounts for better emission results from B25 fuel. Obviously further retarding the injection timing away from TDC deteriorates the combustion performance further and reduces engine output torque. The B25 shows less sensitivity to this retardation in main injection probably due to higher oxygen content compared to baseline diesel fuel.

6.5.2 1500 RPM 17% pedal

During this operating condition the demanded main injection for the standard calibration is 3.9° ATDC, and the advanced and retarded injection timings were set at 1.9° ATDC and 5.9° ATDC respectively, Figure 6.17.

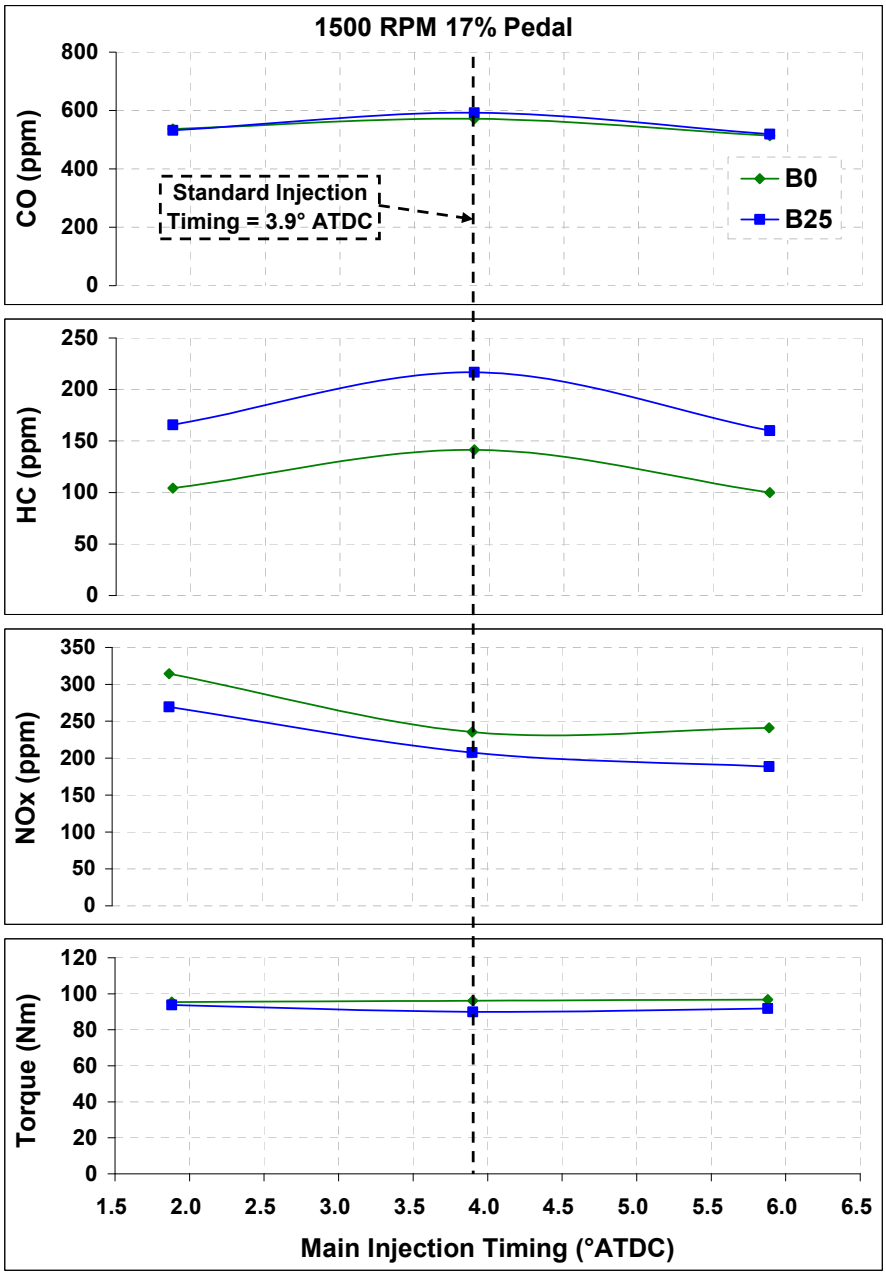

Figure 6.17, the effect of main injection timing swing on engine out emissions and performance at 1500RPM and 17% pedal

Advancing the injection timing to 1.9° ATDC reduced the engine out CO emissions by 6% and 10% for the baseline diesel and B25 fuels respectively. Also, the HC emissions were reduced by 26% and 24% for the baseline diesel and B25 fuels respectively compared to the standard calibration as a result of better combustion efficiency when the fuel is injected into higher pressure and temperature conditions whereas the NO_X emissions increased by about 34% and 30% for the baseline diesel and B25 fuels respectively compared to the standard calibration. In the mean time, earlier injection did not seem to affect the engine output torque with baseline diesel fuel, but it did increase by 4% with B25.

On the other hand, further retarding the injection timing has reduced the engine out emissions of CO and HC and the percentage reduction is very similar with both fuels. However, the NO_X emissions reduced by 9% with B25 and no significant change were observed with the baseline diesel fuel without any major change in engine out torque. To investigate the effect of injection timing swing on combustion process, the cylinder pressure and rate of heat release curves were investigated, see Figure 6.18.

Retarding the injection timing is a common technique used to reduce engine out NO_X emissions [130] which appears to be more beneficial for B25 fuel during this operating condition. Furthermore, retarding the injection timing leads to have smoother combustion process with longer combustion durations and lower cylinder pressure peaks which leads to lower NO_X emissions during this condition. Retarding the main injection has reduced the engine out emissions of CO and HC with both fuels by 10% and 25% respectively. The NO_X emissions dropped by 9% with B25 and increased by 2% with the baseline diesel fuel without any significant impact on the engine out torque.

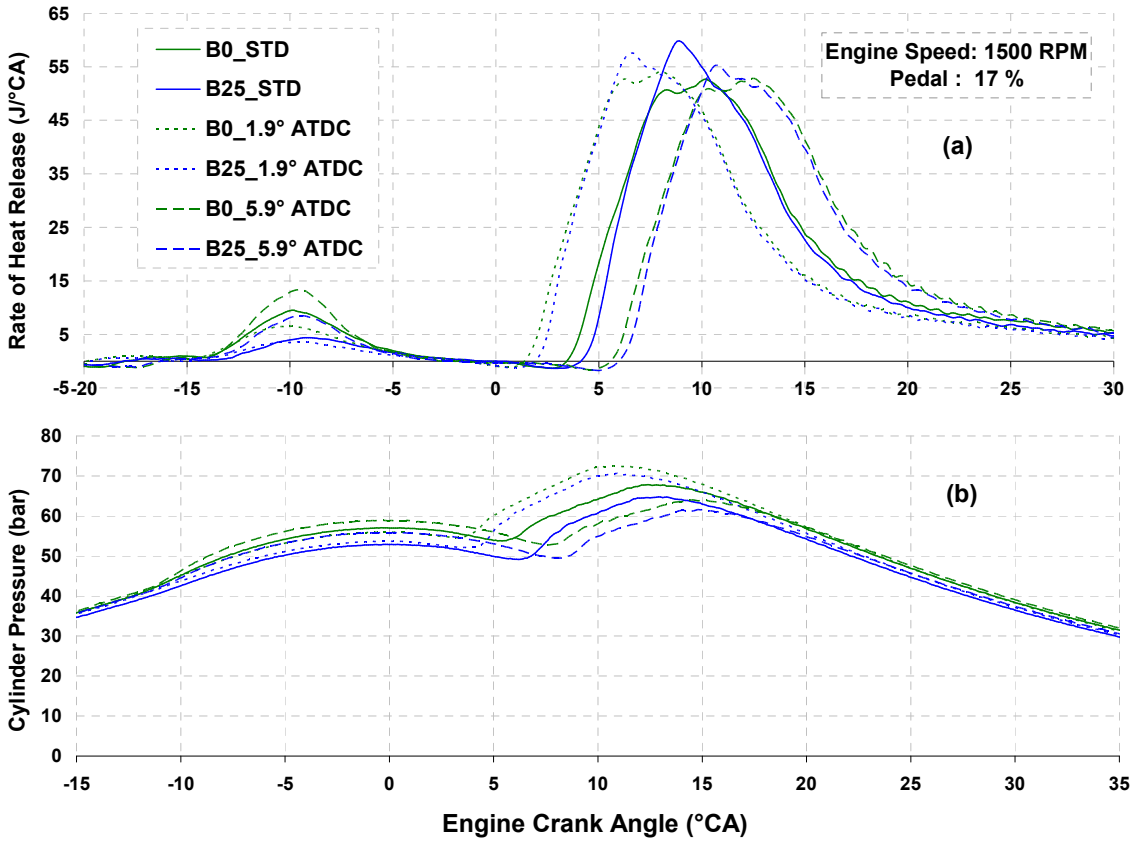

Figure 6.18, effect of main injection variation on (a) rate of heat release and (b) cylinder pressure at 1500 RPM and 17% pedal position

6.5.3 2250 RPM 15% pedal

The effect of fuel injection timing swing on the engine out emissions and performance during this operating condition are shown in Figure 6.19. The standard injection timing is 3.9° ATDC, and the advanced and retarded injection timings were 1.9° ATDC, and 5.9° ATDC respectively. Advancing the injection timing improved the combustion performance significantly with both fuels and the overall values of CO, HC were reduced significantly similar to the 1500 RPM 10% pedal condition. But this resulted in a significant penalty, NO_X emissions increased by 30% and 23% for the baseline diesel and B25 respectively compared to the standard calibration. The CO emissions reduced by 13% and HC emissions reduced by 31% for both baseline diesel and B25 fuels, and the improvement in the engine output torque is 5% and 16% for the baseline diesel and B25 fuels respectively compared to the standard injection timing. The sensitivity of engine performance and emissions to this advancement in main injection timing was more

beneficial with B25 compared to baseline diesel due to its lower percentage increase in NO_X emission and higher percentage increase in engine out torque.

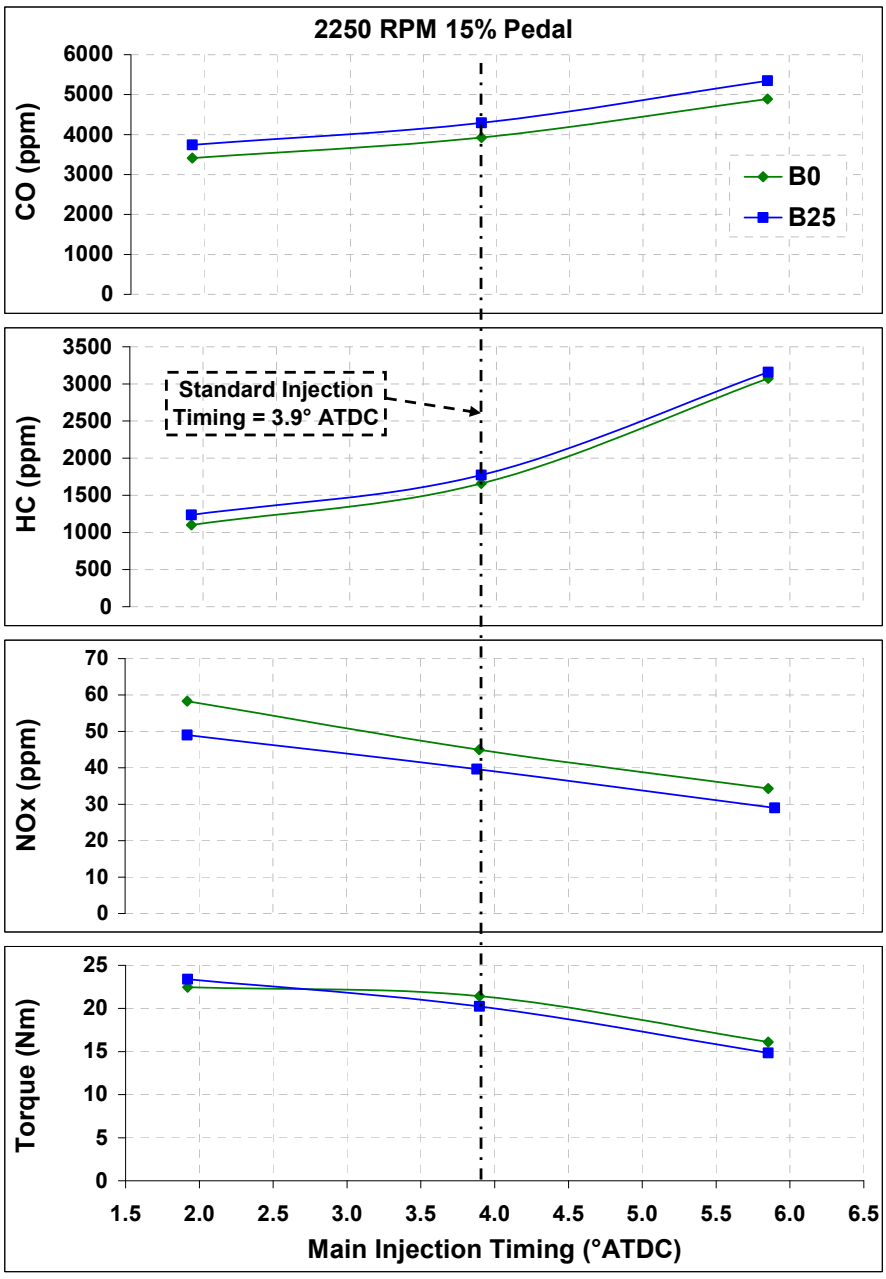

Figure 6.19, the effect of main injection timing swing on engine out emissions and performance at 2250RPM and 15% pedal

Retarding the injection timing during this high speed condition deteriorates the combustion performance significantly and engine output torque reduces by more than 25% and the impact on the engine out torque and emissions is very similar with both fuels.

6.5.4 2250 RPM 22% pedal

The standard injection timing for the test engine at this operating condition is 3.4° ATDC, and the advanced and retarded injection timings were set at 1.4° ATDC, and 5.4° ATDC respectively. The effect of adjusting the injection timing on engine out emissions and performance are shown Figure 6.20.

The observation from Figure 6.20 is that the sensitivity of engine performance and emissions to variations in main injection timing is very similar with both fuels. Advancing the injection timing improves the engine performance and emissions except for NO_X. The change in engine out emissions are very similar with both fuels, however the percentage increase in engine out torque is slightly higher with B25. The engine output torque increased by 4% with B25 but did show any significant change with baseline diesel fuel when the injection timing was advanced.

Similar to the 1500 RPM and 17% pedal condition, further retarding the injection timing does not seem to change the engine performance with reduction in engine out emissions compared to the standard calibration. Both fuels showed similar reduction in engine out emissions of CO and HC by 6% and 24% respectively when injection timing was retarded compared to the standard injection timing, the engine out NO_X emissions reduced by 3% with B25 but did not show any significant change with baseline diesel fuel.

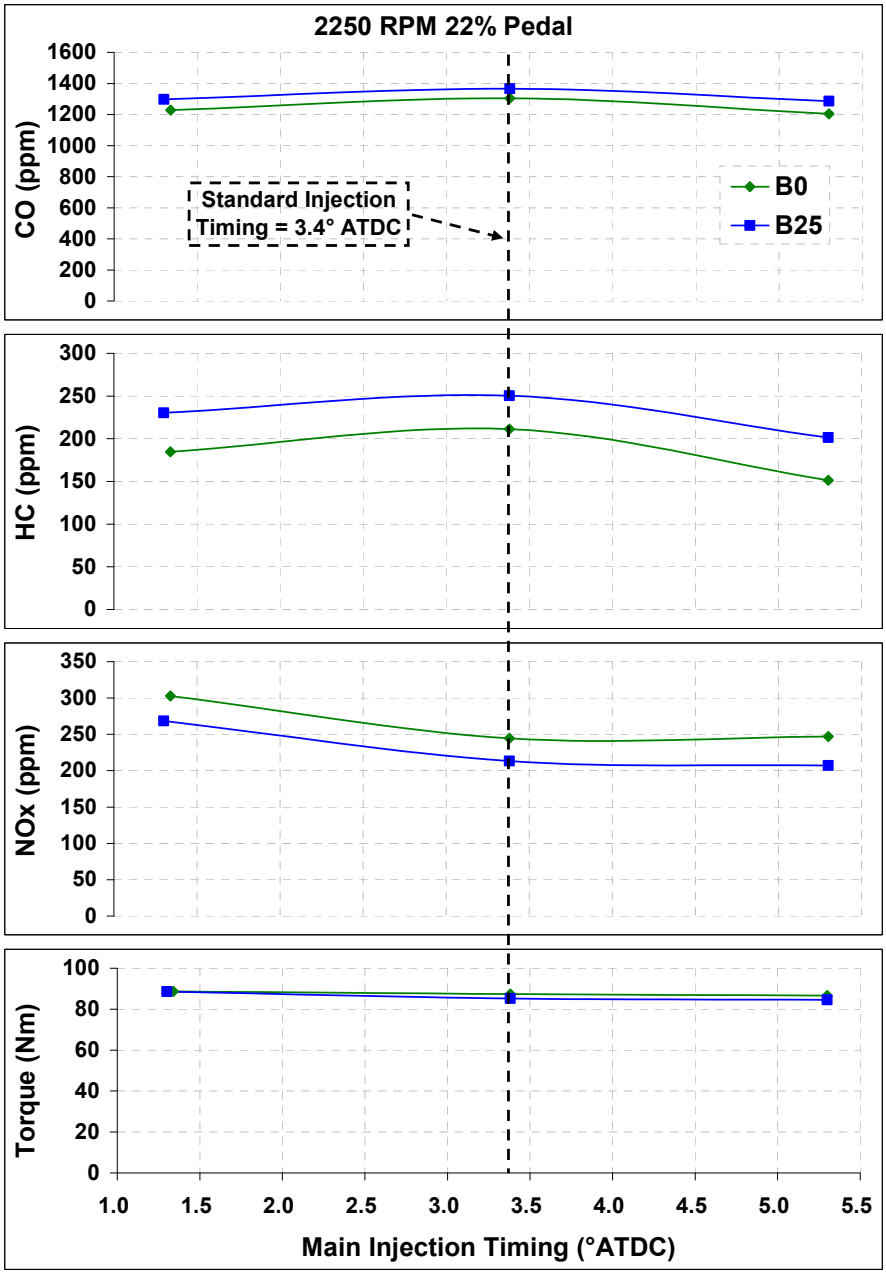

Figure 6.20, the effect of main injection timing variation on engine out emissions and performance at 2250RPM and 22% pedal

6.6 Varying Pilot Injection Timing

The objective of this experimental investigation was to analyse the sensitivity of the engine performance and emissions when fuelled with B25 to changes in pilot injection timing, and compare the results to baseline diesel fuel.

The pilot injection timing is varied through the ECU calibration tool (ATI vision) by changing the value of the pilot injection timing adder. The variations in the pilot injection timing to be investigated are +2° CA and -2° CA from the standard calibration with both fuels during all engine operating conditions.

6.6.1 1500 RPM 10% pedal

Varying the pilot injection timing through the ATI adder produced new injection signals from the engine ECU to the injector solenoid valve. The ECU adjusts the injection timing by controlling the current passing through the injector solenoid valve. The demanded injection timings for both pilot and main injection are shown by plotting the solenoid valve voltage versus cycle crank angle. Figure 6.21 clearly shows the variations in the pilot injection with constant main injection timing for both fuels.

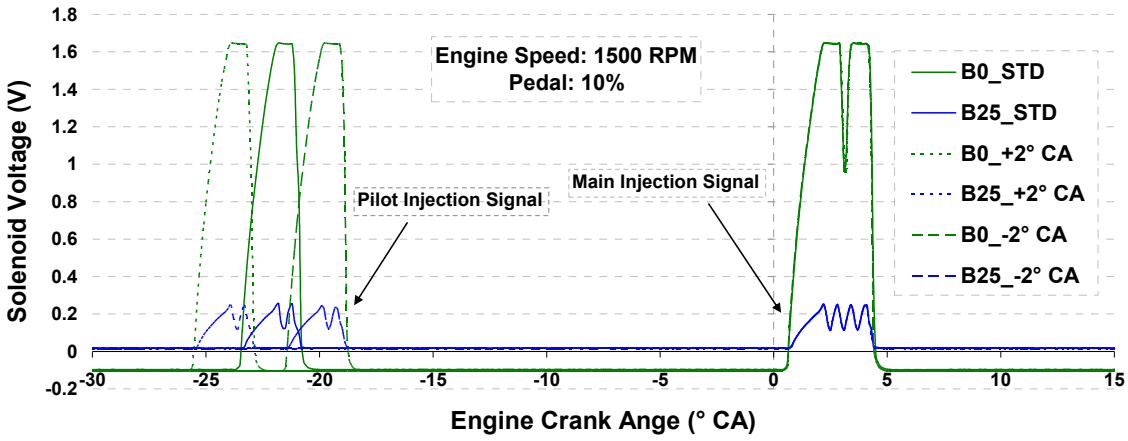

Figure 6.21, ECU demand injection signal with variations of pilot injection timing at the 1500 RPM and 10% pedal position

The effect of swinging the pilot injection timing on engine out emissions and performance for the 10% pedal position is shown in Figure 6.22. It is clearly noticeable and expected that the engine is better optimized to run with baseline diesel fuel with standard calibration, the engine is producing less CO and HC emissions with slightly higher NO_X. Advancing the pilot injection timing by 2° CA, in other words earlier pilot injection, increased engine out CO emissions by 52% with both fuels compared to the standard

condition, and more than 100% increase HC emissions. On the other hand, advancing the pilot injection timing reduced the NO_X emissions by 50% and 45% and increased engine output torque by 45% and 40% with baseline diesel and B25 fuels respectively.

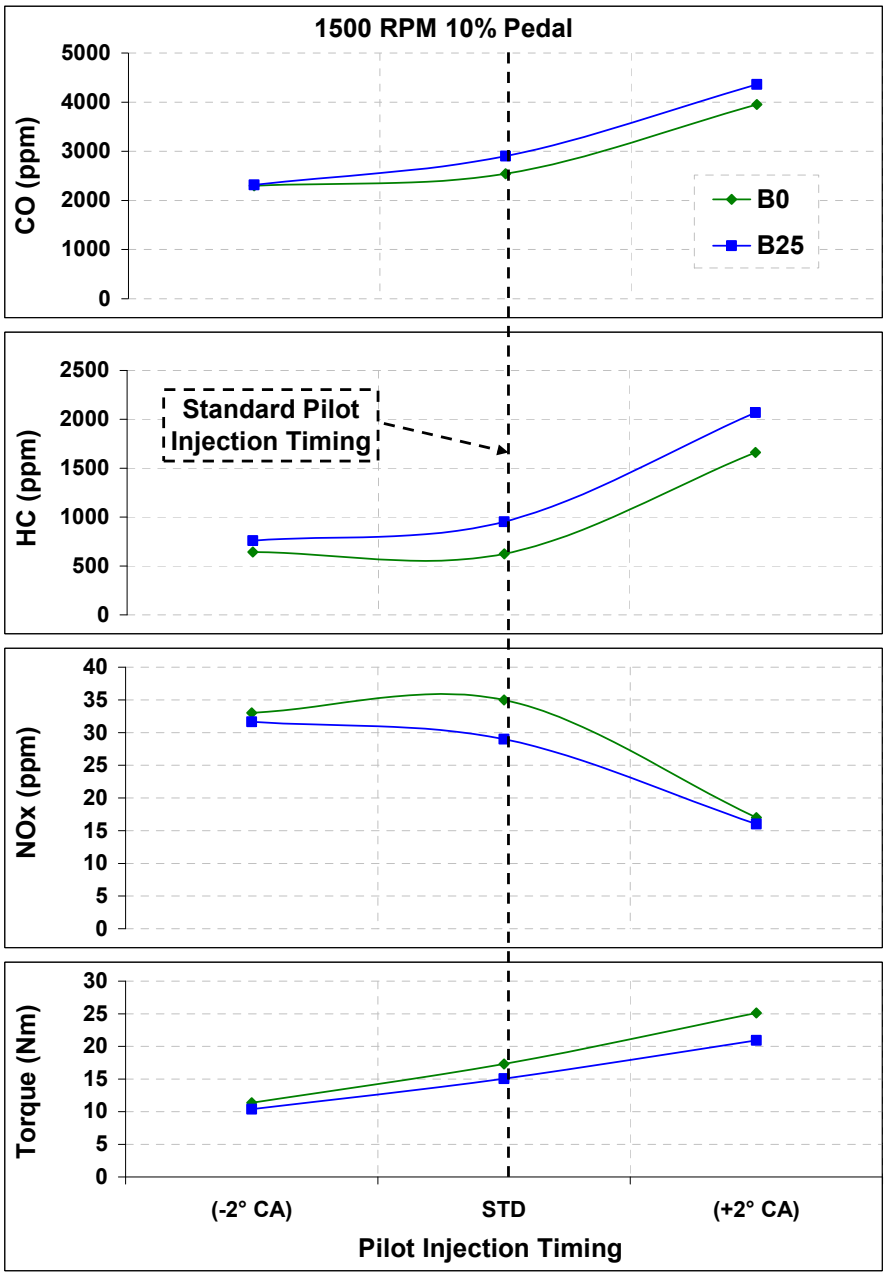

Figure 6.22, the effect of pilot injection timing variation on engine out emissions and performance at 1500RPM and 10% pedal

Retarding the pilot injection timing by 2° CA reduced engine output torque drastically (more than 30%) with both fuels, but the impact is slightly higher in the case of baseline diesel fuel which brings its value very close to the B25 fuel. The NO_X emissions increased by 9% and decreased by 6% with B25 and baseline diesel fuels respectively compared to the standard calibration. The CO emissions reduced by 20% and 10% with B25 and baseline diesel respectively compared to the standard calibration, and HC emission decreased by 20% in the case of B25 and did not show any change with baseline diesel fuel. To investigate the effect of injection timing swing on the combustion process, the cylinder pressure and rate of heat release curves for this operating condition are plotted in Figure 6.23.

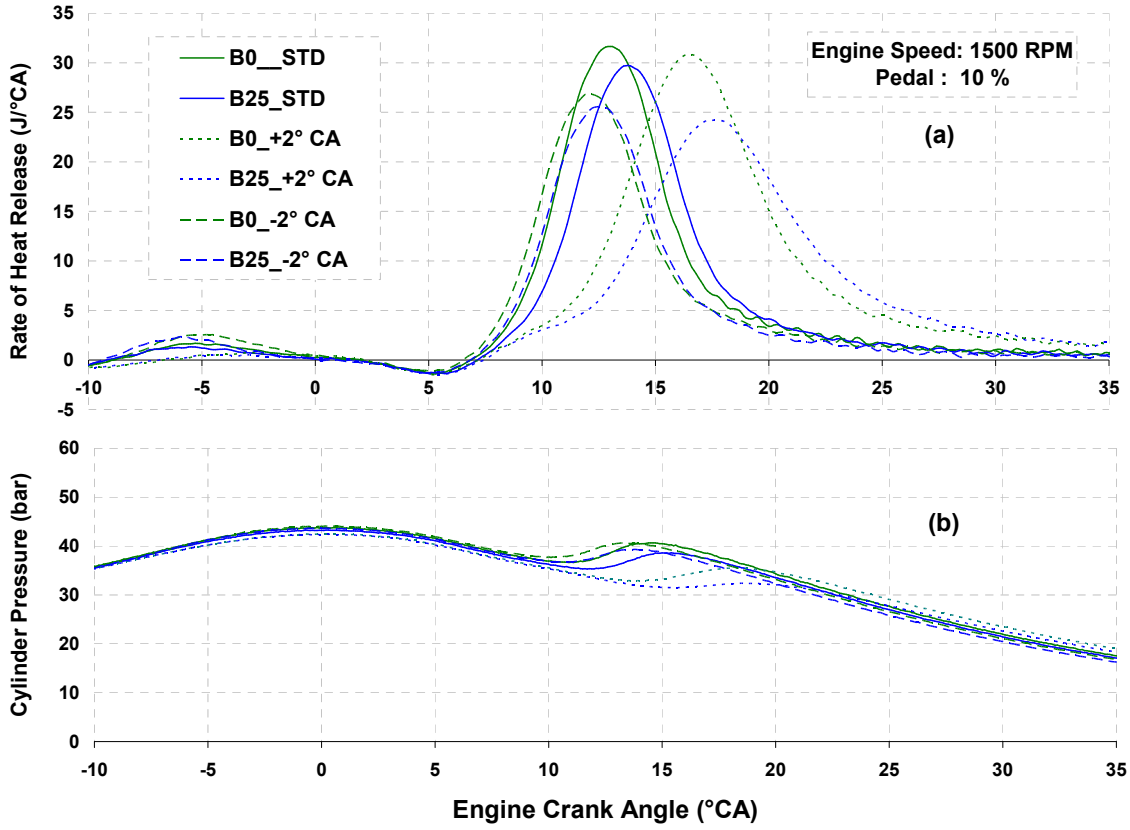

Figure 6.23, the effect of pilot injection timing variation on (a) rate of heat release and (b) cylinder pressure at 1500 RPM and 10% pedal position

Advancing pilot injection timing has retarded the main combustion compared to the standard calibration as shown by the delayed rate of heat release curves of both fuels. Earlier pilot will expand the duration period between the pilot injection and main

injection, thus increase the available time for the fuel to over mix and lead to a formation of excessive lean air-fuel mixture, resulting in higher CO and HC emissions observed in Figure 6.22 [130]. The delayed combustion and more expanded heat release curve probably explain the higher engine output torque produced, and the reduction in combustion pressures justifies the lower NO_X emissions as the pilot injection timing advanced. The combustion of B25 is further delayed and shows even slower rate of heat release profile and higher percentage reduction in cylinder pressure compared to the baseline diesel fuel which is probably due to a compromised atomization and evaporation process.

On the other hand, retarding the pilot injection timing advances the main combustion slightly because it shortens the duration between the pilot and main injections. The earlier combustion is due to the fact that the pilot fuel is still burning when the main injection occurs. Quicker and less expanded rate of heat release curve explains the reduction in engine output torque and the increase in NO_X emissions. B25 fuel shows less sensitivity to the pilot injection retardation, the CO and HC emissions show higher percentage reduction with slight increase in NO_X compared to baseline diesel in addition to lower reduction in engine out put torque.

6.6.2 1500 RPM 17% pedal

The effect of swinging the pilot injection timing on engine out emissions and performance for the 17% pedal position is shown in Figure 6.24. The first impression from this plot is that increasing or decreasing the pilot injection timing does not seem to improve the engine performance or emissions during this operating condition, both cases show significant increase in NO_X emissions and a drop in engine output torque. The HC emissions show a significant drop in both cases, but the CO emissions increase and decrease with advanced and retarded pilot injection timing respectively. The impact of advancing the pilot injection timing is less significant on engine out performance, CO, and HC emissions with B25 compared to the baseline diesel fuel; however the percentage increase in NO_X emission is slightly higher with B25 compared to baseline diesel fuel.

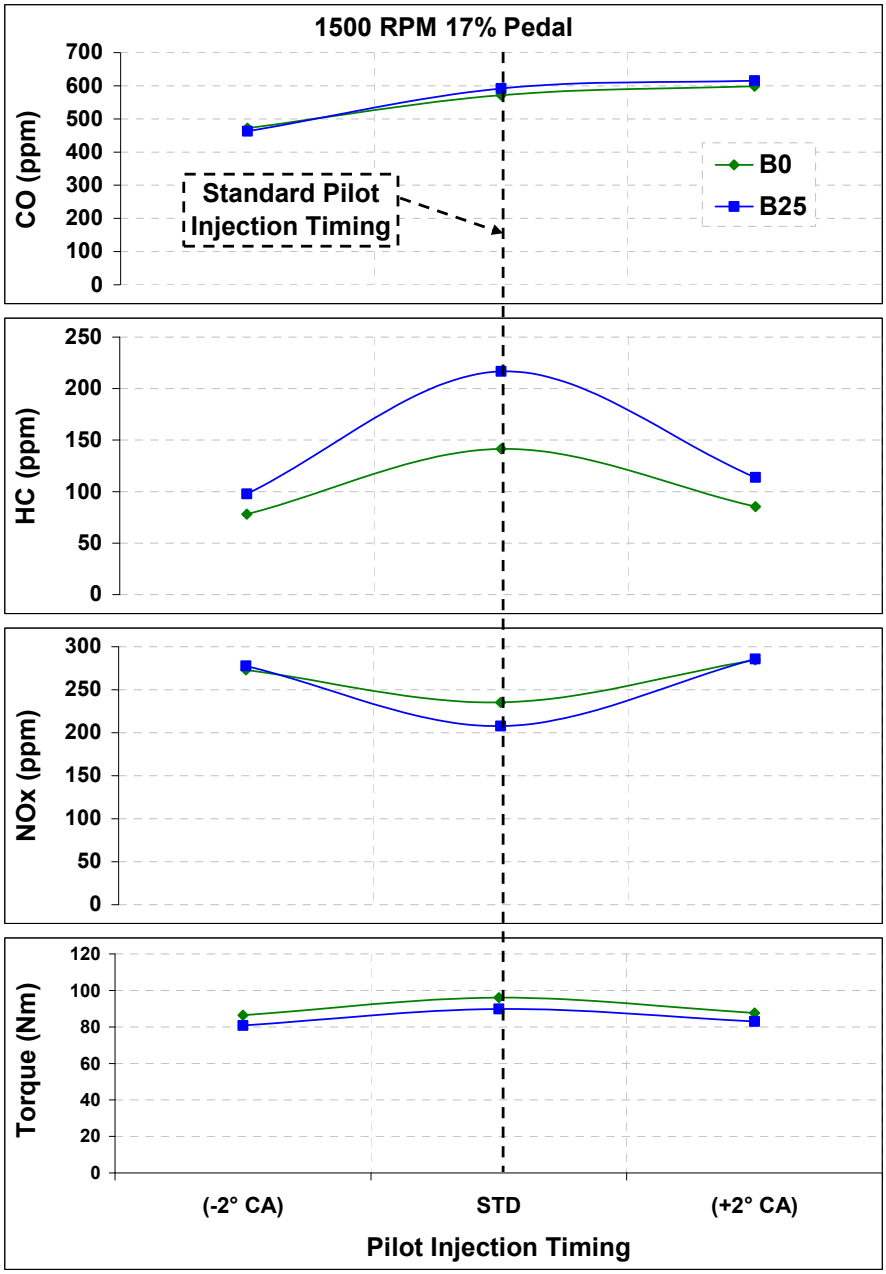

Figure 6.24, the effect of pilot injection timing variation on engine out emissions and performance at 1500RPM and 17% pedal

Similar to the previous condition, retarding the pilot injection timing advances the main combustion slightly due to the fact that it is injected closer to TDC and temperatures are higher during this higher load condition, which explains lower engine out emissions of both CO and HC. The B25 fuel shows less sensitivity to the pilot injection retardation, the CO and HC emissions show higher percentage reduction with slight increase in NO_X compared to baseline diesel.

6.6.3 2250 RPM 15% pedal

The effect of swinging the pilot injection timing on engine out emissions and performance for the 2250 RPM 15% pedal position is shown in Figure 6.25.

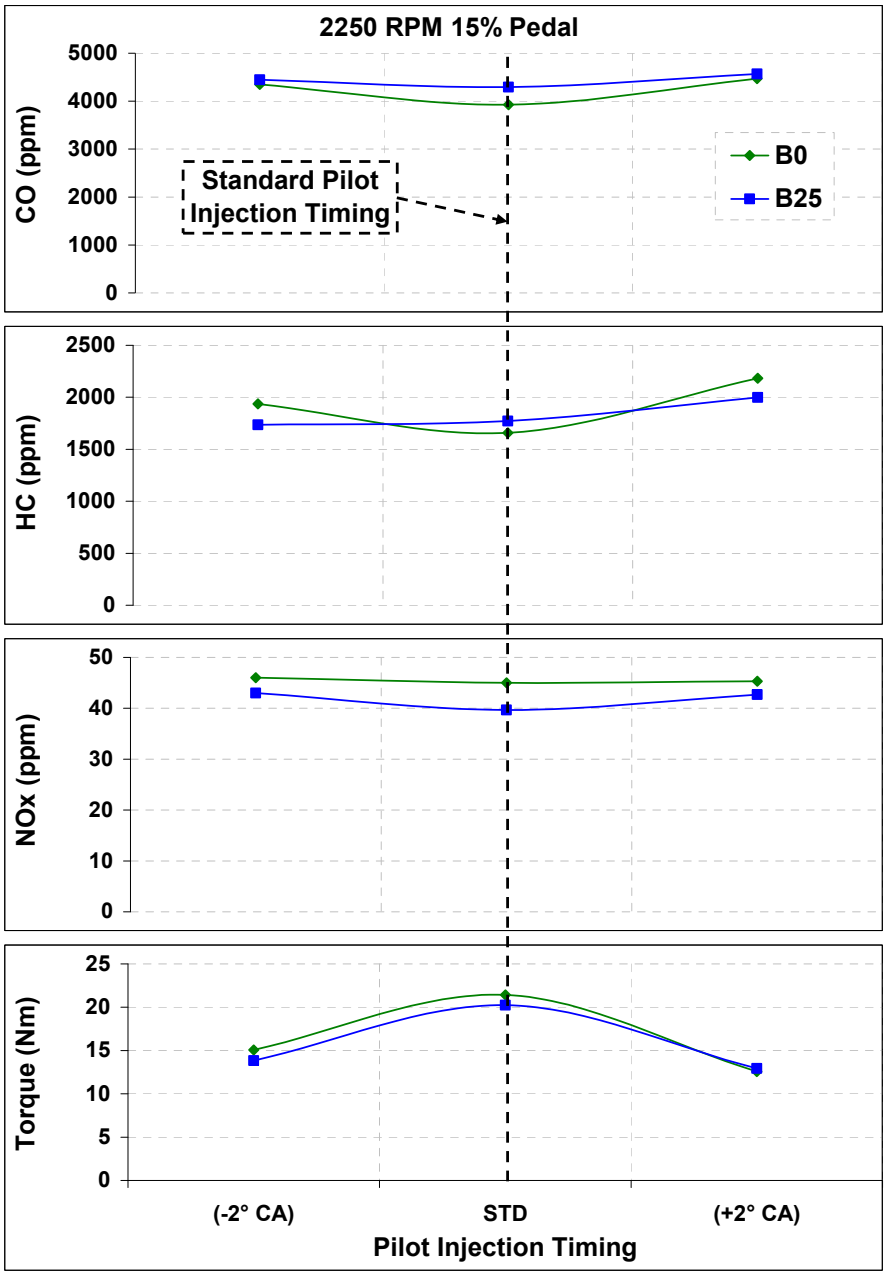

Figure 6.25, the effect of pilot injection timing variation on engine out emissions and performance at 2250RPM and 15% pedal

Similar to the previous condition, varying the pilot injection timing does not seem to improve the engine performance or emissions during this operating condition, significant reduction in engine output torque in addition to general increase in all emissions can be observed.

Advancing the pilot injection timing clearly deteriorates the combustion process which is concluded from the increase in CO and HC emissions and a significant drop in engine power. The rate of heat release and cylinder pressure curves for this operating condition is shown in Figure 6.26. Unlike the lower engine speed condition, advancing the pilot injection did not retard the start of main combustion process probably due to less time available during this higher engine speed condition.

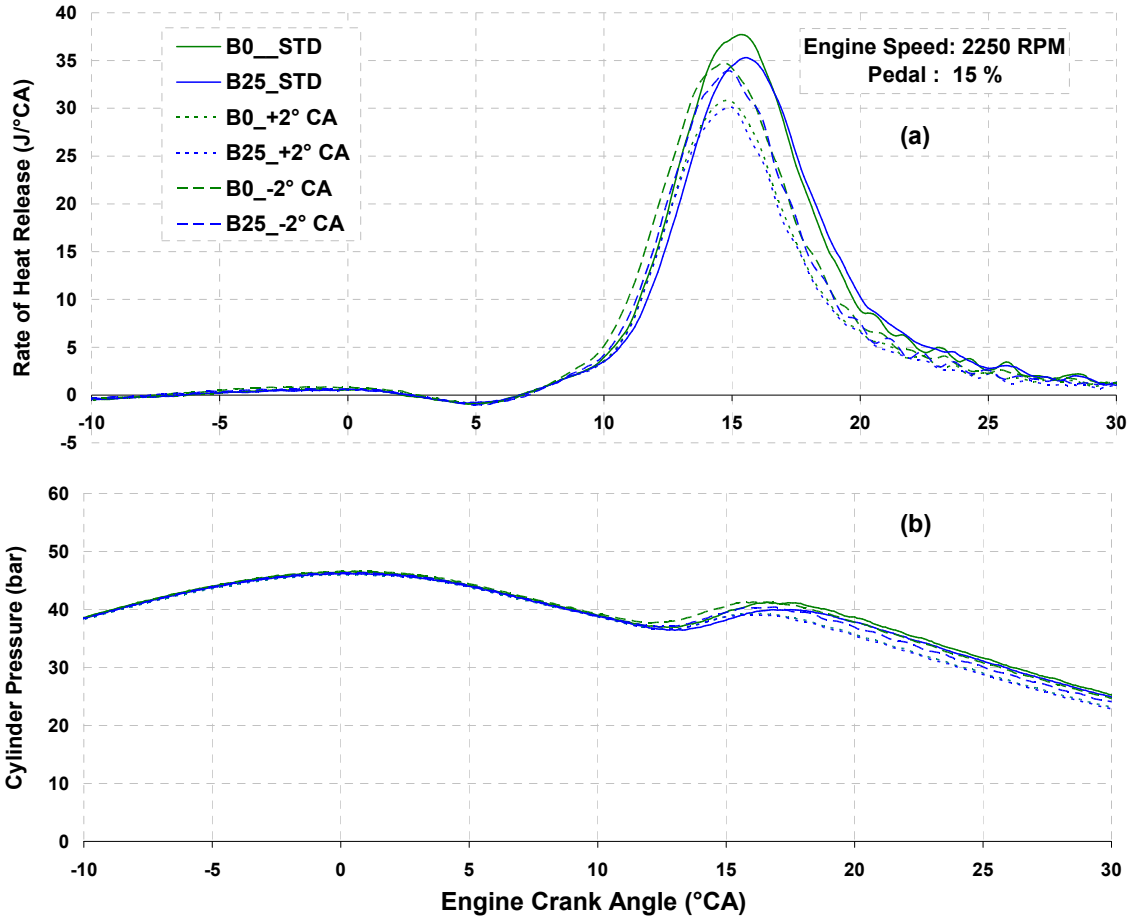

Figure 6.26, the effect of injection timing variation on (a) rate of heat release and (b) cylinder pressure at the 2250 RPM and 15% pedal position

B25 shows slightly less sensitivity to the variation in pilot injection timing during this operating condition by having lower percentage drop in engine power and lower percentage increase in CO and HC emissions.

6.6.4 2250 RPM 22% pedal

The effect of swinging the pilot injection timing on engine out emissions and performance during this operating condition is plotted in Figure 6.27.

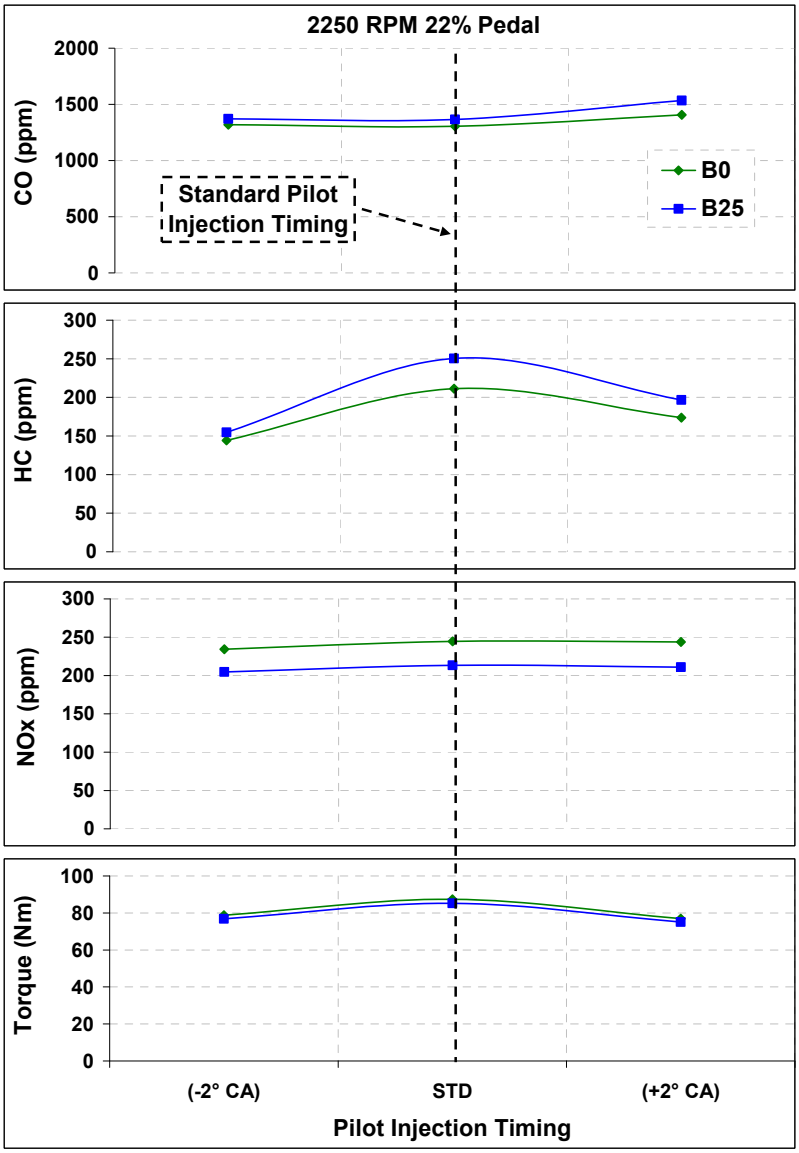

Figure 6.27, the effect of pilot injection timing variation on engine out emissions and performance at 2250RPM and 22% pedal

Very similar engine performance and emissions sensitivity can be seen from both fuels by varying the pilot injection timing. Advancing or retarding the pilot timing reduces the engine power by about 11% with both fuels compared to the standard calibration, and the impact is also similar on NO_X emissions. Little sensitivity difference can be observed between both fuels regarding the impact of varying the pilot timing on engine out emissions of CO and HC, where both fuels show an increase in CO emissions and a decrease in HC emissions by advancing or retarding the pilot timing.

6.7 Conclusions

The objective of this work was to determine the sensitivity of engine performance and emissions to calibration changes when the engine is operated with B25 compared to baseline diesel fuel. This study was performed by altering the main engine parameters of EGR rate, fuel line rail pressure, and both main and pilot injection timing. The following observations are made:

- Increasing the EGR rate resulted in a higher percentage reduction in NO_X emissions and a reduced engine torque penalty with B25 compared to the baseline diesel fuel particularly at higher load conditions due to the higher oxygen content. For all fuels, emissions of CO increased and HC's reduced with increasing EGR rate however, at the 1500 RPM and 17% pedal position condition, the increase in CO emissions with B25 was only 30% of that seen for baseline diesel and, in the case of HC emissions, an additional 10% reduction in levels was observed.
- Increased EGR also resulted in a reduction in engine out NO_X emissions for all fuels, but a further 8% reduction was observed with baseline diesel.
- The engine torque reduced by 3.5% with baseline diesel at high EGR rates, but no change was measured with B25.
- Increasing rail pressure improved the engine out torque at all experimented conditions, in addition it caused an increase in CO and HC emissions at lower load conditions due to the possibility of cylinder wall wetting, and caused an increase in NO_X emissions at higher load conditions due to a possible improvement in the combustion process. However, these emissions changes were less pronounced

when using B25 fuel, possibly as a result of the higher injection pressures improving fuel atomization and enabling sufficient evaporation to mitigate the impact of the higher viscosity of biodiesel. At 1500 RPM and 10% pedal, the observed increases in CO and HC emissions were 15% and 50% respectively lower when using B25 compared to baseline diesel. However, the increase in NO_X emissions and engine torque with B25 was seen to be 13% and 2% higher respectively than that observed with baseline diesel.

- Swinging the main injection timing had a variable impact on the engine performance and emissions dependent on engine operating condition, and in most cases B25 showed reduced sensitivity. Retarding the main injection timing by 2° CA at the 1500 RPM and 17% pedal condition reduced the engine out emissions of CO and HC with both fuels. A further 10% reduction in NO_X emissions and 2% increase in engine torque were only observed for B25. Similarly, at 2250 RPM and 15% pedal, the percentage increase in NO_X emissions was 7% lower and the improvement in the engine output torque was 11% higher with B25. At this condition, similar percentage reductions in CO and HC emissions were observed with both fuels.
- Varying the pilot injection timing did not improve the engine performance or emissions under most operating conditions, and both baseline diesel and B25 fuels showed similar sensitivity to this factor.

These findings can be very beneficial and should be considered by engine optimization engineers in determining the optimal engine calibration for B25 in order to achieve improved engine performance and reductions in exhaust emissions.

Chapter 7 Biodiesel Oxidation Catalyst Performance

7.1 Introduction

The conversion efficiency of a diesel oxidation catalyst (DOC) is mostly affected by the exhaust gas temperature, with other factors such as different hydrocarbon species [97, 111-115]. The performance of a DOC could be affected by variations in HC species due to their different storage characteristics through adsorption or condensation, and different reaction rates on the catalyst surface. One study suggested that the DOC is not equally active for all HC species, and they are grouped by the number of carbon atoms that exist in the molecular chain (C_2 to C_{12+}) [97]. Others stated that since different fuels are used, the exhaust gas of diesel and biodiesel fuels contain a different range of HC species that have different reactivity and storage characteristics on the catalyst surface [111-115], in addition this variation in HC species also might affect the conversion efficiencies of both HC and CO emissions.

In the vehicle trial investigation using RME biodiesel reported in Chapter 3 it was concluded that the average catalyst performance efficiency reduced as the percentage of RME increased with a reduction in engine-out exhaust gas temperature. An attempt to investigate the affect that HC species from RME fuel on the conversion efficiency was performed by examining idle periods during the NEDC. Unfortunately, the actual catalyst brick temperature could not be measured directly during the experimental study; instead it was approximated by using the post catalyst temperatures. This chapter reports the findings of a comprehensive study, conducted to evaluate the impact of RME fuel blends on catalyst performance by utilizing a catalyst instrumented with various thermocouples. The availability of catalyst brick temperature will allow the determination of an accurate light-off curve which can be used to identify any possible impacts from different HC speciation from both RME biodiesel and baseline diesel fuels. The light-off curve is determined by comparing the catalyst conversion efficiency of a given emission species against the catalyst brick temperature, thus isolating exhaust gas temperature and speciation effect on catalyst performance [137].

7.2 Background

DOCs have been used in diesel engines since about 1991, mostly based on Platinum, which oxidize CO, HC and to some extent PM in the exhaust gas to CO_2 and water. More recently, they are usually combined with diesel particulate filters (DPF) in one enclosure (see Figure 7.1) and attached to automotive exhaust systems. The catalyst consists of a ceramic or metallic monolithic honeycomb support, in which a special washcoat is deposited on it. As the exhaust gases pass through the support channels, the oxidation process takes place [92].

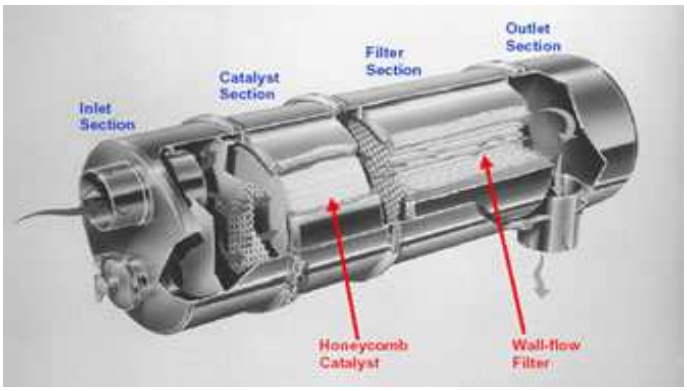

Figure 7.1, Diesel Particulate Filter combined with Oxidation Catalyst [132]

A DOC can achieve a significant reduction of CO and HC emissions up to 99 % for CO emissions, which is considered a milestone for meeting new European light duty diesel emission standards [133]. The availability of the catalyst, with an inherently oxygen rich atmosphere, provides a chemical shortcut in which CO and HC emissions are oxidized more rapidly and at lower temperatures to CO_2 and water, on the other hand makes it very difficult to chemically remove NO_X emissions. The pure oxidizing environment of the diesel engine exhaust gas suppresses the possibility of efficient NO_X removal, however under some operating conditions, low NO_X conversion efficiency can be achieved with the availability of the main reducing gases, such as various species of HCs, in a process called passive de-NO_X [134-136]

The oxidation of CO begins on the outer surface of the catalytic sites where it is converted to CO_2 in the presence of oxygen with the conversion efficiency increasing with increasing catalyst temperature until full conversion is achieved [92]. The oxidation of HCs involves a slightly more complicated process, where the engine out HC emissions passes through several stages before getting oxidized in the catalytic converter as described by Eastwood [137]. The HCs adsorb or condense onto the cold catalyst surface until it's too warm to retain the stored HCs but still too cold for oxidation to occur. If conversion efficiency is monitored, at first a good conversion is seen due to the storage effect then, as the HCs are released again, the conversion drops and might show a negative value since the temperature is not high enough for oxidation. Finally, when the catalyst temperature rises sufficiently, the oxidation process begins and the conversion efficiency increases. As the HCs undergo several stages of condensation, evaporation, and oxidation over the catalyst surface, it is expected that different species of HCs will certainly behave differently through these processes due to their physical and chemical variations. The light (low molecular weight) HCs are expected to pass through catalyst surface with minimal condensation when the catalyst is cold and constitute the "cold start" emissions, whereas the heavier HCs will mostly condensate on the catalyst surface and do not evaporate until the higher temperature is reached.

The principle of passive de-NO_X is based on selecting NO_X to react with HCs on the catalyst surface instead of oxygen, and this mutual annihilation offers removal of these two emission components [137]. Unfortunately this process is limited by a narrow catalyst temperature range and the availability of minimum HC concentrations in the exhaust gas to make up the required (HC/NO_X) ratio. The temperature range varies according to the precious material used in the catalyst, but it is roughly between 200 to 350°C for most of the commonly used materials. This is because at low temperatures HC oxidation is very slow, and at high temperatures HC is more easily oxidized by oxygen in the exhaust and it is only within this window that the HCs are oxidized by the NO_X [78]. The possibilities of any impact of using RME fuel blends on the passive de-NO_X process inside a diesel oxidation catalyst is expected, as it might vary or shift the oxidation temperature window, change the (HC/NO_X) ratio or alter the reaction speed due to its different HC species.

7.3 Aims and Objectives

The main aim of the work reported in this chapter, is to investigate the thermal and chemical impact of using RME biodiesel on the performance of a diesel oxidation catalyst. In order to achieve this, the following objectives are set:

- Identify if the trends in conversion efficiency observed during the vehicle trial study in Chapter 3 are repeatable on a transient engine dynamometer over the NEDC cycle.
- Evaluate the impact of using RME blends on exhaust gas and catalyst brick temperatures.
- Via the determination of catalyst light-off curves, asses the impact of HC speciation on DOC performance when using RME blends.

7.4 Experimental Facility

The experimental work was carried out within the Powertrain and Vehicle Research Centre (PVRC) in the Department of Mechanical Engineering at the University of Bath. Details about the experimental facility are given in section 5.3 of Chapter 5. For this work, the engine test facility was equipped with an instrumented catalyst.

The catalytic converter used in this study is a production diesel oxidation catalyst (DOC) supplied by Johnson Matthey (JM) inherited from a previous research project conducted on the same facility. The catalyst monolith was instrumented with 20 K-type thermocouples distributed along the axial and radial directions as shown in the schematic in Figure 7.2. The thermocouples were inserted at various positions, ten of which were aligned along the axial direction and the other ten along two radial positions.

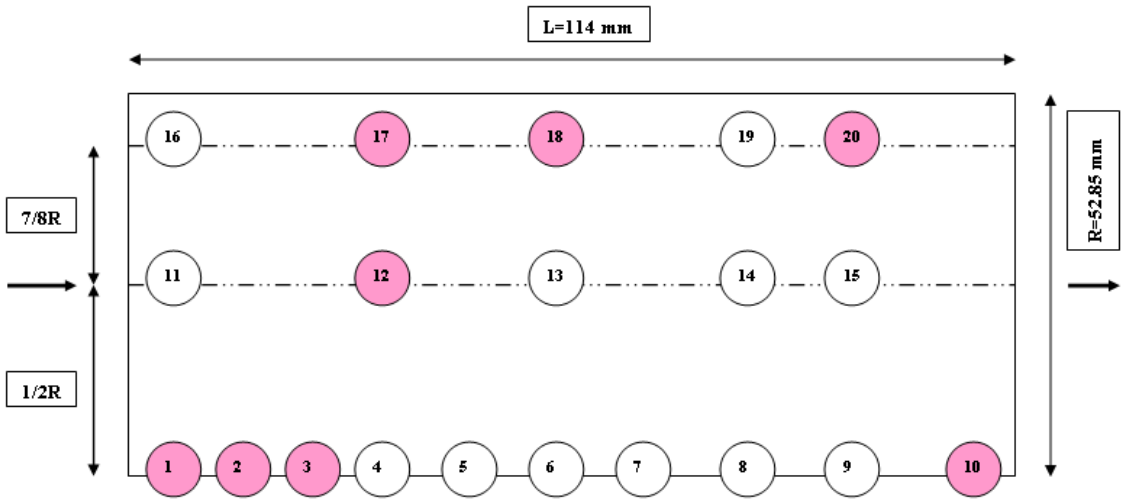

Figure 7.2, Schematic of thermocouple distribution inside the DOC catalyst, with broken ones coloured in pink

In addition, the exhaust system was also equipped with pre and post catalyst gas thermocouples to measure the inlet and outlet gas temperatures. All temperatures were recorded on the test bed data acquisition system.

7.5 Approach

The performance of the diesel oxidation catalyst with different blends of RME was studied, and the results compared to the results of the baseline diesel fuel. The investigations were conducted according to the following procedures:

- NEDC cycles with engine and catalyst conditioned prior to test and left to "soak" to ensure cold engine start. Baseline diesel fuel and blends of B25 and B50 were examined with total cycle catalyst conversion efficiency calculated on a gravimetric basis, using pre and post catalyst emissions measurements.
- Differences in exhaust gas and catalyst brick temperatures for baseline diesel, B25 and B50 fuels were examined using the second by second data over the NEDC.
- A transient experimental test was conducted in an attempt to obtain accurate catalyst light-off curves when using baseline diesel and B50 fuels in order to isolate the impact of exhaust gas chemical composition on catalyst performance.

7.6 DOC Performance during NEDC

To investigate the effect of RME biodiesel on the performance of diesel oxidation catalyst during the standard legislative procedure, the engine is operated with RME blends (B25 and B50) in addition to baseline diesel fuel over the NEDC. The engine ran over automated NEDC cycles which consists of two major parts, the first part simulates urban driving and the second part is one that simulates extra urban, as explained in chapter 3 [Figure 3.4]. The initial results from emission analysers were in volumetric basis (ppm) and they were converted to gravimetric basis using the following equations:

$$M = \frac{C_{exh}}{1 \times 10^6} \times \rho_g \times Q_{exh}$$

Equation 7.1

Where,

M , Is the mass of each pollutant (grams/second)

C_{exh}, Is the raw concentration of the pollutant in (ppm)

ρ_g , Is the gas density in (kg/m^3)

Q_{exh} , Is the exhaust volume flow rate (m^3/second) calculated from air and fuel flow values

The engine was conditioned and operated every day from cold, with only one experiment per day conducted to ensure consistent experimental conditions and repeatability. The standard deviation of the average variations in the cylinder head temperature did not exceed ±2°C before starting each experimental procedures. The catalyst conversion efficiency over the entire NEDC is obtained by calculating the ratio of the total engine out mass emissions to the tailpipe values for CO, HC, and NO_X emissions, see Figure 7.3.

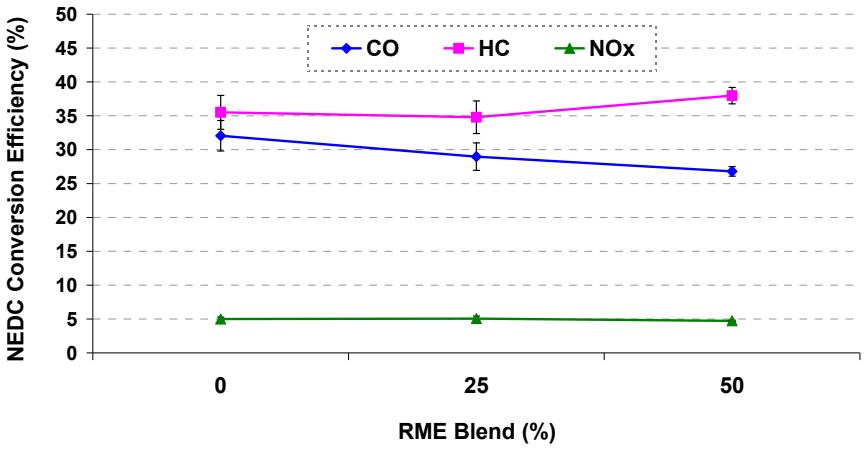

Figure 7.3, NEDC catalyst conversion efficiency

In general, the catalyst conversion efficiency for CO emissions reduced as the percentage of RME increased, conversion reduced by 10% and 16% for B25 and B50 respectively compared to baseline diesel. In the other hand, NO_X conversion is not expected in DOC due to purely oxidation environment, and the conversion seen here is passive NO_X and not what the DOC was designed to do. The passive NO_X conversion reduced by 5% with B50 RME but no change was observed when using B25. The catalyst conversion efficiency of HC emissions showed the opposite trend to both CO and NO_X emissions, with the conversion efficiency improving with the addition of RME to the fuel especially with B50. The HC conversion efficiency did not show any significant change with B25, but increased by 7% when the engine was fuelled with B50 RME compared to the baseline diesel fuel.

7.6.1 NEDC CO Emissions

The accumulated engine out and tailpipe mass emissions of CO and HCs produced during the NEDC for all fuel blends are plotted in Figure 7.4, and for the NO_X emissions in Figure 7.5. The engine out CO emissions reduced by 16% with B25 RME compared to baseline diesel fuel, but did not show any further decrease with B50 RME.

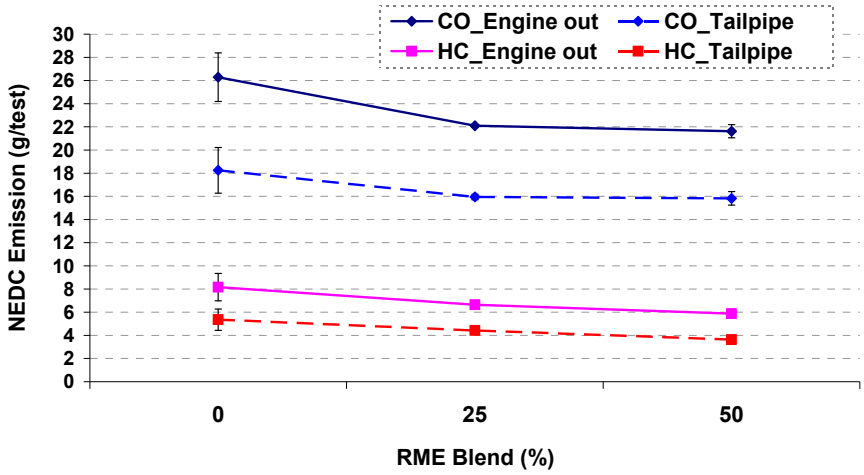

Figure 7.4, Total NEDC engine out and tailpipe CO and HC emissions for all fuel blends

In spite of the reduction in the actual mass value of CO emissions with B25 RME blend seen Figure 7.4 compared to the baseline diesel fuel, the catalyst conversion efficiency dropped by 10% as seen in Figure 7.3. The CO catalyst conversion efficiency continued to reduce with B50 blend even though the actual CO mass emission produced is very similar to B25 blend. This indicates a possibility of either thermal or chemical or a combined effect from the use of RME fuel blends on the catalyst performance, which will be reported later in this chapter.

7.6.2 NEDC HC Emissions

The HC engine out emissions showed a continuous reduction trend as the percentage RME increased in the fuel blend, it reduced from 8.2 (g/test) in case of baseline diesel fuel to 6.6 and 5.9 (g/test) with B25 and B50 biodiesel blends respectively. However, the HC catalyst conversion efficiency did not show any significant change with the B25 blend, and actually improved slightly with the B50 blend compared to the baseline diesel fuel as seen in Figure 7.3. With the expected reduction in catalyst performance with RME blends, the slight increase in HC conversion efficiency in the case of B50 blend seems to contradict this theory and to explain this observation, two scenarios are proposed. Firstly, the higher catalyst conversion efficiency of HC emissions with B50 fuel seen in Figure 7.3 is most likely caused by the significant reduction in engine out mass concentration of HC compared to the baseline diesel fuel seen Figure 7.4 and not actually higher performance

of the oxidation catalyst. Secondly, the chemical affect of HC speciation from the use of RME blends on the catalyst performance, which will be investigated later in this chapter.

7.6.3 NEDC NO_X Emissions

The engine out NO_X emissions did not show any significant change with B25 RME (considering the error bars), but it did show 10% increase with B50 compared to the baseline diesel fuel, see Figure 7.5.

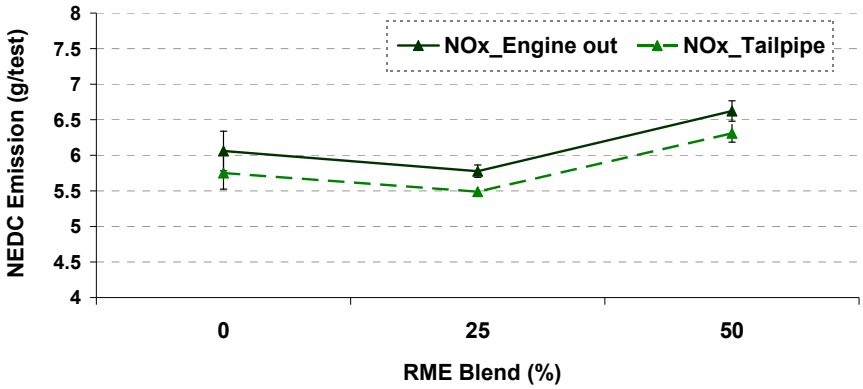

Figure 7.5, NEDC engine out and tailpipe NO_X emission for all fuel blends

As discussed in literature review section 2.4.5.2, most of the published literature indicated a slight increase in NO_X emissions when using biodiesel fuel and the percentage increase is directly dependant on the physical and chemical properties of FAME and engine technology. The FAME properties, such as carbon chain length, number of double bonds and oxygen content, are the main factors that alter the combustion behaviour of the fuel, leading to the expected increase in NO_X emissions [34 , 7, 10, 24 and 64]. Furthermore, the reduction in passive NO_X emissions observed in Figure 7.3 with B50 biodiesel could be due to the expected lower catalyst performance of the DOC or the lower mass concentrations of HC emissions with B50, which might affect the passive de-NO_X process discussed in section 7.2.

Examination of total cycle NEDC emissions confirms earlier results in chapter 3 that the use of biodiesel blends have an impact on catalyst performance. It is unclear if these

differences are caused by variation in catalyst operating temperature or chemical effects, therefore, the thermal impact of biodiesel blends on the performance of DOC during the NEDC, compared to baseline diesel fue needs to be investigated.

7.7 Thermal Impact of Using RME Biodiesel

7.7.1 Catalyst Brick temperature

To investigate the variations in the exhaust gas temperature and its consequent effect on the catalyst brick temperature with all three fuel blends, the pre catalyst temperature and catalyst brick temperature during the NEDC is plotted in Figure 7.6. The engine out temperature is obtained from a thermocouple positioned in the gas stream in the exhaust manifold just before catalyst inlet, and the catalyst brick temperature is the average temperature reading of all working thermocouples distributed inside the catalyst structure (see Figure 7.2). Unfortunately 8 thermocouples from total of 20 were not working when this catalyst was inherited from a previous experimental project, and this study continued with the remaining working thermocouples as replacing the faulty thermocouples could cause damage to the catalyst brick and the other instrumentation.

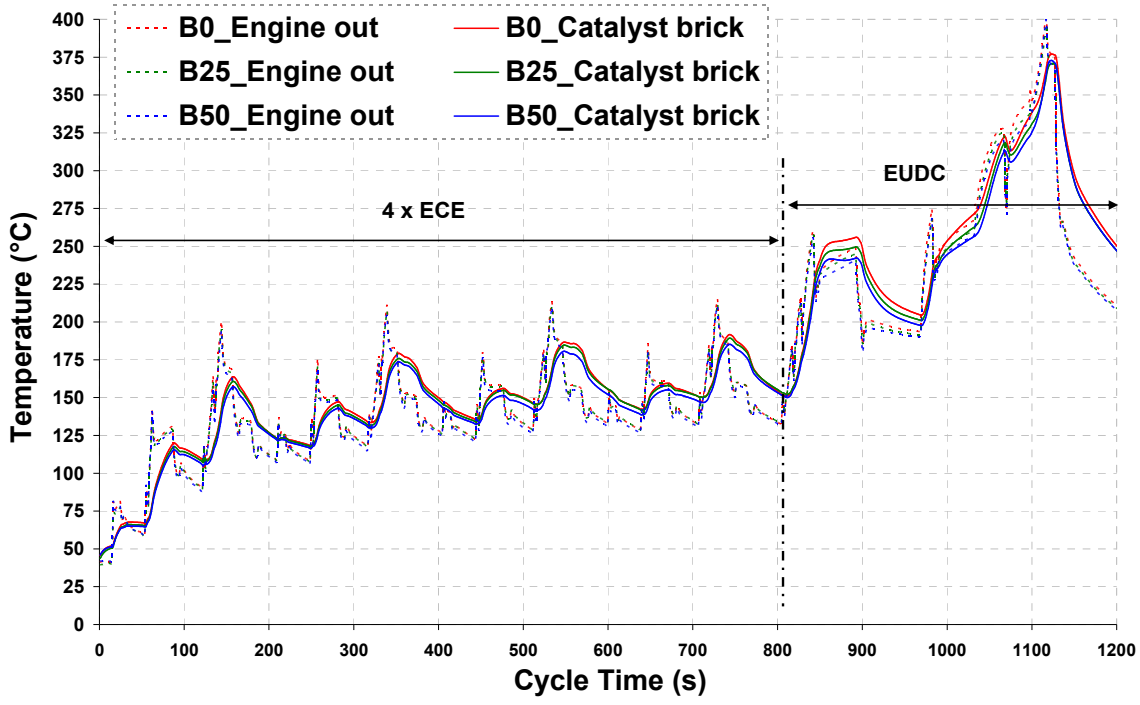

Figure 7.6, Engine out and average catalyst brick temperature for all fuel blends during NEDC

The observations from Figure 7.6 are summarized in the following points:

- The engine out exhaust gas temperature of baseline diesel fuel is always slightly higher than both biodiesel blends, and this trend is also reflected on the catalyst brick temperature. This reduction in exhaust temperature is also reported by many authors [60, 71, and 72] suggesting that the higher heating value and changes in fuel injection and combustion characteristics are the main reasons. This indicates that the catalyst is consistently hotter during the NEDC when the engine is operated with baseline diesel fuel compared to both biodiesel blends, which may partially explain the higher catalyst conversion efficiency seen in Figure 7.3.

- The temperature difference between all fuel blends for both engine out gas temperatures and brick temperature is more obvious during the EUDC portion of the cycle due to the higher load, and the variation is less significant during the ECE segments, especially when looking at the difference between baseline diesel and B25 fuels. The average brick temperature during the first 800 seconds are 141°C, 140°C, and 138°C, and during the last 400 seconds are 260°C, 255°C, and 252°C for baseline diesel, B25 and B50 respectively. The average reduction in catalyst brick temperature during the entire NEDC is 2% and 3% for B25 and B50 RME fuel blends respectively relative to baseline diesel.

- The fluctuations in the average brick temperature are much less pronounced than the engine out temperatures due to the thermal inertia of the catalyst brick releasing stored heat energy when the vehicle decelerates especially during the first half of the cycle when the catalyst temperature is below 150°C.

- Towards the end of ECE portion of the cycle and beginning of the EUDC, the catalyst temperature frequently exceeds that of the exhaust gas during the cruising periods, which is most likely caused by the exothermic reaction within the catalyst indicating higher catalyst conversion efficiency.

- The higher catalyst brick temperature is very distinct with baseline diesel fuel towards the end of NEDC which indicates the reduction in energy available in the exhaust gas (manifesting as lower gas temperatures) with increasing blend ratio

which might have delayed catalyst light-off and consequently reduced the overall catalyst performance observed over the NEDC when using biodiesel fuel blends.

To further investigate the impact of RME fuel blends on catalyst performance, the temperature profiles within the catalyst brick for all fuel blends are plotted in Figure 7.7. The front-face temperature readings are obtained from thermocouple number 11 (see Figure 7.2), as it represents the most frontal working sensor to the incoming exhaust gas. Similarly, the back-face readings are obtained from thermocouple number 9, as it represents the most rear working thermocouple within the catalyst brick.

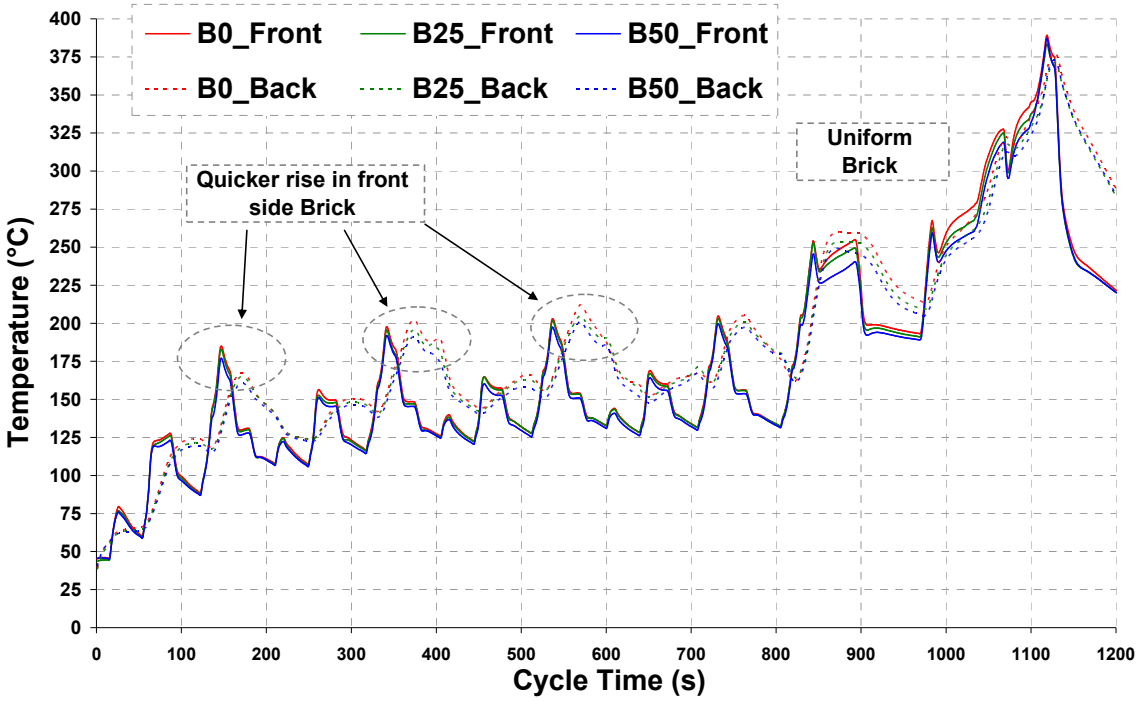

Figure 7.7, Temperature profile inside catalyst brick for all fuel blends during NEDC

The front-face of the catalyst is expected to initially heat up earlier, as the hot exhaust gas hits it first, than the back-face due to the thermal energy loss as the gas passes through the entire catalyst area. The temperature builds up inside the catalyst brick during the NEDC until the exothermic reaction begins. The temperature at which more than 50% or 60% (both used in literature) of the engine out emissions is being converted is usually defined as the catalyst light-off temperature [137]. The full conversion is reached at the end of

ECE and beginning of EUDC part of the cycle, where both the front-face and back-face catalyst brick temperatures are very close to each other and the exothermic reaction is occurring inside the catalyst. However after approximately 350 seconds of the cycle, occasional higher temperature peaks at the back-face of the catalyst can be observed compared to the front-face temperatures with baseline diesel fuel indicating a start of the exothermic reaction. This frequent higher exothermic reaction intensity, earlier in the cycle and even before reaching the full conversion, supports the previously discussed point of higher catalyst performance when the engine is operated with baseline diesel fuel compared to biodiesel blends.

The following section will discuss the impact of catalyst brick temperature and the occurrence of the exothermic reaction with RME blends on the continuous second-by-second catalyst conversion efficiency during NEDC.

7.7.2 Continuous Conversion Efficiency

So far it has been shown that the use of RME fuel blends have lowered the engine out exhaust gas temperature and consequently reduced the catalyst brick temperature, which resulted in a less intensive exothermic oxidation reaction compared to baseline diesel fuel. The impact of a reduced exothermic reaction on the catalyst conversion efficiency of CO, HC, and passive NO_X reduction was then investigated and the findings are reported in this section, by analysing the second-by-second emission concentrations produced during the NEDC.

7.7.2.1 Continuous CO Conversion

Figure 7.8 shows the continuous second by second catalyst conversion efficiency of CO emission for all three fuel blends through the entire NEDC procedure.

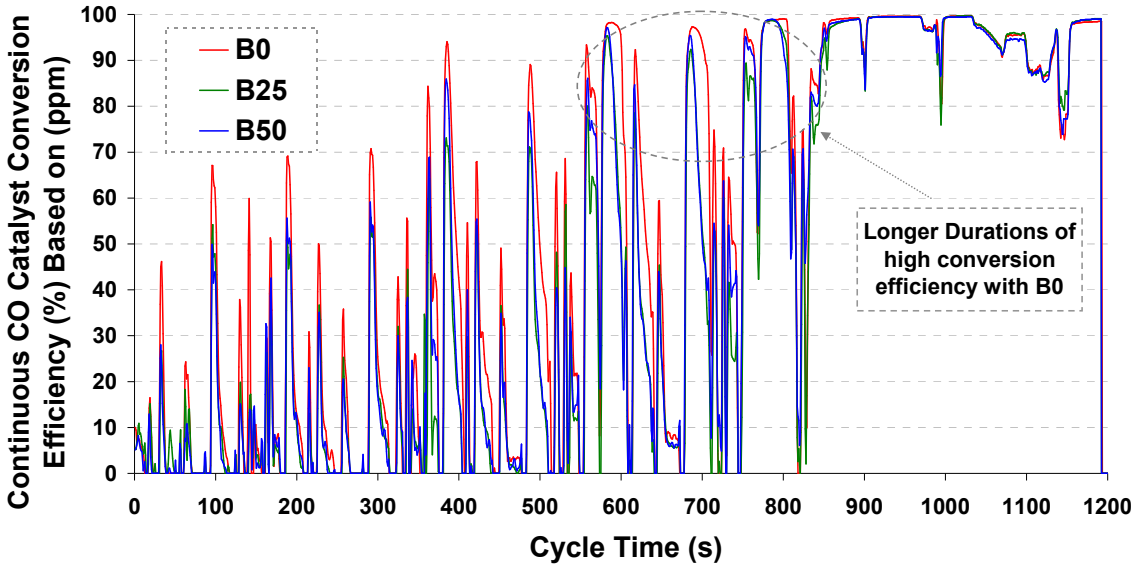

Figure 7.8, Continuous catalyst CO conversion efficiency for all fuel blends

Observations from Figure 7.8 are summarized in the following points:

- During the initial 500 seconds of the cycle, the CO conversion efficiency with baseline diesel fuel always show higher peak values when compared to B25 and B50 RME blends. During this period the catalyst brick temperature is below 150°C on average (see Figure 7.6), and the catalyst has not reached the necessary light-off temperature.
- Between 550 and 800 seconds, similar peak values can be seen with all fuel blends but with baseline diesel fuel, longer durations of high conversion efficiencies can be observed, see Figure 7.8. During this period, the catalyst is starting to light-off and is in transition to reach its full conversion efficiency.
- After 800 seconds, all fuels show very similar conversion values. Despite the brick temperature being lower with both biodiesel fuel blends during this period (see Figure 7.6), full conversion efficiency is achieved as the catalyst brick has already achieved light-off.

7.7.2.2 Continuous HC Conversion

The continuous HC conversion efficiency during the NEDC is plotted in Figure 7.9, and observations from this figure are summarized here:

- The high conversion efficiency during the first 100 seconds of the cycle is due to the fact that most of the HCs emitted are adsorbed or condensed on the cold catalyst surface.
- From 150 to 350 seconds, the HCs are released again when the catalyst has not achieved light-off and the conversion efficiency drops since the catalyst is still cold and the oxidation reaction has not began.
- At approximately 750 seconds, the conversion efficiency starts to rise again due to higher engine exhaust temperature, and also due to the reduction in HC emission concentrations produced as the engine warms up.
- Clear variations can not be observed with the use of biodiesel fuel blends due to fact that the HC light-off characteristics are more complicated, as discussed in the background section, and also the engine out concentrations showed variations with RME blends compared to the baseline diesel fuel.

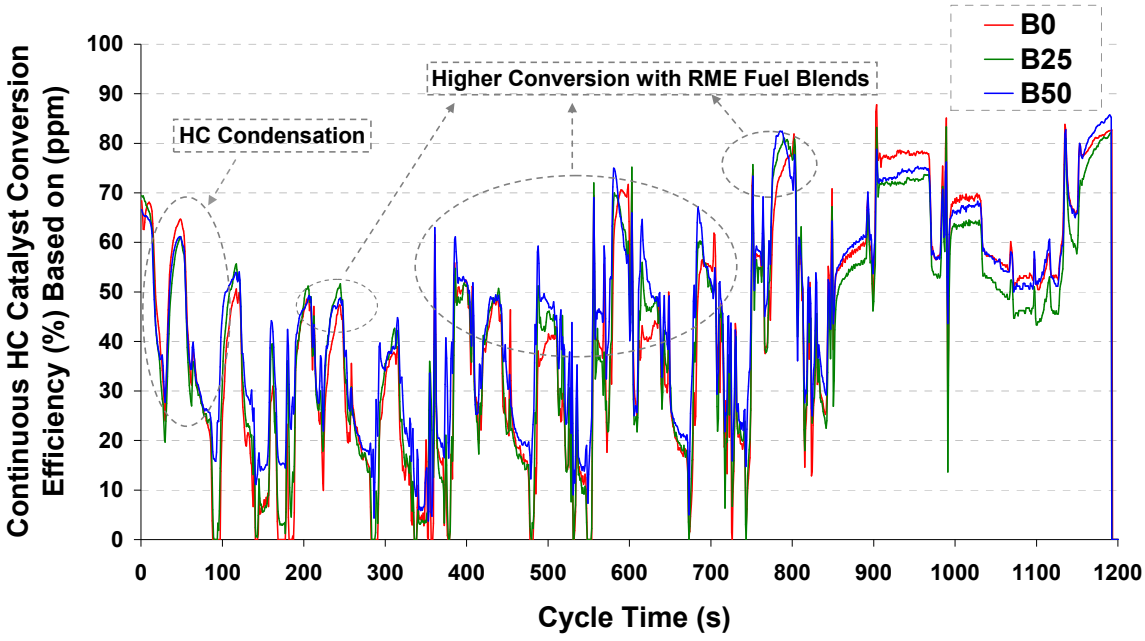

Figure 7.9, Continuous catalyst HC conversion efficiency for all fuel blends

- Slightly higher conversion can be seen during most of the ECE part of the cycle with RME blends which might be attributed to either slightly lower engine out

concentrations of HC emissions, or due to variations in chemical composition compared to baseline diesel fuel which might react differently with catalyst surface material (speciation).

- Higher conversion efficiencies for biodiesel blends during the ECE do not seem to be explainable by thermal effects as both exhaust gas and brick temperatures are slightly lower with RME fuel blends during the entire cycle, see Figure 7.6.
- During the EUDC, the baseline diesel fuel shows higher conversion efficiency occasionally which might be caused by its higher catalyst brick temperature seen in Figure 7.6.

7.7.2.3 Continuous Passive NO_X Conversion

The continuous NO_X passive conversion efficiency for all fuel blends during the NEDC procedure is presented in Figure 7.10. The average catalyst conversion efficiency during the NEDC did not exceed 5% with all fuel blends as seen in Figure 7.3, and dropped slightly as the percentage of RME increased in the fuel blend.

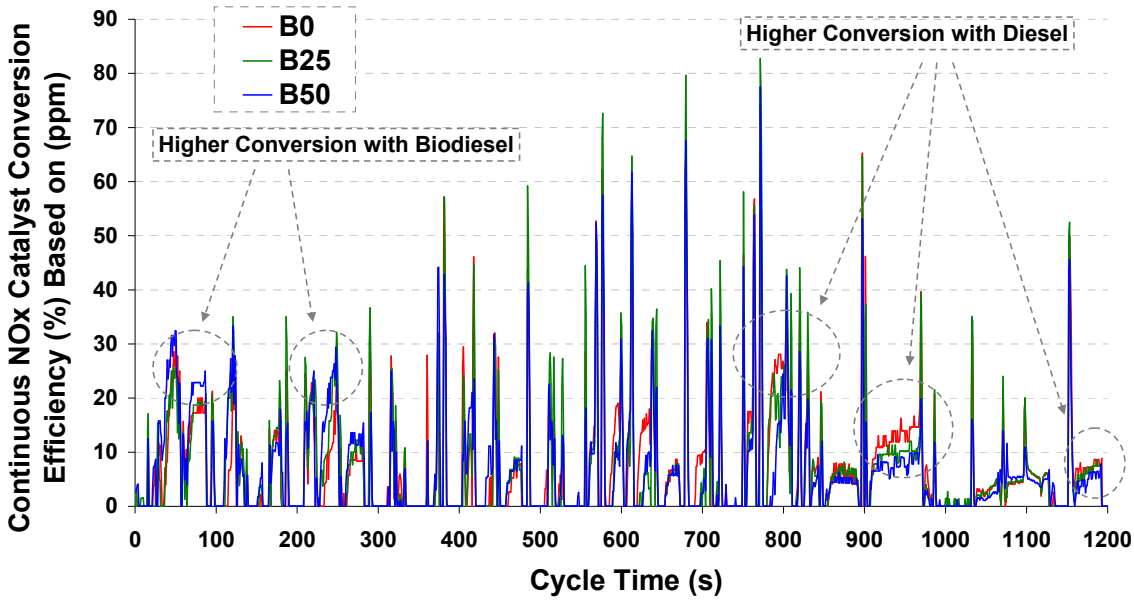

Figure 7.10, Continuous catalyst NO_X passive conversion efficiency for all fuel blends

The observations from Figure 7.10 are summarized in the following points:

- During the first 350 seconds, the average conversion efficiency is generally very low even though the engine out HC emissions is expected to be very high due to cold engine condition. This is probably attributed to the low catalyst brick temperature in addition to the HC condensation during this period of the NEDC, and no clear trend or variation could be seen with the use of RME fuel blends except occasional short segments of higher conversion.
- Half way through the cycle (600 to 700 seconds) several few high conversion peaks and slightly higher average conversion efficiency can be spotted. Higher conversion efficiency during this period is most likely caused by higher catalyst brick temperature which ranges between 145 to 245°C, and the availability of HCs in the engine out exhaust gas, which might have provided the correct NO_X: HC ratio and temperature window for the de-NO_X process.
- At the end of the cycle (post 800 seconds) and more specifically during most of the EUDC part, the average conversion efficiency drops down again with all fuel blends even though the brick temperature is very high. The two main factors are high NO_X concentration in the engine out exhaust gas expected due to hot engine conditions, and less availability of HCs as reducing agent for the efficient passive de-NO_X process to take place.
- It is very difficult to distinguish any variations in continuous NO_X emissions between the baseline diesel fuel and RME blends.

In summary, the use of biodiesel fuel blends have lowered the engine out exhaust temperature and consequently reduced the catalyst brick temperature during the NEDC, which resulted in less intensive exothermic oxidation reaction with biodiesel compared to baseline diesel fuel, and impacted on the DOC performance especially for CO. Reduced exhaust gas temperatures with biodiesel fuel is reported by few authors [60, 71, and 72], but no other work could be found that investigates the impact of biodiesel on the performance of DOC. While there is clearly a temperature difference when using biodiesel blends, it is not clear if this is the reason for the reduction in CO conversion efficiency observed over the NEDC, or if variations in exhaust gas chemical composition also contribute. Therefore, the impact of chemical variations from the use of RME fuel blends must be investigated.

7.8 Chemical Impact of Using Biodiesel on DOC

The previous section identified the thermal impact of biodiesel blends on the exhaust gas and catalyst brick temperatures, and the knock on effect on performance of the catalyst compared to baseline diesel fuel. This section reports an investigation to ascertain if the chemical impact of using biodiesel on the performance of the oxidation catalyst due to its different HC composition. The instantaneous catalyst conversion efficiency for CO, HC, and NO_X is plotted against the average catalyst brick temperature for all three fuel blends regardless of the difference in exhaust gas temperature. This will realise for each fuel blend, the catalyst conversion efficiency at a given brick temperature during the NEDC which is called the catalyst light-off curve. The catalyst light-off temperature is the temperature at which the conversion efficiency of the inlet gas emissions reaches a specific value, usually 50%. Comparing these curves from different fuel blends will provide some insights regarding any HC speciation impact on the performance of the diesel oxidation catalyst.

The transient nature of the NEDC introduces a lot of challenges into performing this investigation due to frequent accelerations and decelerations encountered during this procedure, which will vary many critical parameters such as exhaust flow (consistent residence time in the catalyst) and the amount of emissions emitted. Therefore, only the idling periods of the cycle will be selected in order to ensure consistent exhaust flow rate and lower variations in engine out emissions with different fuel blends. Also, to get better representative curves, very narrow range of catalyst conversion efficiency will be selected in order to minimize any possible miss alignments between engine out and tailpipe emission measurements. Finally to get a clearer trend, a histogram was produced of catalyst conversion efficiency values in 5°C increments.

7.8.1 CO Light-off Curve: NEDC Idle periods

The CO light-off curve for all three fuel blends is plotted in Figure 7.11.

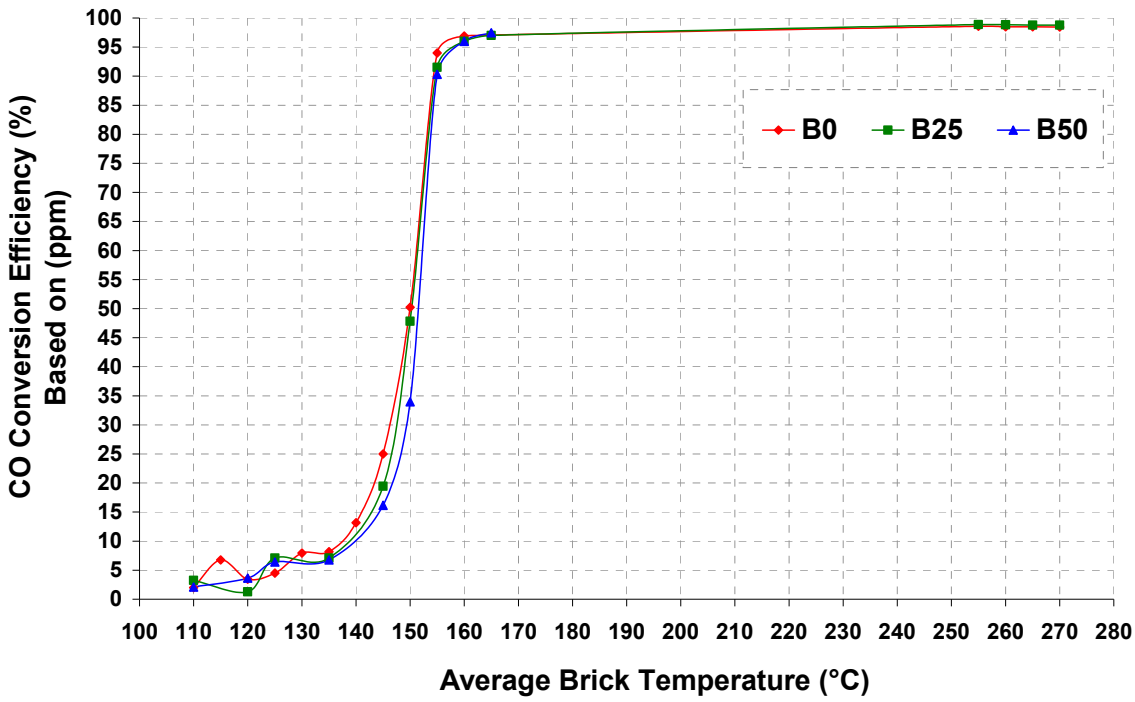

Figure 7.11, CO light-off curve during idle periods of the NEDC for all fuel blends

The observations for Figure 7.11 are summarized in the following points:

- The CO light-off temperature is approximately 150°C for all fuel blends if defining 50% conversion efficiency as the start of catalyst light-off.
- Slightly higher conversion efficiency can be observed with baseline diesel fuel until the brick temperature reaches 150°C compared to both RME blends.
- The conversion efficiency between 150 to 160°C brick temperatures shows slightly higher values with baseline diesel fuel.
- For brick temperature above 160°C, all fuels show very similar CO conversion efficiency ranges between 96 to 99%.

7.8.2 HC Light-off Curve: NEDC Idle periods

The HC light-off curve for all three fuel blends is plotted in Figure 7.12.

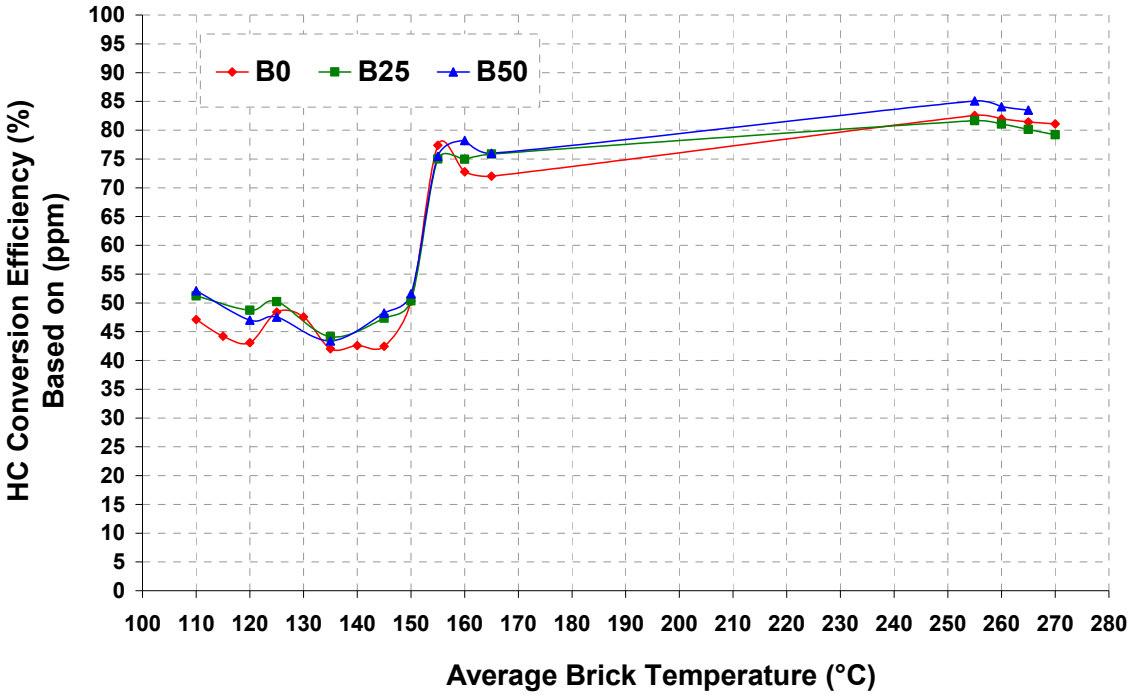

Figure 7.12, Averaged HC light-off curve during the idle periods of the NEDC for all fuel blends

The observations from the HC light-off curves are summarized in the following points:

- Similar to the CO light-off curve, the HC light-off temperature is around 150°C for all fuel blends.
- Unlike the CO light-off curve, the high conversion efficiency earlier in the cycle is caused by HC adsorption or condensation onto the cold catalyst surface. The higher HC conversion with both RME blends during this period is probably caused by either lower HC concentrations in the exhaust gas or their higher molecular weight leading to more condensation compared to baseline diesel fuel.
- The conversion efficiency drops slightly as the brick temperature increases, due to HC evaporation off the catalyst surface, until it reaches around 140°C when it starts to rise again.
- The conversion efficiency between 150 to 155°C brick temperature shows very similar trends with all fuel blends as the conversion efficiency jumps from 50% to more than 75%.
- As the brick temperature increases above 155°C, a slight variation in conversion efficiency is apparent between the baseline diesel fuel and both biodiesel blends.

This is most likely caused by much lower HC concentrations in the exhaust gas when the engine is operated with biodiesel.

- Finally above 160°C, the HC conversion efficiency reaches its maximum value and settles in the ranges of 80 to 85%.

7.8.3 Passive NO_X Light-off Curve: NEDC Idle periods

The passive NO_X catalyst light-off curve for all three fuel blends is plotted in Figure 7.13.

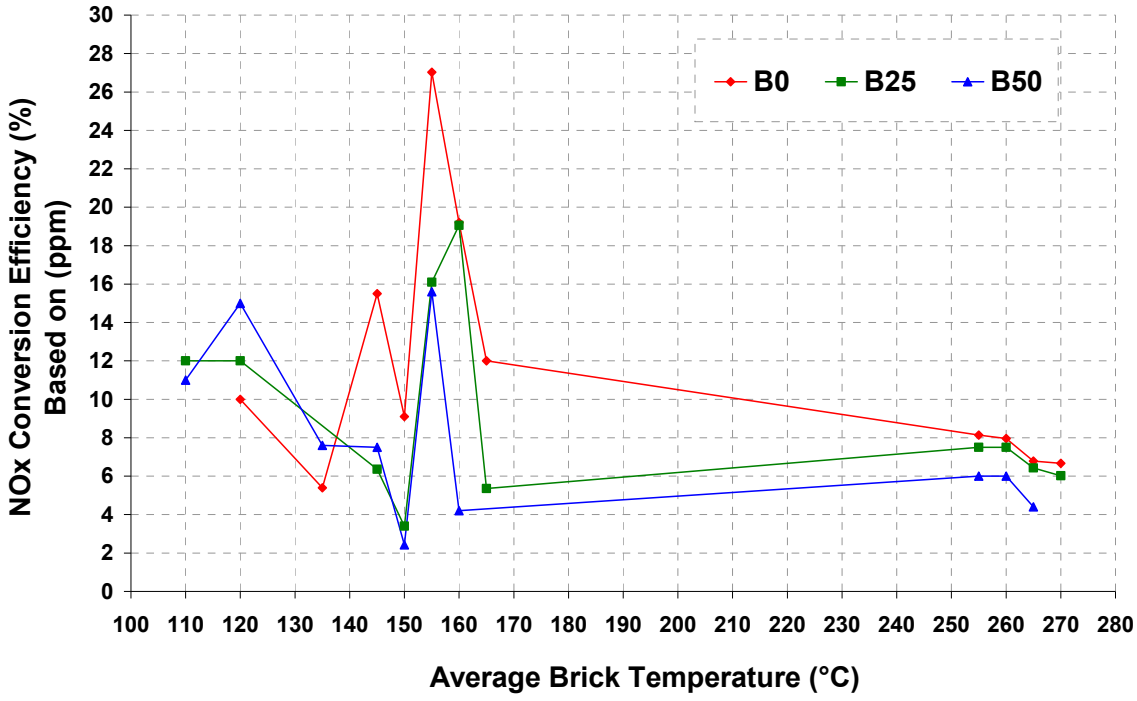

Figure 7.13, Averaged NO_X light-off curve during the idle periods of the NEDC for all fuel blends

The outcome of the NO_X passive conversion curve is variable due to the dependency of NO_X conversion on variable factors such as exhaust temperature and HC concentrations in order for the passive de-NO_X process to take place. The general observations that can be made from the NO_X light-off curves are summarized in the following points:

- With relatively low catalyst brick temperatures (until 150°C), the NO_X passive conversion fluctuates at around 10% conversion with all fuel blends, and all fuel blends show a very similar NO_X light-off temperature which is around 155°C.

- During the higher conversion period (from 150 to 160°C), the NO_X conversion efficiency peaks at about 27%, 19%, and 16% for baseline diesel, B25, and B50 fuels respectively. The higher conversion efficiency during this period is probably because it met the required passive de-NO_X criteria with the certain temperature window and availability of HCs. This period corresponds to the end of the ECE part of the NEDC (see Figure 7.6) at which time the brick temperature is hot enough and the engine is still emitting enough HCs for the passive de-NO_X process to take place.
- The NO_X conversion efficiency is always higher when the engine is fuelled with baseline diesel fuel compared to both RME blends; this is most likely attributed to the higher concentration of HC in the engine out emissions when using baseline diesel fuel.
- After the brick temperature exceeds 160°C, the conversion efficiency drops as the brick temperature increases and settles at around 6%. This period corresponds to the EUDC part of the cycle, and the very low concentrations of HCs during this period is the main factor in having lower NO_X conversion efficiency.

This section reported the investigation carried out to determine the chemical impact of different exhaust gas HC species from the combustion of biodiesel blends on the DOC compared to baseline diesel fuel. The dynamic nature of the NEDC introduced additional complexity into performing this investigation and, in order to overcome the discreet nature of the data which was obtained from examining the NEDC idle periods, specific light-off test needed to be performed. While determination of light-off curves by the catalyst industry is commonplace using specific rigs and synthetic exhaust gas, obtaining this data from a running engine is more challenging. The experimental work undertaken to obtain these light-off curves for different fuel blends is discussed in the following sections.

7.9 Further Investigations into Chemical Impact of biodiesel on DOC

In the previous section, data analysis was conducted to investigate the possibilities of determining any chemical impact of different HC species from biodiesel fuel blends on the DOC compared to baseline diesel fuel using NEDC data. However, due to the nature of the NEDC, many additional challenges were introduced which cast doubt on the accuracy of the results obtained. The objective of this experimental work was to further investigate the chemical effect of RME fuel blends on the catalyst light-off temperature by using a specifically designed procedure.

7.9.1 Transient Engine Ramp

This procedure calls for increasing the engine load gradually by ramping up the pedal position from a lower fixed point to a higher fixed point over a given duration and then ramp down following the same procedure. An engine speed of 2000 RPM was set with a varying pedal position from 11% to 15% representing about 7 Nm to 47 Nm respectively when the engine was fuelled with baseline diesel fuel. The ramp time allowed for the pedal position to reach 15% from 11% was set as 600 seconds which was hoped to be slow enough to ensure that the brick temperature closely matches the exhaust gas temperature during the ramp. This procedure was controlled via the test cell control computer. Several skirmish experiments were performed to ensure that the catalyst undergoes light-off during this transient engine ramp procedure with both baseline diesel and the B50 fuel blend. The pedal ramp procedure and associated brick temperatures and CO conversion efficiency for the baseline diesel fuel are shown in Figure 7.14.

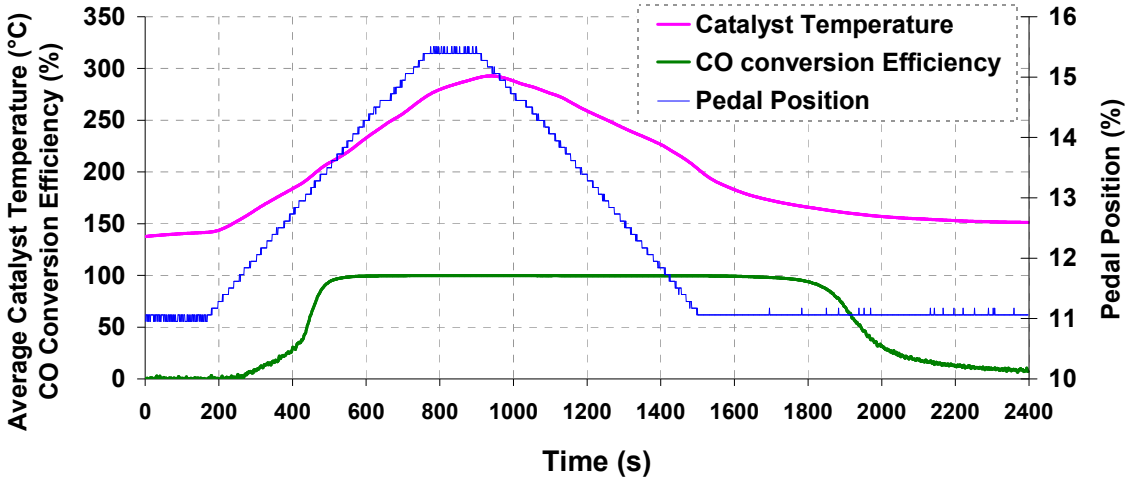

Figure 7.14, Effect of transient engine ramp on catalyst brich temperature and CO conversion efficiency

7.9.1.1 Light-off Curves during Transient Engine Ramp

The light-off curves for CO, HC, and NO_X are plotted in Figure 7.15, Figure 7.16, and Figure 7.17 respectively. The light-off curve for B50 biodiesel fuel blend starts earlier with higher conversion efficiencies as the brick temperature increases compared to baseline diesel fuel. The CO light-off temperature is 187°C for B50 fuel blend and 192°C for the baseline diesel fuel when the engine is ramped up, and these results were repeatable within +/- 2°C. During ramping down the catalyst did not reach the light-down temperature within the 600 seconds ramp, however the engine conditioned for approximately 400 seconds on average at 11% pedal to reach the light-down temperature with 50% conversion efficiency. The CO light-down temperature occurred at slightly higher temperature with baseline diesel fuel at 159°C, and 157°C for B50 fuel blend.

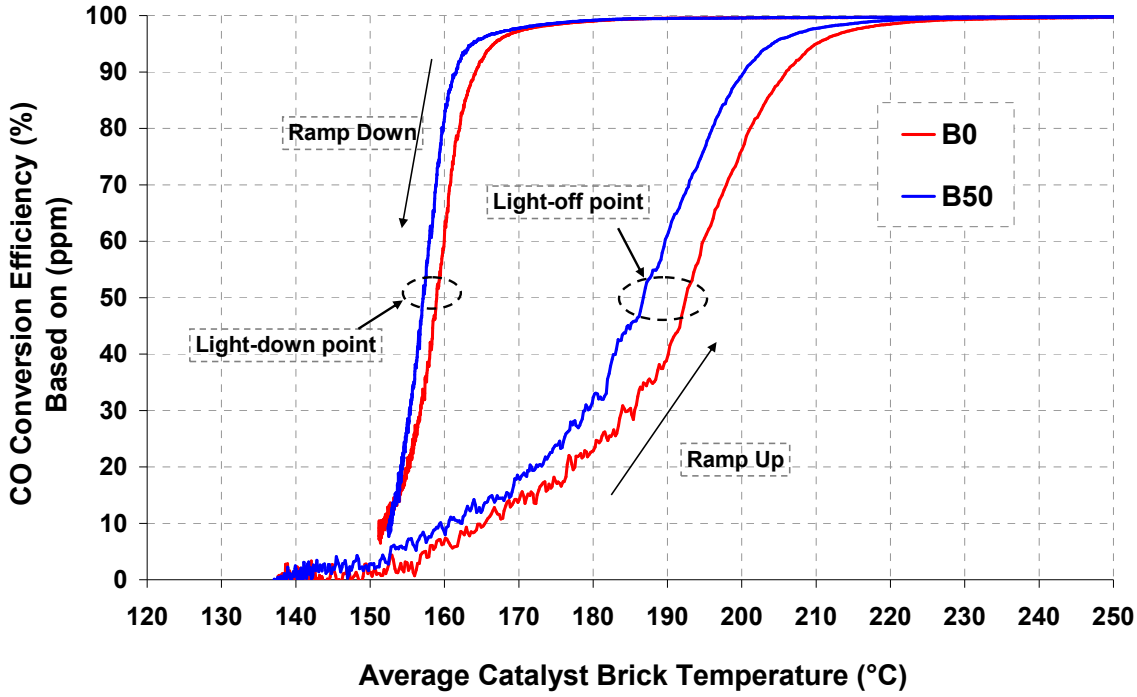

Figure 7.15, CO Light-off curve for baseline diesel and B50 in transient engine ramp condition

A similar trend was observed in HC light-off curve as shown in Figure 7.16, the HC light-off temperature is 192°C for B50 fuel blend and 199°C for the baseline diesel fuel. The maximum conversion efficiency is the same for both fuels (about 87%), but it is reached at a brick temperature 15°C lower with B50 biodiesel compared to baseline diesel fuel. The HC light-off curve starts with reasonably high conversion values (30%), it decreases slightly as the brick temperature increases and finally rises to the maximum conversion efficiency. The initial high conversion value of HCs is due to adsorption or condensation on the catalyst surface at lower temperatures, and then followed by desorption or vaporisation once the temperature increases.

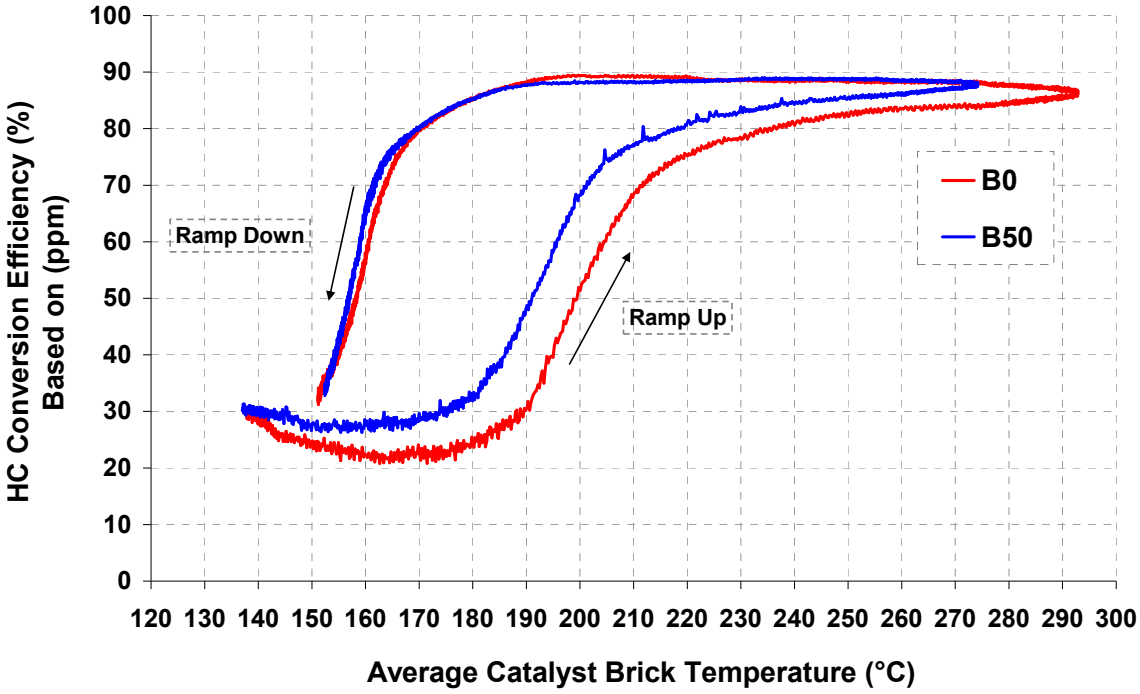

Figure 7.16, HC Light-off curve for baseline diesel and B50 in transient engine ramp condition

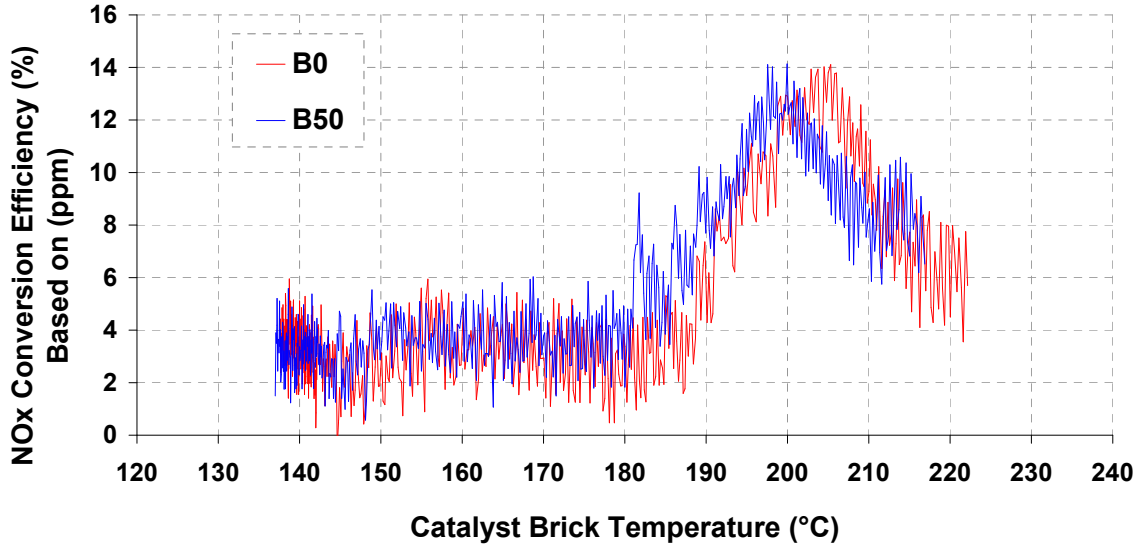

Figure 7.17, NO_X Light-off curve for baseline diesel and B50 in transient engine ramp condition

The NO_X conversion curve also showed earlier light-off with B50 compared to the baseline diesel fuel. Figure 7.17 shows that the average conversion is similar for both fuels before light-off which is about 4%, and the maximum NO_X conversion efficiency reached is 14%, but at a temperature 5°C lower for B50 fuel. The passive de-NO_X

conversion obtained here depends on two factors as discussed earlier, availability of HC and the correct temperature window which vary with both fuels.

At first glance the catalyst light-off curves of CO, HC, and NO_X emissions indicate that the catalyst performance is better when the engine is fuelled with B50 than the baseline diesel fuel due to the earlier light-off and delayed light-down temperatures. In other words, at a given temperature, baseline diesel and B50 fuels have different conversion rates. For example, when the gas temperature is 188°C, the CO version efficiency is 50% for B50 but only 30% for the baseline diesel fuel. This result does not agree with the preliminary findings in the vehicle trials in chapter 3 section 3.5.6.3 with earlier light-off temperature in case of baseline diesel fuel. It is suspected that the HC speciation influence is a valid argument with this limited information in hand. Before jumping to any conclusion, a study of amount of CO, HC, and NO_X emissions emitted by engine when operated with both baseline and B50 fuels is required to validate these results.

7.9.1.2 Emissions Investigation during Transient Engine Ramp

The engine out CO, HC, and NO_X emissions during the ramp tests are plotted in Figure 7.18, Figure 7.19, and Figure 7.20 respectively. Pedal position points were selected in order to have a valid comparison between fuel types. The concentrations of CO and HC are higher with the baseline diesel fuel compared to the B50 blend, except for NO_X emissions where B50 shows slightly higher concentrations. Until the light-off temperature point, the emissions from baseline diesel fuel are higher by more than 15% and 20% for CO and HC emissions respectively compared to B50 blend.

Higher concentrations of CO and HC emissions are passing over the catalyst washcoat surface when using baseline diesel fuel prior to the catalyst achieving sufficient light-off temperature. In other words, the catalyst is always exposed to higher concentrations of CO and HC when the engine is fuelled with baseline diesel fuel compared to B50 blend throughout the experimental procedure.

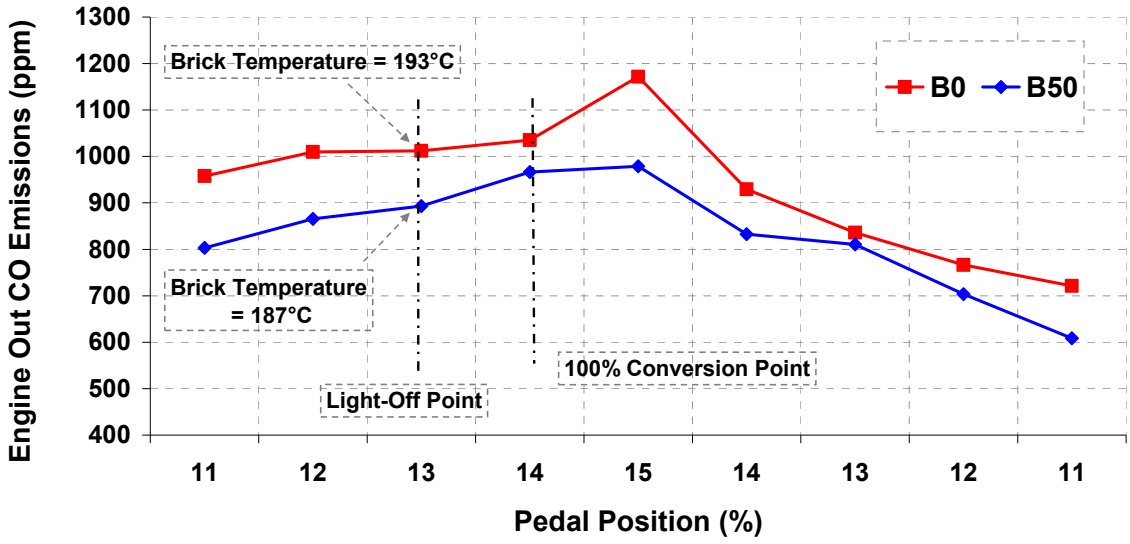

Figure 7.18, Engine out CO emissions during ramping up and down the pedal position, standard calibration

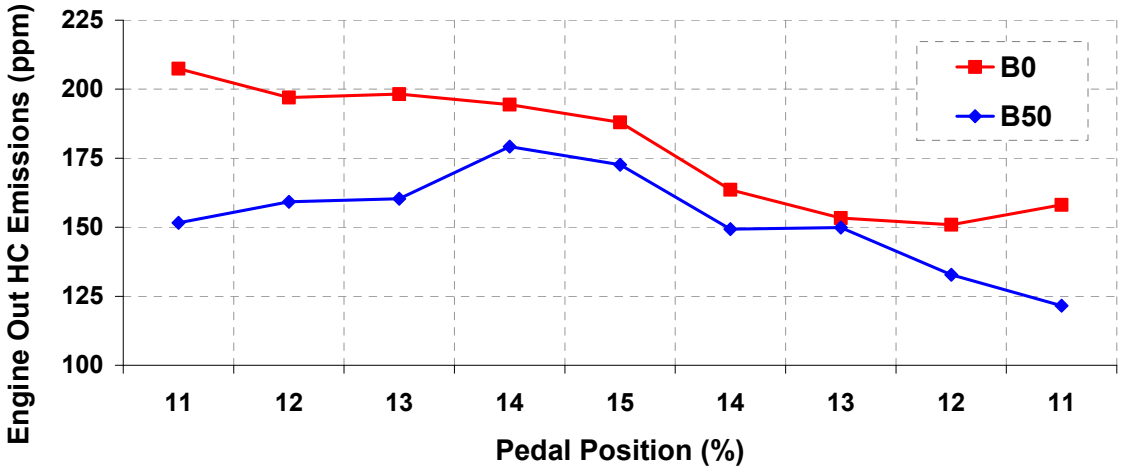

Figure 7.19, Engine out HC emissions during ramping up and down the pedal position, standard calibration

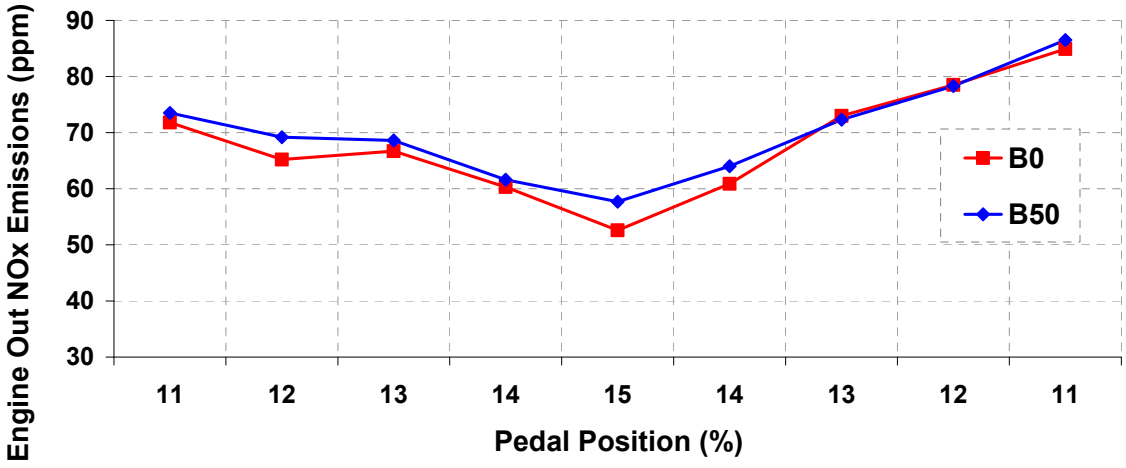

Figure 7.20, Engine out NOx emissions during ramping up and down the pedal position, standard calibration

The limited surface capacity of the catalyst before it achieves light-off temperature might have caused lower calculated conversion efficiency at lower catalyst temperatures in case of baseline diesel fuel due to its much higher CO and HC concentrations. Once the catalyst is hot enough, the conversion efficiency is sufficient to convert the majority of emissions regardless of concentrations and fuel type. On the other hand, the slight increase in NO_X emissions shown in Figure 7.20 with B50 can not be used to explain the shift in the NO_X light-off curve, since the limited passive NO_X conversion depends mainly on the availability of HC within a specific temperature range, which both varies with B50 compared to the baseline diesel fuel.

Due to the large differences in pre catalyst emissions concentrations when using different fuel types, it is not possible to definitely comment on the influence exhaust gas speciation may have on catalyst performance. In order to determine a fair light-off comparison, the differences in exhaust gas emissions concentrations between different fuels must be minimized, while maintaining a consistent exhaust flow rate. The following section describes experimental work undertaken to obtain light-off curves under similar exhaust gas emissions concentrations.

7.9.2 Altering the engine calibration

In order to achieve similar engine out emissions to the baseline diesel fuel, the engine calibration was be modified when using biodiesel. Initially EGR rate was increased for the blend B50 in order to increase engine out emissions of both CO and HC emission to levels closer to those seen for the baseline diesel fuel. Increasing the EGR rate by 10% reduced the difference in engine out CO emissions between B50 and the baseline diesel fuel to approximately 5% prior to light-off instead of 15% observed under standard conditions. However this method did not reduce the difference in HC emissions considerably, where the B50 fuel blend still produced 15% lower HC emissions, on average, compared to the baseline diesel fuel.

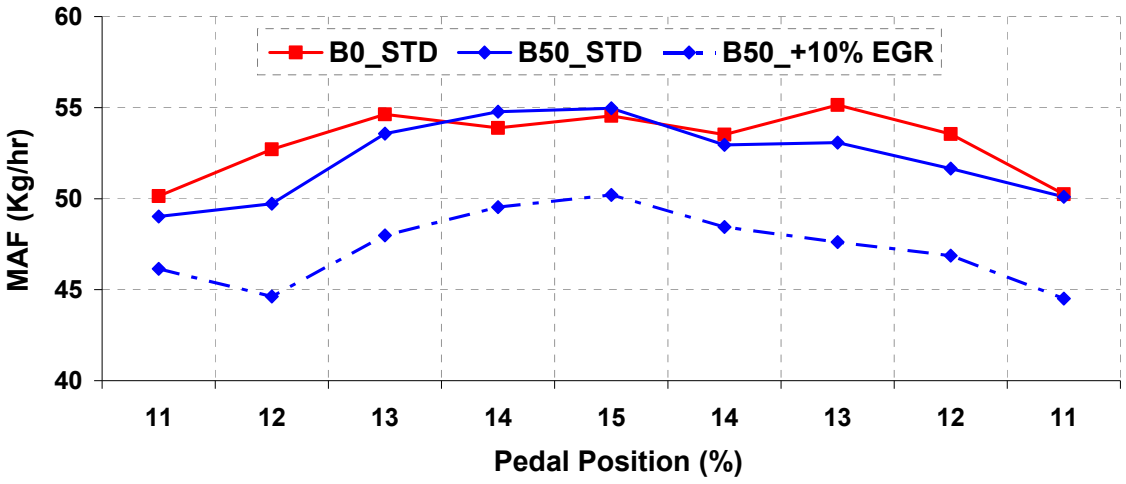

Figure 7.21, Effect of EGR change with B50 RME fuel blend on engine MAF

In addition, the increase in EGR rate introduced an additional variable of a reduction in engine mass air flow (MAF) as shown in Figure 7.21, which would lead to a corresponding reduction in exhaust flow rate and an increased residence time of the exhaust gas within the catalyst. The increased residence time would promote lighter conversion efficiencies, as reported by E. Zervas [138] that CO and HC conversion is greatly influenced from variations in space velocity. The author reported decrease in catalyst conversion efficiency with increasing space velocity due to the decrease of residence time thus the decrease of contact time of CO and HC with the oxidation catalyst.

Increasing the EGR rate by 10% had significant impact on the engine MAF value, with an average reduction of 15% compared to the baseline diesel fuel. As already stated, this drop in engine MAF with B50 fuel will have a direct impact on the catalyst conversion efficiency, due to increased exhaust gas residence time over the catalyst surface compared to baseline diesel fuel. Due to the issue of longer residence time this data can not be used to identify any variations in light-off temperatures between both fuels, and an alternative method of reducing emissions concentrations differences while maintaining the exhaust flow rate needed to be found.

Several other modifications to the engine calibration were trialled in order to bring the engine out emissions of B50 closer to the baseline diesel fuel. The closest match was

achieved when combining changes to both EGR rate and injection timing. The EGR rate was increased by 6% and the injection timing advanced by 2°CA, in order to increase the engine out emissions. Also, the engine speed was increased by approximately 50 RPM for B50 fuel to match the baseline diesel MAF value. The engine out CO, HC and NO_X emissions, after modifying the engine calibration during pedal ramps, are plotted in Figure 7.22, Figure 7.23, and Figure 7.24 respectively.

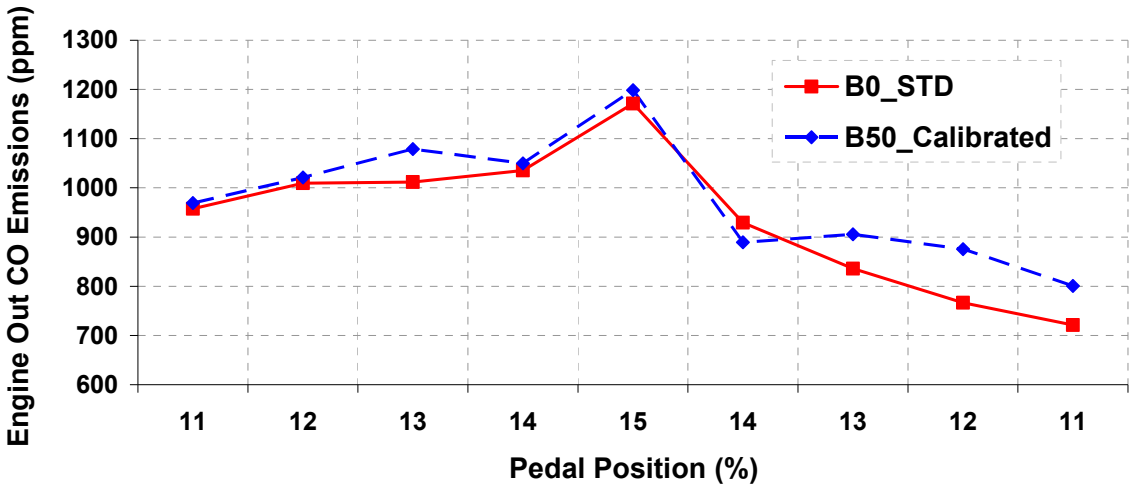

Figure 7.22, Engine out CO emissions during ramp tests using modified engine calibration

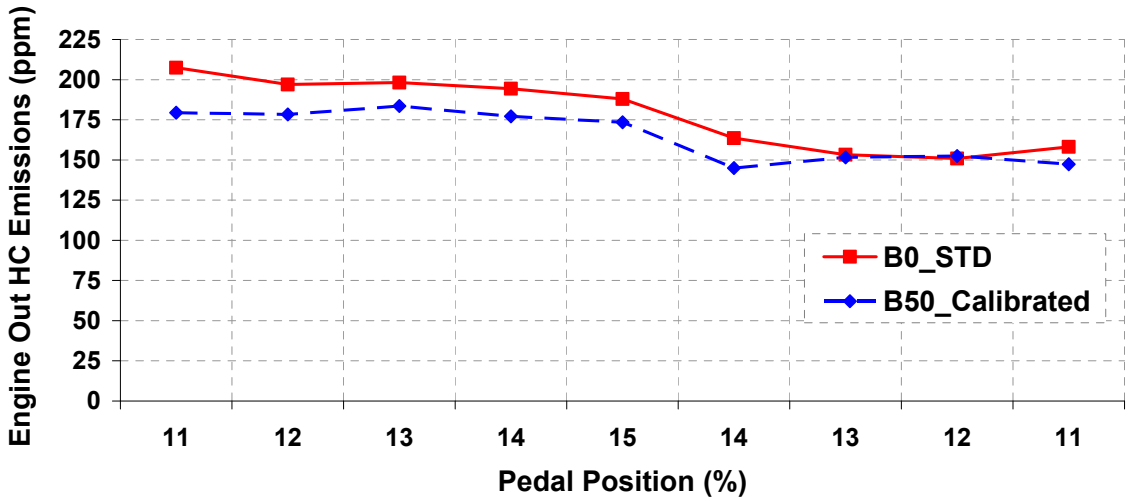

Figure 7.23, Engine out HC emissions during ramp tests using modified engine calibration

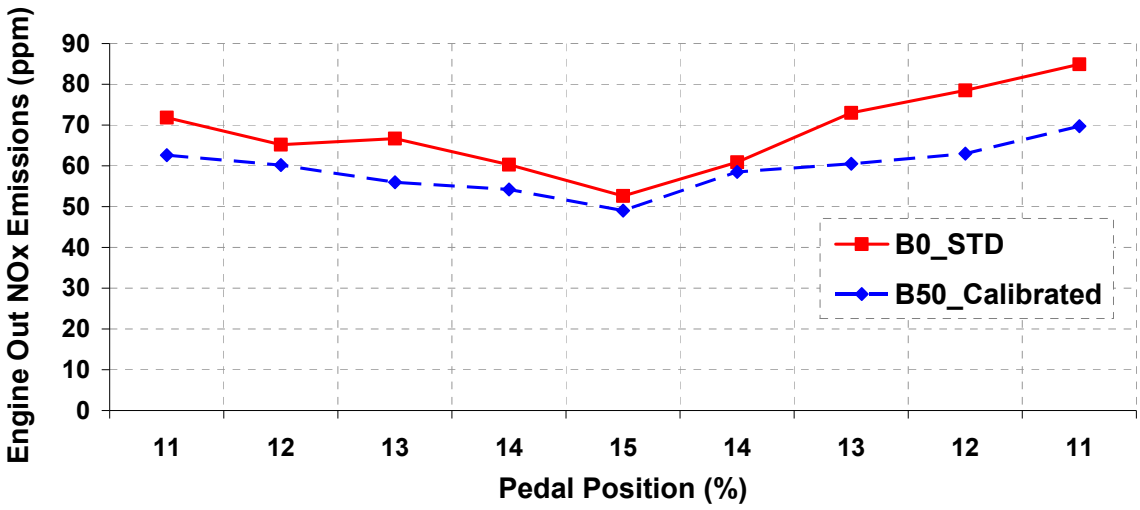

Figure 7.24, Engine out NO_X emissions during ramp tests using modified engine calibration

The B50 CO emissions during the ramp tests with modified engine calibration, closely matched with the baseline diesel fuel as shown in Figure 7.22 with an average difference of less than 5% especially during the ramping up process were the catalyst has not yet achieved light-off. Also, the HC emission trend from the modified calibration in Figure 7.23 shows reduced variation when compared to the standard calibration, with an average difference of less than 8%. This is the closest possible trend that could be achieved during this operating procedure. Despite closer agreement of CO and HC emissions, the NO_X emissions were adversely impacted with lower values from B50 compared to baseline. This is most likely due to increasing the EGR rate by 6% to achieve higher CO and HC emissions. This variation in NO_X emissions, with B50 should not have large impact on the catalyst light-ff curve of CO and HC emissions since NO_X conversion in the DOC is a passive secondary reaction. The MAF value with B50 fuel was also closely matched to the baseline diesel fuel with the modified calibration to ensure similar gas residence time over catalyst surface with both fuels.

The new modified CO catalyst light-off curve for both fuels is plotted in Figure 7.25. With the modified calibration, the light-off temperature for CO with B50 fuel has increased from 187°C to 193°C, which is only one degree hotter than the light-off temperature of the baseline diesel fuel. Also, the CO light-down temperature occurred

earlier with the modified calibration at 162°C which is also a higher temperature than for the baseline diesel fuel.

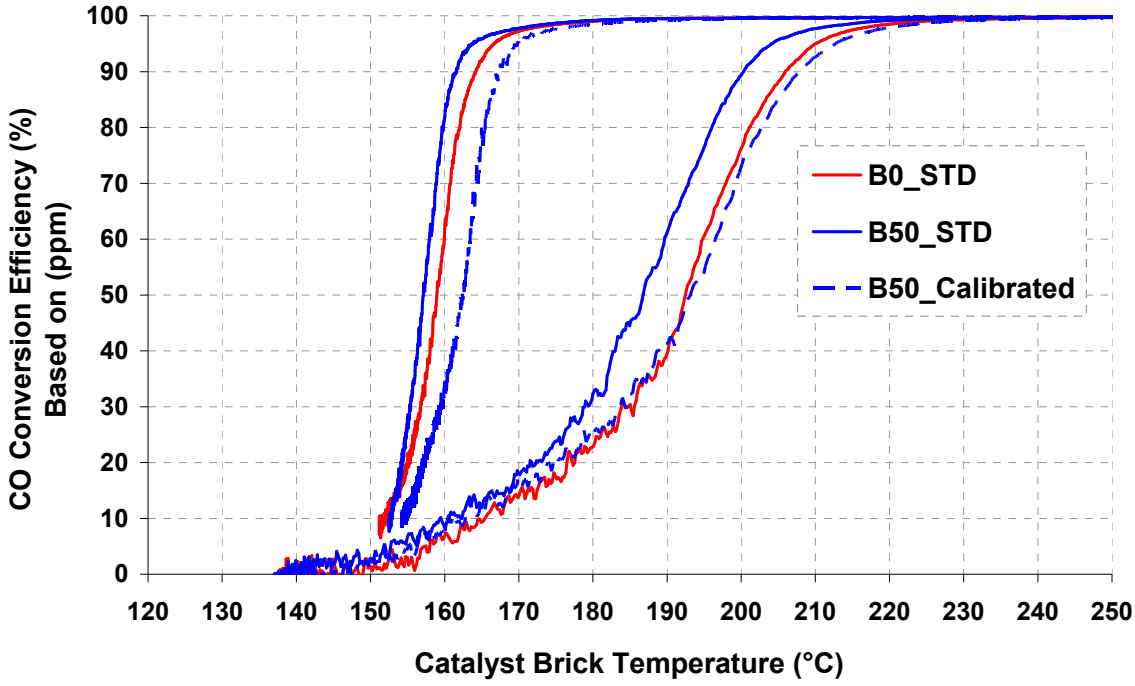

Figure 7.25, Light-off curve for CO emissions for baseline diesel and B50, and with modified calibration

The hesteresis effect observed between the light-off and light-down curves is largely attributed to CO self-inhibition as reported by Arnby *et* al. [146], and was experimentally demonstrated by Ye [145]. The catalyst inlet gas temperature is relatively low during engine ramp-up which leads to CO self-inhibition on the catalyst surface and reduced vacant active sites until light-off occurs. Once the catalyst has lit-off, the heat released from the oxidation reaction increases the CO desorption rates and counteracts the CO self-inhibition process [146 and 147]. However, during engine ramp-down the cartalyst brick temperature is higher, leading to far reduced CO self-inhibition rates leading to lower catalyst light-down temperatures.

Similarly, the HC light-off temperature with B50 increased from 192°C to 202°C when the engine calibration was modified, which is two degree hotter than the light-off temperature of baseline diesel fuel as shown in Figure 7.26.

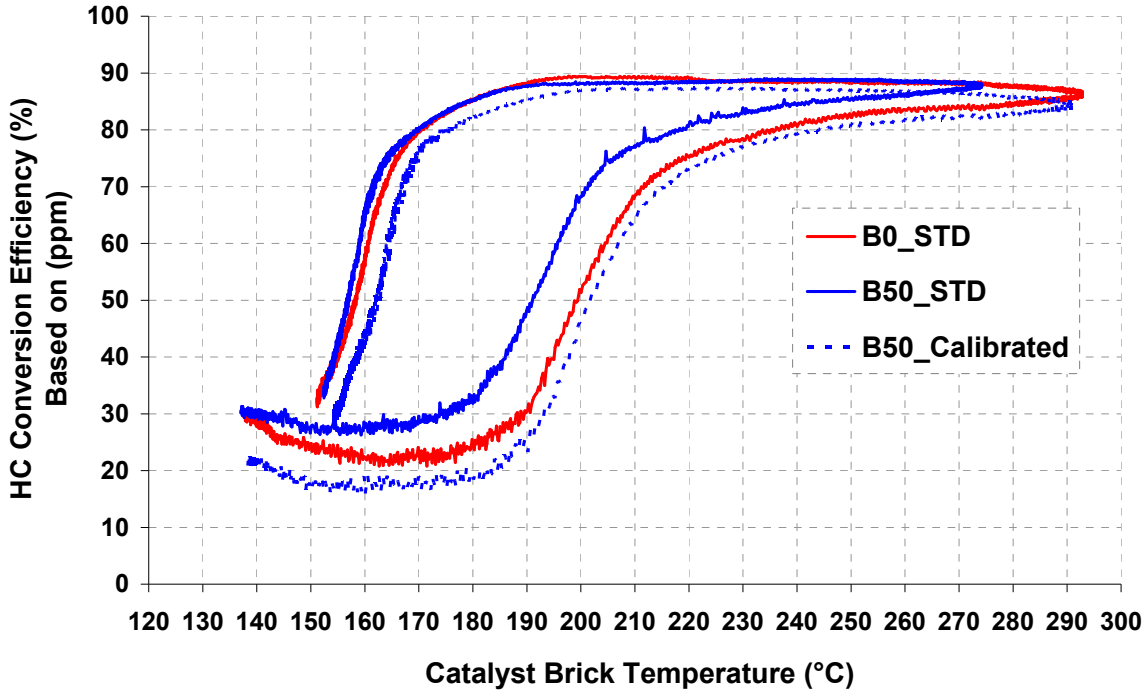

Figure 7.26, Light-off curve for HC emissions for baseline diesel and B50, and with modified calibration

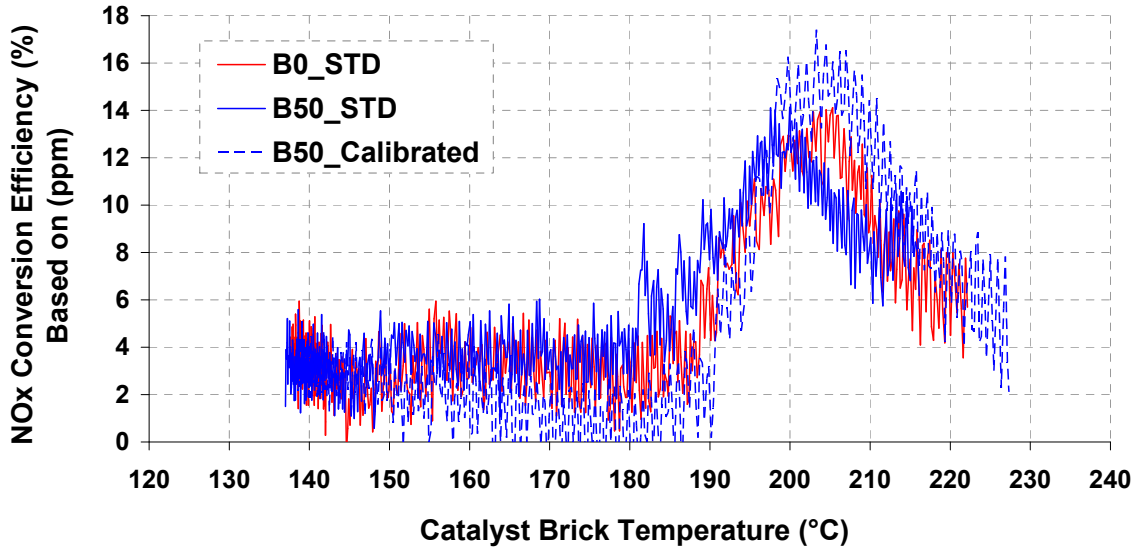

Figure 7.27, Light-off curve for NO_X emissions for baseline diesel and B50, and with modified calibration

The NO_X conversion efficiency is also affected with the modified engine calibration, as shown in Figure 7.27. At lower brick temperatures, the average NO_X conversion dropped

to approximately 2% with the modified engine calibration compared to standard conditions. However, the peak conversion temperature is similar to baseline diesel but with higher peak conversion efficiency close to 17%, which is probably caused by the reduction in NO_X emissions manifesting from the calibration changes.

The repeatability of this experimental procedure, with modified engine calibration, showed slight variations in the light-off curves and temperatures for all exhaust gas emissions. The light-off temperature value range was +/- 3°C to the values shown in Figure 7.25 and Figure 7.26, which puts it either before or after the light-off temperature of the baseline diesel fuel. This indicates that the light-off temperatures for both fuels are within the range of experimental error and therefore, there is no statistically significant variation in light-off temperature between B50 and the baseline diesel fuel. This would imply that gas speciation does not significantly impact on catalyst performance, and instead, that exhaust gas temperature, is the more significant factor.

7.10 Conclusions

The aim of this work was to investigate the impact of using biodiesel on the performance of a diesel oxidation catalyst, and to determine if differences were due to temperature or chemical effects. The following conclusions can be drawn from this work:

- Earlier results obtained during the vehicle trial (chapter 3) were confirmed on the engine test bed, with differences in catalyst performance over the NEDC measured when using biodiesel blends.
- It was shown that the engine out exhaust gas temperature with baseline diesel fuel was consistently higher than those observed for biodiesel blends over the NEDC. The average NEDC catalyst brick temperature reduced by 2% and 3% for B25 and B50 fuel blends respectively.
- The use of biodiesel reduced the energy released during the exothermic reaction inside the DOC compared to the baseline diesel fuel, which lead to lower overall catalyst performance when using biodiesel fuel blends.

- Catalyst light-off curves showed very similar responses when the engine out emissions of CO and HCs were closely matched to the baseline diesel fuel. No statistically significant difference in the light-off temperatures for B50 biodiesel and baseline diesel were found suggesting that exhaust gas HC speciation (chemical impact) when using B50 fuel did not have a significant impact on catalyst performance.

The results suggest that exhaust gas temperature, and the energy released during the exothermic reactions within the catalyst, are the most significant cause of variations in catalyst performance when using biodiesel blends.

Chapter 8 Final Conclusions

8.1 Overall Conclusions

The aim of this work was to perform a comprehensive investigation on the use of biodiesel fuel in modern production diesel engines, and to asses its impact on emissions, performance and fuel consumption. The final conclusions are made in relation to the specific project objectives as outlined in chapter 1:

1. "*To conduct a review of published literature regarding biodiesel, in particular the environmental impact of using fatty acid methyl esters (FAME), variations in their feedstock and commercial production, and finally reviewing their physical and chemical properties and their impact on engine performance and emissions*."

A review of current literature was conducted and the following conclusions were drawn:

- The factors most affecting the physical and chemical properties of FAMEs are their carbon chain length and number of double bonds (un-saturation level).
- The cetane number, kinematic viscosity and crystallisation temperature of FAMEs increase as the chain length and saturation level increases in the fatty acid molecules, and its resistance to oxidation decreases with an increasing number of double bonds.
- FAMEs are compatible with most of the elastomers used in diesel engines and can improve fuel lubricity. Higher viscosity and surface tension of biodiesel fuels leads to poorer atomization of the fuel spray.
- The average fuel consumption increases with biodiesel use due to its lower calorific value compared to petroleum diesel fuel, and a reduction in engine out emissions of CO, HC and PM with biodiesel is reported by the majority of studies due to higher oxygen content which allows faster and more complete combustion of the fuel compared to petroleum diesel.

- An increase in NO_X emissions is reported with biodiesel use due to physical and chemical properties, such as cetane number and density. Studies suggest that increases in NO_X emissions could be linked to the molecular structure of the fatty acids with the level of un-saturation being most significant.
- Biodiesel fuel properties were found to have a significant effect on the combustion process especially in the case of pump-line-nozzle fuel injection systems, but the impact reduces significantly when common rail fuel injection systems are used.
- Simulation studies with biodiesel using CFD models reported contradictory results due to inability of the models to account for some biodiesel fuel properties. No literature could be found which examined the use of one-dimensional simulation packages to investigate the combustion of biodiesel fuels in compression ignition engines.
- Adjusting the EGR rate and injection timing can mitigate some of the negative effects of biodiesel use, such as an increase in NO_X emissions and fuel economy, by optimising the combustion process.
- Whilst there have been studies investigating the impact of biodiesel use on diesel particulate filters, no published work could be found examining the impact of biodiesel fuel on the performance of diesel oxidation catalysts (DOC).
- All literature reviewed, discussed studies which examined biodiesel performance at room temperature (20-25°C approx.). The author could find no studies examining the interaction between ambient operating temperature and engine performance and emissions when using biodiesel fuels.
- Many studies discuss the impact of injection timing and EGR rate on engine emissions when using biodiesel, however, no literature could be found which examined the impact of other calibration parameters, such as rail pressure and pilot injection timing, on engine performance and emissions with biodiesel fuels.

2. "*Undertake experimental vehicle work over a standard legislative drive cycle to assess the variations in performance and emissions when using several biodiesel blends at various ambient temperature conditions*."

An experimental programme was undertaken using a vehicle tested on the chassis dynamometer facility at the University of Bath. The following conclusions were drawn:

- Tailpipe CO NEDC emissions increased with increasing blend ratio at all ambient temperatures, increasing by 15% at -5°C and 30% at 25°C for B50. This increase in tailpipe emissions was observed despite measured reductions in the engine-out (pre-catalyst) levels and was shown to be due to a reduction in catalyst conversion efficiency when using biodiesel blends compared to baseline diesel fuel.
- No statistically significant changes in tailpipe THC emissions were observed, for all blend ratios and ambient temperatures, with variations falling within the 95% confidence interval for each blend ratio. However, the engine-out THC emissions reduced by up to 25% with increasing biodiesel blend compared to baseline diesel.
- The tailpipe NO_X emissions increased by 2% at -5°C and 4% at 25°C for a B50 blend compared to baseline diesel fuel. The engine out NO_X emissions showed very similar values and trends to the tailpipe results since very little NO_X conversion is expected by the oxidation catalyst.
- The tailpipe PM emissions reduced by 16.5% at 25°C with B50 blend and the smoke opacity reduced by 45% and 36% at 25°C and 10°C ambient temperatures respectively compared to baseline diesel fuel.
- The engine out exhaust gas temperature was found to be lower when the vehicle was running with biodiesel blends compared to baseline diesel fuel, demonstrating an inversely proportional relationship with the blend ratio. The average NEDC exhaust gas temperature for B50 reduced by approximately 4°C compared to baseline diesel fuel for tests run at 25°C ambient conditions.

- The fuel consumption increased as the percentage of biodiesel increased in the fuel. B5 and B10 blends showed very little increase compared to baseline diesel, however the percentage increase ranged from up to 3% for B20, 7% for B30 and from 9% for B50 blends.

- Increasing the blend ratio and ambient temperature decreased the test vehicle's maximum tractive force. This reduction was in the order of 5% for the B50 blend at low vehicle speeds and 6–10% at higher speeds compared to baseline diesel fuel.

3. "*To asses the ability of the engine simulation software Ricardo WAVE, to predict the impact of biodiesel fuel on the combustion process of diesel engines by investigating the sensitivity of the software to changes in important fuel properties*."

A sensitivity study using Ricardo WAVE found that:

- The lower heating value and hydrogen content were found to be the most influential fuel properties affecting the calculation of the droplet mean diameter within the WAVE simulation, and other properties, such as specific heat capacity, cetane number and surface tension had only very minor impacts.
- The current fuel evaporation model was not suitable for predicting the spray evaporation of fuels with specific ranges of physical properties such as biodiesel fuels. Also, the basic combustion models may be too simplistic to consider the fuel's physical properties in the calculation, and the more sophisticated diesel jet model was also limited to the effect of the fuel properties on the actual heat release.
- WAVE's basic combustion models were not suitable for accurately predicting the impact of the different physical and chemical properties of biodiesel.

4. "*Undertake experimental work on an engine test bed to analyse the differences in combustion and emission characteristics of certain biodiesel blend compared to baseline diesel fuel*."

An experimental study was conducted using a 2.0L Ford diesel engine mounted on a transient engine dynamometer and concluded that:

- The cylinder pressure and combustion profiles for biodiesel fuel are similar to that of the baseline diesel fuel when a similar torque is demanded from the engine. Earlier SOC of pilot fuel by up to 1.0° CA with B50 biodiesel compared to baseline diesel fuel was observed, but the SOC of the main charge did not show any significant variations. The percentage increase in fuel demand during the lower load conditions was up to 16%, and up to 8% at higher load conditions for B50 compared to baseline diesel fuel.

- The maximum cylinder pressure decreased slightly (1-2%) with biodiesel when the engine was operated at pedal positions matched to those for diesel fuel. The use of biodiesel blends reduced the engine output power compared to baseline diesel fuel. Using B50 reduced the engine power by up to 14% and 8% during the lower and higher pedal positions respectively.
- The average engine out CO and HC emissions showed a general reduction as the percentage of biodiesel increased in the fuel at all engine operating conditions, and the NO_X emissions showed an increase as the blend ratio increases at all engine operating conditions examined.

5. "To a*ssess the sensitivity of a modern production diesel engine to calibration changes, when using a B25 blend compared to baseline diesel fuel*."

An experimental study into the effects of calibration changes was conducted using a 2.0L Ford diesel engine mounted on a transient engine dynamometer and concluded that:

- Increasing the EGR rate resulted in a higher percentage reduction in NO_X emissions and a reduced engine torque penalty with B25 compared to the baseline diesel fuel particularly at higher load conditions due to the higher oxygen content.
- Increasing rail pressure improved the engine out torque at all experimented conditions, in addition it caused an increase in CO and HC emissions at lower load conditions due to the possibility of cylinder wall wetting, and caused an increase in NO_X emissions at higher load conditions due to a possible improvement in the combustion process. However, these emissions changes were less pronounced when using B25 fuel.
- Retarding the main injection timing by 2° CA at the 1500 RPM and 17% pedal condition reduced the engine out emissions of CO and HC with both fuels. A further 10% reduction in NO_X emissions and 2% increase in engine torque were only observed for B25. Similarly, at 2250 RPM and 15% pedal, the percentage increase in NO_X emissions was 7% lower and the improvement in the engine output torque was 11% higher with B25. At this condition, similar percentage reductions in CO and HC emissions were observed with both fuels.

- Varying the pilot injection timing did not improve the engine performance or emissions under most operating conditions, and both baseline diesel and B25 fuels showed similar sensitivity to this factor.

6. "*Investigate the impact of different blends of RME biodiesel on the performance of a diesel oxidation catalyst, and assess its thermal and chemical effects*."

An experimental study into the effects of biodiesel on diesel oxidation catalyst performance was conducted using a 2.0L Ford diesel engine mounted on a transient engine dynamometer and concluded that:

- The engine out exhaust gas temperatures when running with baseline diesel fuel were always higher than for biodiesel blends with the average NEDC catalyst brick temperatures reduced by 2% and 3% for B25 and B50 blends respectively.
- This reduction in energy in the exhaust gas with increasing blend ratio resulted in a delay in the catalyst light-off time, or longer periods of lower conversion efficiency. The use of biodiesel reduced the exothermic reaction intensity inside the oxidation catalyst compared to the baseline diesel fuel which resulted in lower overall catalyst performance.
- At matched engine pedal positions, higher catalyst conversion efficiency was obtained with biodiesel blends compared to baseline diesel fuel due to a significant reduction in engine out emission concentrations of CO and HC. As the catalyst was exposed to lower concentrations of emissions with fixed catalyst surface capacity and gas residence time, percentage conversion appears to increase despite lower masses of emissions being oxidised.
- The catalyst light-off curve showed a slightly earlier rise when the engine was fuelled with baseline diesel fuel and engine out emissions of CO and HCs were closely matched. However, the light-off temperatures for biodiesel blends and baseline diesel were within the range of experimental error and no solid evidence of HC speciation effects (chemical impact) of B50 fuel could be found from the results obtained in this work.

8.2 Recommendations for Future Work

- Results from vehicle full load testing in chapter 3 reported that, other than the LHV of biodiesel, the performance of the VGT and the variations in MAF also affected the overall performance of the vehicle as the ambient temperature varied. Additional investigations could reduce the impact of these two factors.
- Findings from chapter 6 can be used by engine optimization engineers to determine the optimal engine calibration for biodiesel fuel in order to achieve improved engine performance and a reduction in exhaust emissions.
- Improving the experimental procedure for the determination of oxidation catalyst performance by matching the exhaust gas emissions concentrations between different fuels more closely, while maintaining a consistent exhaust flow rate could produce more accurate light-off curves to determine HC speciation effects when using biodiesel fuels.
- Investigate methods to sense the presence of biodiesel blend ratio in the fuel which will allow the engine ECU to optimize its calibration for better performance and emissions.

Chapter 9 References

1. Environmental Protection Agency (EPA), 2002. A Comprehensive Analysis of Biodiesel Impacts on Exhaust Emissions, Draft Technical Report: EPA.
2. Stone, R., 1999. Introduction to Internal Combustion Engine. 3rd edition. Palgrave: Macmillan Press Ltd.
3. Emission Standards, European Union. Cars and light trucks [online]. Available from: http://www.dieselnet.com/standards/eu/ld.php [Accessed 2008].
4. Lapuerta, M., Armas, O. and Rodriguez-Fernandez, J. Effect of biodiesel fuels on diesel emissions. Progress in Energy and Combustion Science, 34 (2008) 198–223.
5. Agarwal, A. K., 2007. Biofuels (alcohols and biodiesel) applications as fuels for internal combustion engines. Progress in Energy and Combustion Science, 33 (2007) 233-271.
6. Nabi, M. N., Rahman, M.M., Akhter, M. S., 2009. Biodiesel from cotton seed oil and its effect on engine performance and exhaust emissions. Applied Thermal Engineering. 29 (11-12): 2265-2270.
7. Knothe, G., Gerpen, J. and Krahl, J., 2005. The biodiesel Handbook, AOCS Press.
8. Alam, M., Song, J., Zello, V. and Boehman, A., 2006. Spray and combustion visualization of a direct-injection diesel engine operated with oxygenated fuel blends. IMechE, Int. J. Engines Res. Vol. 7.
9. Altiparmak, D., Keskin, A., Koca, A. and Guru, M. Alternative fuel properties of Tall oil fatty acid methyl ester-diesel fuel blends. Bioresource Technology 98 (2007) 241-246.
10. Chuk, C., 2007. From Cultivation to Combustion-A scientific Review of Biodiesel. University of Bath.
11. The official Site of The National Biodiesel Board, Environmental Sustainability [online]. Available from: http://www.biodiesel.org/resources/sustainability/default.shtm. [Accessed 2008].
12. Cheng, V. M., Wessol, A. A., Baudouin, P., BenKinney, M. T. and Navick, N. J. Biodegradable and nontoxic hydraulic oils, *SAE Paper*, 1991, No. 910964.
13. Ma, F. and Hanna, M. A., 1999. Biodiesel production-a review. Bioresource Technology (70) 1-15.

14. Holmberg, K. and Osterberg, E., 1989. Process for the transesterification of triglycerides in an aqueous micro emulsion reaction medium in the presence of lipase enzyme. US patent: No. 4839287, 1989.
15. Strong, C., Erickson, C. and Shukla, D., 2004. Evaluation of Biodiesel Fuel-Literature Review. Western Transportation Institute College of Engineering Montana State University, January 2004.
16. Sanjeev, M., Suhas, K., Winfried, D., Stefan, K. On Road Testing of Advanced Common Rail Diesel Vehicles with Biodiesel from the Jatropha Curcas plant, *SAE Paper,* 2005, No. 2005-26-356.
17. Schonborn, A., Ladommatos, N., Allan, R., Williams, J. and Rogerson, J. Effect of the Molecular Structure of Individual Fatty Acid Alcohol Esters (Biodiesel) on the Formation of NO_X and Particulate Matter in the Diesel Combustion Process, *SAE paper*, 2008, No. 2008-01-1578.
18. U.S. Department of Energy, 2006. Biodiesel Handling and Use Guidelines, 3rd Edition, September 2006.
19. Knothe, G. The Lubricity of Biodiesel, *SAE Paper*, 2005, No. 2005-01-3672.
20. Knothe, G., 2005. Dependence of biodiesel fuel properties on the structure of fatty acid alkyl esters. Fuel Processing Technology 86 (2005) 1059-1070.
21. Gopinath, A., Puhan, S. and Nagarajan, G., 2009. Relating the cetane number of biodiesel fuels to their fatty acid composition: a critical study, Proc. IMechE J. of Automotive Engineering Vol. 223 Part D.
22. Knothe, G. and Ryan, T., 2003. Cetane numbers of branched and straight chain fatty esters determined in an ignition quality tester. Fuel 82 (2003) 971-975.
23. Sinha, S. and Agarwal, A. K., 2007. Experimental investigation of the combustion characteristic of a biodiesel (rice-bran oil methyl ester) fuelled direct injection transportation diesel engine. Proceedings IMechE J. of Automobile Engineering Vol. 221 part D.
24. Lapuerta, M., Armas, O. and Fernandez, J. R. Effect of the Degree of Unsaturation of Biodiesel Fuels on NO_X and Particulate Emissions, *SAE paper*, 2008, No. 2008-01-1676.
25. Chiu, C., Schumacher, L. G. and Suppes, G. J., 2004. Impact of cold flow improvers on soybean biodiesel blend. Biomass and Bioenergy 27(5): 485-491.
26. Copeland, K., Hardy, R., Jeff, J., Selvidge, C. and Walztoni, K., 2006. Blending biodiesel with diesel fuel in cold locations. U.S. Patent: No. 0037237, 2006.

27. Kivevele, T., Agarwal, A. K., Gupta, T. and Mbarawa, M. Oxidation Stability of Biodiesel Produced from Non-Edible Oils of African Origin, *SAE paper*, 2011, No. 2011-01-1202.
28. Karavalakis, G., Karonis, D. and Stournas, S. Evaluation of the Oxidation Stability of Diesel /Biodiesel Blends using the Modified Rancimat Method, *SAE paper*, 2009, No. 2009-01-1828.
29. Lin, C. Y. and Chiu, C. C., 2009. Effects of Oxidation during Long-term Storage on the Fuel Properties of Palm Oil-based Biodiesel. Energy & Fuels 23 (2009) 3285-3289.
30. Bannister, C. D., Chuck, C. J., Bounds, M. and Hawley, J. G., 2010. Oxidative stability of biodiesel fuel. IMechE J. of Automobile Engineering Vol. 225.
31. Benvenutti, L. H., Miyamoto, R. N. Effects of the Use of B5 Blends (5 % biodiesel) over the Engine Oil of Light Pickups in Fleet Test, *SAE paper*, 2008, No. 2008-36-0294.
32. Paligova, J., Jorikova, L. and Cvengros, J., 2008. Study of FAME Stability. Energy & Fuels 22 (2008) 1991-1996.
33. McCormick, R. L., Ratcliff, M., Moens, L. and Lawrence, R., 2007. Several factors affecting the stability of biodiesel in standard accelerated tests. Fuel Processing Technology 88 (2007) 651-657.
34. Jaroonjitsathian, S., Akarapanjavit, N., Sa-norh, S. S., In-ochanon, R., Wuttimongkolchai, A. and Tipdecho, C. Evaluation of 5 to 20% Biodiesel Blend on Heavy-duty Common-rail Diesel Engine, *SAE paper*, 2009, No. 2009-01-1894.
35. Devlin, C., Passut, C., Campbell, R. and Jao, T. Biodiesel Fuel Effect on Diesel Engine Lubrication, *SAE paper*, 2008, No. 2008-01-2375.
36. Miyashita, K., Takagi, T., 1986. Study on the oxidative rate and prooxidant activity of free fatty acids. Journal of the American Oil Chemists Society 63 (10): 1380-1384.
37. Knothe, G., 2002. Structure Indices in FA Chemistry. Journal of the American Oil Chemists Society 79 (9) 847.
38. Conceicao, M. M., Fernandes, V. J., Araujo, A. S., Farias, M. F., Santos, I. M. and Souza, A. G., 2007. Thermal and Oxidative Degradation of Castor Oil Biodiesel. Energy & Fuels 21 (2007) 1522-1527.
39. Jain, S. and Sharma, M. P., 2010. Prospects of biodiesel from Jatropha in India: A review. Renewable and Sustainable Energy Reviews. 14 (2): 763-771.

40. Ogawa, T., Kajiya, S., Kosaka, S., Tajima, I. and Yamamoto, M. Analysis of oxidative deterioration of biodiesel fuel, *SAE paper*, 2008, No. 2008-01-2502.
41. Demirbas, A., 2008. Biodiesel: a realistic fuel alternative for diesel engines. London. Springer.
42. Dinkov, R., Hristov, G., Stratiev, D. and Aldayri, V. B., 2009. Effect of commercially available antioxidants over biodiesel/diesel blends stability. Fuel 88 (2009) 732–737.
43. Dodos, G. S., Zannikos, F. and Stournas, S. Effect of metals in the oxidation stability and lubricity of biodiesel fuel, *SAE paper*, 2009, No. 2009-01-1829.
44. Paligova, J., Jorikova, L. and Cvengros, J., 2008. Study of FAME Stability. Energy & Fuels 22 (2008) 1991-1996.
45. Lamprecht, D. Elastomer Compatibility of Blends of Biodiesel and Fischer-Tropsch Diesel, *SAE paper*, 2007, No. 2007-01-0029.
46. Bessee, G. B. and Fey, J. P. Compatibility of Elastomers and Metals in Biodiesel Fuel Blends, *SAE paper*, 1997, No. 971690.
47. National Biodiesel Board, Materials Compatibility [online]. Available from: http://www.biodiesel.org. [Accessed 2009].
48. Nakai, T. and Ogishi, H. Verification of Influences of Biodiesel Fuel on Automotive Fuel-line Rubber and Plastic Materials, *SAE paper*, 2010, No. 2010-01-0915.
49. Terry, B., 2005. Impact of Biodiesel on Fuel System Component Durability. Technical Report, Octel Company limited.
50. Joint FIE Manufacturers Statement. Fuel Requirements for Diesel Fuel Injection Systems [online]. Available from: http://www.globaldenso.com/en/topics/files/common_position_paper.pdf. [Accessed 2009].
51. Mitchell, K. Diesel fuel lubricity – base fuel effects, *SAE paper*, 2001, No. 2001-01-1928.
52. Andreae, M., Fang, H. and Bhandary, K. Biodiesel and Fuel Dilution of Engine Oil, *SAE paper*, 2007, No. 2007-01-4036.
53. Fang, H., Alleman, T. and McCormick, R. Quantification of Biodiesel Content in Fuels and Lubricants by FTIR and NMR Spectroscopy, *SAE paper*, 2006, No. 2006-01-3301.

54. Devlin, C., Passut, C., Campbell, R. and Jao, T. Biodiesel Fuel Effect on Diesel Engine Lubrication, *SAE paper*, 2008, No. 2008-01-2375.
55. Thornton, M., Alleman. T., Luecke, J. and McCormick, R. Impacts of Biodiesel Fuel Blends Oil Dilution on Light-Duty Diesel Engine Operation, *SAE paper*, 2009, No. 2009-01-1790.
56. Peterson, A., Lee, P. and Lai, M. Impact of Biodiesel Emissions Products from a Multi-cylinder Direct Injection Diesel Engine on Particulate Filter Performance, *SAE paper*, 2009, No. 2009-01-1184.
57. Parsons, G., 2007. Impact of Biodiesel Use on the Lubrication of Diesel Engines. The 13th annual Fuels and Lubes Asia Conference, Bangkok.
58. Fang, H., Whitacre, S., Yamaguch, E. and Boons, M. Biodiesel Impact on Wear Protection of Engine Oils, *SAE paper*, 2007, No. 2007-01-4141.
59. Massa, C. and Benvenutti, L. H. Fleet Test Evaluation of B5 Blends (5% Biodiesel) in Pickups, *SAE paper*, 2008, No. 2008-36-0293.
60. Tatur, M., Nanjundaswamy, H., Tomazic, D., Thornton, M. and McCormick, R. L. Biodiesel Effects on U.S. Light-Duty Tier 2 Engine and Emission Control Systems – Part 2, *SAE paper*, 2009, No. 2009-01-0281.
61. Agarwal, A. K., Bijwe, J. and Das, L. M., 2003. Effect of Biodiesel Utilization of Wear of Vital Parts in Compression Ignition Engine. ASME, Vol. 125 pp 604-611.
62. Ra, Y., Reitz, R. D., McFarlane, J. and Daw, C. S. Effects of Fuel Physical Properties on Diesel Engine Combustion using Diesel and Bio-diesel Fuels, *SAE paper*, 2008, No. 2008-01-1379.
63. Bittle, J. A., Knight, B. M. and Jacobs, T. J. The Impact of Biodiesel on Injection Timing and Pulsewidth in a Common-Rail Medium-Duty Diesel Engine, *SAE paper*, 2009, No. 2009-01-2782.
64. Zhang Y. and Boehman, A., 2007. Impact of Biodiesel on NO_X Emissions in a Common Rail Direct Injection Diesel Engine. Energy & Fuels 21 (2007) 2003-2012.
65. Ertunc, M. T., 2003. Investigation of Oxides of Nitrogen Emissions from biodiesel Fuelled Engines. PhD dissertation, Iowa state University, Ames.
66. Boehman, A., Morris, D., Szybist, J. and Esen, E., 2004. The Impact of the Bulk Modulus of Diesel Fuels on Fuel Injection Timing. Energy & Fuels 18 (2004) 1877-1882.

67. Szybist, J. P. and Boehman, A. L. Behaviour of Diesel Injection System with Biodiesel Fuel, *SAE paper*, 2003, No. 2003-01-1039.
68. Grimaldi, C. and Postrioti, L. Experimental Comparison Between Conventional and Bio-derived Fuel Sprays from a Common Rail Injection System, *SAE paper*, 2000, No. 2000-01-1252.
69. Tatur, M., Nanjundaswamy, H., Tomazic, D. and Thornton, M. Effects of Biodiesel Operation on Light-Duty Tier 2 Engine and Emission Control Systems, *SAE paper*, 2008, No. 2008-01-0080.
70. Kawano, D., Ishii, H., Goto, Y., Noda, A. and Aoyagi, Y. Optimization of Engine System for Application of Biodiesel Fuel, *SAE paper*, 2007, No. 2007-01-2028.
71. Williams, A., McCormick, R. L., Hayes, R. R., Ireland, J. and Fang, H. L. Effect of Biodiesel Blends on Diesel Particulate Filter Performance, *SAE paper*, 2006, No. 2006-01-3280.
72. Fukuda, K., Kohakura, M., Kaneko, T., Furui, K., Tsuchihashi, K., Hasegawa, T., Saitou, K., Baba, H., Shibuya, M., Nakamura, O., Okada, M., Hosono, K., Hirata, K., Kawatani, T. and Sugiyama, G. Impact Study of High Biodiesel Blends on Performance of Exhaust Aftertreatment Systems, *SAE paper*, 2008, No. 2008-01-2494.
73. Boehman, A., Song, J. and Alam, M., 2005. Impact of Biodiesel Blending on Diesel Soot and the Regeneration of Particulate Filters. Energy & Fuels 19 (2005) 1857-1864.
74. Sharp, C. A., Howell, S. A. and Jobe, J. The Effect of Biodiesel Fuels on Transient Emissions from Modern Diesel Engines, Part 1 Regulated Emissions and Performance, *SAE paper*, 2000, No. 2000-01-1967.
75. Pepiot-Desjardins, P., Pitscha, H., Malhotra, R., Kirbyc, S. R. and Boehman, A. L., 2008. Structural group analysis for soot reduction tendency of oxygenated fuels. Combustion and Flame 154 (2008) 191–205.
76. Szybist, J. P., Song, J., Alam, M. and Boehman, A. L., 2007. Biodiesel combustion, emissions and emission control. Fuel Processing Technology 88 (2007) 679-691.
77. Cheng, W. L., Lee, C. F. and Ruan, D. F. Comparisons of Combustion Characteristics of Biodiesels in a High Speed Direct Injection Diesel Engine, *SAE paper*, 2008, No. 2008-01-1638.

78. Choi, C. Y., Bower, G. R. and Reitz, R. D. Effect of Biodiesel Blended Fuels and Multiple Injections on D.I. Diesel Engines, *SAE paper*, 1997, No. 970218.
79. Cheng1, A. S., Upatnieks, A. and Mueller, C. J., 2005. Investigation of the impact of biodiesel fuelling on NOx emissions using an optical direct injection diesel engine. IMechE, Int. J. of Engine Research Vol.7.
80. Graboski, M. S., McCormick, R. L., Alleman, T. L. and Herring, A. M., 2003. The Effect of Biodiesel Composition on Engine Emissions from DDC Series 60 Diesel Engine. Final Report.
81. Knothe, G., Sharp, C. A. and Ryan, T. W., 2006. Exhaust Emissions of Biodiesel, Petrodiesel, Neat Methyl Esters, and Alkanes in New Technology Engine. Energy & Fuels 20 (2006) 403-408.
82. McCormick, R. L., Tennant, C. J., Hayes, R. R., Black, S., Ireland, J., McDaniel, T., Williams, A. and Frailey, M. Regulated Emissions from Biodiesel Tested in Heavy-Duty Engines Meeting 2004 Emission Standards, *SAE Paper*, 2005, No. 2005-01-2200.
83. Camden Council, 2004. Camden Council Biodiesel Trial, third and final Progress Report. June 2004.
84. Newcastle City Council, 2004. Newcastle City Council Biodiesel Trial, Emission Testing Program. Final Report December 2004.
85. Karavalakis, G., Bakeas, E. and Stournas, S. An Experimental Study on Impact of Biodiesel Origin and Type on the Exhaust Emissions from a Euro 4 Pick-up Truck, *SAE Paper*, 2010, No. 2010-01-2273.
86. Karavalakis, G., Tzirakis, E., Zannikos, F., Stournas, S., Bakeas, E., Arapaki, N. and Spanos, A. Diesel/Soy Methyl Ester Blends Emissions Profile from a Passenger Vehicle Operated on the European and the Athens Driving Cycle, *SAE Paper*, 2007, No. 2007-01-4043.
87. McGill, R., Storey, J., Wagner, R., Irick, D., Aakko, P., Westerholm, M., Olof-Nylund, N. and Lappi, M. Emission Performance of Selected Biodiesel Fuels, *SAE Paper*, 2003, No. 2003-01-1866.
88. Yoshida, K., Taniguchi, S., Kitano, K., Tsukasaki, Y., Hasegawa, R. and Sakata, I. Effects of RME30 on Exhaust Emissions and Combustion in a Diesel Engine, *SAE paper*, 2008, No. 2008-01-2499.

89. Georgios, F., Zissis, S. and Georgios, M. Experimental Evaluation of Cottonseed Oil Diesel Blends as Automotive Fuels via Vehicle and Engine Measurements, *SAE Paper*, 2007, No. 2007-24-0126.
90. Arapaki, N., Bakeas, E., Karavalakis, G., Tzirakis, E., Stournas, S. and Zannikos, F. Regulated and Unregulated Emissions Characteristics of a Diesel Vehicle Operating with Diesel/Biodiesel Blends, *SAE Paper*, 2007, No. 2007-01-0071.
91. Tzirakis, E., Karavalakis, G., Zannikos, F. and Stournas, S. Impact of Diesel/Biodiesel Blends on Emissions from a Diesel Vehicle Operated in Real Driving Conditions, *SAE Paper*, 2007, No. 2007-01-0076.
92. Bielaczyc, P. and Szczotka, A. A Study of RME-Based Biodiesel Blend Influence on Performance, Reliability and Emissions from Modern Light-Duty Diesel Engines, *SAE Paper*, 2008, No. 2008-01-1398.
93. Lin, B. F., Huang, J. H. and Huang, D. Y., 2008. Effects of Biodiesel from Palm Kernel Oil on the Engine Performance, Exhaust Emissions, and Combustion Characteristics of a Direct Injection Diesel Engine. Energy & Fuels 22 (2008) pp 2796-2804.
94. Kawano, D., Ishii, H. and Goto, Y. Effect of Biodiesel Blending on Emission Characteristics of Modern Diesel Engine, *SAE paper*, 2008, No. 2008-01-2384.
95. Karra, P. K., Veltman, M. K. and Kong, S. C., 2008. Characteristics of Engine Emissions Using Biodiesel Blends in Low-Temperature Combustion Regimes. Energy & Fuels Vol.22.
96. Sharp, C., Howell, S. and Jobe, J. The Effect of Biodiesel Fuels on Transient Emissions from Modern Diesel Engines, Part II Unregulated Emissions and Chemical Characterization, *SAE paper*, 2000, No. 2000-01-1968.
97. Ballesteros, R., Hernandez, J. J., Lyons, L. L., Cabanas, B. and Taipa, A., 2008. Speciation of the semivolatile hydrocarbon engine emissions from sunflower biodiesel. Fuel 87 (2008) 1835-1843.
98. Mendera, K. Z., 2005. Burn Rate Profiles for Compression Ignition Engine Model. Journal of KONES Internal Combustion Engines, vol.12, 1-2.
99. Brakora, J. L., Ra, Y., Reitz, R. D., McFarlane, J. and Daw, C. S. Development and Validation of a Reduced Reaction Mechanism for Biodiesel Fuelled Engine Simulation, *SAE paper*, 2008, No. 2008-01-1378.

100. Szybist, J. P., Mcfarlane, J. and Bunting, B. G. Comparison of Simulated and Experimental Combustion of Biodiesel Blends in a Single Cylinder Diesel HCCI Engine, *SAE paper*, 2007, No. 2007-01-4010.

101. Ali, M. Y., Mehdi, S. N. and Reddy, P. R., 2008. Modelling and Simulation of Compression Ignition Engine Process with Bio-diesel. International journal of Engineering, Vol.88, pp 32-36.

102. Ireland, J., McCormick, R., Yanowitz, J. and Wright, S. Improving Biodiesel Emissions and Fuel Efficiency with Fuel-Specific Engine Calibration, *SAE paper*, 2009, No. 2009-01-0492.

103. Senatore, A., Cardone, M., Buono, M., Rocco, V., Allocca, L. and Vitolo, S. Performances and Emissions Optimization of a CR Diesel Engine Fuelled with Biodiesel, *SAE paper*, 2006, No. 2006-01-0235.

104. Lujan, J. M., Bermudez, V., Tormos, B. and Pla, B., 2009. Comparative analysis of a DI diesel engine fuelled with biodiesel blends during the European MVEG-A cycle: Performance and emissions (II). Biomass and Bioenergy 33 (2009) 948-956.

105. Yoon, S. H., Suh, H. K. and Lee, C. S., 2009. Effect of Spray and EGR Rate on the Combustion and Emission Characteristics of Biodiesel Fuel in a Compression Ignition Engine. Energy & Fuels 23 (2009) 1486-1493.

106. Zhang, X., Gao, G., Li, L., Wu, Z., Hu, Z. and Deng, J. Characteristics of Combustion and Emissions in a DI Engine Fueled with Biodiesel Blends from Soybean Oil, *SAE paper*, 2008, No. 2008-01-1832.

107. Hawley, J. G., Brace, C. J., Cox, A., Ketcher, D. and Stark, R. Influence of Time-Alignment on the Calculation of Mass Emissions on a Chassis Rolls Dynamometer, *SAE paper*, 2003, No. 2003-01-0395.

108. Bannister, C. B., Hawley, J. G., Brace, C. J, Cox, A., Ketcher, D. and Stark, R. Further Investigations on Time-Alignment, *SAE paper*, 2004, No. 2004-01-1441.

109. MODDE 7 design of experiments software package, help menu.

110. Eriksson, E., Johansson, E., Kettaneh-Wold, N., Wikstrom, C. and Wold, S. Design of Experiments principles and Applications. Umetrics Academy, training booklet.

111. Philips, P. R., Chandler, G. R., Jollie, D. M., Wilkins, A. J. and Twigg, M. V. Development of Advanced Diesel Oxidation Catalyst, *SAE paper*, 1999, No. 1999-01-3075.

112. Knafl, A., Busch, S. B., Han, M., Bohac, S. V., Assanis, D. N., Szymkowicz, P. G. and Blint, R. D. Characterising Light-Off Behaviour and Species-Resolved Conversion Efficiencies During In-Situ Diesel Oxidation Catalyst Degreening, *SAE paper*, 2006, No. 2006-01-0209.

113. Payri, F., Bermudez, V. R., Tormos, B. and Linares, W. G., 2009. Hydrocarbon emissions speciation in diesel and biodiesel exhausts. Atmospheric Environment 43 (2009) 1273-1279.

114. Adams, K. M., Cavataio, J. V., Sale, T., Rimkus, W. A. and Hammerle, R. H. Laboratory screening of diesel oxidation catalysts and validation with vehicle testing: the importance of hydrocarbon storage, *SAE paper*, 1996, No. 962049.

115. Bohac, S. V., Han, M., Jacobs. T. J., Lopez, A. J., Assanis, D. N. and Szymkowicz, P. G. Speciated Hydrocarbon Emissions from an Automotive Diesel Engine and DOC Utilizing Conventional and PCI Combustion, *SAE paper*, 2006, No. 2006-01-0201.

116. Ricardo Inc., 2009. WAVE 8.1 user's manual.

117. Wave Build V8.1 Help, 2009. Engine Formulation and Basic Elements.

118. Tate, R. E., Watts, K. C., Allen, C. A. and Wilkie, K. I., 2006. The densities of three biodiesel fuels at temperatures up to 300°C. Fuel 85 (2006) 1004-1009.

119. Goodrum, J. W., 1996. Biodiesel Bus Demonstration in Atlanta '96 Olympics: Thermal Techniques for Detecting Biodiesel Fuel Quality. University of Georgia, U.S.A published paper.

120. Acaroglu, M. and Demirbas, A., 2007. Relationships between Viscosity and Density Measurements of Biodiesel Fuels. Energy Source Part A, 29 (2007) 705-712.

121. Griend, V., Feldman, L. and Peterson, C. L., 1988. Properties of Rape Oil and its Methyl Ester Relevant to Combustion Modelling. American Society of Agricultural Engineers, presentation meeting 88-6507.

122. Varde, K. S., 1984. Bulk modulus of vegetable oil – diesel fuel blends. Fuel Vol. 63.

123. The Lee Company, Viscosity of various fluids [online]. Available from: http://www.microhydraulics.com. [Accessed 2008]

124. Swern, D., 1979. Bailey's Industrial Oil and Fat Products. New York: Wiley.

125. Golovitchev, V. I. and Yang, J., 2009. Construction of combustion models for rapeseed methyl ester bio-diesel fuel for internal combustion engine applications. Biotechnology Advances 27 (2009) 641-655.

126. Pogorevc, P., Kegl, B. and Skerget, L., 2008. Diesel and Biodiesel Fuel Spray Simulation. Energy & Fuels 22 (2008) 1266-1274.

127. Watson, N., Pilley, A. D. and Marzouk, M. A Combustion Correlation for Diesel Engine Simulation, *SAE paper*, 1980, No. 800029.

128. Wave knowledge centre V7.2, Engine Manual, Formulation and Basic Elements.

129. Hiroyasu, H., Masataka, A. and Michihiko, T. Empirical Equations for the Sauter Mean Diameter of a Diesel Spray, *SAE paper*, 1989, No. 890464.

130. Heywood, J. B., 1988. Internal Combustion Engine Fundamentals. New York: McGraw Hill Book Company.

131. Woschni, G. A universal applicable equation for the instantaneous heat transfer coefficient in the internal combustion engine, *SAE paper*, 1967, No. 670931.

132. Hawley, J. G., Brace, J. and Wallace, F. J., 1998. Handbook of Air Pollution from Internal Combustion Engines: Chapter 10 Combustion-Related Emissions in CI Engines. Academic Press Limited.

133. Philips, P. R., Chandler, G. R., Jollie, D. M., Wilkins, A. J. and Twigg, M. V. Development of Advanced Diesel Oxidation Catalysts, *SAE paper*, 1999, No. 1999-01-3075.

134. Held, W., Konig, A., Richter, T. and Puppe, L. Catalyst NO_X Reducing in Net Oxidizing Exhaust Gas, *SAE paper*, 1990, No. 900496.

135. Iwamoto, M. and amada, H., 1991. Removal of Nitrogen Monoxide from Exhaust Gases through Novel Catalytic Processes. Catalysis Today 10 (1991) 57.

136. Monroe, D. R., DiMaggio, C. L., Beck, D. and Matekunas, F. A. Evaluation of a Cu/Zeolite Catalyst to Remove NO_X from Lean Exhaust, *SAE paper*, 1993, No. 930737.

137. Eastwood, P., 2000. Critical Topics in Exhaust Gas Aftertreatment, Baldock, UK: Research Studies Press Ltd.

138. Zervas, E., 2008. Parametric Study of the Main Parameters Influencing the Catalyst Efficiency of A Diesel Oxidation Catalyst: Parameters Influencing The Efficiency of A Diesel Catalyst. Int. Journal of Automotive Technology Vol. 9 No. 6, pp.641-647.

139. Feldman, B., 2004. *Diesel Engine Modelling in WAVE.* Thesis (Bachelor of Science). The Pennsylvania State University, USA.

140. O'Sullivan, M., 2009. *Investigating the Usage of Biodiesel and Diesel-Biodiesel Blends in Ricardo WAVE.* Thesis (MSc). University of Bath, UK.

141. Piddock, M., 2010. *Engine Optimization for Downsizing by Experiment and by Simulation.* Thesis (PhD). University of Bath, UK.

142. Kerschbaum, S. and Rinke. G., 2004. Measurement of the temperature dependent viscosity of biodiesel fuels. Fuel 83 (2004) 287-291.

143. Chakravarthy, K., McFarlane, J., Daw, S., Ra, Y., Reitz, R. and Griffin, J. Physical properties of bio-diesel and implications for use of bio-diesel in diesel engines. *SAE paper*, 2007, No. 2007-01-4030.

144. Rochaya, D., 2007. Numerical simulation of spray combustion using bio-mass derived liquid fuels. 2007.

145. Ye, Shifei, 2010. *Oxidation Catalyst Studies on a Diesel Engine*. Thesis (PhD). University of Bath, UK.

146. Amby, K., Torncrona, A., Anderson, B. and Skoglundha, M., 2004. Investigation of Pt/γ – Al_2O_3 Catalyst with locally High Pt Concentrations for Oxidation of CO at Low Temperature. Journal of Catalysis, 221, 252-261.

147. Carlsson, P., Skoglundha, M., Thorma, P. and Anderson, B., 2004. Low-temperature CO Oxidation over a Pt/AL_2O_3 Monolith Catalyst Investigated by Step-response Experiments and Simukations. Topics in Catalysis, 30/31, 375-381.

Chapter 10 Appendices

Appendix A: Baseline Diesel Fuel Specification

FUEL SPECIFICATION					
Batch No :	REFERENCE / LINE FUEL - DK 2567				TANK 19 & 27
Fuel Type :	DIESEL				
Supplier:	SHELL				
Specification :	XE-M4CX725-A				
Fuel Certified Date	20-Jun-07				
PROPERTY	**UNIT**	**MIN**	**RESULTS**	**MAX**	**ASTM method**
Cetane Number		52	**52.8**	54	IP41, ISO 5165
Cetane Index		50			IP380
Distillation					IP 123
Initial Boiling Point			**165**		
50 % Evaporate	° C	245	**270**	280	IP123
95 % Evaporate	° C	345	**349**	350	IP123
Final Boiling Point	° C		**359**	370	IP123
Oxidation Stability	mg/100ml			2.5	IP40 ISO 7536
Recovery	% Vol				
Residue	% Vol		**1**		
Calorific Value - Gross	MJ/kg		**45.52**		BS2869
Calorific Value - Gross	BTU/lb		**19570**		BS2869
Calorific Value - Nett	MJ/kg		**42.59**		BS2869
Calorific Value - Nett	BTU/lb		**18310**		BS2869
Viscosity, Kinematic @ 40° C	mm^2/s	2.5	**2.748**	3.5	IP 71
Flash Point	° C	55			IP 34
Copper corrosion			**1A**	1	IP 154
Sulphur Content (UVF)	ppm		**7**		D5453
Lubricity			**234**	400	IP450
Neut No. (Strong acid)	mgKOH/g		**<0.01**	0.2	IP177
Carbon Residue - Conradson	% Wt			0.2	IP398
Ash	% Wt			0.01	IP 4
Cloud Point	° C		**-11**		IP 219
Cold Filter Plugging Point	° C		**-18**	-15	IP 309
Carbon content	% mass		**86.5**		
Hydrogen content			**13.46**		
H/C Ratio			**1.854**		
Oxygen	% mass				
Water Content	mg/Kg		**68**	100	ASTM D1744
Total Contamination	mg/kg				IP440
Aromatics	% v/v		**20**		IP156 ISO 3937
PCA Hydrocarbons	% mass	3		6	IP391
Density @ 15 °C	kg/l	0.833	**0.833**	0.837	ASTM D1298

Appendix B: RME Biodiesel Fuel Specification

Interim Laboratory Test Report No.		**08-000369-0-WTHU**	
BP Coryton Technical Centre			
Test		**Method**	**001-00**
Net calorific value	Mj/kg	D240	39.99
Density at 15 oC	kg/m3	ISO 12185	883.2
Kinematic Viscosity at 40 oC	mm2/s	EN ISO 3104	4.564
Flash Point	°C	EN ISO 3679*	182.0
Sulphur Content	mg/kg	EN ISO 20846*	1.8
Microcarbon Residue 10% (ASTM D1160)	% (m/m)	EN ISO 10370	0.17
Cetane Number		EN ISO 5165	49.5
Water	mg/kg	EN ISO 12937	210
Total Contamination	mg/kg	EN 12662*	6
Copper Corrosion 3 hrs.at 50 oC		EN ISO 2160	1
Oxidation Stability, 110 oC	Hours	EN 14112*	10.8
Acid Number	mgKOH/g	EN 14104*	0.18
Iodine Value	g/100gFAME	EN 14111*	112
Linolenic Acid Methyl Ester	% m/m	EN 14103*	9.41
Polyunsaturated Methyl Ester	% m/m	EN 14103*	<1
Ester Content	% m/m	EN 14103*	97.7
Methanol Content	% (m/m)	EN 14110*	0.01
Monoglyceride Content	% m/m	EN 14105*	0.57
Diglyceride Content	% m/m	EN 14105*	0.15
Triglyceride Content	% m/m	EN 14105*	0.03
Free Glycerol	% m/m	EN 14105*	<0.01
Total Glycerol	% m/m	EN 14105*	0.17
Sodium	mg/kg	EN 14108*	<0.1
Potassium	mg/kg	EN 14109*	<0.1
Calcium	mg/kg	EN 14538*	<0.1
Magnesium	mg/kg	EN 14538*	<0.1
Phosphorus	mg/kg	EN 14107*	0.2
Cold Filter Plugging Point	°C	EN 116	-20
Carbon Content	wt/wt		77
Hydrogen Content	wt/wt		12
Oxygen Content	wt/wt		11

(^^) Test subcontracted to another laboratory.

Appendix C: The Student T Test P values

Emission Species		**Ambient Temperature**		
		25°C	10°C	-5°C
Tailpipe	CO	*0.0003*	*0.0075*	0.0634
	THC	**0.19**	**0.5149**	**0.2652**
	NO_X	*0.0095*	*0.1151*	**0.2494**
	PM	*0.0077*	**0.4054**	**0.2999**
Engine-Out	CO	0.0772	**0.1398**	**0.9649**
	THC	*0.0001*	*0.0219*	*0.0187*
	NO_X	*0.0077*	*0.0417*	**0.1425**
	Fuel Consumption (AVL 733)	*0.0003*	*0.0038*	*0.0017*

10.1, The student T test P values for baseline diesel and B50 fuel blends

Confidence intervals in which the means are different are given by 1-p. Italic numerals indicate greater than 95 percent confidence, upright numerals greater than 90 percent confidence, and bold red coloured numerals are not considered statistically significant.